Universitat Autònoma de Barcelona

NEW INSIGHTS IN THE STUDY AND CHARACTERIZATION OF FUNGAL METALLOTHIONEINS AND THEIR RELATIONSHIP WITH THE PATHOGENIC ACTIVITY

Selene Gil Moreno

PhD THESIS:

NEW INSIGHTS IN THE STUDY AND CHARACTERIZATION OF FUNGAL METALLOTHIONEINS AND THEIR RELATIONSHIP WITH THE PATHOGENIC ACTIVITY

Author

Selene Gil Moreno

Directors

Dr. Mercè Capdevila

Dr. Òscar Palacios

Departament de Química

Facultat de Ciències

Doctorat en Química, RD 99/2011, 2017

Universitat Autònoma de Barcelona

ABBREVIATIONS

^{o}C	degrees centigrade
µ	micra
µM	micro molar
aa	amino acid/s
AIDS	acquired immune deficiency syndrome
Asp	aspartic acid
apo-MT	apo-metallothionein
BC	before Christ
ca	*circa* (around)
CD	circular dichroism
cm	centimetre
Cys	cysteine
Da	dalton
DNA	deoxyribonucleic acid
EC protein	Early Cysteine-labelled protein
EPR	electron paramagnetic resonance
eq	equivalents
ESI-MS	ElectroSpray ionization mass spectrometry
etc	etcetera
EXAFS	Extended X-Ray absorption fine structure
g	grams
GE Healthcare	Glutathione Sepharose 4B
Gln	glutamine
Glu	glutamic acid
GST	Glutathione S-Transferase
Gly	glycine
h	hour/s
His	histidine
ICP-AES	Inductevely Coupled Plasma Atomic Emission Spectroscopy
IPTG	Isopopyl-β-D-1-thiogalactopyranoside
kDa	kilo Dalton

kV	kilo Volt
l	litre
LB	Luria-Bertani
Lys	lisine
mM	milli molar
min	minutes
ml	millilitre
MT/MTs	metallothionein/s
MW	mass weight
m/z	mass-to-charge ratio
nm	nano metres
NMR	Nuclear Magnetic Resonance
PBS	Phosphate Buffered Saline
PCP	pneumocystis pneumonia
PEEK	polyether ether ketone
pGEX	GST expression vector
RNS	reactive nitrogen species
ROS	reactive oxygen species
rpm	revolutions per minute
spp	species
Thr	threonine
Tris	tris(hydroximethyl)aminomethane
UV	ultraviolet
UV-Vis	ultraviolet-visible
v/v	volume-volume ratio
XRD	X-Ray Diffraction

INDEX

ABSTRACT

1. ABSTRACT

Metallothioneins (MTs) constitute a superfamily of metalloproteins with low molecular weight characterized by an extraordinary cysteine (Cys) content, which provides them the ability to coordinate heavy-metal ions through the corresponding metal-thiolate bonds. These proteins are polymorphic in a huge number of organisms studied up to now, besides great similarities have been found between MTs from different organisms. These observations suggest that a diversification of MTs have been produced as a consequence of successive gene duplication events in or between different taxa. In each case, the activity that the MT needs to accomplish in the organism may have produced the evolution to serve different molecular metal-related functions, such as essential metal ion homeostasis (Zn^{2+} or Cu^{+}), the defence in front of toxic metal ions (*i.e.* Cd^{2+}, Pb^{2+} or Hg^{2+}), the scavenging of free radicals and reactive oxygen species (ROS), and a wide range of cell stresses. Therefore, MTs in a given organism exhibit preferences for specific metal ion coordination and also to form complexes with a concrete number of metal ions bonded, independently of the degree of their similarity at protein sequence level. For this reason, the present PhD thesis work has been based first on classify a huge number of MTs, belonging to fungi organisms, in four families, according to their amino acid sequence length. Once classified the MTs, a study of the similarities between their amino acid sequences have been plausible, and also a comparison between their protein/metal coordination abilities and specificity for different metal ions. In order to elucidate these last-mentioned capabilities, the biosynthesis of the MTs in different metal content environments has been necessary. MTs biosynthesis and folding about their cognate metal ions result in the formation of energetically optimized complexes. But, when the synthesis takes place about non-cognate metal ions, normally a mixture of species is produced, by reflecting the amount of metal ions available in its molecular environment, or by contrast the synthesis may not be successful.

With the study of all these properties, attempts to clarify the functions of MTs in each organism are possible. In this PhD thesis work, MTs from fungi organisms, most of them pathogenic, have been studied, due to the importance to discover the role of the MTs in the process of virulence and pathogenicity. Advances in these findings may help the humanity at biological and medical level.

INTRODUCTION

2. KINGDOMS IN THE TREE OF LIFE

Over the years, the classification of living organisms has provoked a lot of controversy. During the age of Aristotle (384-322 BC) living beings were classified as animals or plants, but over the time and the technological advances, new proposals were performed (Table 1).

<table>
<tr><th>Linnaeus 1735[1]</th><th>Haeckel 1866[2]</th><th>Chatton 1925[3][4]</th><th>Copeland 1938[5][6]</th><th>Whittaker 1969[7]</th><th>Woese et al. 1977[8][9]</th><th>Woese et al. 1990[10]</th><th>Cavalier-Smith 1993[11][12][13]</th><th>Cavalier-Smith 1998[14][15][16]</th><th>Ruggiero et al. 2015[17]</th></tr>
<tr><td>2 kingdoms</td><td>3 kingdoms</td><td>2 empires</td><td>4 kingdoms</td><td>5 kingdoms</td><td>6 kingdoms</td><td>3 domains</td><td>8 kingdoms</td><td>6 kingdoms</td><td>7 kingdoms</td></tr>
<tr><td rowspan="2">(not treated)</td><td rowspan="2">Protista</td><td>Prokaryota</td><td>Monera</td><td>Monera</td><td>Eubacteria</td><td>Bacteria</td><td>Eubacteria</td><td rowspan="2">Bacteria</td><td>Bacteria</td></tr>
<tr><td></td><td></td><td></td><td>Archaebacteria</td><td>Archaea</td><td>Archaebacteria</td><td>Archaea</td></tr>
<tr><td rowspan="4">Vegetabilia</td><td rowspan="4">Plantae</td><td rowspan="4">Eukaryota</td><td rowspan="3">Protista</td><td rowspan="3">Protista</td><td rowspan="3">Protista</td><td rowspan="4">Eucarya</td><td>Archezoa</td><td rowspan="2">Protozoa</td><td rowspan="2">Protozoa</td></tr>
<tr><td>Protozoa</td></tr>
<tr><td>Chromista</td><td>Chromista</td><td>Chromista</td></tr>
<tr><td rowspan="2">Plantae</td><td rowspan="2">Plantae</td><td rowspan="2">Plantae</td><td rowspan="2">Plantae</td><td rowspan="2">Plantae</td></tr>
<tr><td>Fungi</td><td>Fungi</td><td>Fungi</td><td>Fungi</td></tr>
<tr><td>Animalia</td><td>Animalia</td><td>Animalia</td><td>Animalia</td><td>Animalia</td><td>Animalia</td><td>Animalia</td><td>Animalia</td><td>Animalia</td><td>Animalia</td></tr>
</table>

Table 1. Evolution in the classification of living beings over the years.

The system proposed in 1969 by Whittaker[7] has become one of the most popular standards of classification, and this is widely used even nowadays. This classification divides the organisms in five kingdoms, as shows the Tree of Life in Figure 1. The simplest organisms are located on the lower part of the tree, including monera and protista groups, illustrating their primitive origin. And the more complex organisms are in the branches of the tree, divided into animalia, fungi and plantae groups.

Whittaker's classification is mainly based on differentiate between 4 different aspects: prokaryotic or eukaryotic organism, unicellular or multicellular organism, cell wall presence and phototrophic or heterotrophic organism (Figure 2).

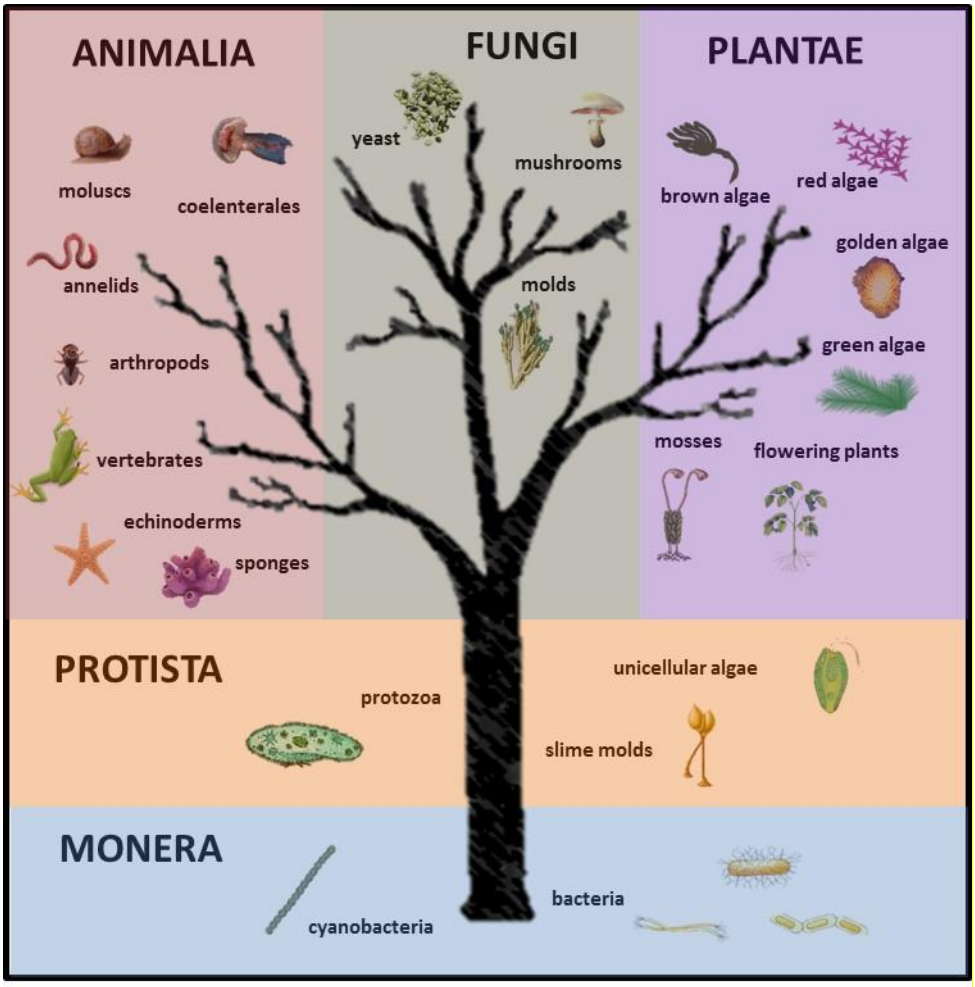

Figure 1. Whittaker's five-kingdom Tree of Life.[7]

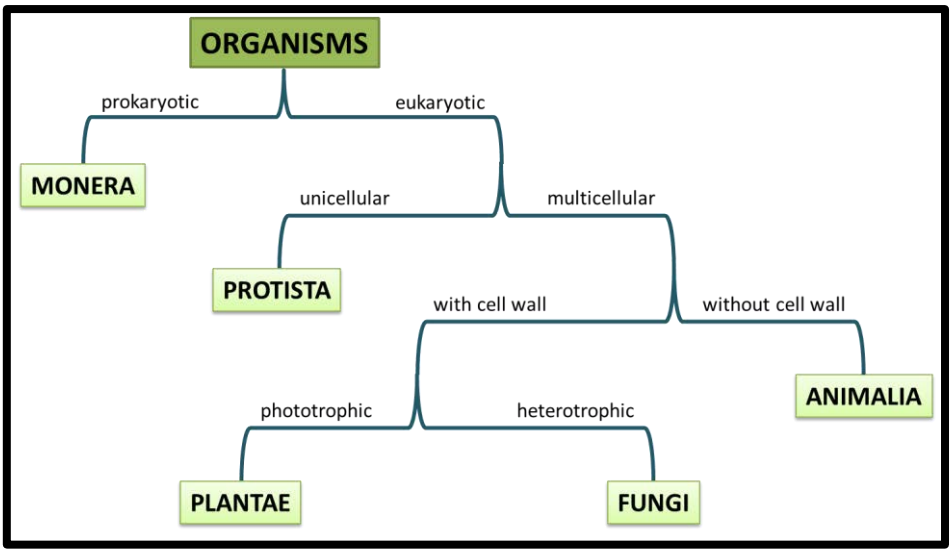

Figure 2. Criteria used in the five kingdoms Whittaker's classification.

3. FUNGI KINGDOM

The word *fungus* comes from the latin word for mushrooms. However, the fungi kingdom also comprises a wide variety of organisms besides them, like yeast and molds (see Figure 1). Fungi are eukaryotic unicellular, multicellular, or syncytial spore-producing organisms that can be found in both, terrestrial and aquatic, environments. These organisms are heterotrophic, due to the lack of photosynthetic pigments. But, in contrast to animals, which typically feed by ingestion, fungi obtain their nutrients by extracellular digestion due to the activity of secreted enzymes, followed by the absorption of solubilized breakdown products.[18] The production of numerous small spores greatly facilitates recruitment of new resources, even more than the production of a few large propagules. Colonization of a food source, once reached, is achieved most efficiently by the growth of a system of branching tubes, the hyphae, which together make up the mycelium. Hyphae are generally quite uniform in different taxonomic groups of fungi, but not all fungi grow as hyphae. Some of them grow as discrete yeast cells that are divided by fission or budding. Asexual and sexual reproductions are found to exist in almost all species, leading to alternate haploid and diploid life cycles. Asexual reproduction happens via vegetative spores, mycelial fragmentation, or yeast budding. On the other hand, sexual reproduction occurs through meiotic generation of haploid cells which can be extremely divergent between species depending on their mating preferences; and hence heterothallic fungi spores mate with different type, while homothallic mate with theirselves. Either way, sexual and asexual spores are very efficiently spread in order to ensure reproduction success.[19][20]

3.1 Fungi in humankind history

Fungi have been present in different aspect in human life since many centuries ago. Egyptian, Greek and Roman already used yeast for fermentation processes to elaborate bread, wine, and beer.[21] Fungi exist in every environment on Earth and play very important roles in most ecosystems. They figure prominently in different aspects of the human diet: as edible mushrooms (morels, shiitake mushrooms, chanterelles, truffles, etc.), and for food preparation (cheese ripening, wine fermentation, alcoholic beverages production, bread production, etc.). Unfortunately, not all fungi are edible or healthy. There are poisonous species with toxicities ranging from slight digestive problems, allergic reactions, or hallucinations to severe organ failures and death.[22] However, fungi are also used by humans with medicinal proposals (production of antibiotics, vitamins, anti-cancer drugs, immune suppressants, etc.) or as pesticides. The latter applications take advantage of the

pathogenicity of some fungi. For example, certain fungi can inhibit the growth or kill a specific bacterium allowing to heal an infected patient (the genre *Penicillium,* that produces penicillin), or they can infect a specific insect to avoid damage in a harvest (*Beauveria bassiana*).[23] In addition to infecting bacteria and insects, fungi can affect also plants and humans. Examples of this are the rice blast fungus *Magnaporthe oryzae*, and, in the case of humans, *Candida* spp. (which provokes candidiasis), *Aspergillus* spp. (aspergillosis) or *Cryptoccoccus neoformans* (cryptoccoccosis), being particularly susceptible persons with immuno-deficiencies.[24][25][26]

3.2 Fungi classification

About 99,000 species of fungi have been nowadays studied, and new species are described at the rate of approximately 1200 per year.[27][28] It is believed to exist more than 1.5 million of fungal species living in Earth.[29] Most of the introductory books to mycology divide the fungi kingdom in four different groups or phylum: *ascomycota, basidiomycota, chytridiomycota* and *zygomycota*.[18][30] More recent studies, based on genome structure and phylogenetic analysis, have allowed the recognition of additional phyla in the classification of fungi, giving rise to eight different groups (Figure 3). [27][31][32] Ascomycota and basidiomycota are the largest and more important groups between these eight phyla, for this reason the vast majority of the organisms studied in this thesis work are inside these two divisions. Table 2 briefly summarize the most important aspects of each phylum. Ascomycota and basidiomycota include the most recognized organisms like yeast, molds and edible fungi, and also the most important human and plant pathogens.

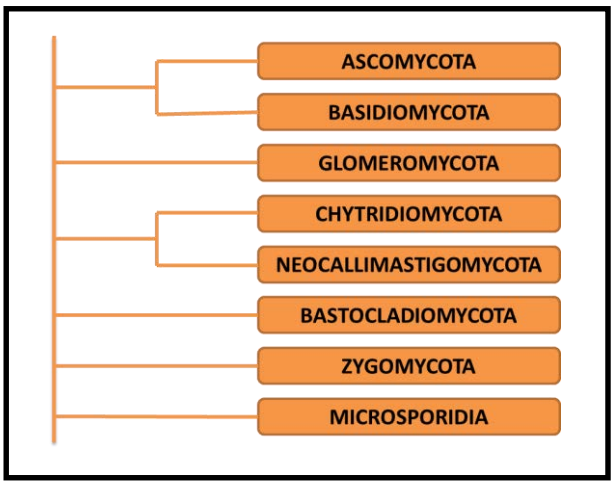

Figure 3. Classification of fungi in 8 different phyla. Adapted from Blackwell (2011) and Hibbet (2007).[27][32]

PHYLUM	GENERAL FEATURES	FOUND IN THE NATURE	EXAMPLES
Ascomycota	Largest phylum Asexual reproduction by spores Sexual reproduction by ascospores	Yeasts, molds, morels, truffles, human and plant pathogens	*Saccharomyces* spp. *Aspergillus* spp. *Fusarium* spp.
Basidiomycota	Reproduction by basidiospores	Edible fungi, human and plant pathogens	*Crytococcus neoformans* *Agaricus bisporus*
Glomeromycota	Asexual reproduction by spores	Parasites or symbionts of plants by mycorrhiza	*Gigaspora margarita*
Chytridiomycota	Saprophytes Terrestrial and aquatic Uniflagellated	Plant and human parasites	*Synchytrium endobioticum*
Neocallimastigomycota	Anaerobic Zoospores multiflagelled	Present in digestive tracts of herbivores	*Neocallimastix patriciarium*
Bastocladiomycota	Saprophytes Terrestrial and aquatic Anisogamic sexual reproduction Asexual reproduction by zoospores	Invertebrate and plant pathogens	*Allomyces macrogynus* *Blastocladiella emersonii*
Zygomycota	Formation of zygospores (sexual) and sporangiospores (asexual)	Bread moulds, some plant and animal parasites	*Rhizopus* spp.
Microsporidia	Unicellular	Intracellular animal parasites	*Trachipleistophora hominis*

Table 2. General features of the 8 fungi phyla.

3.3 Fungal interaction with other organisms

Fungi are extremely diversified and versatile organisms able to establish numerous interactions with other living beings. Some of these interactions may be beneficial for all partners involved (mutualistic interaction or symbiosis), whereas others are detrimental for at least one partner (parasitic or pathogenic interaction). Despite the fact that fungi can maintain associations with a wide variety of organisms, fungal-plants and fungal-human interactions have been the more studied due to their economical and sociological importance.[33][34]

3.3.1 Interactions between plants and fungi

The most well-known symbiotic interactions between plants and fungi are lichens (the result of an algae and a fungus) and mycorrhizal fungi. In both cases, fungus takes profit of the nutrients produced by the plant, whereas the plant is benefited by the protection of the fungus filaments.

In the case of parasitic or pathogenic interactions, fungi take advantage of the plant to obtain nutrients, even though the plant can be damaged. There are cases where the fungal parasite is able to obtain nutrients of the plant without hurting them, but plants do not gain any benefit. Some examples of these parasitic or pathogenic interactions are rust, anthracnose, mildew, or black moulds. Table 3 summarize the ten most well-known fungal pathogens which cause diseases to different plants. Especially relevant is *Botrytis cinerea*, which can affect more than 200 plant species.

FUNGAL PATHOGEN	DISEASE	HOST
Magnaporthe grisea	Rice blast	Rice
Botrytis cinerea	Grey mould	More than 200 plant species (vide is the most important)
***Puccinia* spp.**	Rust disease	Wheat mainly
Fusarium graminearum	Fusarium head blight	Grain
Fusarium oxysporum	Panama disease and other diseases	Banana
Blumeria graminis	Powdery mildew	Grasses, including wheat and barley
Mycosphaerella graminicola	Septoria tritici blotch disease	Wheat
***Colletotrichum* spp.**	Broad-range	Anthracnose
Ustilago maydis	Corn smut	Corn
Melampsora lini	Flax rust	Flax

Table 3. Top 10 fungal pathogens in molecular plant pathology.[35]

3.3.2 Interactions between animals and fungi

There are few cases of mutualistic relationship between fungi and animals. The two most representative ones are the fungi present in the gut of herbivores and the relationship between leaf cutter ants and *Leucocoprinus* spp. The former interaction consists on helping the animal in the digestive process whereas the fungi receive nutrients. On the latter, ants feed the fungal garden as the source of their own food.

But normally, the relationships between animals and fungi are pathogenic and more than 400 fungi can provoke several diseases. Most of them are known as dermatophytes, they cause only superficial infections at the skin or appendages. The fraction of fungi resulting in fatal or chronic diseases is

small. In this case, they produce systemic infections involving vital organs or the central nervous system (see Table 4).[36][37] There are several examples of widely known diseases, like candidiasis or cryptococcosis, which awakes a strong interest in the field.

FUNGAL PATHOGEN	DISEASE	SYMPTOMS
***Aspergillus* spp.**	Aspergillosis	Allergy, fever, cough, chest pain.
Blastomyces dermatitidis	Blastomicosis	Febrile pneumonia with cough, asthenia and dyspnoea.
***Candida* spp.**	Candidiasis	Redness and itching. Fatal in immunodeficient patients.
***Coccidioides* spp.**	Coccidioidomycosis (Valley Fever)	Flu-like symptoms, dyspnoea, weakness, depression and weigh loss. Fatal in immunodeficient patients.
Cryptococcus neoformans	Cryptococcosis	Cutaneous wound, pulmonary infection or meningitis. Opportunistic infection for acquired immune deficiency syndrome (AIDS) patients. Often fatal.
Histoplasma capsulatum	Histoplasmosis	Pneumonia-like symptoms and fever. High mortality in immunodeficient patients.
Pneumocystis jirovecii	Pneumocystis pneumonia (PCP)	Lung infection in immunodeficient patients.
Sporothrix schenckii	Sporotrichosis	Nodular lesions or bumps in the skin. Rare times can affect lungs, joints, bones and brain.
Penicillium marneffei	Penicillosis	Lethal system infection, with fever and anaemia.

Table 4. Summary of the most important fungal pathogens which can cause human diseases, as well as the main symptoms that they produce.

3.4 Toxicity of metals in fungi

The study of the interaction between toxic metals and fungi has long been of scientific interest, due to the importance of fungicidal preparations in control of pathogens and preservation of materials.[38] As already happens in other organisms, some metals are essential for fungi, for example K, Na, Mg, Ca, Mn, Fe, Cu, Zn, Co, or Ni. While others, like Al, Cd, Ag, Au, Hg, or Pb can result toxic at very low concentrations, by causing exert harmful effects in different ways. Toxic mechanisms include: the blocking of functional groups of biologically important molecules (as enzymes and transport systems); the displacement or substitution of essential metal ions from biomolecules and functional

cellular units; conformational modification, denaturation and deactivation of enzymes; and disruption of cellular and organellar membrane integrity.[38][39]

Cell membrane is an initial site of action for toxic metal ions[40], producing loss of mobile cellular solutes and increasing permeability of the cell to external materials. The metal toxic effects are varied, from membrane lipid peroxidation and breakdown of biological macromolecules, to production of toxic free radicals as a result of reactions with thiols or enzymes.[41]

The fungal survival in the presence of toxic metal ions depends on several factors: intrinsic biochemical and structural properties; physiological and genetic adaptation (including morphological changes); and environmental modification of the metallic speciation, availability, and toxicity. In terms of metallic toxicity, it is possible to distinguish between metallic resistance and metallic tolerance. The first is defined as the ability of an organism to survive metallic toxicity by means of a mechanism produced in direct response to the metallic species concerned. The second consist on the ability of an organism to survive metal toxicity by means of intrinsic properties and environmental modification of toxicity.[42]

Biological mechanisms implicated in fungal survival in metal-rich environments include extracellular precipitation, complexation, crystallization, biosorption, transport, impermeability, intracellular compartmentalization sequestration, and transformation of metallic species by oxidation, reduction, etc.[43][44] Other mechanisms include the synthesis of sulphur-rich molecules in order to bind toxic metal ions, such as metallothioneins and glutathione.

4. METALLOTHIONEINS

Metallothioneins are a very special family of metalloproteins characterized by their exceptional abilities to bind heavy metal ions and by their low mass weigh. The first MT was discovered on 1957, by Margoshes and Vallee, in the horse kidney cortex.[45] Few years later, Kägi and Vallee called them "metallothioneins" due to their high metal and cysteine residues content.[46] MTs constitutes a big family of proteins that are present in a wide variety of living beings, unicellular (cyanobacteria, yeasts, protozoa, and more recently mycobacteria[47]) and pluricellular ones (vertebrates, invertebrates and plants). The most common features of MTs are:[48]

- Low molecular weight (3-10 kDa).
- High cysteine content (*ca.* 30%) in their amino acid sequences.
- High coordinating and ion-exchange capability, through the corresponding metal-thiolate bonds.
- Low rate of hydrophobic and aromatic residues, as well as histidine and arginine.
- Three-dimensional structure acquired due to the metal-MT clusters formed. In their apo form, without metals bound, MTs do not exhibit a defined secondary structure.
- High thermal stability and kinetic lability.
- Characteristic cysteine motifs -XCXCX-, -XCCX-, -XCCCX- (X as an amino acid different from cysteine) in certain MTs.

Among all these, the most important feature of these proteins is their high cysteine content. This amino acid is the main responsible for coordinating metal ions in proteins, even though histidines are also able to bind them. In living beings, MTs have been found coordinating essential metal ions like Zn(II) and Cu(I), and also toxic ones like Cd(II), Hg(II), Ag(I), or Pb(II). Additionally, *in vitro* studies demonstrated that MTs are able to coordinate also other metal ions like Au(I), Bi(III), Fe(II), Ni(II), Pt(II), or Tc(IV).[49] Moreover, it is important to highlight that there is a great diversity in length and sequence composition among the studied MTs, providing differentiation in binding abilities, which must probably produce a variety of structures and biological functions among them.

4.1 MTs production methods

The most used MT production methods until the 90's were based on inducing the target MT synthesis in living organisms by different routes, followed by subsequent isolation and purification from the tissues where this was expressed.

Induction of MTs in living beings can be provoked by different factors, depending on the organisms and the MT, such as the presence of certain metal ions, radical agents, ultra violet (UV) radiation, or certain hormones. With the direct induction on the desired organism, MTs are normally obtained in native form, but it has two important disadvantages: the extremely long and difficult purification process, and the low concentration of the MTs obtained.[50]

Another alternative method, less used, is the chemical synthesis of polypeptide chains on solid supports. In this case, the sequences are produced without the presence of any metal ion, thus producing the apo-metallothioneins (apo-MT). Some fungal[51][52] and mammalian[53][54][55] MTs have been obtained following this method. However, this methodology also has some limitations, as it is the difficulty of synthesize long chains or also the complex protection of cysteine residues against oxidation.

An alternative to the previous methods is the use of genetic engineering techniques, known as deoxyribonucleic acid (DNA) recombinant technique.[56] This method consists in taking benefit of the protein synthesis mechanism inherent in some bacteria (Figure 4). Circular DNA sequences are introduced inside the bacteria containing: genetic information of the target MT, transcription and translation signals, together with additional genetic information for stability and transmission inside the cell. Then, the process of synthesis, induced by IPTG (Isopopyl-β-D-1-thiogalactopyranoside, molecule commonly used in genetic expression induction), is produced inside the cells, and followed by subsequent isolation and purification to obtain large amounts of the sequenced protein.

The cell media where the proteins are induced can be enriched with different metal ions, in order to allow the protein to bind the metal ion selected in each case. When the media is enriched with Zn(II), the *in vivo* Zn-MT production is obtained, as well as Cd-MT and Cu-MT productions from Cd(II) and Cu(II) enriched cells, respectively.

This technique allows producing proteins with high purity and identical properties to the native ones.[57] The technique also allows to modify the amino acid sequences of the protein, in order to provoke mutations into the native forms or reproduce partially the whole protein.

All proteins used in this Thesis work have been obtained by recombinant DNA synthesis by the group of Dr. Silvia Atrian at the *Universitat de Barcelona*. They have a long experience on producing MTs by this method since 1995.[58]

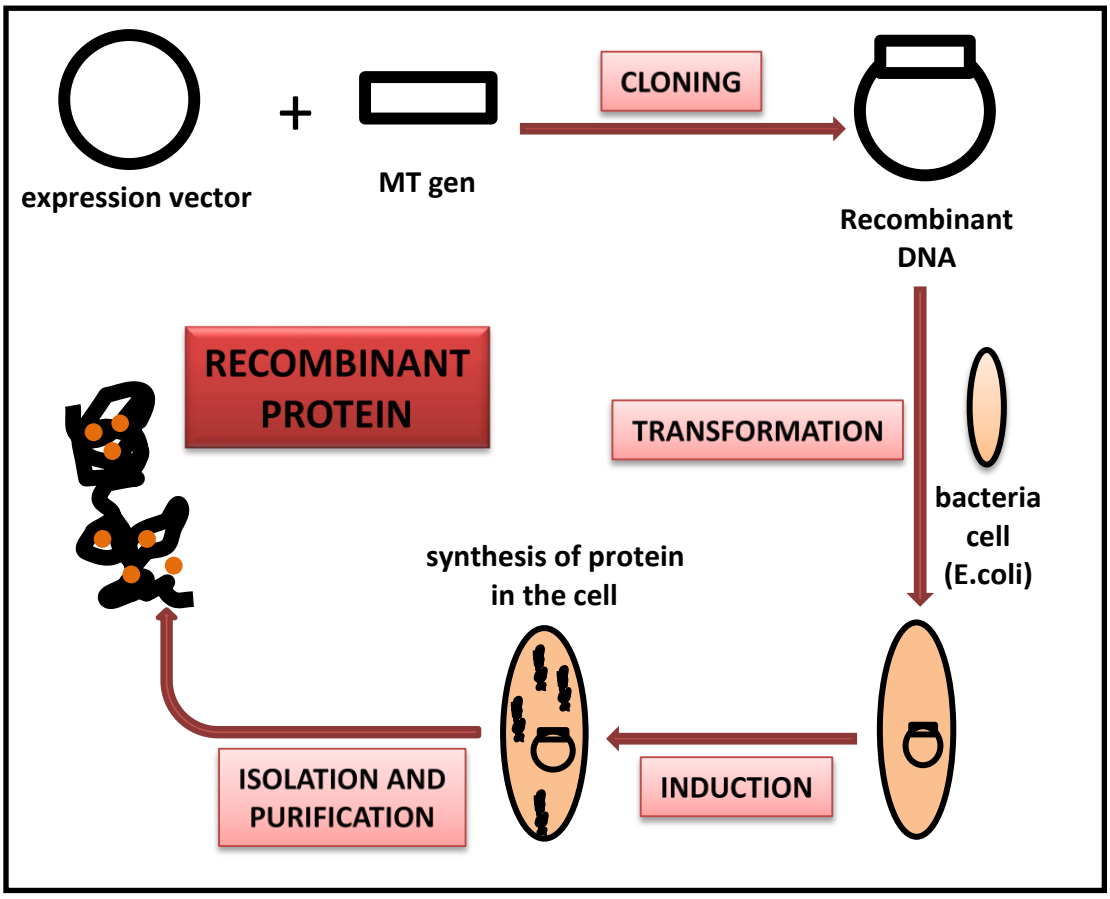

Figure 4. MT production procedure by the use of the recombinant DNA methodology.

4.2 MTs structure

As already mentioned, MTs adopt a three-dimensional folding when they are coordinated to metal ions, mainly through metal-SCys bonds, and to a lesser extent, through metal-NHis. In contrast, apo-MTs exhibit a disordered structure of *random coil*. The high flexibility of peptide chain allows thiolates to accommodate each metal ion in their preferential coordination environment. However, this flexibility also hinders the study of three-dimensional structure. For this reason, only a few structures have been solved, by nuclear magnetic resonance (NMR) or X-Ray diffraction (XRD) (Table 5).

Organism	Metallothionein	Technique
Mammal (human, rat, and rabbit)	Cd_7-MT2	NMR[59][60][61]
Mammal (rat)	Zn_2Cd_5-MT2	XRD[62]
Mammal (mouse)	Cd_7-MT1	NMR[63]
Mammal (mouse and human)	Cd_4-αMT3	NMR[64][62]
Fish (*N. coriiceps*)	Cd_7-ncMT	NMR[65]
Crustacean (*C. sapidus*)	Cd_6-MT1	NMR[66]
Crustacean (*H. americanus*)	Cd_6-MT1	NMR[67]
Echinoderm (*S. purpuratus*)	Cd_7-MTA	NMR[68]
Yeast (*S. cerevisiae*)	Cu_7-Cup1, Ag_7-Cup1	NMR[69][70]
Yeast (*S. cerevisiae*)	Cu_8-Cup1	XRD[71]
Bacteria (*Synechoccus*)	Zn_4-SmtA	NMR[72]
Fungus (*N. crassa*)	Cu_6-NcMT	NMR[73]
Plant, wheat (*T. aestivum*)	Zn_4-β_E-E_C-1	NMR[74]

Table 5. MT structures solved by NMR or X-Ray diffraction so far

Most of the solved structures have two separate domains, and each domain contains one metal-thiolate cluster. This is the case of mammalian MT2 (Figure 5), one of the most studied MTs, and very similar to the other major isoform MT1. The N-terminal domain (β domain) of mammalian MT2 is formed by 3 divalent metal ions in tetrahedral environment, bonded to 9 cysteine thiolates ($M_3(SCys)_9$). The C-terminal domain (α domain) is a cluster constituted by 4 divalent ions in tetrahedral environment and 11 cysteine thiolates ($M_4(SCys)_{11}$) (M=Zn and/or Cd).

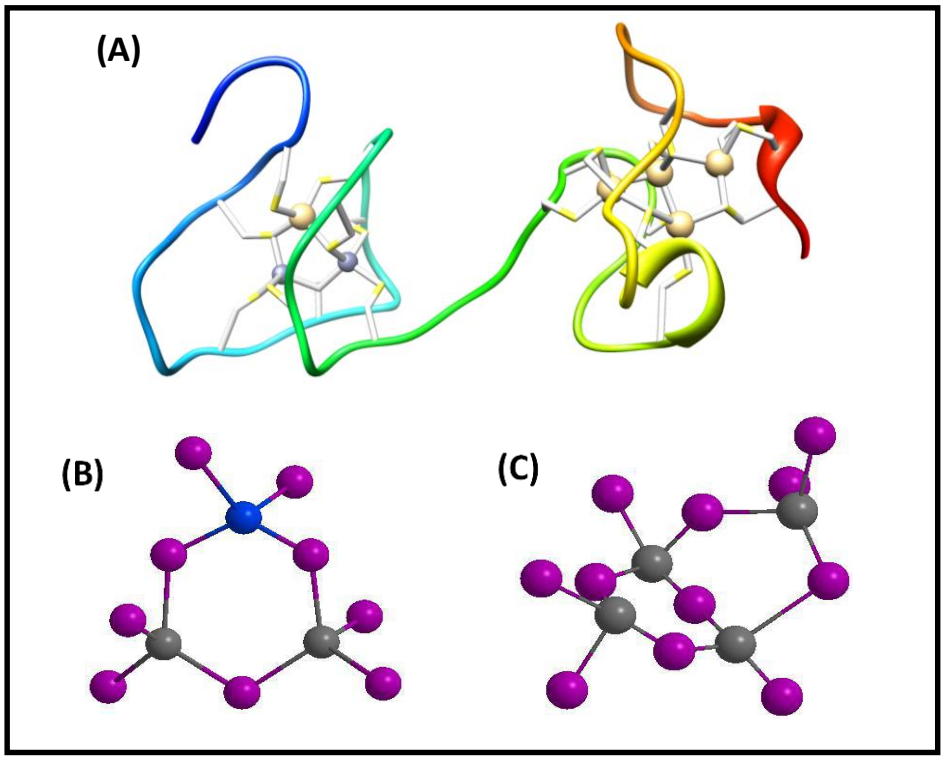

Figure 5. Three-dimensional structure of mammalian Zn_2Cd_5-MT2, solved by X-Ray Diffraction, showing (B) the β domain formed by the aggregate Cd_1Zn_2-$(SCys)_9$, and (C) the α domain formed by the aggregate Cd_4-$(SCys)_{11}$.

In the case of Cu-MTs, the clusters formed always contain Cu(I), that can be coordinated by two or three cysteine ligands in lineal or trigonal-planar geometry.[49][75][76] However, data related to Cu-MT structures is limited, due to the broad signals obtained for Cu(I) nuclei in NMR spectroscopy studies[77] and the difficulty to obtain mono-crystals to elucidate by XRD. Despite this drawback, the structure of *Saccharomyces cerevisiae* MT (Cup1) was solved by XRD[71] (Figure 6) and NMR[69][70], and also the structure of *Neurospora crassa* MT (Nc-MT) by NMR have been recorded [73], besides some X-Ray absorption and Extended X-Ray absorption fine structure (EXAFS) information.[78] In both cases, the protein forms a single cluster, Cu_8-$(SCys)_{10}$ and Cu_6-$(SCys)_7$, respectively.

These two MTs, NcMT and Cup1, are the most widely studied fungal MTs so far. The research about their structures provides important progress in the knowledge of this particular organisms' group. Due to the importance for the development of this thesis, the studies of these MTs will be further detailed in section 5.

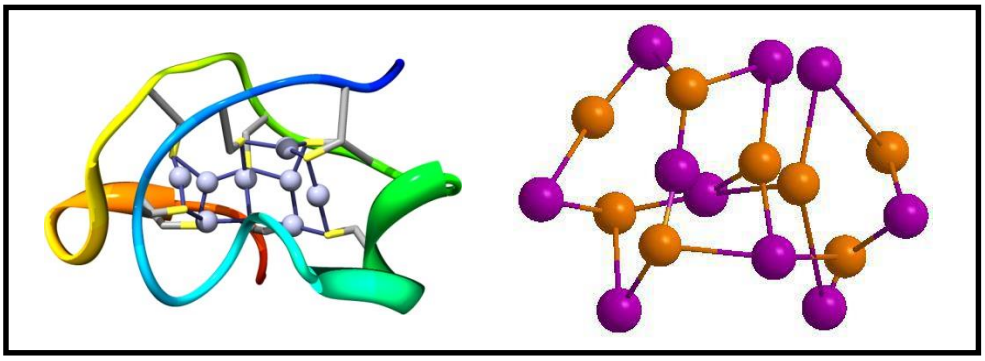

Figure 6. Three dimensional structure of Cu_8-Cup1 of *Saccharomyces cerevisiae* fungus solved by XRD and the aggregate Cu_8-$(SCys)_{10}$ formed

Despite cysteine and histidine are the main coordinating amino acids that form the metal clusters in proteins, it has been shown that chloride and sulfide can participate as additional ligands in metal-MT aggregates. The participation of chloride as additional ligand in MTs is not so common, but some cases have been discovered during the last years: Cd_7-MT2[79], MtnB of *D.melanogaster*[80] and MT4 of mouse.[81] On the other hand, the contribution of sulfide have acquired more relevance being an important ligand for MTs with Cu-thionein character (as is explained in section 4.3).

4.2.1 Sulfide anions

The participation of sulfide anions (S^{2-}) as additional ligands was observed for the first time in phytochelatines (PCs).[82][83] Phytochelatines or cadistines are enzymatic peptides with the general formula $(\gamma\text{-Glu-Cys})_n$Gly present in plants, fungus and algae. They coordinate divalent metal ions through cysteines and sulfide anions, by forming structures where the peptide covers the so called *crystallite*, a metallic sulphide mono crystal (Figure 7).[84]

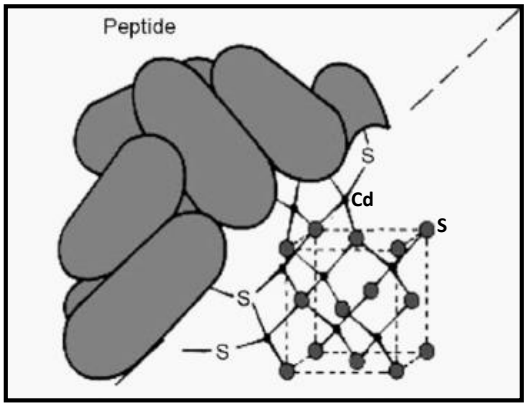

Figure 7. In Cd-PCs aggregates, peptide covers CdS mono crystals (*crystallites*), which bind PC through Cd-SCys bonds.[84]

Thereafter, in the studies of *Q. suber* MT (QsMT) by the use of recombinant biosynthesis, they were observed the first evidences of participation of additional sulfide ligands in metal-MT complexes.[85] However, the presence and participation of these ligands were confirmed by the research group where this thesis has been carried out.[86] The most important proportion of sulfide ligands could be observed in certain Cd-MT productions forming the expected Cd_x-MT species, but also Cd_xS_y-MT species coexisting. Consequently, a study was designed in order to determine the presence of these species in both, recombinant and natives MTs,[87] concluding that MTs with more Cu-thionein character are assisted for the presence of sulfide in order to form stable clusters with Cd(II) (Cu-thionein features are explained in section 4.3). Besides, other groups have been taken benefit of this property by synthesizing metallic nanoparticles recombinantly in *E. coli*.[88]

4.3 MTs classification

Usually proteins are classified according to their functionality (oxygenases, reductases, proteases, etc.). In the case of MTs there is a big controversy, because, despite the different possible functions attributed, the main physiological role is still a matter of debate in the community. For this reason, different classifications of MTs have been proposed over the years.

The first classification, proposed on 1985 established a division of MTs in three groups, based on the similarity of their sequences with the first known MT, the one from horse kidney cortex:[89][90]

- Class I is constituted by MTs with similar sequence to the MT from horse kidney and structured in two domains. This group contains a wide variety of mammalian MTs, but also some other vertebrate and invertebrate MTs.
- Class II is constituted by MTs with a big heterogeneity in their sequences. The amino acid sequences cannot be aligned between them either with the equine MT. MTs from this group have mainly a single domain, and have been isolated from fungi, plants, invertebrates, and some bacteria.
- Class III is constituted by enzyme sourced MTs isolated from plants, algae and some fungi. This group also include the above mentioned phytochelatines (section 4.2.1).

In 1997, Binz and Kägi proposed a new classification for MTs based on phylogenetic relationships and sequential criteria. This new proposal divides MTs in families, subfamilies, subgroups, isoforms, and subisoforms, but providing as many MT types as taxonomic groups known.[91]

However, these two classifications do not provide functional or evolutionary information about MTs, because they are based on sequence similarity. For this reason, in 2001, our group proposed a new classification, based on both, amino acid sequences and preferences for essential metal ions such as Zn(II) and Cu(I).

Zn(II) and Cu(I) can be found physiologically bonded to MTs in living beings. Thus, the different coordination environment exhibited by these two metal ions (tetrahedral for Zn(II) and trigonal planar and linear for Cu(I)) can lead to the formation of different clusters and thus, different protein conformation. This may confer different structures to the same MT when binding Zn(II) or Cu(I). Consequently, taking into account that the function of the proteins is normally determined by its structure, the characteristic function of a particular MT must be determined by the metal ion bonded.

Therefore, to classify MTs according to these assumptions, their coordinating abilities in front of Zn(II) and Cu(I) had to be evaluated. Additionally, MTs coordination abilities in front of Cd(II) were also evaluated, because the behaviour of MTs with this metal ion is an important factor that helps to classify them, as will be further explained.

Zn-, Cd- and Cu-MTs were recombinantly produced in *E. coli* cultures, in order to analyse their *in vivo* binding capabilities. Besides, the cultures enriched with Cu(II) have been produced in two different aeration conditions, normal oxygenation and low oxygenation, due to the difference in the MTs copper-binding abilities depending on the aerobic or anaerobic status of the producing host cells.[92] With all these parameters, the study of a large number of different MTs allowed to propose a gradation from genuine Zn-thioneins to strict Cu-thioneins (Figure 8). [93][94]

The factors taken into account to classify the different MTs in the gradation are:[95]

1) Presence or absence of Zn(II) in the metal-complexes synthesized in Cu(II) media.
2) Presence or absence of sulfide ligands in the *in vivo* Cd-MT preparations.
3) Presence or absence of Zn(II) in biosynthesized Cd-MT preparations.
4) Reluctance grade for Zn(II) exchange by Cd(II) on *in vivo* Zn-MT titrations.
5) The number of Cu(I) equivalents (according with the number of cysteines) necessary for *in vitro* reproduces the *in vivo* Cu-MT species.

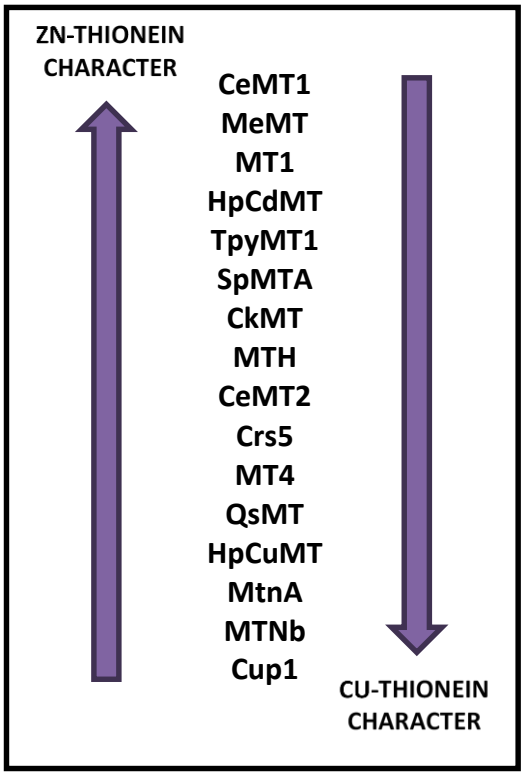

Figure 8. MTs gradation according to their Zn- or Cu-thionein character proposed in 2008.[95]

Completely opposite features were observed in genuine Zn and Cu-thioneins by studying all the previous factors. (Table 6 and Figure 9).

GENUINE Zn-THIONEINS	GENUINE Cu-THIONEINS
Single species observed in Zn(II) and Cd(II)-enriched bioproductions	Mixture of species observed in Zn(II) and Cd(II)-enriched bioproductions
Heterometallic Zn_xCd_y-MT species observed in Cd(II)-enriched bioproductions	Presence of S^{2-} ligands observed in Cd(II)-enriched bioproductions
Reluctance for *in vitro* Zn/Cd exchange	Easy *in vitro* Zn/Cd exchange
Heterometallic Zn_xCu_y-MT species observed in Cu(II) enriched bioproductions, regardless of the oxygenation grade	Homometallic Cu-MT species observed in Cu(II) enriched bioproductions, regardless of the oxygenation grade

Table 6. Comparison between features of genuine Zn-thioneins and Cu-thioneins.

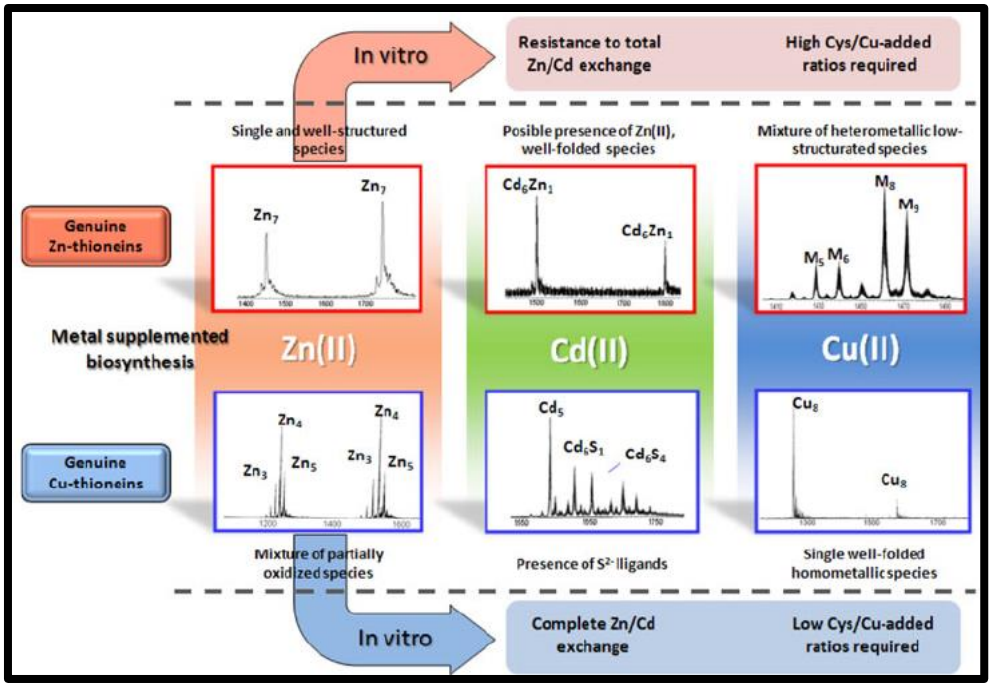

Figure 9. Experimental data and deductive process followed to classify MTs according to their Zn- or Cu-thionein character.[95]

The most prominent feature of genuine Zn-thioneins is the formation of single well-structured Zn-MT species in Zn(II)-enriched bioproductions. Zn(II) ions bonded to these species present high reluctance for *in vivo* and *in vitro* Zn/Cd exchange, giving rise to heterometallic Zn_xCd_y-MT complexes. Besides, when Zn-thioneins are produced in Cu(II) culture bioproductions, they present the particularity to form mixtures of Zn_xCu_y-MT species. On the other hand, genuine Cu-thioneins form single well-structured Cu-MT species in Cu(II)-enriched bioproductions, while in Zn(II)- enriched bioproductions they tend to form mixtures of Zn-MT species. Additionally, these kinds of MTs form Cd_xS_y-MT complexes in Cd(II) culture bioproductions. All this suggests that Cu-thioneins are designed to bond monovalent ions, so, they need the presence of Zn(II) or sulfide ligands to stabilize metal-complexes when binding divalent metal ions.

Among all the classified MTs, Cup1 from yeast is the MT with the most Cu-thionein character known so far[96] and CeMT1 from nematode the one with the most Zn-thionein character. A good example of a MT with intermediate character is CkMT from chicken[97] which participate in both, Zn(II) and Cu(I) metabolism (Figure 8).

4.4 MTs reactivity and functions

Nowadays the specific physiological functions of MTs are still not well known, despite the huge research literature published about them during several decades. The only general agreement about MTs' biological roles is that their main function depends on the organism where they are found.

In order to attribute different functions to MTs, it is necessary to understand their inherent features and reactivity:[48]

- Metal-binding capacity. MTs are polydentate ligands with high affinity for metal ions due to the presence of thiolate groups.
- Metal exchange. The exchange is based on the affinity of thiolate for different metals (Fe(II) ≈ Zn(II) ≈ Co(II) < Pb(II) < Cd(II) < Cu(I) < Au(I) ≈ Ag(I) < Hg (II) < Bi(III)).[49] According to this gradation, species with Fe(II) or Zn(II) will tend to react and change their metallic content easily.
- Metal transfer between biomolecules. MTs can be acceptors or donators of metal ions, promoting the metal transfer between different proteins or other biomolecules.
- Redox activity. Thiolate groups of MTs are susceptible to be oxidized by soft agents and radical species.

The diverse reactivity of MTs enables them to participate in multiple physiologic processes:

- Detoxification of metals. This is the first and long assumed biological function of MTs. They seem to have high ability to bind toxic metals, following the order of metal-thiolate affinity gradation above mentioned. For this reason, MTs help to avoid cell damage and maintain a favourable physiologic situation by sequestering toxic metal ions.[98][99][100]
- Metal ion homeostasis. Apart from toxic metals that can cause cell damage, all physiologic metals, present normally in organisms, as Cu(I) or Zn(II), can be poisonous at high concentrations. For this reason, MTs help to maintain the physiologic metal concentrations on biological systems in-between the corresponding range.[101][102]
- Antioxidant agents. MTs present in oxidative stressed cellular media have been found living together with oxygen (ROS) and nitrogen (RNS) reactive species, produced by UV or X-Rays radiation. MTs participate in the radical elimination process by suffering an oxidation of their thiolate groups and releasing metal ions.[103][104][105][106]
- Molecular carbine. MTs might participate in the folding of other proteins, such as other metalloproteins or transcription factors.[107]

Besides these four functions described above, other less-known functions have been attributed to MTs. These proteins can take part on metabolic control, for example, by regulating the cellular energy balance.[108] Also, they can exhibit an antiapoptotic role[109] or help in cellular protection and regeneration too.[110][111][112]

4.5 MTs in living beings

More than 250 MTs are known so far, because they are present in practically all living organisms. Nevertheless, the most extend studies have been focus in mammal, fungi and, more recently, in plant MTs.

Four MT-coding gens have been isolated from mammals. These coding gens induce the different isoforms MT1, MT2, MT3, and MT4, which can also present subisoforms (differentiated by 1 or 2 amino acids among them). These four isoforms show a high amino acid sequence similarity, being possible to align their 20 cysteine residues. However, they present differences in their expression pattern, because MT1 and MT2 are expressed ubiquitous and constitutively, MT3 is expressed in nervous system while MT4 in the stratified squamous epithelium.[113][114]

The structural and chemical perspective of invertebrate MTs has been poorly studied. MT system from insects,[115] crustaceans,[66][116][117] echinoderms,[68] molluscs,[118] and nematodes[119][120] have been studied, especially focusing on the physiologic role and their use as biomarkers for contamination.[121]

The first evidences about a plant MT was on 1987, when Kennedy and his collaborators isolated a protein from wheat seed, known as EC protein (*Early Cysteine-labelled protein*), which contained large Zn(II) amounts. Thereafter, a wide range of MT gens have been found, mainly related with Cu homeostasis on vegetal tissues.[122][123]

Within all organisms, we are going to focus on fungal MTs, because this thesis work is going to deepening on the role of MTs in the different fungi functions, especially pathogenic activity.

5. FUNGAL MTs

MTs concerning fungi have been poorly investigated over the years. Fortunately, their interest has increased in the last decades. The first discovered fungal MT was a Cu-MT from the yeast *Saccharomyces cerevisiae,* the so called Cup1. There are notable differences between these MT and horse MTs, and for this reason Cup1 was assigned to the class II in the three-class system.[124] Subsequently, when MTs were proposed to be classified into 15 families, by Binz and Kägi, the different fungal MTs were assigned to six different families, numbered 8 to 13 (Table 7).[125][89]

Family 8 is the subgroup with the largest number of known MT sequences. In general, MTs that constitute this family are very small, about 25 amino acid residues each. Coordination of copper ions, rather than divalent Zn(II) or Cd(II), is a characteristic feature of this group and it is commonly observed in fungal MTs. However, their most striking property is the similarity of their sequence with the N-terminal domains of mammalian MTs. Families 9 and 10 contains one member each, both from *Candida glabrata*. Family 11 has four members from *Yarrowia lipolytica*. The cysteine part of these members is limited to the second half of the sequence, starting with an unusual motif of three cysteine residues followed by a spacer, and a structure like -CXCXXCXCXXCXC- in the last 13 residues. Finally, families 12 and 13 are constituted by two different MTs from *Saccharomyces cerevisiae.*

FAMILY	EXAMPLE OF A MEMBER	CYS PATTERNS
8	*Neurospora crassa* MT	**-CXC-** **-CXCXXC-**
9	*Candida glabrata* MT1	**-CXC-** **-CXCXXC-** **-CXXXCXC-**
10	*Candida glabrata* MT2	**-CXC-** **-CXCXXC-** **-CXXXCXC-**
11	*Yarrowia lipolytica* MT3	**-CXC-** **-CCC-**
12	*Saccharomyces cerevisiae* CUP1	**-CC-** **-CXC-** **-CXCXCXXC-** **-CXXXCXCXXXC-**
13	*Saccharomyces cerevisiae* CRS5	**-CC-** **-CXC-** **-CXXC-** **-CXXXC-** **-CXCXXC-**

Table 7. Classification of fungal MTs according to Binz and Kägi's division[125][89]

Among all fungal MTs, yeast MTs has been the most deeply studied due to the importance of *Saccharomyces cerevisi*ae and its first discovered MT, Cup1-MT. *S. cerevisiae* has been adopted as a model organism among unicellular eukaryotes, for this reason its Cup1 isoform is the Cu-thionein most characterized up to know, providing a huge quantity of studies of MTs from similar organisms. However, there are two non-yeast MTs less studied, which have been important in the advances on this field, as they are considered the traditional and archetypical fungal MTs: *Neurospora crassa* MT (NcMT) and *Agaricus bisporus* MT (AbMT). A brief summary of the study of yeast and non-yeast MTs is detailed below.

5.1 Yeast MTs widely characterized

5.1.1 *Saccharomyces cerevisiae* MTs

An exclusively Cu(I)-loaded MT, called Cup1 and classified in the family 12 of Binz and Kägi's division, was found and isolated in 1975.[126] The protein, which confers Cu-resistance to the fungus *Saccharomyces cerevisiae*, was purified and characterized by D.R. Winge in 1984.[127] This MT is formed by 53 amino acids and 20% of cysteine content, lower than the 30% for mammalian MTs. In total, it contains 12 Cys residues and, unlike vertebrate MT, one histidine.

Cup1-MT is encoded by *CUP1* gene, which is induced by Cu(I) and Ag(I), but not by other metal ions, like Cd(II) or Zn(II). For this reason, Cup1-MT is found containing Cu(I) under physiological conditions. X-ray photoelectron spectrometry, EXAFS, and NMR techniques have been used to characterize the structure of the cluster formed by Cup1 (replacing Cu(I) by Ag(I) in the case of NMR, to observe M-Cys connectivities).

The crystal structure of Cu_8-Cup1 was solved, being the unique Cu-MT cluster whose structure is known up to now.[71] After X-Rays diffraction studies, the Cup1-MT cluster is known to be formed by 8 Cu(I) ions bonded by 10 of the 12 cysteines present in the sequence. In this structure 6 Cu(I) ions are coordinated trigonally by cysteine thiolates, whereas two are bound in a linear mode, which are more labile (Figure 10). For this reason, in solution, Cu_8-Cup1 consists of a mixture with stoichiometries of six to eight Cu(I) per MT molecule.

By contrast, NMR studies show different results. Seven, instead of eight, different frequencies were found in the NMR spectra, showing a linear coordination mode for three Ag(I) ions, whereas four Ag(I) ions are bound in a trigonal mode (Figure 10).

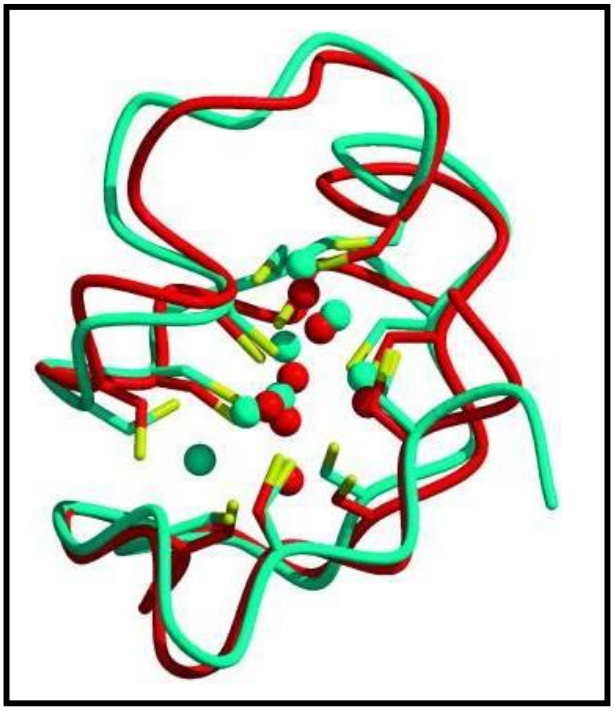

Figure 10. Superposition of Cu_8-Cup1 crystal structure obtained from X-Rays diffraction (cyan line) compared to the NMR model of the polypeptide chain fold in a Cu_7-Cup1 complex (red line). Yellow lines are cysteine side chains, cyan spheres are the Cu_8-atoms and red spheres are the Cu_7-atoms. (Adapted from Calderone 2005).[71]

Although *CUP1* gene is not induced by Cd(II) or Zn(II), Cup1 is able to bind these metals. When this MT is synthesized in Zn-supplemented cultures, it can coordinate from 3 to 5 Zn(II) ions per molecule, while it renders Cd_5-Cup1 and Cd_6S_4-Cup1, or Cd_7S_7-Cup1 complexes when synthesized by Cd-enriched bacteria.[87]

Another MT gene, called *CRS5*, was found in 1994 in *Saccharomyces cerevisiae*. This gene is also induced by high levels of Cu(I) in order to synthesize the Crs5 isoform, a protein with 69 amino acid residues and 19 cysteines, classified in the family 13 according to Binz and Kägi's division.[128][129] This MT is able to bind 11-12 Cu(I) ions by molecule, but Cup1 contributes more to copper resistance due to its capacity of tandem amplification.

Different studies about the coordination capabilities of Crs5 have been performed the last years, allowing its classification as an intermediate between Cu-thioneins and Zn-thioneins, but slightly closer to Zn-thioneins.[92] This is due to the stability of Zn complexes formed in Zn-supplemented cultures, homometallic Cd species expressed in Cd-rich media, and heterometallic Zn, Cu complexes in Cu-supplemented media. Despite this fact, in anaerobic physiological conditions, homometallic Cu complexes are able to be obtained.

5.1.2 *Candida glabrata* MTs

Two distinct Cu-inducible MTs have been well characterized in the human pathogen *Candida glabrata*, designated as MT-1 and MT-2.[130] MT-1 appears to consist on only one member, while two subisoforms have been isolated for MT-2.[131]

MT-1 has 62 amino acid residues, 18 of which are cysteines, while MT-2 has 51 amino acid residues with 16 cysteines. Unusual aromatic residues, tyrosine and histidine, are also found in the sequence of both MTs. In the case of MT-1, the sequence Cys-X-Cys-Pro-Asn and the sequence Cys-Gly-Asp-Lys-Cys-Glu-Cys-Lys are found twice, suggesting that the protein has been formed by evolution consisting in gene duplication. The same phenomenon is observed for MT-2, but with a different sequence Gln-Thr-Cys-Lys-Cys. Their sequence similarity is limited and for this reason MT-1 has been classified in family 9 while MT-2 in family 10 (see section 5).

The expression of MT-1 and MT-2 is regulated by Cu(I) and Ag(I), but not by divalent metal ions like Zn(II) or Cd(II). The metal-binding properties of both MTs have not yet been examined in detail. The only studies performed have been based on luminescence and UV absorption, determining a stoichiometry of 11-12 Cu(I) ions for MT-1 and 10 Cu(I) ions for MT-2.[131][132]

5.1.3 *Yarrowia lipolytica* MTs

Yarrowia lipolytica is a dimorphic heterothallic fungus belonging to the phylum *Ascomycota*. The genome of this fungus encodes four high similar MTs (MTP1, MTP2, MTP3 and MTP4) which are all classified in the family 11 in Binz and Kägi division. MTP1 and MTP3 are formed by 55 amino acid residues, of which 9 are cysteines, while MTP2 and MTP4 have 54 amino acid residues with also 9 cysteines in their sequence. These 9 cysteine residues are perfectly aligned between all four MTs, and they are located in the second half of the protein sequence with a characteristic triplet (-CCC-) and the fragment CXCXXCXCXXCXC at C-terminus (Figure 11). The expression of the *MTPs* genes is copper-dependent.[133]

```
MTP1 MEFTTAMFGTSLIFTT-STQSKHNLVNNCCCSSSTSESSMPASCACTKCGCKTCKC 55
MTP3 MEFTTAMLGASLISTT-STQSKHNLVNNCCCSSSTSESSMPASCACTKCGCKTCKC 55
MTP2 MEFTSALFGASLVQSKHKTTKKHNLVDSCCCSKPTEK--PTNSCTCSKCACDSCKC 54
MTP4 MEFLNANFGASLIQSKHKTTKKHNLVNSCCCSKPAEK--PTNSCTCSKCACDSCKC 54
```

Figure 11. Alignment between *Yarrowia lipolytica* MTs.

5.1.4 *Schizosaccharomyces pombe* MT

Schizosaccharomyces pombe is a type of yeast belonging to the phylum *Ascomycota*. Various studies show the presence of a gene that codifies a specific MT in this organism, called Zym1. This protein is composed by 50 amino acid residues, 12 of which are cysteines. The synthesis of this MT is induced principally by Zn(II), and, to a lesser extent, by Cd(II) and oxidative environments (like H_2O_2), when the concentration of Zn(II) is low. For this reason, Zym1 is known to confer clear Zn-tolerance to cells. However, a decreasing in its synthesis results in only a small decrease in tolerance to zinc. This fact suggests the presence of alternative mechanisms in the organism, being these undefined processes the principal detoxifying agents and leading the main role of Zym1 as unknown until now.[134]

5.2 Non-Yeast MTs widely characterized

5.2.1 *Neurospora crassa* MT

From the ascomycete *Neurospora crassa,* a MT with 25 amino acid residues was isolated, which is considered one of the traditional archetypical fungi MTs. This MT, belonging to the family 8 of Binz and Kägi classification, has a sequence very similar to the N-terminal domain (so called β-domain) of mammalian MTs. It has a total of 7 cysteines, which can be perfectly aligned with the mammalian ones.[135]

The gene which synthesize *Neurospora crassa* MT (NcMT) is only induced by copper, not by divalent ions like Cd(II), Zn(II), Co(II), or Ni(II).[136] Various studies about this MT were performed with circular dichroism (CD), electronic absorption spectroscopy (AES) and electron paramagnetic resonance (EPR), concluding that it is able to bind up to 6 Cu(I) ions forming a $Cu(I)_6S_7$ cluster.[137]

Later, the *in vitro* features of NcMT were tested by titration of the protein with different metal ions and the subsequent analysis by electronic absorption spectroscopy and EPR. The results obtained confirm that Zn(II), Cd(II), Co(II), and Hg(II) can also be bonded by the protein.[138] When Zn(II) was introduced in the culture media, a cluster with 3 metal ions, Zn_3-NcMT, was formed. Different results were observed between the titration with Cu(I) of this cluster Zn_3-NcMT and the apo-NcMT form. In the first case a Cu_6-NcMT specie were obtained after the addition of Cu(I), while in the second case the result of the titrations produced a Cu_4-NcMT specie.[102][73]

After all these studies, various attempts to determine the structure of the cluster Cu_6-NcMT were conducted. However, the signal problems of Cu(I) in NMR techniques and the mixture of species

obtained when Cu(I) was substituted by Ag(I) made difficult to accomplish this objective. Despite this fact, polypeptide fold of the protein was determined by ^{1}H-NMR proton-proton interactions by showing also the cysteine side chains. With the ribbon diagram, the possible positions of the 6 Cu(I) ions were modelled (Figure 12).[73][139]

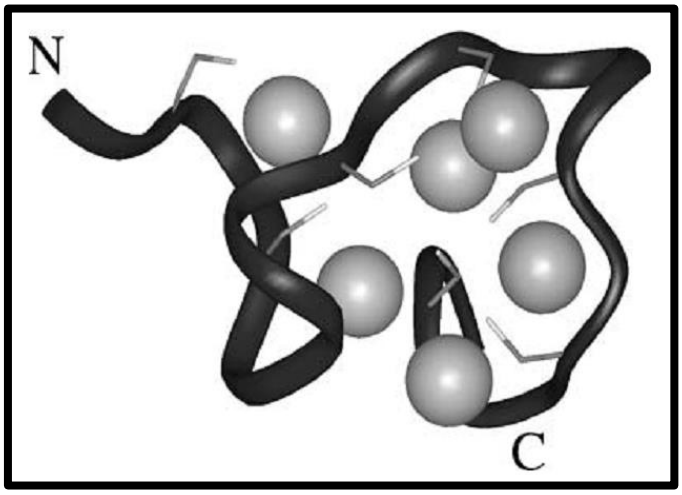

Figure 12. Backbone fold of NcMT solved by NMR with the hypothetical positions of the 6 Cu(I) ions.[139][73]

But Cu(I) is known can adopt variable coordination numbers by binding in linear or trigonal environments. Consequently, the hypothesis of this cluster structure cannot be totally confirmed with the studies performed.

5.2.2 *Agaricus bisporus* MT

Agaricus bisporus is a mushroom which contains only one metallothionein. Together with NcMT, MT from *Agaricus bisporus* (AbMT) is considered the other traditional, archetypical fungal MT. Both sequences are highly similar (Figure 13), even though *N. crassa* belongs to the *Ascomycota* phylum and *A. bisporus* to the *Basidiomycota*. They share an 80% of similarity in their sequence, and AbMT also has 7 cysteines which are exactly in the same position than the NcMT ones.

```
MGDCGCSGASSCNCGSG-CSCSNCGSK   N.crassa
MGDCGCSGASSCTCASGQCTCSGCG-K   A.bisporus
```

Figure 13. Alignment between NcMT and AbMT.

AbMT consists on a 25 amino acid protein that binds copper in the organism. The calculated total amount of this metal in the protein by Atomic Absorption Spectroscopy is 5,8 Cu(I) per molecule,

almost coinciding with the 6 Cu(I) determined for NcMT. In addition, synthesis of AbMT is also induced only by copper, not by Zn(II) or Cd(II).[140]

5.3 Other reported fungal MTs

Although the vast majority of fungal MTs are Cu-thioneins, there is a small group of them induced by other metals. For example *Hebeloma mesophaem*, which has three MT isoforms, HmMT1, HmMT2, and HmMT3. HmMT1 binds specifically Zn(II) and Cd(II) whereas HmMT2 and HmMT3 bind Ag(I).[141] In the case of *Hebeloma cylindrosporum*, the HcMT1 isoform is induced by Cu(I) while HcMT2 is induced by both, Cu(I) and Cd(II), conferring to cells tolerance to both metals.[142] The same situation is also repeated for *Paxillus involutus* and *Gigaspora margarita*, whose MT genes (*Pimt1* and *Gmarmt1*) are induced by Cu(I) and Cd(II) conferring also cellular tolerance against both metal ions.[143][144]

On the other hand, the two MTs from the fungus *Russula atropurpurea* bind specifically Zn(II) ions accumulated in the cytoplasm,[145] and the three MTs from *Amanita strobiliformis* sequester Ag(I) in macro fungal fruit bodies and mycelia, hyperaccumulating this metal.[146]

Another typical fungal MT studied is the *Glomus intraradices* MT. Its gene is induced by copper, and the presence of this MT confers Cu-tolerance to cell.[147] The MT from the parasite arthropod *Beauveria bassiana* (BbMT) or the two MT genes from the plant pathogenic fungus *Colletotrichum gloesporioides* (*Cap3* and *Cap5*) are all induced by Cu(I) and Cd(II), showing their potential function in heavy metal resistance.[146][148] Moreover, the MT from the aquatic fungi *Heliscus lugdensus* is Cd-induced, being the Cd detoxification its primarily function.[149]

Other fungal MTs have been found in *Uromyces fabae*, *Phaeosphaeria nodorum,* or *Laccaria bicolor*, but they have not been fully characterized so far. Table 8 shows a list of all fungal MTs studied until today.

Fungus and MT name	Phylum	Length (aa)	Cys number	Pathogen	Induced by	Report
***H. lugdunensis* MT**	*Ascomycota*	24	8	No	Cd	Jaeckel, P. (2005)[150]
***U. fabae* MT**	*Basidiomycota*	24	6	Yes	?	Hahn, M. (1997)[151]
***P. nodorum* MT**	*Ascomycota*	25	7	Yes	?	Hane, J.K. (2007)[152]
***C. gloesporioides* Cap3**	*Ascomycota*	26	7	Yes	Cu, Cd	Hwang, C.S. (1995)[153]
***C. gloesporioides* Cap5**	*Ascomycota*	27	8	Yes	Cu, Cd	Hwang, C.S. (1995) [153]
***P. anserina* PaMT1**	*Ascomycota*	26	7	No	Cu	Averbeck, NB. (2001)[154]
***C. albicans* CUP1**	*Ascomycota*	33	6	Yes	Cu	Weissman, Z. (2000)[155]
***C. albicans* CRD2**	*Ascomycota*	76	12	Yes	Basal levels	Riggle, P.J. (2000)[156]
***A. strobiliformis* MT1a**	*Basidiomycota*	34	6	No	Ag	Osobova, M. (2011)[146]
***A. strobiliformis* MT1b**	*Basidiomycota*	34	7	No	Ag	Osobova, M. (2011) [146]
***A. strobiliformis* MT1c**	*Basidiomycota*	34	6	No	Ag	Osobova, M. (2011) [146]
***H. mesophaeum* HmMT1**	*Basidiomycota*	59	13	No	Zn, Cd	Sacky, J. (2014)[141]
***H. mesophaeum* HmMT2**	*Basidiomycota*	58	13	No	Ag	Sacky, J. (2014) [141]
***H. mesophaeum* HmMT3**	*Basidiomycota*	52	13	No	Ag	Sacky, J. (2014) [141]
***H. cylindrosporum* HcMT1**	*Basidiomycota*	59	13	No	Cu	Bellion, M. (2007)[143]
***H. cylindrosporum* HcMT2**	*Basidiomycota*	57	13	No	Cu, Cd	Bellion, M. (2007) [143]
***G. margarita* GmarMT1**	*Glomeromycota*	65	13	No	Cu, Cd	Lafranco, L. (2002)[144]
***S. pombe* Zym1**	*Ascomycota*	50	12	No	Zn	Borrelly, GPM. (2002)[134]
***G. intraradices* ntMT**	*Glomeromycota*	71	12	No	Cu	González-Guerrero, M. (2005)[147]
***B. bassiana* MT**	*Ascomycota*	?	?	Yes	Cu, Cd	Kameo, S. (2002)[148]
***P. tinctoricus* MT**	*Basidiomycota*	35	7	No	?	Voiblet, C. (2001)[157]
***P. involutus* PiMT1**	*Basidiomycota*	34	7	No	Cu, Cd	Courbot, M. (2004)[158]
***L. edodes* MT**	*Basidiomycota*	34	7	No	?	Kwan, HS. (2002)[159]
***R. atropurpurea* RaZBP1**	*Basidiomycota*	53	6	No	Zn	Sacky, J. (2016)[160]
***R. atropurpurea* RaZBP2**	*Basidiomycota*	53	6	No	Zn	Sacky, J. (2016) [160]
***L. bicolor* MT1**	*Basidiomycota*	37	8	No	Cd	Reddy, MS. (2014)[161]
***L. bicolor* MT2**	*Basidiomycota*	58	14	No	Cu, Cd	Reddy, MS. (2014) [161]

Table 8. Summary of other fungal MTs described in the literature

5.4 Pathogenic fungi MTs

Among all fungal MTs, probably pathogenic fungi are one of the most interesting. They are becoming an important field of study due to their relation in crop care and human diseases, so, huge progress in their knowledge allows the development of new biotechnological and biomedical tools.

Magnaporthe grisea is a pathogenic fungus widely studied, responsible of rice blast fungus disease[162], while *Cryptococcus neoformans* is the pathogenic fungus responsible of human cryptococcosis.[163]

The MT found in the fungus *Magnaporthe* grisea is known as MMT1, which has 22 amino acid residues and 6 cysteines, being the smallest MT reported until today. MMT1 exhibits a high preference for zinc, resulting in a great ability to play an antioxidant role by releasing these metal ions when ROS are in the media. Although its synthesis is not induced by any metal ion, there are some environmental stresses which produce the *MT* gene expression. Two possible roles have been proposed for MMT1. First, it can act as antioxidant to confront plant defence mechanism that involves a rapid oxidative burst, localized in the infection points. Second, MMT1 may be required for cell wall differentiation in the appressorium, being necessary in the developmental biology of plant pathogenic fungi.[162]

In *C. neoformans* two unusually long MTs were found, CnMT1 and CnMT2. CnMT1 is a 122 amino acid protein, with 25 cysteines, whereas CnMT2 comprises 183 amino acid residues with 37 cysteines. These particularly long MTs seem to be formed by Cys-regions separated by portions without cysteines called spacers. The cysteine pattern in the Cys-segments is highly similar to the NcMT sequence, indicating a probable evolutionary common origin from the same ancestor.[164][165] CnMT1 and CnMT2 exhibit an extraordinary high capacity to bind copper, not observed previously. CnMT1 is able to bind up to 16 Cu(I) ions per molecule whereas CnMT2 binds up to 24 Cu(I) ions, producing homometallic species. Both CnMTs bind Cu(I) through the cooperative construction of Cu_5-clusters, which suggests that each Cys-fragment can bind 5 Cu(I) ions forming a characteristic cluster. Besides Cu(I), additional experiments with other metals were performed resulting in other metal-CnMTs complexes. The recombinant synthesis in Zn(II) and Cd(II) metal enriched media produces Zn-CnMTs and Cd-CnMTs complexes, but with poor yield and stability.

During *C. neoformans* infection, one of the mechanisms used by innate immune cells to create an adverse environment to fight against the invaders is to hyperaccumulate copper inside the phagosome through macrophages.[166] Meanwhile, a metalloregulatory transcription factor activates

the transcription of CnMTs under copper excess conditions, to chelate these metal ions. *Ding et al.*[164] conducted *in vitro* mice experiments to confirm the idea of the requirement of CnMTs for virulence and infection.

5.5 New division of fungal MTs

Following the strategy of studying and comparing the sequences of all known fungal MTs, a new division, different from Binz and Kagi's fungal classification, has been proposed on the last years.[167] This new division is based on the length and different Cys motifs of fungal MTs, providing four different subfamilies. Subfamily 1 (Figure 14) comprises the shortest fungal MTs, which contain between 6 to 8 cysteines arranged principally in three different Cys patterns. *N. crassa* MT and homologous fungal MTs are placed in this group. Subfamily 2 (Figure 15) is for medium-length MTs, which contain 9 cysteines and only 2 Cys patterns. Only human opportunistic fungal MTs represent this group so far. Subfamily 3 (Figure 16) comprises yeast, moulds and dimorphic fungi MTs, with sequences similar to *C. albicans* CRD2, containing from 12 to 20 cysteines arranged in different Cys patterns. Finally, Subfamily 4 (Figure 17) is constituted by the extremely long fungal MTs, with more than 22 cysteines and modular structure. *C. neoformans* MTs and *T. mesenterica* are classified in this group.

This innovative classification may allow us to hypothesize the functional features and the different roles in metal metabolism and infectivity processes of the different MTs. For this reason, the classification of new fungal MTs discovered inside of these subfamilies, with the subsequent study of their coordination abilities, allow making progress in the unknown functions of MTs. A classification of already known fungal MTs and new discovered MTs is presented hereafter (Figure 14 to 17).

```
U.fabae_MT                ------------MNP--CSSN--CSCGAS---CTCSGCSSHKK 24
C.gloeosporioides_Cap3    ------------MSGCGCASTGTCHCGKD---CTCAGCPHK-- 26
A.bisporus_MT             -------------GDCGCSGASSCTCASGQ--CTCSGCGK--- 25
N.crassa_MT               ------------MGDCGCSGASSCNCGSG---CSCSNCGSK-- 26
F.oxysporum_MT            -----------MAGDCGCSGASSCNCGSS---CSCSGCGK--- 26
M.perniciosa_MT1       MIATEFTVVNAHCGSSTCNCGEN--CACKPGE--CKC-------- 33
H.lugdunensis_MT          -------------SPCTCST---CNCAGACNSCSCTSCSH--- 24
P.nodorum_MT              ------------MSPCNCQT---CSCSGDCSGCSCSSCSH--- 25
C.gloeosporioides_Cap5    ------------MAPCSCKS-CGTSCAGSCTSCSCGSCSH--- 27
B.dermatitidis_MT1        ------------MSPCNCN-----CCAGDCNSCSCTSCSVP-- 24
U.reesi_MT                ------------MSPCSCN-----CCSGNCNSCSCSNCSH--- 23
A.nidulans_MT             ------------MSPCTCN-----CCSGECNSCSCSSCKH--- 23
A.oryzae/flavus_MT        ------------MSPCSCN-----CCSGNCNSCSCSDCKH--- 23
A.niger_MT                ------------MAPCECK-----CCSGSCNSCSCSNCKH--- 23
C.posadasii_MT1           ------------MNPCSCN-----CCSGNCNNCSCGSCGH--- 23
```

Figure 14. Subfamily 1: short MTs (6-8 Cys).This subfamily is characterized by contain -CXC-, -CC- and -CXCXXC- patterns.

```
P.brasiliensis_MT          MGCGCGS-ECSCSGPQNCVCGTSGGGSTCHCTSCTVS 36
C.posadasii/immitis_MT2    MGCGCGTGSCSCNGPQNCSCPS--D--TCHCTTCGK- 32
H.capsulatum_MT            MACGCGNNSCPCDGPQSCTCSS-GGGSSCGCTTCK-- 34
B.dermatitidis_MT2         MGCGCGDDKCPCEGPKTCSCSS-SG--TCGCTTCGK- 33
```

Figure 15. Subfamily 2: medium MTs (9 Cys). This subfamily exhibits only the -CXC- and -CXCXXC- patterns.

```
S.cerevisiae_CUP1   MFSELINFQNEGHECQCQCGSCKNNEQCQKSCSCPTG----CNSDDK-----------
C.albicans_CRD2     -----------MACSAAQ---CVCAQKST-CSCGKQPALKCNCSKASVENVVPSSNDA
S.brasiliensis_MT   ---------MVSSTCCGKGGAECVCAQNAT-CSCGKQSALHCNCDRAATENNTAGDR--
S.apiospermum_MT    --------MSPADTCCRKGEGACVCAQQAT-CSCGKQSALHCTCDKAAVENTISGPS--
N.crassa_MT2        ----MSAPVAKASTCCGKSAE-CICAKQAT-CSCGKQSALHCTCDKANSENAVEGPR--
C.glabrata_MT2      --------MPEQVNCQYD----CHCSN----CACENT----CNCCAKPA----------
Y.lypolitica_MT5    -----------MACSTN----CSCPKPCTNCACEKA----CTCSP-------------


S.cerevisiae_CUP1   CPCGNKSEETKKSCCSGK-----------------------------------------
C.albicans_CRD2     CACGKRNKSS---CTCGANAICDGTDGETDFTNLK-----------------------
S.brasiliensis_MT   CSCGQRPAGA---CTCATNPSEVNTANETDFTTRK-----------------------
S.apiospermum_MT    CSCGSRPVGQ---CTCENATVENQKPTGATCGCGARPAGSCTCNNSANETDFTTKK---
N.crassa_MT2        CSCRARPAGQ---CTCDRASTENQKPTGNACACGTRPADACTCEKAADGGFKPTDLETD
C.glabrata_MT2      CACTNSASNE---CSCQT-----------CKCQT-----CKC----------------
Y.lypolitica_MT5    CSCES--------CKCAKA-----------CECEKSTT—CKCESCKCEGSCKC------


S.cerevisiae_CUP1   ----------------------------------------------------------  61
C.albicans_CRD2     ----------------------------------------------------------  76
S.brasiliensis_MT   ----------------------------------------------------------  79
S.apiospermum_MT    ---------------------------------------------------------- 101
N.crassa_MT2        FTTKN------------------------------------------------------ 112
C.glabrata_MT2      ----------------------------------------------------------  52
Y.lypolitica_MT5    ----------------------------------------------------------  59
```

Figure 16. Subfamily 3: long MTs (12-20 Cys). Different Cys patterns: -CXC-, -CC-, -CXCXXC-, -CX$_{2\text{-}4}$CXC-.

```
T.mesenterica_MT    MSAPVETKEKSCGCQPAPAVQSCNCSNEGN--CTCAPGKCACSSCSSDSIKKTGK-CGG
C.neoformans_MT1    ---------MACNCPPQKNTA-CCSTSEAQDKCTCQKGNCECKACPNSTKTSESGGKAS
C.neoformans_MT2    ---------MAFNPNPEKTTS-CCSTSKAQDKCTCPKGKCECETCPKSTKTPGSGPCNC


T.mesenterica_MT    SEG--------------CTCEAGKCDCASCPGSSGQVKACTCGTS---CSCPPGECTCA
C.neoformans_MT1    T-------CNCGGSGEACTCPPGQCACDKCPKKAKSVSTCGCGGSGAACSCPPGKCACD
C.neoformans_MT2    GVKEKVSTCGCNGSGAACTCPPGQCACDSCPRKAKSVSTCGCGGSAAACSCPPGKCACD


T.mesenterica_MT    GCPNNKGKEKAKDEKAGECSCGPS---CSCPPGECSCAGCSNVKSTGKEKAPAKACECG
C.neoformans_MT1    NCPKQAQEKVSS------CACSGSGAA
C.neoformans_MT2    SCPKQAQEKVSS------CACNGSGGACTCPPGKCSCSGCPAQAKENPADQPTT-CGCQ


T.mesenterica_MT    EE---CSCPPGQCSCANCPAKEKKDACSCSEGCSCPPGQCACANCPHKDEAKGCSCGES
C.neoformans_MT1    ----------------------------------------------------------
C.neoformans_MT2    GVGVACTCPPGQCACDGCPAKAK-----------------------------------


T.mesenterica_MT    CSCPPGECKCANCPKKTEPAKACACGDECSCPPGQCGCADCPGKTS  257
C.neoformans_MT1    ------------------------------------------------  122
C.neoformans_MT2    ------------------------------------------------  183
```

Figure 17. Subfamily 4: extremely long MTs (>22 Cys). Different Cys patterns are identified: -CXC-, -CC- and -CXCXXC-.

6. ORGANISMS OF STUDY

6.1 *Neurospora crassa*

Neurospora crassa is a fungus commonly known as orange bread mold, belonging to the phylum *Ascomycota*. The first historical report of this fungus dates back to 1843, when it was reported as a contaminant of French bakeries. Later, *Neurospora crassa* became an experimental model organism, after its eventful discovery and subsequent studies performed by Bernard O. Dodge[168] and Carl C. Lindegren[169] about sexual reproduction.

Several years later, Beadle and Tatum sought an easily manipulated organism that could be grown on simple media quite rapidly, and might display additional nutrient requirements arising by mutation, when they realized *Neurospora crassa.* In their work, they defined the role of genes in metabolism by taking advantage of this fungus.[170] The success on using *N. crassa* emboldened others to use bacteria, algae, and other fungi in similar studies.

All these supposed the 1900s-mid-century revolution in genetics and biochemistry. For these reason, molecular biology is considered to be born after Beadle and Tatum work in 1958, together with the elucidation of the structure of DNA in 1953.

Since that moment, *N. crassa* has been used for the understanding of several basic and fundamental aspects in biology, a fact that produces a high interest in study all features of this fungus, including its MTs.

During the 80s, one MT was found in *N. crassa*, which was called NcMT. As mentioned in section 5.2.1, this MT was widely studied and characterized with the techniques known until then.[73][78][102][135][136][137][138] Due to its short and simple amino acid sequence, NcMT was considered as an archetypical fungal MT, resulting in a big interest in elucidating its structure and metal binding abilities. For this reason, our group proposed to upgrade the study of the features of NcMT by using modern methodologies available nowadays, as genetic engineering and new spectroscopic techniques.

NcMT has 7 cysteines (among 28 aa) in the amino acid sequence, therefore, this protein has been classified in subfamily 1 inside the new proposal of fungal MT division mentioned in section 4.5. Apart from NcMT, the group of Pr. Silvia Atrian recently discovered two new MTs by screening the entire genome of this organism, which have been called NcMT1 (114 aa, 16 Cys) and NcMT2 (77aa, 7 Cys).

NcMT1 and NcMT2 have been classified in subfamily 1 and subfamily 3, respectively, and they have been also studied and characterized.

6.2 *Fusarium verticillioides*

Fusarium is a large genus of filamentous fungi, belonging to the *Ascomycota* phylum, widely distributed in soil and associated with some plant pathologies. There are a large number of *Fusarium* species, and an important number of them are pathogenic for plants. [171] A smaller part of them also can affect humans and, occasionally, animals.[172] In humans, *Fusarium* species can cause a broad spectrum of infections, including superficial, locally invasive, or disseminated infections, with the last occurring almost exclusively in severely immunocompromised patients.[173] They also may cause allergic diseases and mycitoxicosis in humans and animals by ingestion of contaminated food.[171] Among all the species, twelve have been associated with fusariosis in humans, being the most important *Fusarium solani* (∼50% of cases), *Fusarium oxysporum* (∼20%), and *Fusarium verticillioides* (∼10%). Here it is studied in particular the specie *Fusarium verticillioides*, the most prevalent fungi on maize. In plants, it also causes the bakanae disease, whereas in humans, *F.* verticillioides can infect especially immunocompromised people.[174] As already explained in section 5.4, previous studies about another pathogenic fungus, *Cryptococcus neoformans* demonstrated the role of MTs as pathogenic and virulence factors, due to their extremely high capacity to bind copper.[164][165] For this reason, it seemed interesting to characterize other fungal MTs like *F. verticillioides* MT (FvMT), classified in subfamily 1 in the new fungal division.

6.3 *Candida albicans*

Candida albicans is a dimorphic fungus that grows both as yeast and filamentous cells. This fungus causes the infection candidiasis, being responsible of 50–90% of all cases of candidiasis in humans.[175][176] The parts of the body that are commonly infected by this fungus include the skin, genitals, throat, mouth, and blood. But the really important interest lies in systemic fungal infections produced by *C. albicans*, which have emerged as important causes of morbidity and mortality in immunocompromised patients. The fungus *C. albicans* is a common member of human gut flora and it is detectable in the gastrointestinal tract in 40% of healthy adults,[177] being the overgrowth of the fungus the responsible of candidiasis.[175][176]

In order to analyse the factors responsible of the high resistance to elevated concentrations of copper of the pathogenic fungus *C. albicans,*[155][156] a screening of the fungus genes was performed. Two different genes were found to induce the synthesis of two MTs involved in the copper detoxification role, so called CaCup1 and CaCRD2.[155][156] While CaCup1 is a short MT with only 6 cysteines (35 aa), CaCRD2 is a long MT with 12 cysteines (78 aa). In the new proposed fungal division, CaCup1 is classified in subfamily 1 while CaCRD2 in subfamily 3.

6.4 *Coccidioides posadasii*

Coccidioides posadasii is another pathogenic fungus that, together with *Coccidioides immitis*, is the causative agent of coccidiodomycosis in both animals and humans.[178] *C. posadasii* grows in the soil as infectious cells, called arthroconidia, which are dispersed into the air.[179] When arthroconidia is inhaled by a host a process of division into endospores[180] causes an inflammatory response, resulting in the respiratory disease coccidiodomycosis.[181]

The exposure to the pathogen can result in a wide variety of symptoms: asymptomatic infection; a benign pulmonary infection ("Valley fever"); or even fatal cases of pulmonary disease affecting the skin, bones, central nervous system and other organs.[182]

Two different MTs have been found in *C. posadasii*: CipMT1, which belongs to subfamily 1; and CipMT2, into subfamily 2. In the same way as explained for the other fungal pathogens, it is important to characterize *Coccidioides posadasii* MTs to shed light to their possible role in the pathogenicity of this organism.

6.5 *Uncinocarpus resii*

Uncinocarpus resii is a filamentous fungus scarcely studied. The main interest of this organism lies on its similarity with the dimorphic pathogenic fungi *Coccidioides immitis* and *Coccidioides posadasii*, that suggest phylogenetic connections between them.[183][184][185] *Uncinocarpus resii* and *Coccidioides* spp. have common habitat preferences: they can survive passage through animals and they also have similar morphological features. However, the important factor that distinguishes them is that while *Coccidioides* spp. are pathogenic fungi, *Uncinocarpus resii* is a harmless inhabitant of animals.[186]

The only MT found in *Uncinocarpus resii*, UrMT, is classified in subfamily 1 and is very similar to CipMT1, one MT isoform of *Coccidioides posadasii*. So, the behaviour of CipMT1 and URMT can be compared in order to correlate their characteristics with their roles in the pathogenicity of organisms.

6.6 *Sporothrix brasiliensis*

There are a wide variety of *Sporothrix* species, differing in their ecological niche, frequency, distribution, and virulence, which forms the so called *Sporothrix schenckii* complex.[187] Some of these fungi have the potential to survive in mammalian hosts and are able to cause damage in multiple species of animals, including humans.[188][189] The best known species of this complex are *S. schenckii*, *S. brasiliensis*, *S. globosa*, *S. mexicana*, *S. luriei*, *S. pallida* (formerly *S. albicans*), and *S. schenckii sensu stricto*.

All the above mentioned species, with the exception of *S. pallida*, have been reported to cause sporotrichosis in humans and animals.[190][191][192][193][194] Sporotrichosis affects humans and other mammals, such as cats, dogs, rats, armadillos, and horses. As the fungus is abundant in soil, wood and moss, most infections occur following minor skin trauma in people with outdoor occupations or hobbies, such as gardening, farming, hunting, or other activities involving close contact with vegetation and soil. In humans, the disease can be classified into fixed cutaneous, lymphocutaneous, disseminated cutaneous, and extracutaneous or systemic sporotrichosis.

Among all the *S.* species, *S. brasiliensis* has aroused big interest because, in a murine model, this fungus resulted the most virulent member of *Sporothrix schenckii* complex.[196]

In the same manner as in the other pathogenic fungi, the persistence and survival of the fungus may be related to the presence of MTs. For this reason, the study of the only MT found in this organism, so called SbMT, classified in subfamily 3, seems necessary to shed light on the possible role in the pathogenicity of this organism.

6.7 *Scedosporium apiospermum*

Scedosporium species are filamentous fungi, being *S. prolificans* and *S. apiospermum* the two most important species of this group. They are mainly saprophytes, but they can be also opportunistic pathogens. *Scedosporium* spp. can cause scedosporiosis, and, in particular, *S. apiospermum* is responsible of about 25% of fungi infections in pulmonary transplant patients.[196][197][198] The range of

diseases caused by these fungi is broad, ranging from transient colonization of the respiratory tract to saprophytic involvement of abnormal airways, allergic bronchopulmonary reaction, invasive localized disease, and sometimes disseminated disease. [197][199][200][201] Treatment of *Scedosporium* infections is especially challenging because of their resistance to many antifungal agents.

By following the hypothesis explained for previous pathogenic fungi, MTs are believed to be responsible of this resistance, for this reason, the MT present in *S. apiospermum* has been studied and characterized. SaMT have 16 cysteines in its 103 amino acid sequence, and has been classified in subfamily 3.

6.8 *Cryptococcus neoformans*

Cryptococcus neoformans is an encapsulated yeast and an obligate aerobe[202] that can live in both plants and animals. This organism grows as yeast and replicates by budding, it makes hyphae during mating, and eventually creates basidiospores at the end of the hyphae before producing spores.

The infection produced by *C. neoformans* is termed cryptococcosis. This infection occurs mostly in the lungs,[203] producing fungal meningitis and encephalitis. It is particularly dangerous for AIDS patients, for this reason, *C. neoformans* is sometimes referred to as an opportunistic fungus.[204]

This fungus is a facultative intracellular pathogen[205] that can use host phagocytes to spread within the body.[206][207] In human infection, *C. neoformans* is spread by inhalation of aerosolized basidiospores, and disseminate to the central nervous system.[208] In the lungs, *C. neoformans* cells are phagocytosed by alveolar macrophages.[209] Macrophages produce oxidative and nitrosative agents, creating a hostile environment, to kill invading pathogens.[210] However, some *C. neoformans* cells can survive intracellularly in macrophages.[209] One mechanism by which *C. neoformans* survives the hostile intracellular environment of the macrophage involves metallothioneins, for these reason the two MTs found in the genome of this organism has been studied.[164][165] These two MTs are CnMT1 and CnMT2 and have been classified in subfamily 4.

6.9 *Tremella mesenterica*

Tremella mesenterica is a common jelly fungus in the *Tremellaceae* family of the *Agaricomycotina*. It is typically considered as a saprophytic fungus, but it has also been reported as parasitic to other fungi. This organism is especially found on dead angiosperms, frequently attached on fallen branches, as a parasite of wood decay fungi in the genus *Peniophora*.[211] The gelatinous, orange-yellow fruit body of the fungus, which can grow up to 7.5 cm diameter, has a convoluted or lobed surface that is greasy or slimy when damp. It grows in crevices in bark, appearing during rainy weather. *T. mesenterica* aroused big interest into the medical field, due to the production of the polysaccharide glucuronoxylomannan,[212] which have been associated to a huge number of biological activities, including immunostimulatory, protecting against radiation, antidiabetic, anti-inflammatory, hypocholesterolemic, hepatoprotective, and antiallergic effects.[213][214]

In the genome of this fungus a new extremely large MT have been found. The sequence showed a Cys pattern which can be aligned with the *C. neoformans* MTs, suggesting also a modular structure. This MT, so called TmMT, is the longest MT reported so far, and has been classified in subfamily 4.

OBJECTIVES

7. OBJECTIVES

This PhD thesis has as main objective to increase the current knowledge in the metallothioneins field, concretely by studying the structure and the metal binding behaviour of different fungi MTs in order to deepen in the relation between their structure and their function.

To achieve this general objective, we have centred on accomplish the next specific objectives:

1. Identification of new pathogenic and non-pathogenic fungal MT sequences, comparing them and doing an alignment of their sequences, especially of their cysteines residues.

2. Revisit the metal binding abilities of NcMT described in the bibliography (See section 5.2.1)

3. Study the metal binding preferences of new found MTs, already classified in the new proposed division of fungal MTs (See section 5.5).

4. Description of the modular blocks forming CnMT1 in order to describe their homology with the *N. crassa* fungal MT model.

5. Study of the modular structure and metal binding abilities of TmMT.

RESULTS AND DISCUSSION

8. MTs OF SUBFAMILY 1

In this subfamily we have studied and classified six different MTs of the organisms mentioned in section 6. Even if they are composed by different numbers of amino acids, their behaviour can be compared when considering the number of cysteine residues and their relative position in the sequence (Table 9). The MTs studied are one with 6 cysteines, CaCup1; three with 7 cysteines, NcMT, FvMT and NcMT2; and two with 8 cysteines, UrMT and CipMT1. Interestingly, all of them can be perfectly aligned in their Cys residues.

ORGANISM	MT	SEQUENCE	aa	C
Candida albicans	CaCup1	----------MSKFELVNYASGCSCGA--DCKCASETECKCASKK	35	6
Neurospora crassa	NcMT	----------MGDCGCSGASSCNCGSG--CSCSNCGSK	28	7
Fusarium verticillioides	FvMT	----------MAGDCGCSGASSCNCGSS--CSCSGCGK	28	7
Neurospora crassa	NcMT2	MSDKPSTKADMSSDSGTNTGPSTGAAAASETRDKPVATKPAQTCDCGHTGSCTCTPGD-CACENCPTAIQASHHTK	77	7
Uncinocarpus resii	UrMT	----------MSPCSCN----CCSGNCNSCSCSNCSH	25	8
Coccidioides posadasii	CipMT1	----------MNPCSCN----CCSGNCNNCSCGSCGH	25	8

Table 9. Alignment of MT sequences studied from subfamily 1, with the number of amino acids (aa) and cysteines (in red). Also histidines (in green) and methionines (in blue) are marked.

8.1 CaCup1

The sequence of CaCup1 has 35 amino acids and 6 cysteines (Figure 18A). After recombinant synthesis of this protein in different metal-supplemented cultures, its purity and identity was analysed by ESI-MS (pH 2.4). The peak obtained for the apo-form was 3627 Da. This value correlates with the theoretical mass weight (MW) calculated for CaCup1, 3627.1 Da, thus confirming the identity of the amino acid sequence (Figure 18B).

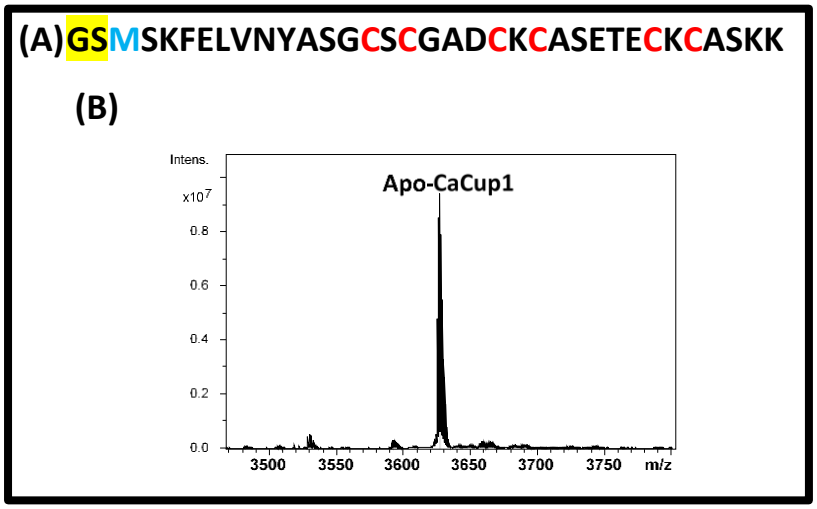

Figure 18. Amino acid sequence of the recombinant CaCup1 isoform and deconvoluted ESI-MS spectrum of the Zn-CaCup1 preparation recorded at pH 2.4, which corresponds to the apo-CaCup1.

Once confirmed the amino acid sequence and the corresponding MW, the behaviour of the protein in the presence of Zn(II), Cd(II), and Cu(II) can be analysed.

8.1.1 CaCup1 binding Zn(II)

According to the data obtained by ESI-MS (Figure 19A), when CaCup1 is synthesized in Zn(II)-enriched media a single specie corresponding to the complex Zn_2-CaCup1 is obtained, result which correlates with the 2,06 Zn(II) per MT value obtained by ICP-AES. Despite the considerable cleanness of the ESI-MS spectrum, the lack of signals after 240 nm in the CD spectrum indicates that the structuration of the protein about Zn(II) is poor. (Figure 19B).

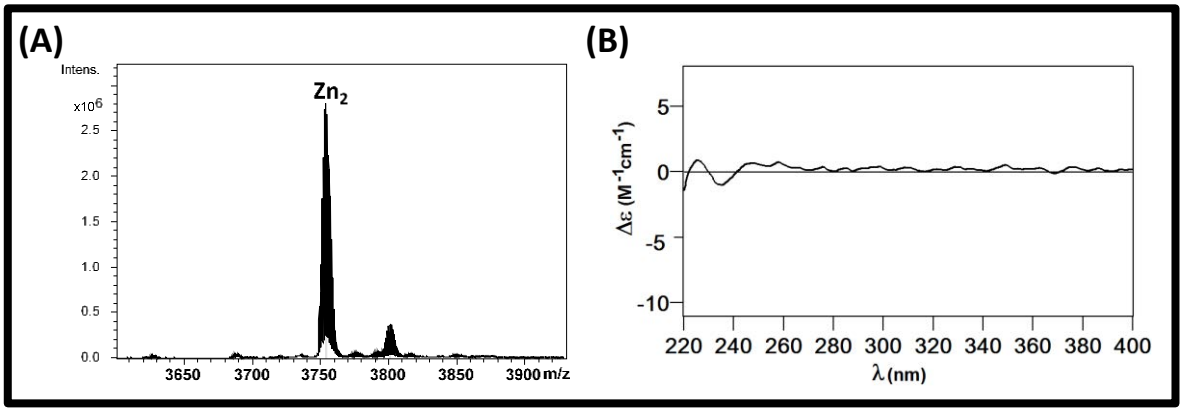

Figure 19. Deconvoluted ESI-MS spectrum of Zn-CaCup1 at pH 7.0 and CD spectrum of the Zn-CaCup1 preparation.

8.1.2 CaCup1 binding Cd(II)

In the case of the synthesis of this protein in Cd(II)-supplemented cultures, the ESI-MS spectrum shows the presence of different Cd_xS_y-CaCup1 complexes and also the specie Cd_5-CaCup1, all of them with similar intensities (Figure 20A). The presence of S^{2-} ligands was corroborated by the low Cd-to-S ratio measured by ICP-AES. On the other hand, the CD spectrum shows a Gaussian band at 250 nm, related with the Cd-Cys bond, and one exciton coupling at 290 nm, characteristic of the Cd-S^{2-} bond.

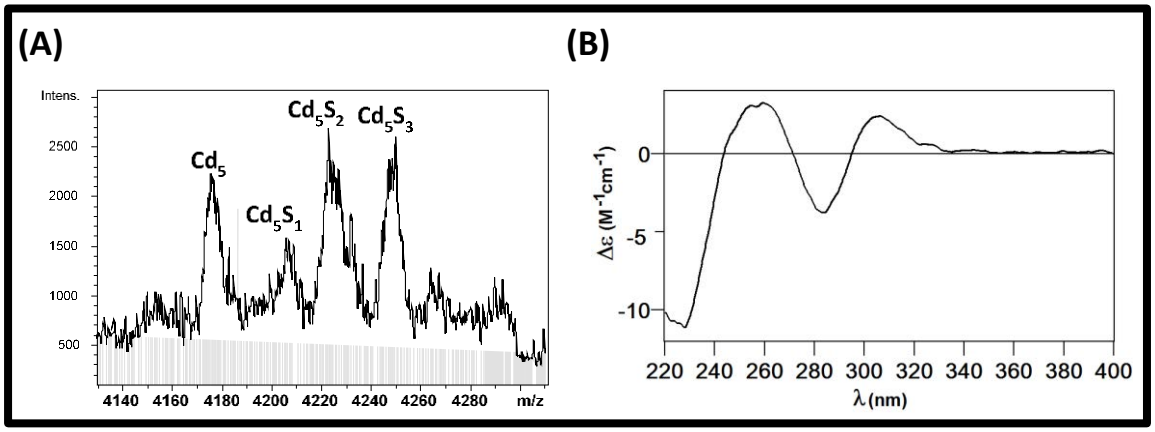

Figure 20. Deconvoluted ESI-MS and CD spectra of the Cd-CaCup1 preparation, recorded both at pH 7.0

8.1.3 CaCup1 binding Cu(I)

When CaCup1 is produced in Cu(II)-enriched media, the ESI-MS results obtained for the productions at normal and low oxygenation of the cultures are significantly different. At normal oxygenation, a mixture of different species is obtained, where the majority ones are Cu_4-CaCup1 and Cu_5-CaCup1. Besides, the apo-form is always present in the mixture, at both neutral and acidic pH, suggesting that this protein has not high preference for Cu(I) (Figure 21A and 21B). By contrast, at low oxygenation the only specie which is observed is Apo-CaCup1, at both pH values recorded, reflecting that any Cu(I) specie is formed. Due to this result, the data of this production is not shown.

In both productions, the concentration of the protein was lower than the detection limit of ICP-AES analysis, thus impairing to confirm the Cu content. Conversely, the CD analysis was possible, by showing low intensity Gaussian bands at 255, 290, and 330 nm (Figure 21C), which correlates with the presence of some Cu clusters.

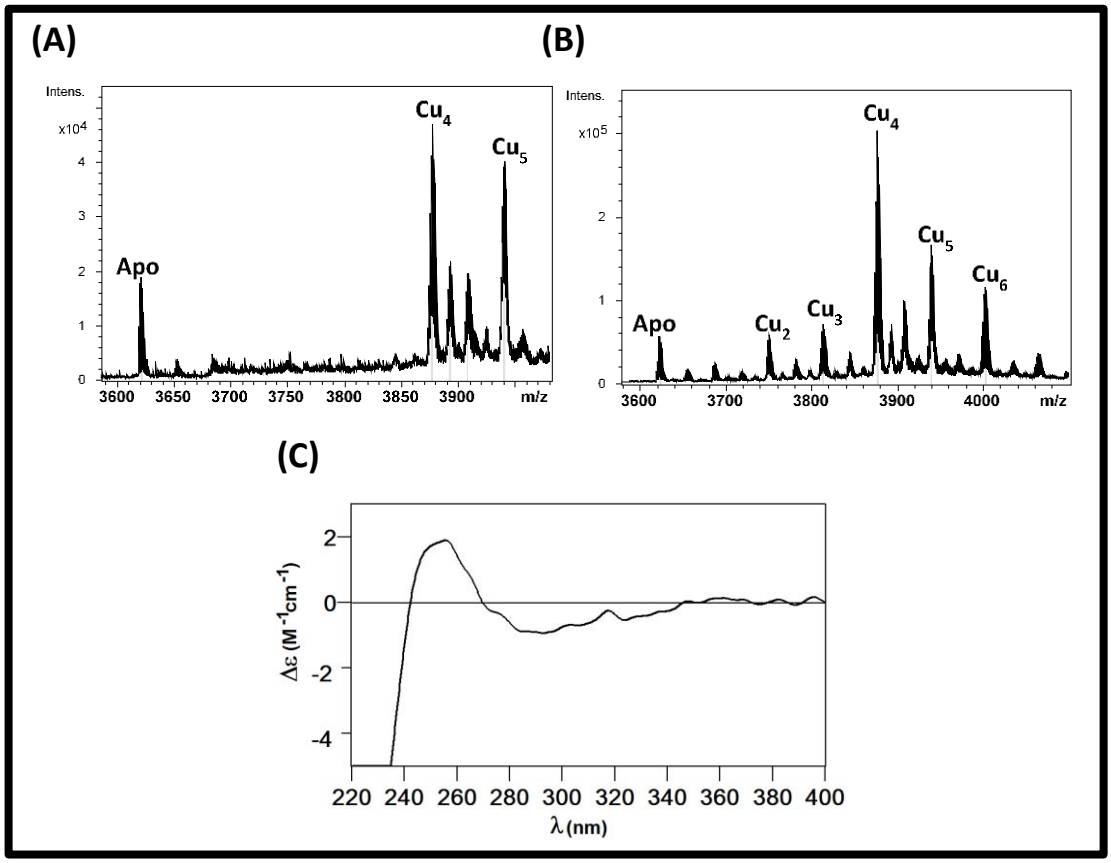

Figure 21. Deconvoluted ESI-MS spectra, recorded at pH 7.0 and 2.4, and CD spectrum of Cu-CaCup1 preparation.

The *in vitro* addition of Cu(I) to the Zn-CaCup1 preparation, followed by CD, UV-Vis and ESI-MS, allows to observe the formation of mainly Cu_4-CaCup1 with 4 Cu(I) equivalents added. According to the CD, ESI-MS and UV-Vis data, the addition of further Cu(I) to the solution do not provoke additional binding of Cu but the unfolding of the formed cluster until rendering the apo-species (Figures 22 and 23).

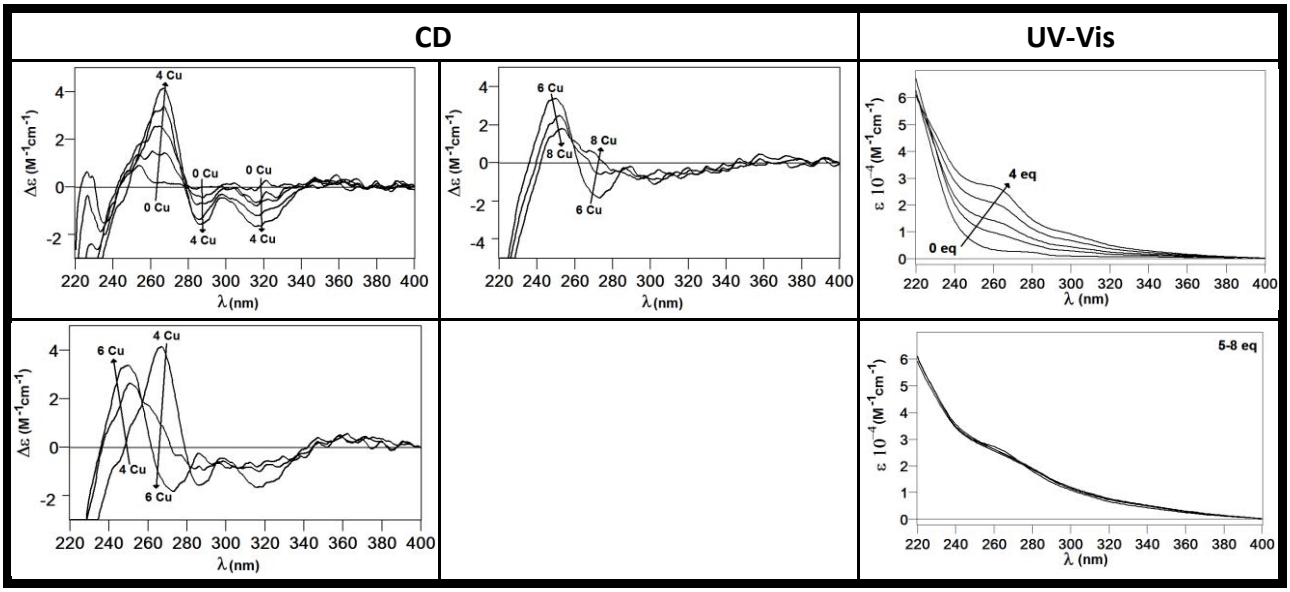

Figure 22. Titration followed by CD and UV-Vis spectroscopies corresponding to the addition of Cu(I) to a solution 20.4 µM of Zn-CaCup1 at pH 7.0 and 25ºC.

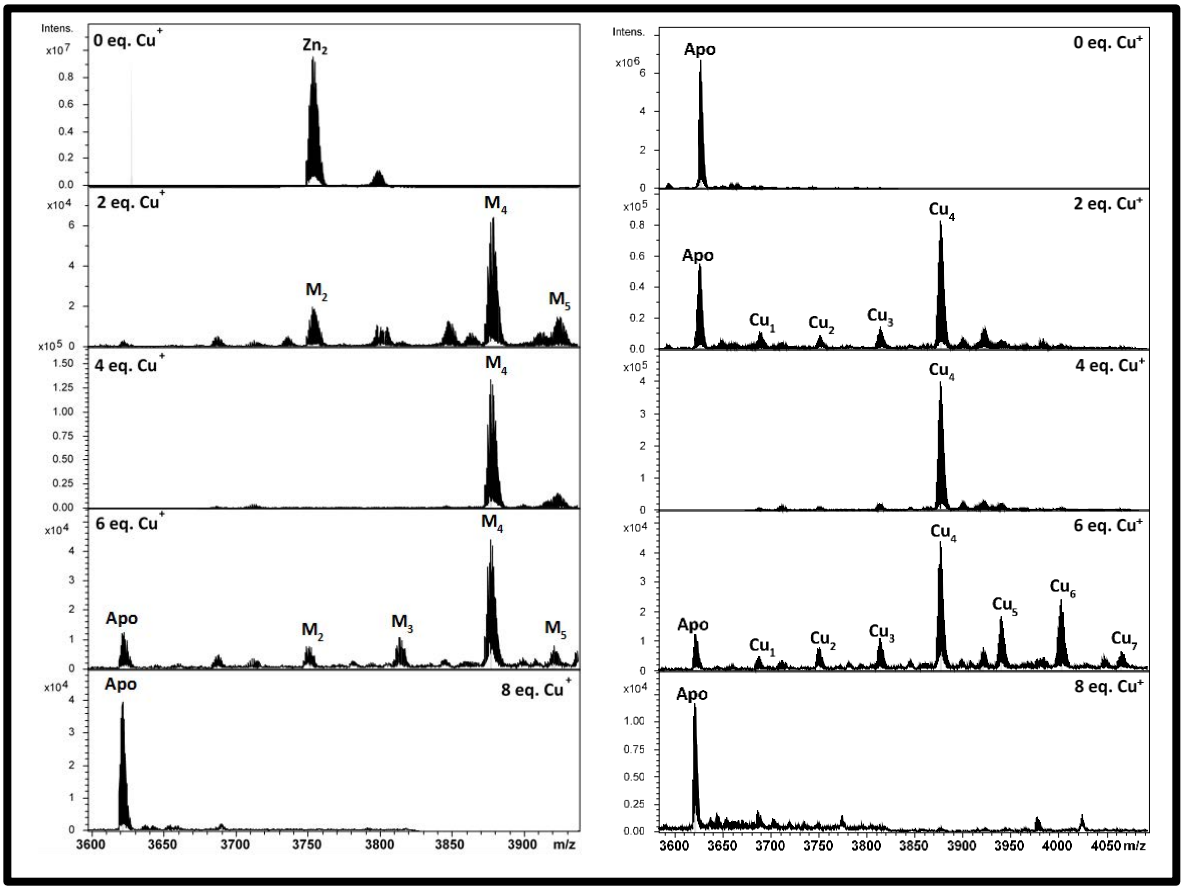

Figure 23. Titration followed by ESI-MS at pH 7.0 and 2.4, corresponding to the addition of Cu(I) to a solution 20.4 µM of Zn-CaCup1.

The results obtained *in vivo* and *in vitro* are slightly different. *In vitro* the Cu(I) is added step by step and the specie Cu_4-CaCup1 is formed properly, but with the addition of excessive Cu(I) equivalents the destabilization of the protein is produced. By contrast, *in vivo*, the excess of copper is present from the beginning of the formation process. This creates a not so stable protein preparation where the apo-form is present together with a mixture of different Cu-species. Therefore, the CD and ESI-MS *in vitro* spectra able to be compared with the *in vivo* spectra correspond to a stage of the titration where the destabilization of the protein is being produced (Figure 24).

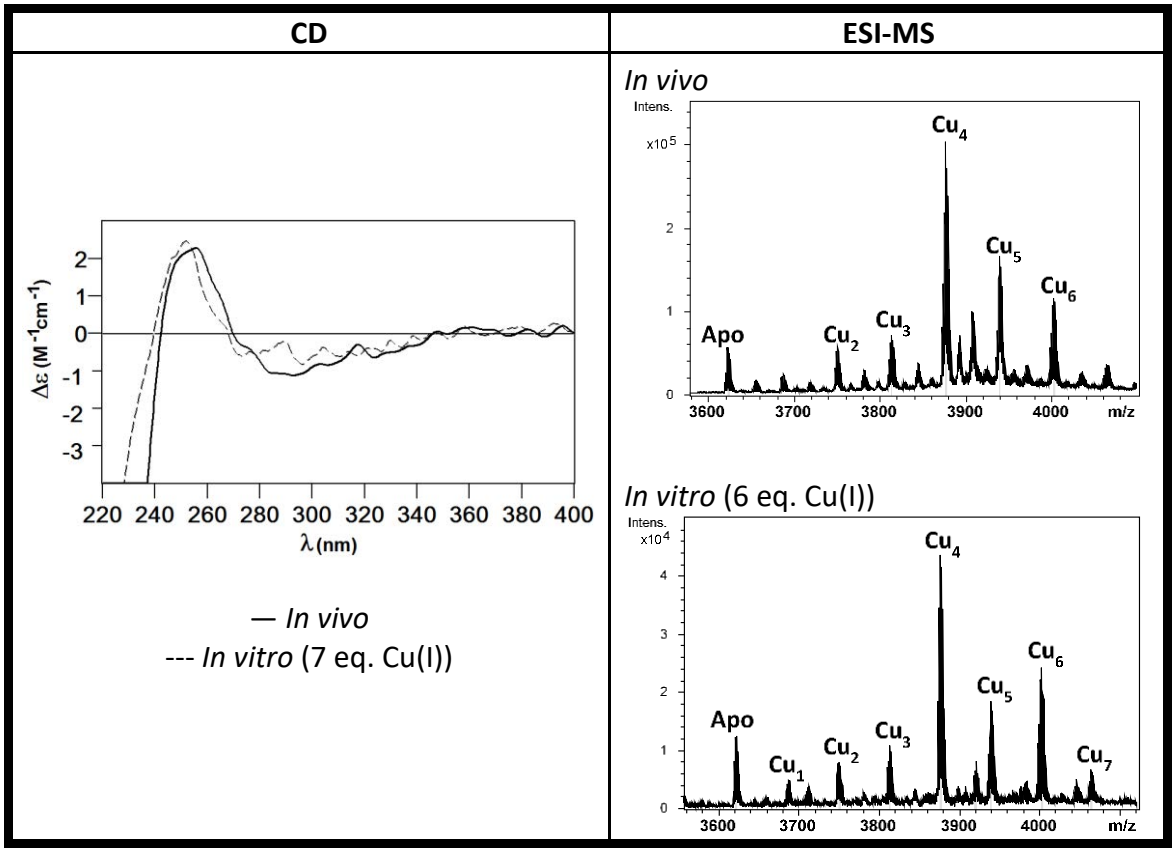

Figure 24. Superposition and comparison of DC and ESI-MS spectra of Cu-CaCup1 preparation *in vivo* and *in vitro*

8.2 NcMT

The sequence of NcMT has 25 amino acids and 7 cysteines (Figure 25A). The protein was synthesized recombinantly in Zn-, Cd- and Cu-metal-supplemented cultures, and after, its purity and identity was analysed by ESI-MS (pH 2.4). The resultant peak obtained for the apo-form was 2509 Da, value which correlates with the theoretical MW calculated for NcMT, 2509.7 Da, thus confirming the amino acid sequence (Figure 25B).

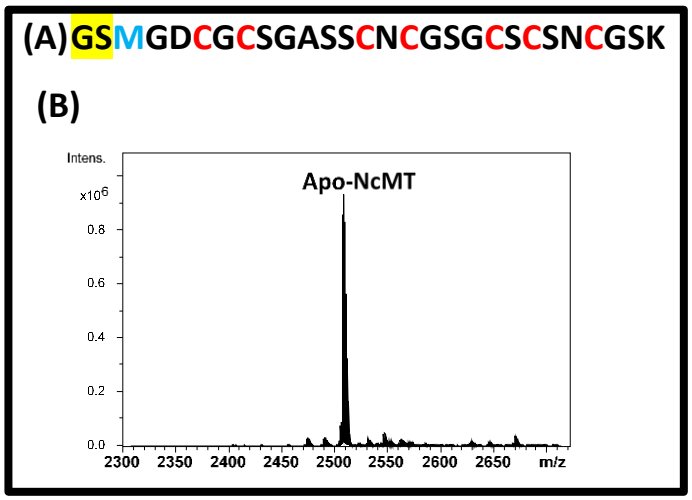

Figure 25. Amino acid sequence of the recombinant NcMT isoform and deconvoluted ESI-MS spectrum of the Zn-NcMT preparation recorded at pH 2.4, which corresponds to the apo-NcMT.

Once confirmed the amino acid sequence and the corresponding MW, the behaviour of the protein in the presence of Zn(II), Cd(II), and Cu(II) can be evaluated.

8.2.1 NcMT binding Zn(II)

According to the data obtained by ESI-MS (Figure 26A), when NcMT is synthesized in Zn(II)-enriched media, the complex Zn_2-NcMT is produced as a majority specie. This result is corroborated by the value 2.05 Zn(II) per MT obtained in ICP-AES analysis. On the other hand, the CD analysis indicates that the structuration of the protein about Zn(II) is poor, because of the lack of signals after 240 nm (Figure 27B).

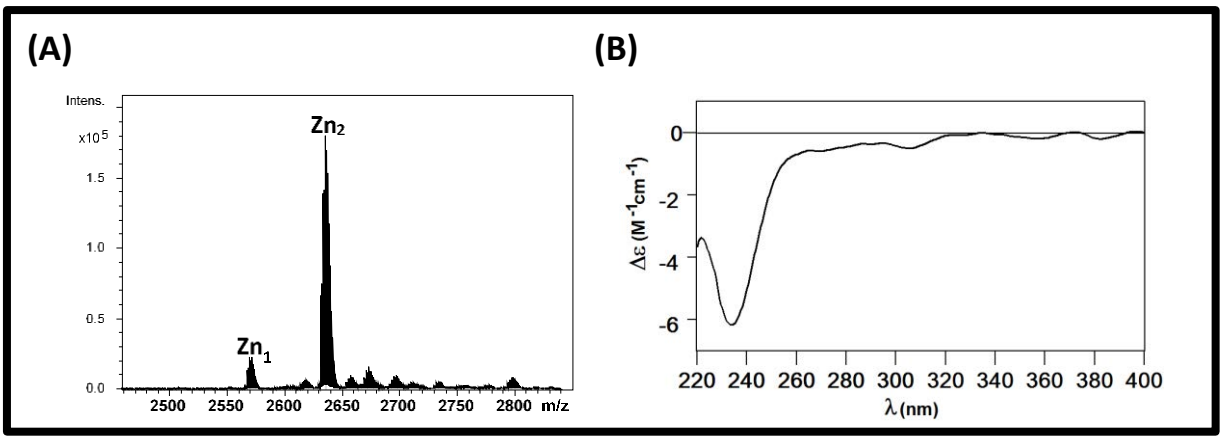

Figure 26. Deconvoluted ESI-MS spectrum of Zn-NcMT at pH 7.0 and CD spectrum of the Zn-NcMT preparation.

8.2.2 NcMT binding Cd(II)

When NcMT is synthesized in Cd(II)-enriched media the results are not satisfactory. By CD, ESI-MS or ICP-AES techniques any protein concentration is detected.

However, the Cd(II) *in vitro* binding of the protein has been tested, by adding Cd(II) to a Zn-NcMT preparation and following the titration by CD, UV and ESI-MS. With the first equivalents of Cd(II), heterometallic species Zn_xCd_x-NcMT are formed suggesting a step by step exchange of the metals. After the addition of 2 equivalents of Cd(II), the Cd_3-NcMT complex is formed as majority specie, being stable during all the titration (Figure 27 and 28).

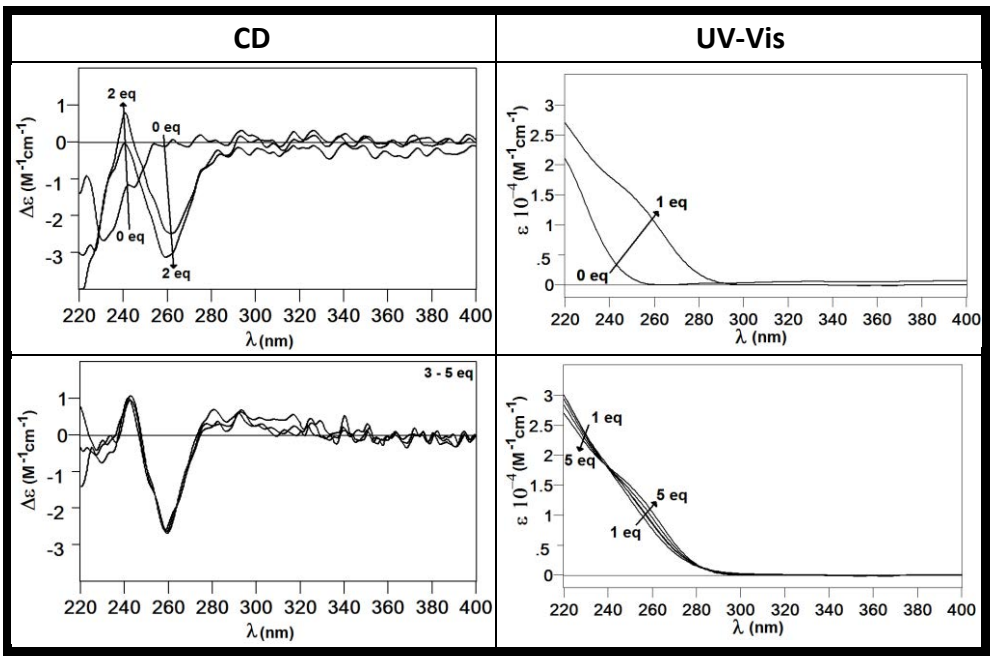

Figure 27. Titration followed by CD and UV-Vis spectroscopies corresponding to the addition of Cd(II) to a solution 15.6 µM of Zn-NcMT at pH 7.0 and 25ºC.

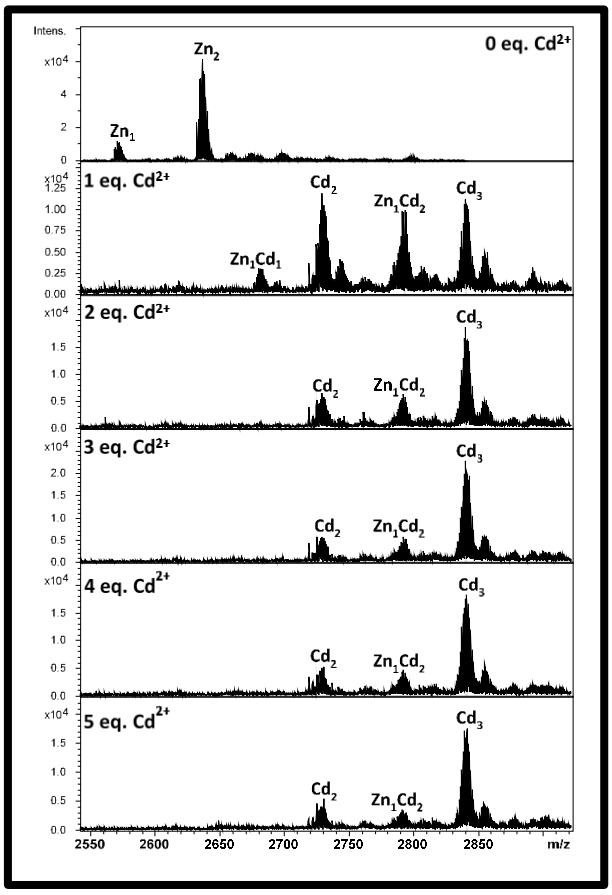

Figure 28. Titration followed by ESI-MS at pH 7.0, corresponding to the addition of Cd(II) to a solution 15.6 µM of Zn-NcMT.

8.2.3 NcMT binding Cu(I)

When NcMT is synthesized in Cu(II)-enriched media, a unique well folded complex Cu_5-NcMT is formed in both cases, normal and low oxygenation, according to ESI-MS results (Figure 29A). ICP-AES analysis reinforces these results giving a value of 5.77 Cu(I) per MT. The proper folding of this complex is confirmed by the CD spectrum (Figure 29B), which shows intense and characteristic bands of Cu-species at 235, 265 and 300 nm.

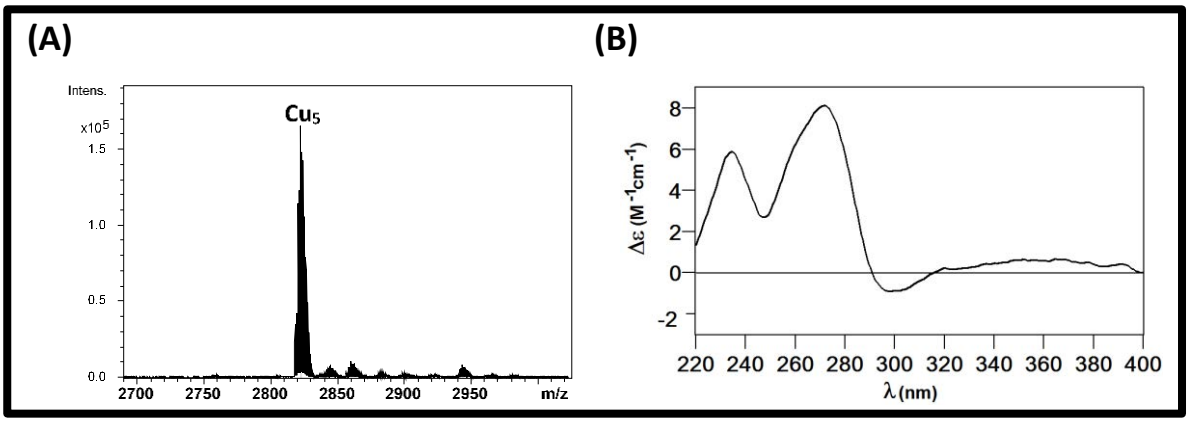

Figure 29. Deconvoluted ESI-MS spectra, recorded at pH 7.0, and CD spectrum of Cu-NcMT preparation.

The *in vitro* addition of Cu(I) to a Zn-NcMT preparation, followed by CD, UV-Vis and ESI-MS, allows also observing the formation of Cu_5-NcMT as majority specie, when 3-4 Cu(I) equivalents are added. According to the CD, ESI-MS and UV-Vis data, the addition of further Cu(I) to the solution do not provoke additional binding of Cu but the unfolding of the formed cluster until rendering the apo-species (Figures 30 and 31).

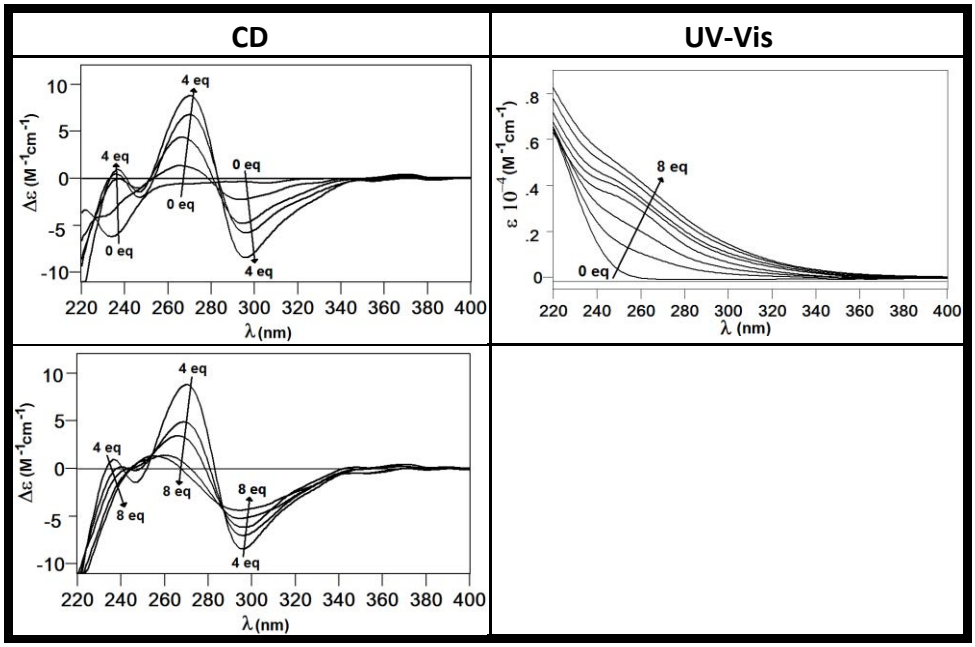

Figure 30. Titration followed by CD and UV-Vis spectroscopies corresponding to the addition of Cu(I) to a solution 15.6 µM of Zn-NcMT at pH 7.0 and 25ºC.

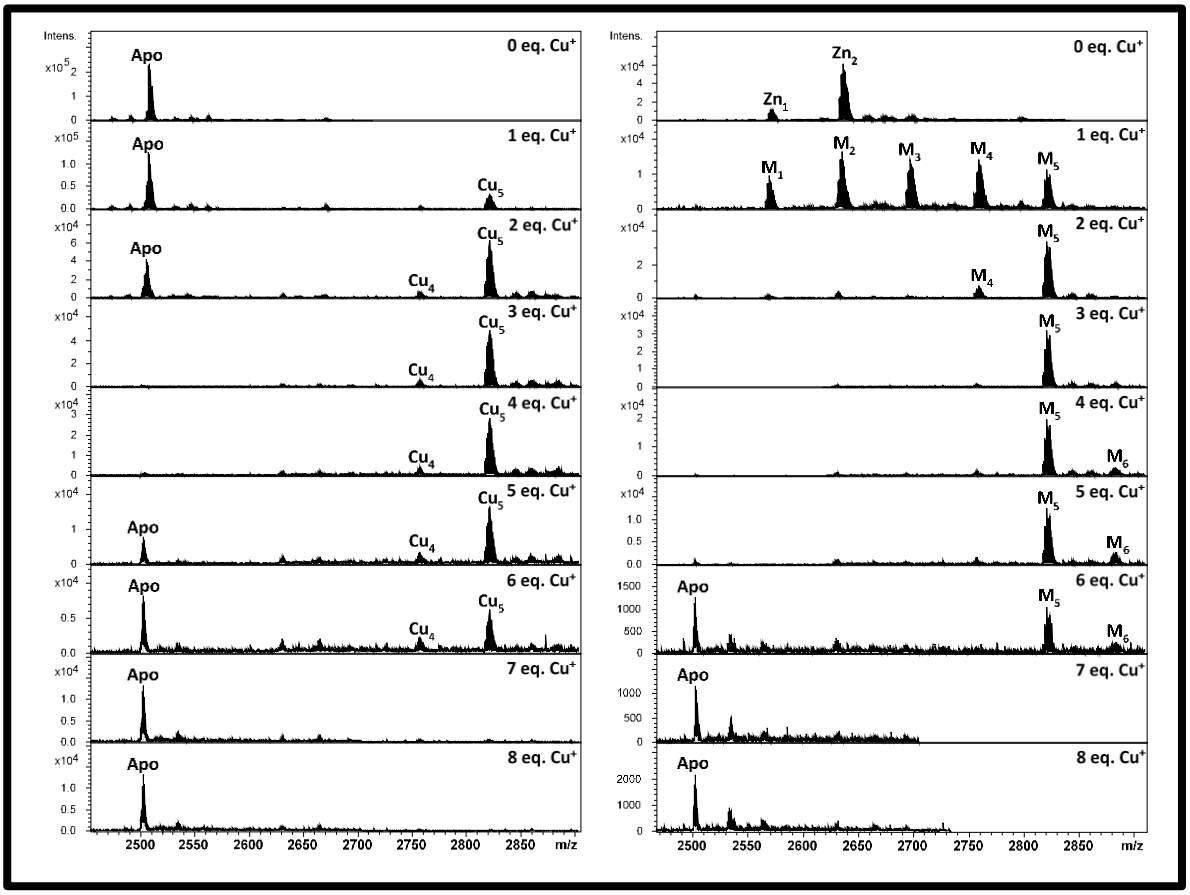

Figure 31. Titration followed by ESI-MS at pH 7 and 2.4 corresponding to the addition of Cu(I) to a solution 15.6 µM of Zn-NcMT.

The same well-structured specie Cu_5-NcMT is formed in both cases, *in vitro* and *in vivo*. Consequently, the ESI-MS and CD *in vivo* spectra of the Cu-preparation can be compared with the *in vitro* spectra, during the stage of the titration where the specie Cu_5-NcMT is present (Figure 32).

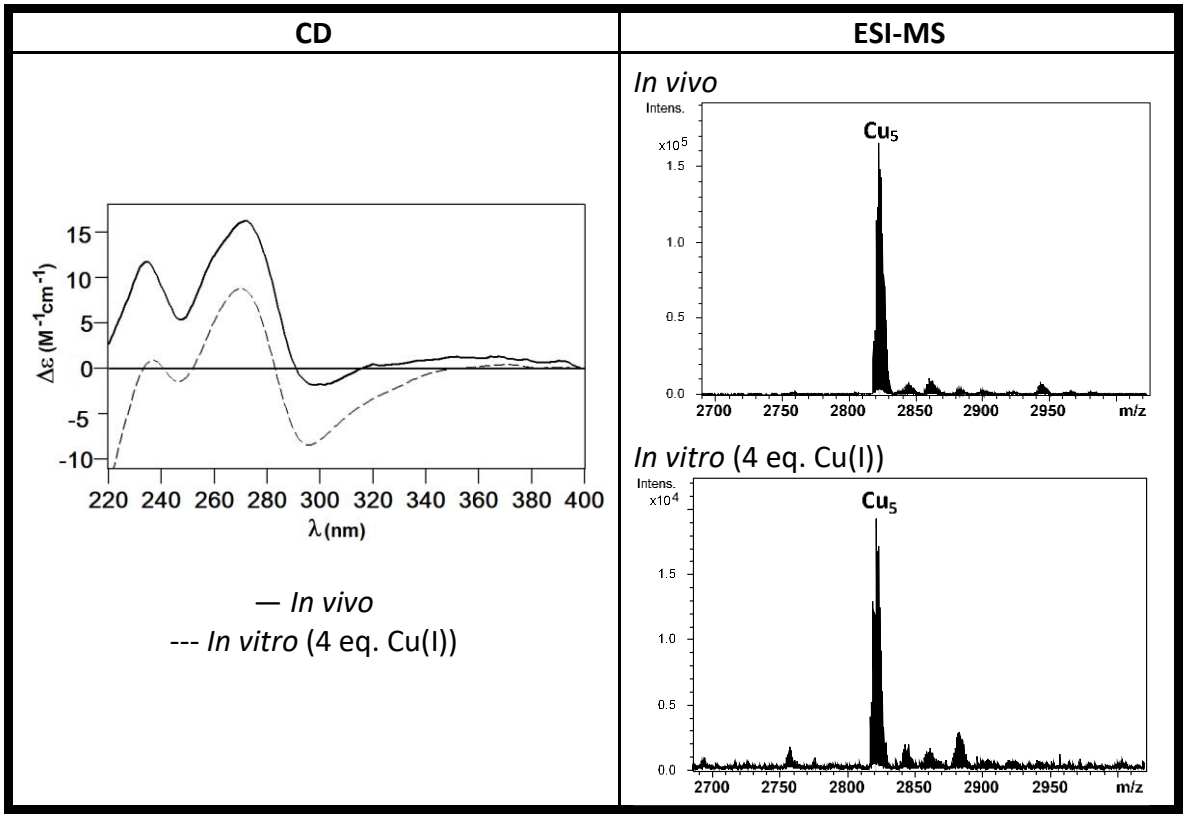

Figure 32. Superposition and comparison of CD and ESI-MS spectra of Cu-NcMT preparation *in vivo* and *in vitro*

8.3 FvMT

The MT sequence found for *F. verticillioides*, FvMT, has a short sequence of 26 amino acids with 7 cysteines (Figure 33A). After synthesize the protein recombinantly in different metal-supplemented cultures, its identity, purity and integrity was confirmed by ESI-MS (pH 2.4). The peak observed for the apo-form was 2467Da, value which resembles with the theoretical value 2466.7 Da calculated for the sequence (Figure 33B).

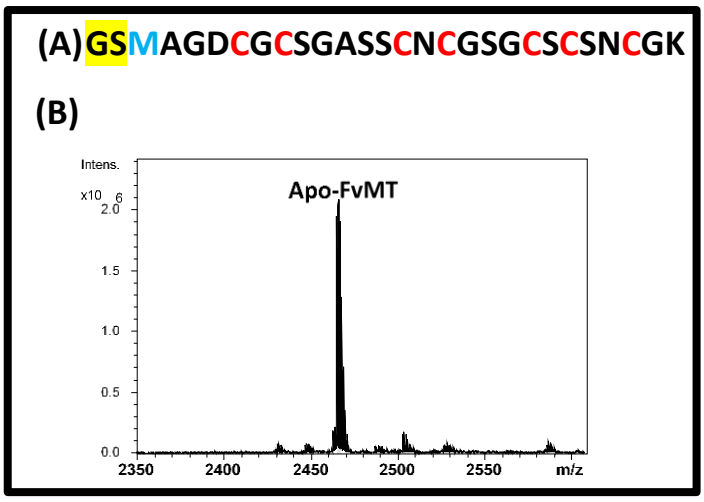

Figure 33. Amino acid sequence of the recombinant FvMT isoform and deconvoluted ESI-MS spectrum of the Zn-FvMT preparation recorded at pH 2.4, which corresponds to the apo-FvMT.

Once determined the amino acid sequence and the corresponding MW, the behaviour of the protein in the presence of Zn(II), Cd(II) and Cu(II) can be studied.

8.3.1 FvMT binding Zn(II)

According to the data obtained by ESI-MS (Figure 34A), the biosynthesis of FvMT in Zn(II)-enriched media produces a mixture of Zn_1-, Zn_2 and Zn_3-FvMT, being Zn_2-FvMT the majority specie. The content of 2.25 Zn(II) per MT obtained from ICP-AES analysis is consistent with this result. The CD spectrum of this preparation shows a non-very defined spectrum, without signals after 240 nm, suggesting a poor structuring of these protein about Zn(II) (Figure 34B).

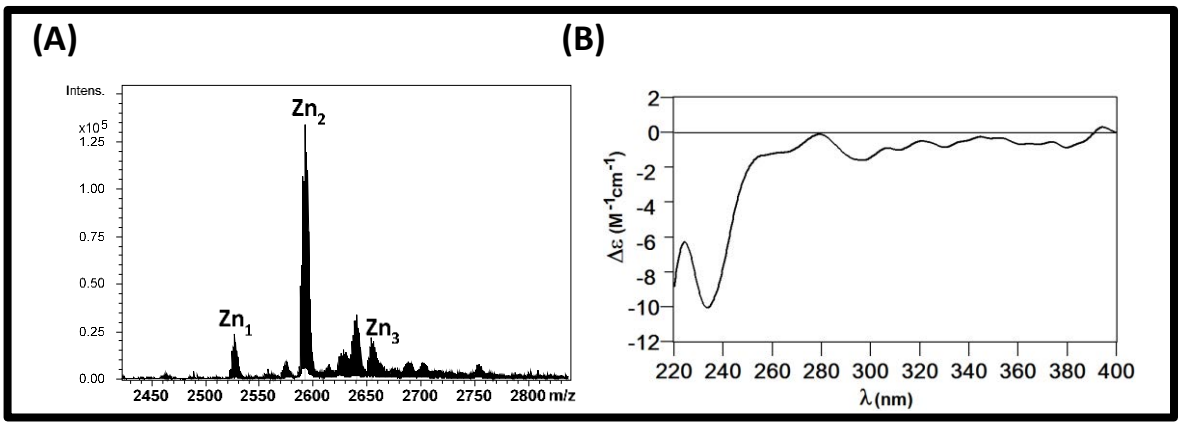

Figure 34. Deconvoluted ESI-MS spectrum of Zn-FvMT at pH 7.0 and CD spectrum of the Zn-FvMT preparation.

8.3.2 FvMT binding Cd(II)

In the case of the synthesis of this protein in Cd(II)-supplemented cultures, the ESI-MS spectrum shows the presence of Cd_xS_y-FvMT complexes where Cd_3S_2-FvMT is the majority specie (Figure 35). The presence of S^{2-} ligands is corroborated by the low Cd-to-S ratio measured by ICP-AES. On the other hand, the concentration of protein obtained was too low, making impossible to overcome the detection limit of the CD technique.

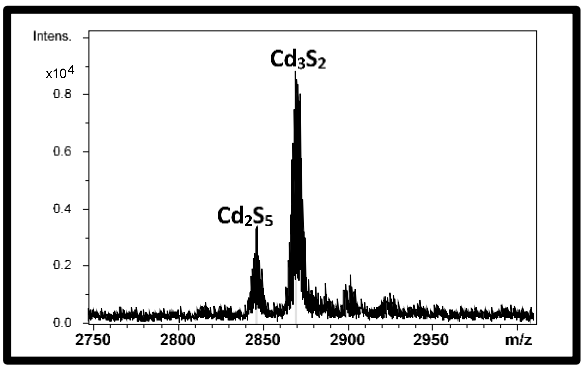

Figure 35. Deconvoluted ESI-MS spectrum of Cd-FvMT preparation at pH 7.

8.3.3 FvMT binding Cu(I)

According to ESI-MS results, in Cu(II)-enriched media cultures, FvMT is produced forming a unique well-folded complex Cu_5-FvMT in both cases, normal and low oxygenation conditions (Figure 36A). ICP-AES analysis reinforces these results giving a value of 5.20 Cu(I) per MT. The proper folding of this complex is confirmed by the CD spectrum (Figure 36B), which shows characteristic bands of Cu-species at 235, 265 and 300 nm.

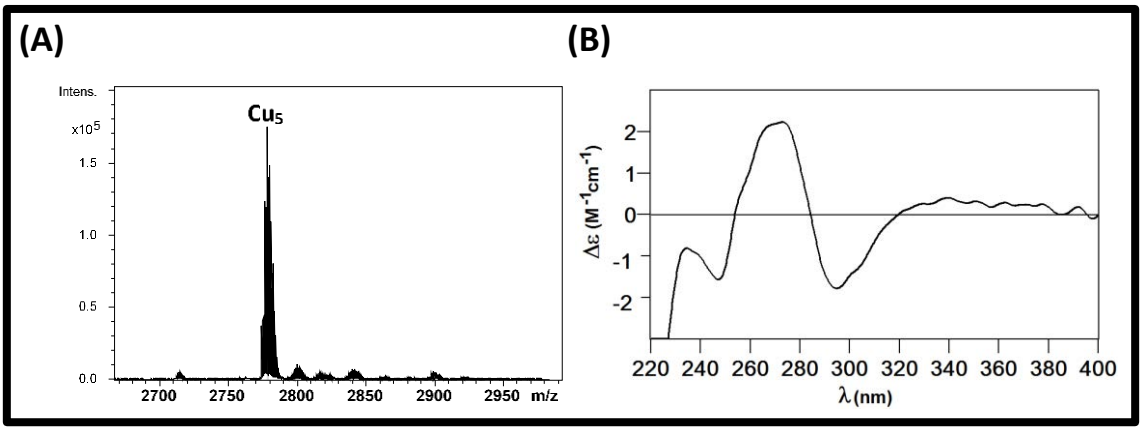

Figure 36. Deconvoluted ESI-MS spectra, recorded at pH 7.0, and CD spectrum of Cu-FvMT preparation.

The *in vitro* addition of Cu(I) to a Zn-FvMT preparation, followed by CD, UV-Vis and ESI-MS, allows also observing the formation of Cu_5-FvMT as majority specie, when 5 Cu(I) equivalents are added.

According to the CD, ESI-MS and UV-Vis data, the addition of further Cu(I) to the solution do not provoke additional binding of Cu but the unfolding of the formed cluster until rendering the apo-species (Figures 37 and 38).

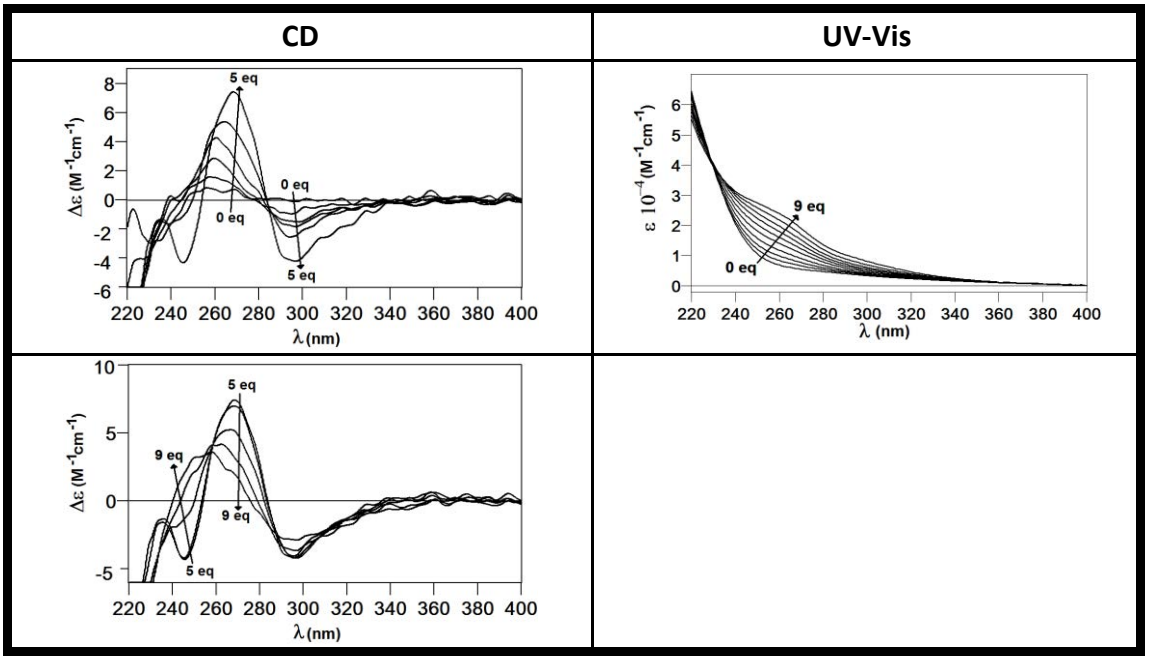

Figure 37. Titration followed by CD and UV-Vis spectroscopies corresponding to the addition of Cu(I) to a solution 19.9 µM of Zn-FvMT at pH 7.0 and 25ºC.

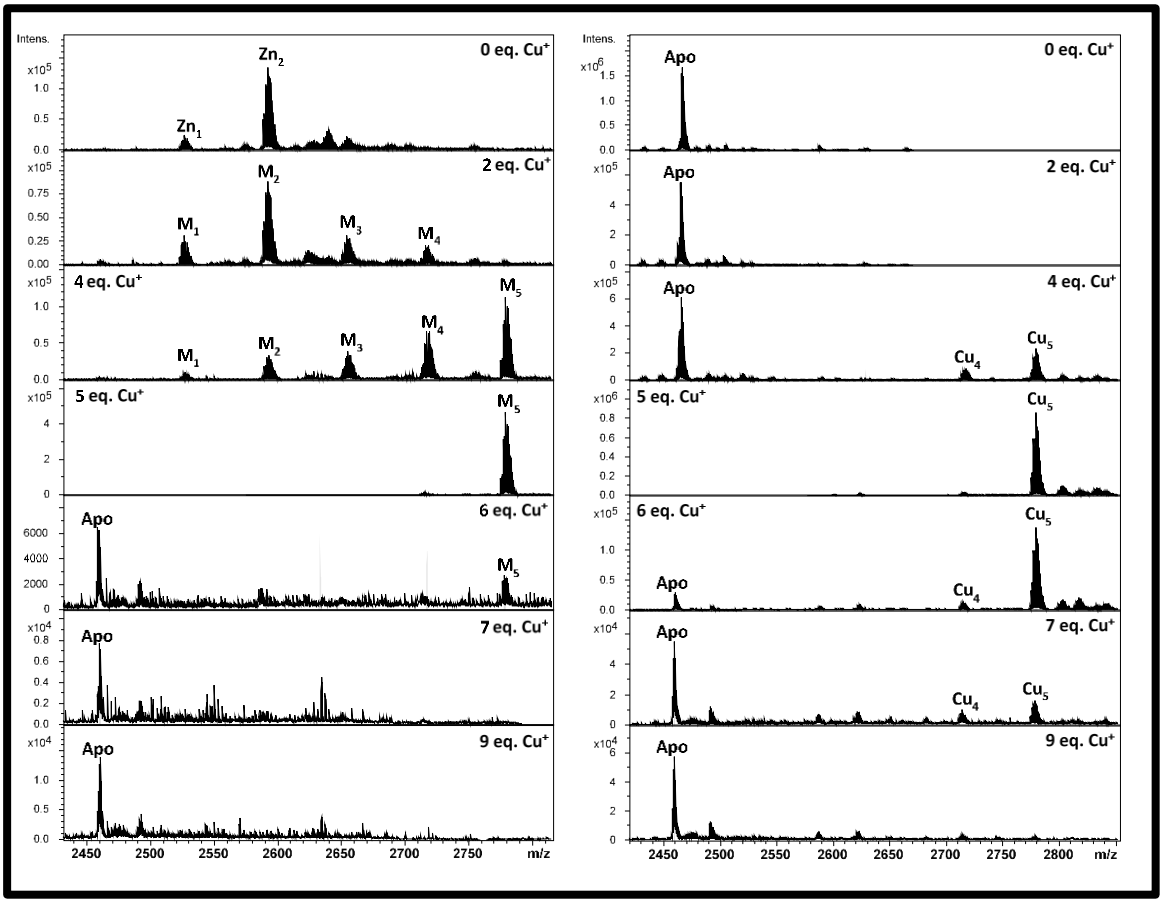

Figure 38. Titration followed by ESI-MS at pH 7 and 2.4 corresponding to the addition of Cu(I) to a solution 19.9 µM of Zn-FvMT.

The same well-structured specie Cu_5-FvMT is formed in both cases, *in vitro* and *in vivo*. Consequently, the ESI-MS and CD *in vivo* spectra of the Cu-preparation can be compared with the *in vitro* spectra, during the stage of the titration where the specie Cu_5-FvMT is present (Figure 39).

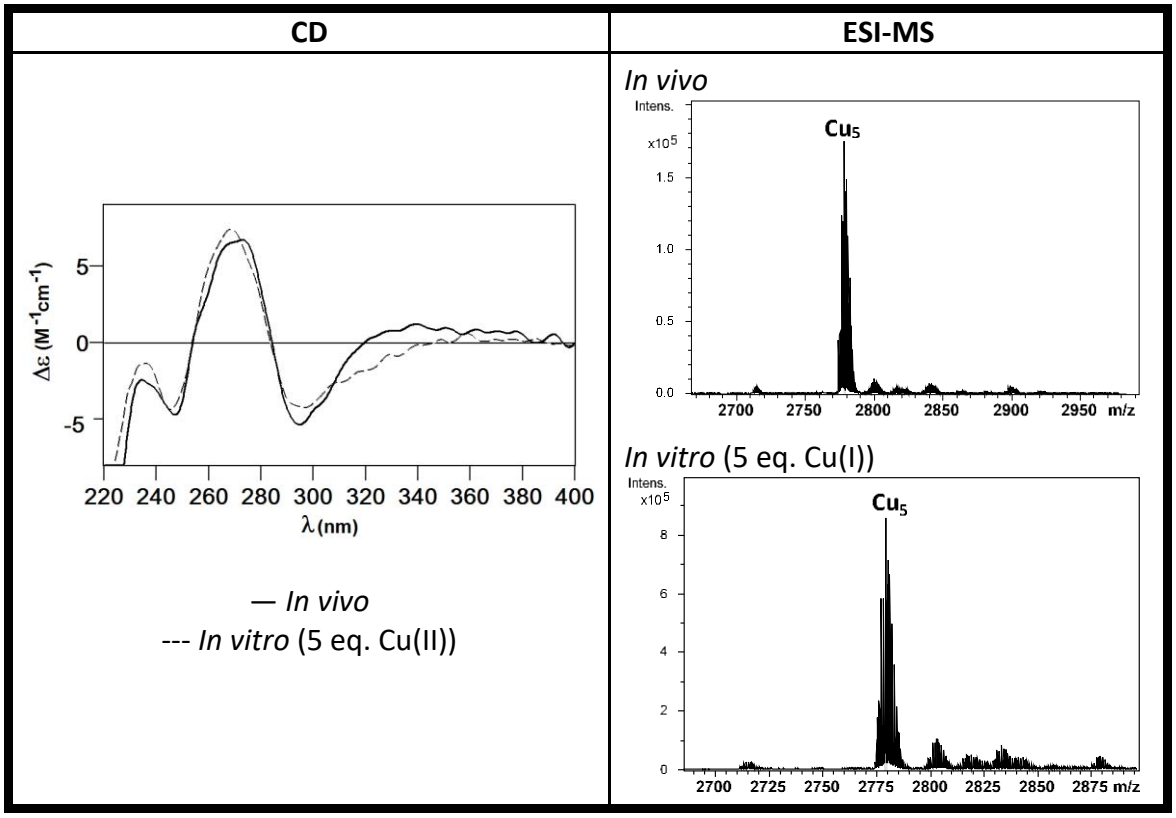

Figure 39. Superposition and comparison of CD and ESI-MS spectra of Cu-FvMT preparation *in vivo* and *in vitro*

8.4 NcMT2

The sequence of this MT is out of the tendency of subfamily 1. Normally the sequences of the proteins found in this group tends to be short, about 20-30 amino acids, but NcMT2 has 75 amino acids in total. The first half of the protein sequence does not have any cysteine while the second half contain the 7 cysteines present in the sequence (Figure 40A). After the recombinant synthesis of NcMT2 in different metal-supplemented cultures, its purity and identity was analysed by ESI-MS (pH 2.4). The resultant peak obtained for apo-form was 7632 Da, value which correlates with the theoretical MW calculated for NcMT2, 7633.0 Da, thus confirming the amino acid sequence (Figure 40B).

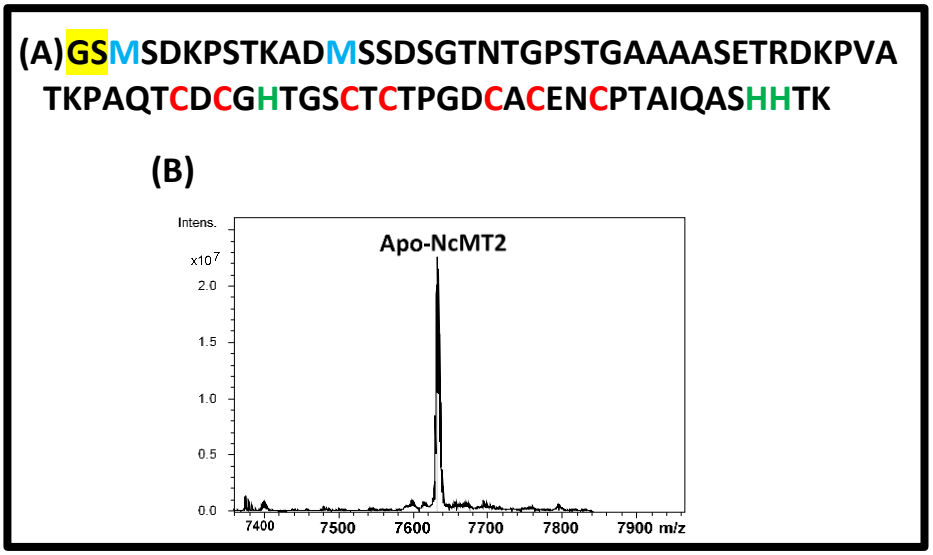

Figure 40. Amino acid sequence of the recombinant NcMT2 isoform and deconvoluted ESI-MS spectrum of the Zn-NcMT2 preparation recorded at pH 2.4, which corresponds to the apo-NcMT2.

Once determined the amino acid sequence and the corresponding MW, the behaviour of the protein in the presence of Zn(II), Cd(II) and Cu(II) can be discussed.

8.4.1 NcMT2 binding Zn(II)

When NcMT2 is synthesised in Zn(II)-enriched media, the results obtained by ESI-MS indicate the formation of an almost equimolar mixture of two different complexes Zn_2-NcMT2 and Zn_3-NcMT2 (Figure 41A). The ICP-AES analysis of this production is quite consistent with the formation of these species, indicating a content of 2,10 Zn(II) per MT. However, the CD analysis indicates that the structuration of the protein about Zn(II) is poor, because of the lack of signals after 240 nm (Figure 41B).

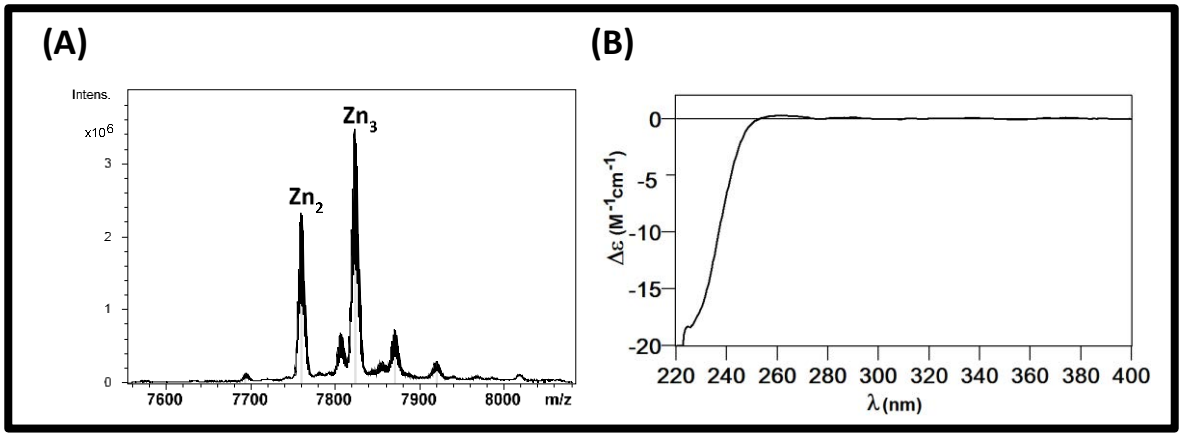

Figure 41. Deconvoluted ESI-MS spectrum of Zn-NcMT2 at pH 7.0 and CD spectrum of the Zn-NcMT2 preparation.

8.4.2 NcMT2 binding Cd(II)

According to the data obtained by ESI-MS (Figure 42A), the biosynthesis of NcMT2 in Cd(II)-enriched media produces the complex Cd_3-NcMT2 as a majority specie, with the presence of traces of Cd_2-NcMT2 and different Cd_xS_y-NcMT2 species. The low Cd-to-S ratio measured by ICP-AES corroborates the presence of S^{2-} ligands in the preparation. The concentration of protein obtained for this production was a little low, producing the collection of a weak-intense CD spectrum. Despite the weak intensity, the spectrum shows a Gaussian band at 250-260 nm, related with the Cd-Cys bond, and one exciton coupling at 290 nm, characteristic of the Cd-S^{2-} bond (Figure 42B).

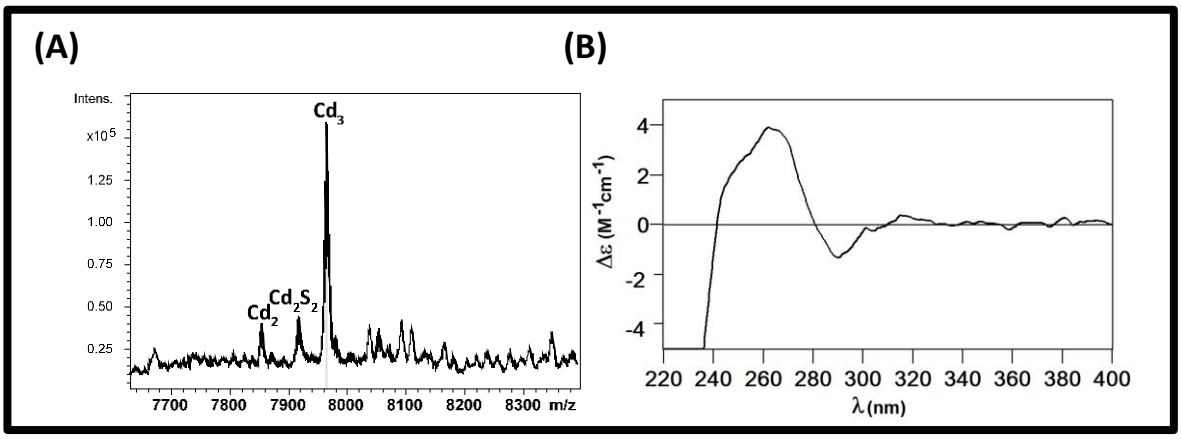

Figure 42. Deconvoluted ESI-MS and CD spectra of the Cd-NcMT2 preparation, recorded both at pH 7.0

8.4.3 NcMT2 binding Cu(I)

When NcMT2 is produced in Cu(II)-enriched media the ESI-MS results for the productions at normal and low oxygenation are the same. In both cases the majority specie formed is Cu_5-NcMT. However, the ESI-MS spectra recorded at pH 7.0 show significant traces of Cu_6-NcMT2 not observed in the spectra recorded at pH 2.4. This fact is probably produced because the conditions used for ESI-MS recorded at pH 2.4 are too high for the stability of Cu_6-NcMT2 complex (Figure 45A and 45B). These results are supported by the value 5.07 Cu(I) per MT obtained by ICP-AES and also by CD spectra, which show different bands at 255, 290 and 300 and 330 nm, characteristic of Cu-MT complexes (Figure 45C).

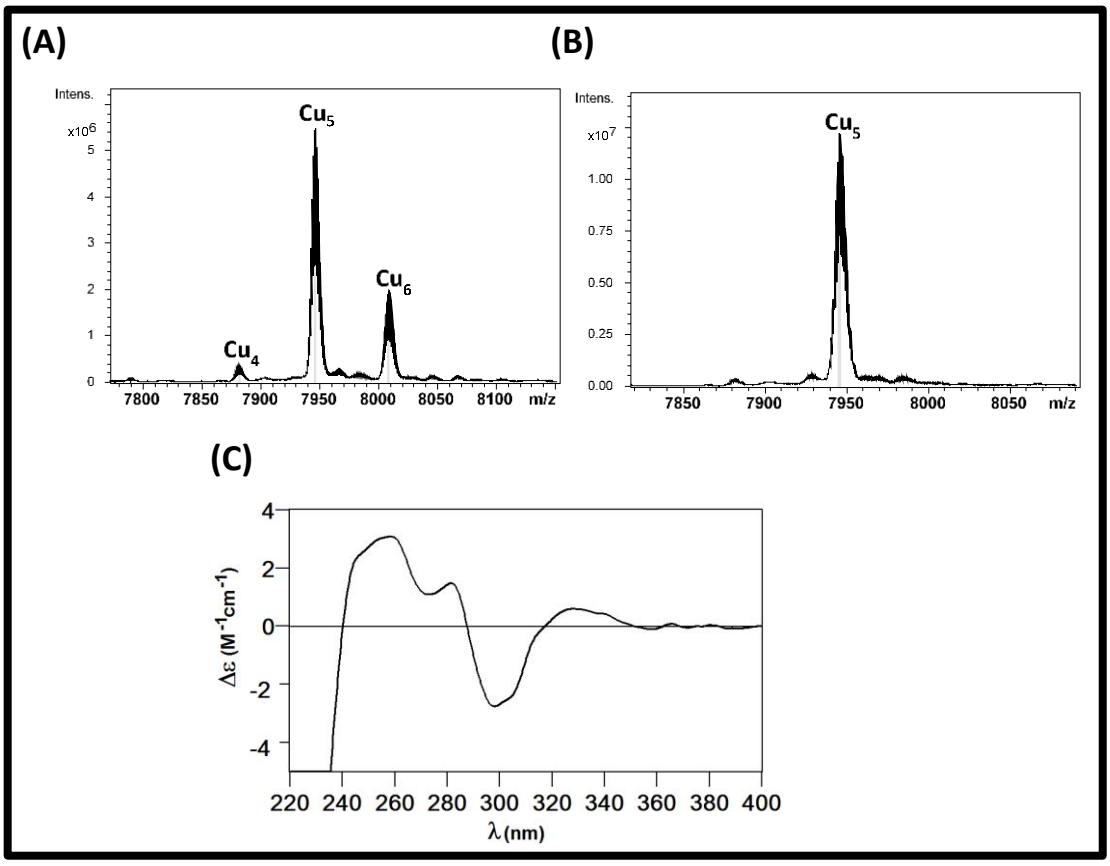

Figure 43. Deconvoluted ESI-MS spectra, recorded at pH 7.0 and 2.4, and CD spectrum of Cu-NcMT2 preparation.

The *in vitro* addition of Cu(I) to the Zn-NcMT2 preparation, followed by CD, UV-Vis and ESI-MS, allows observing the formation of mainly Cu_5-NcMT2 when 5 Cu(I) equivalents are added. According to the CD, ESI-MS and UV-Vis data, the addition of further Cu(I) provokes additional binding of Cu forming the cluster Cu_6-NcMT2, but with less importance than Cu_5-NcMT2. (Figures 44 and 45).

The same well-structured specie Cu_5-NcMT2 is formed in both cases, *in vitro* and *in vivo*. Consequently, the ESI-MS and CD *in vivo* spectra of the Cu-preparation can be compared with the *in vitro* spectra, during the stage of the titration where the specie Cu_5-NcMT2 is present (Figure 46).

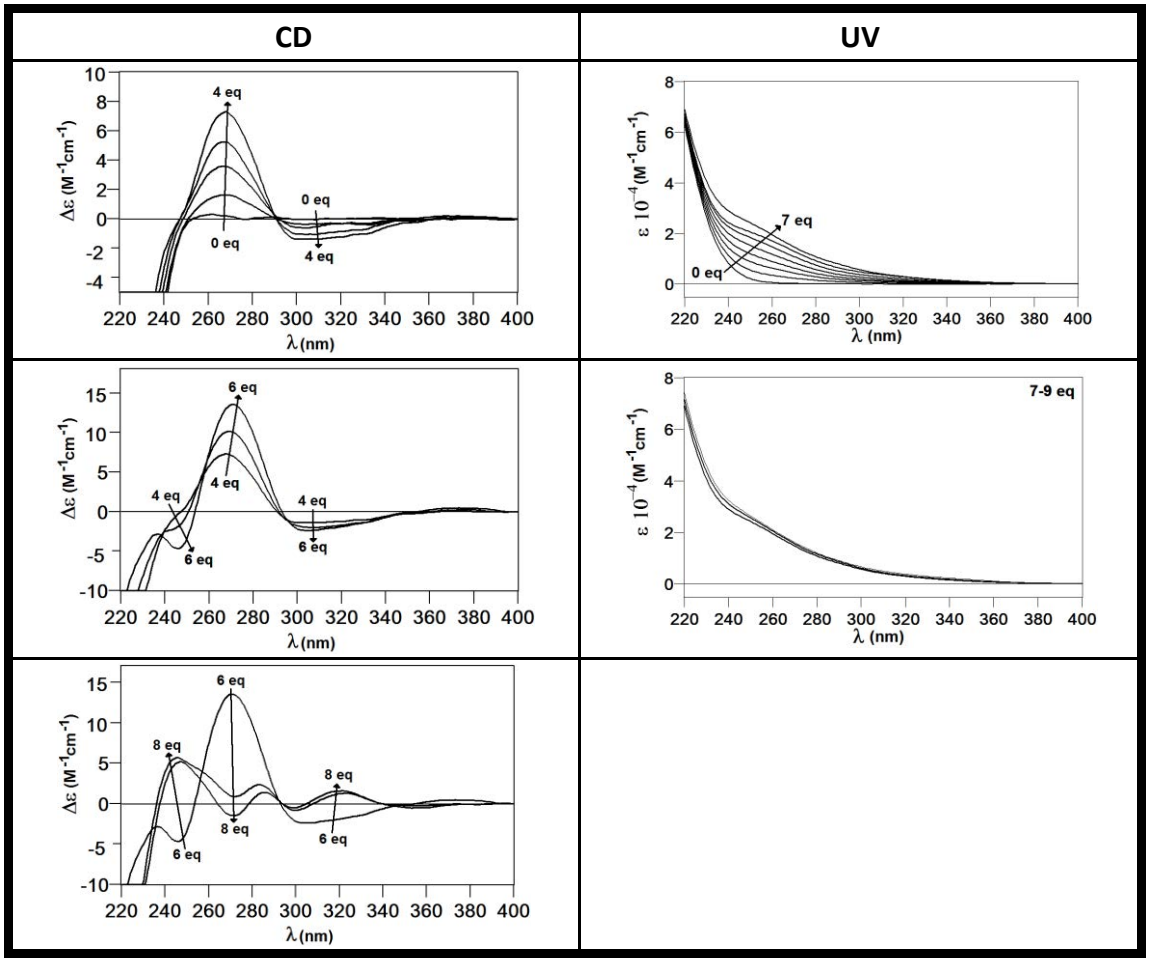

Figure 44. Titration followed by CD and UV-Vis spectroscopies corresponding to the addition of Cu(I) to a solution 18.7 µM of Zn-NcMT2 at pH 7.0 and 25ºC.

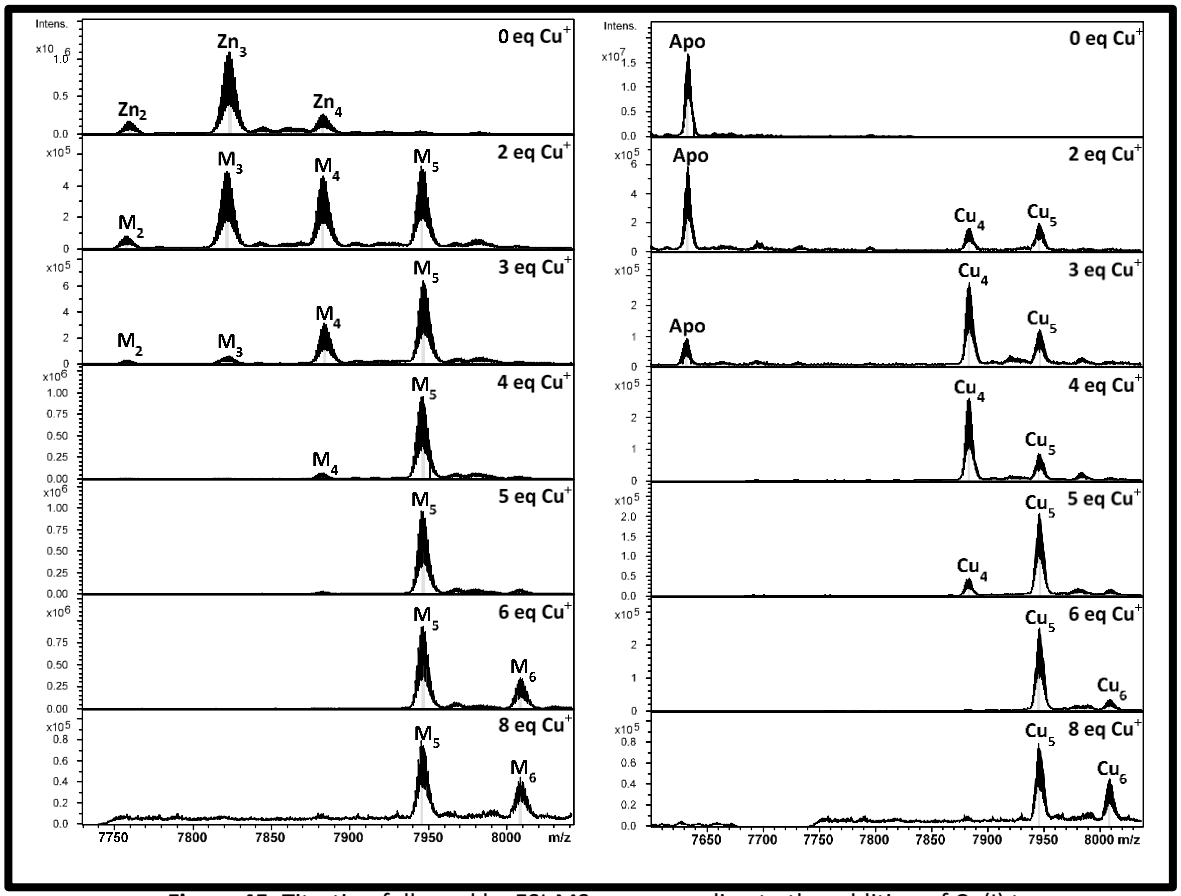

Figure 45. Titration followed by ESI-MS corresponding to the addition of Cu(I) to a solution 18.7 µM of Zn-NcMT2 at pH 7.0 and 2.4.

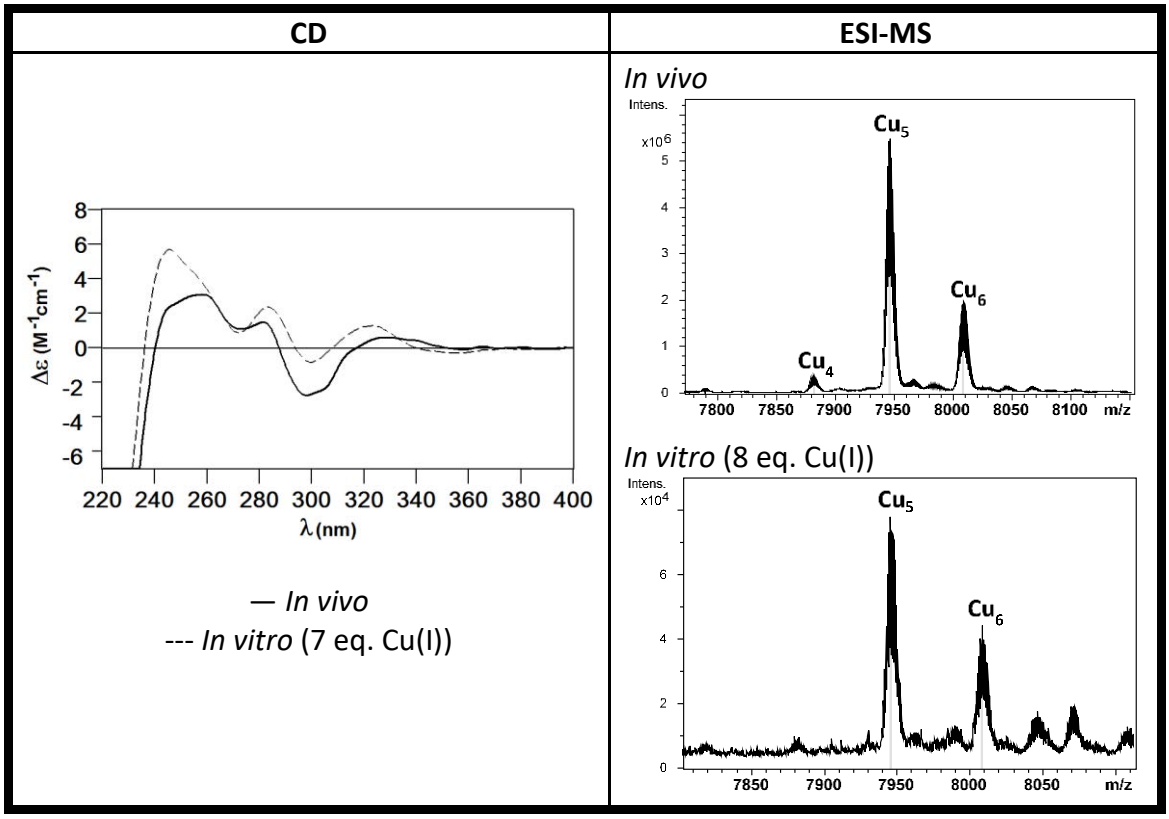

Figure 46. Superposition and comparison of CD and ESI-MS spectra of Cu-NcMT2 preparation *in vivo* and *in vitro.*

8.5 UrMT

The sequence of UrMT has 25 amino acids and 8 cysteines (Figure 47A). After recombinant synthesis of this protein in different metal-supplemented cultures, its purity and identity was analysed by ESI-MS (pH 2.4). The peak observed for the apo-form is 2475 Da, value which resembles with the theoretical MW 2475.7 Da calculated for the identity of the amino acid sequence (Figure 47B).

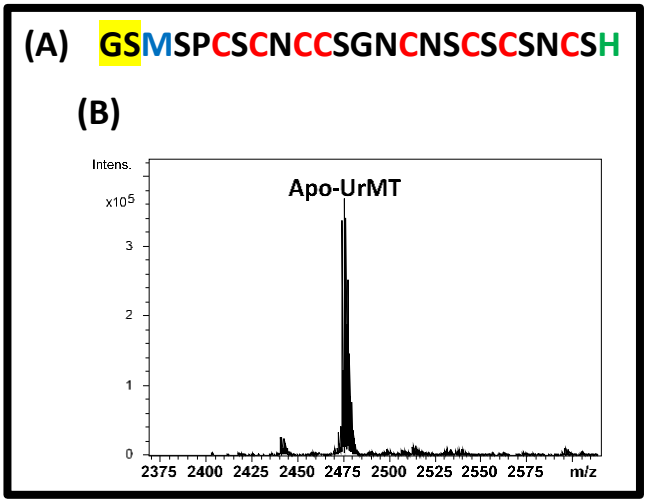

Figure 47. Amino acid sequence of the recombinant UrMT isoform and deconvoluted ESI-MS spectrum of the Zn-UrMT preparation recorded at pH 2.4, which corresponds to the apo-UrMT.

Once determined the MT sequence and the corresponding MW, the behaviour of the protein in the presence of Zn(II), Cd(II) and Cu(II) can be analysed.

8.5.1 UrMT binding Zn(II)

According to the data obtained by ESI-MS (Figure 48A), when UrMT is synthesised in Zn(II)-enriched media a single specie corresponding to the complex Zn_3-UrMT is produced. This result correlates with the value 3.3 Zn(II) per MT obtained by ICP-AES analysis. Despite the considerable cleanness of the ESI-MS spectrum, the lack of signals after 240 nm in the CD spectrum indicates that the structuration of the protein about Zn(II) is poor (Figure 48B).

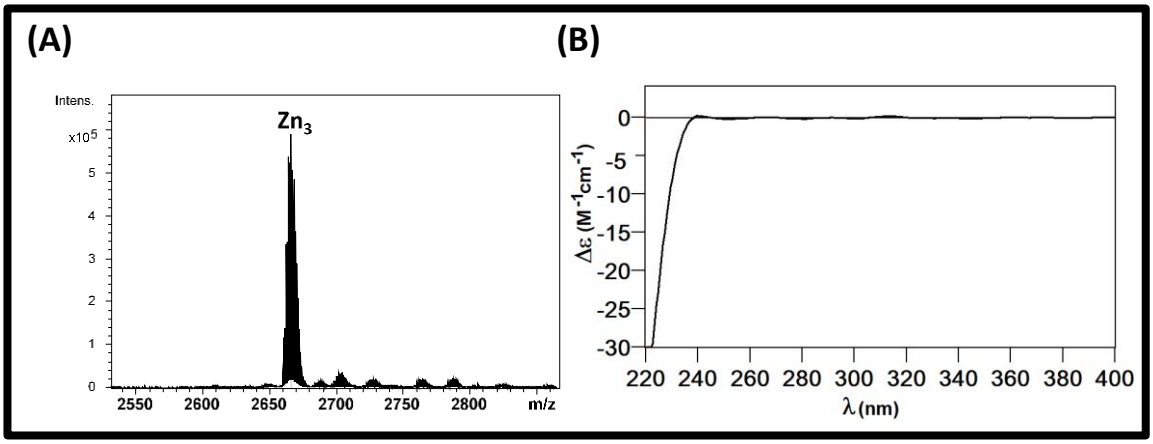

Figure 48. Deconvoluted ESI-MS spectrum of Zn-UrMT at pH 7.0 and CD spectrum of the Zn-UrMT preparation.

8.5.2 UrMT binding Cd(II)

In the case of the synthesis of this protein in Cd(II)-supplemented cultures, the ESI-MS spectrum shows several peaks which corresponds to Cd_3-UrMT, Cd_5-UrMT and different Cd_xS_y-UrMT complexes (Figure 49A). The presence of S^{2-} ligands is corroborated by the low Cd-to-S ratio measured by ICP-AES. On the other hand, the CD spectrum shows a Gaussian band at 260 nm, related with the Cd-Cys bond, and one exciton coupling at 290 nm, characteristic of the Cd-S^{2-} bond (Figure 49B).

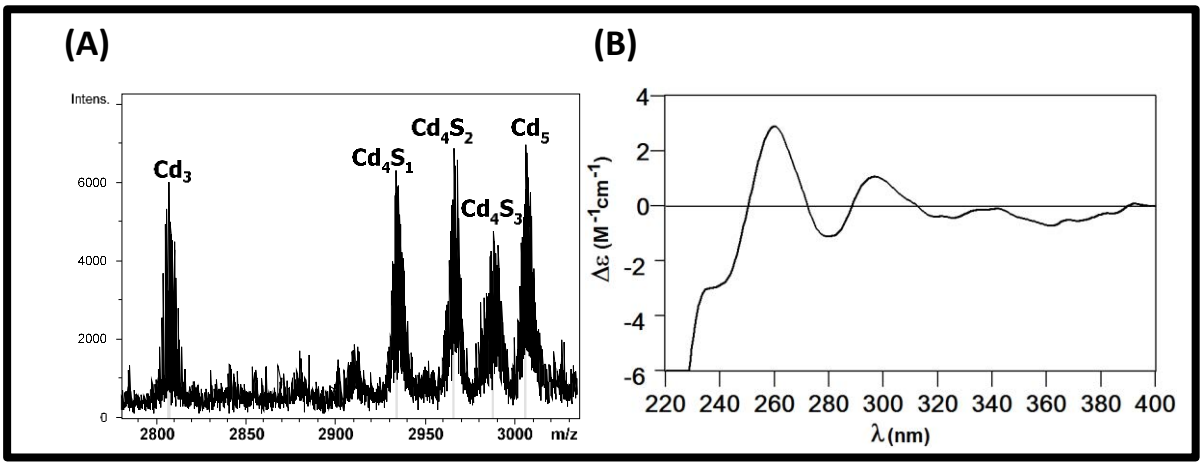

Figure 49. Deconvoluted ESI-MS and CD spectra of the Cd-UrMT preparation, recorded both at pH 7.0

The *in vitro* addition of Cd(II) to the Zn-UrMT preparation, followed by CD, UV-Vis and ESI-MS, allows observing initially the formation of different heterometallic species Zn_xCd_y-UrMT and the complex Cd_3-UrMT as majority specie. The addition of further Cd(II) equivalents provokes the formation of the specie Cd_5-UrMT with more or less the same ratio than Cd_3-UrMT (Figure 50 and 51).

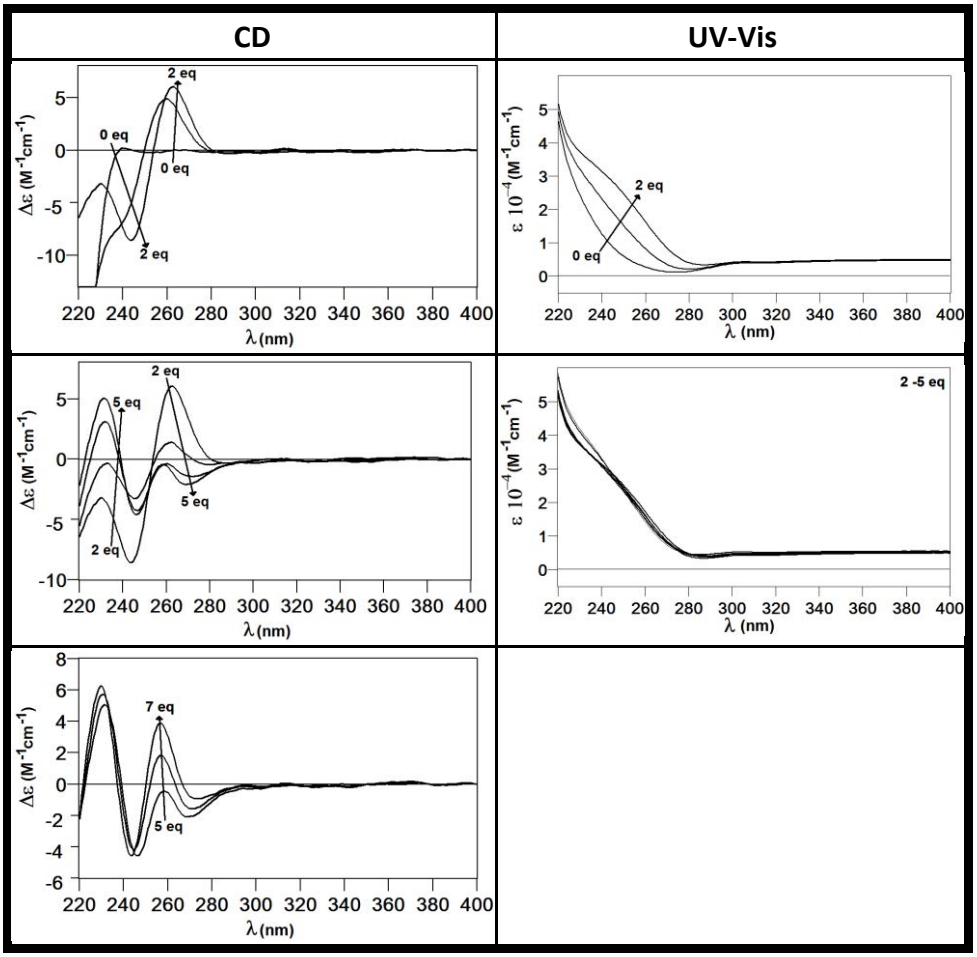

Figure 50. Titration followed by CD and UV-Vis spectroscopies corresponding to the addition of Cd(II) to a solution 14,7 µM of Zn-UrMT at pH 7.0 and 25ºC.

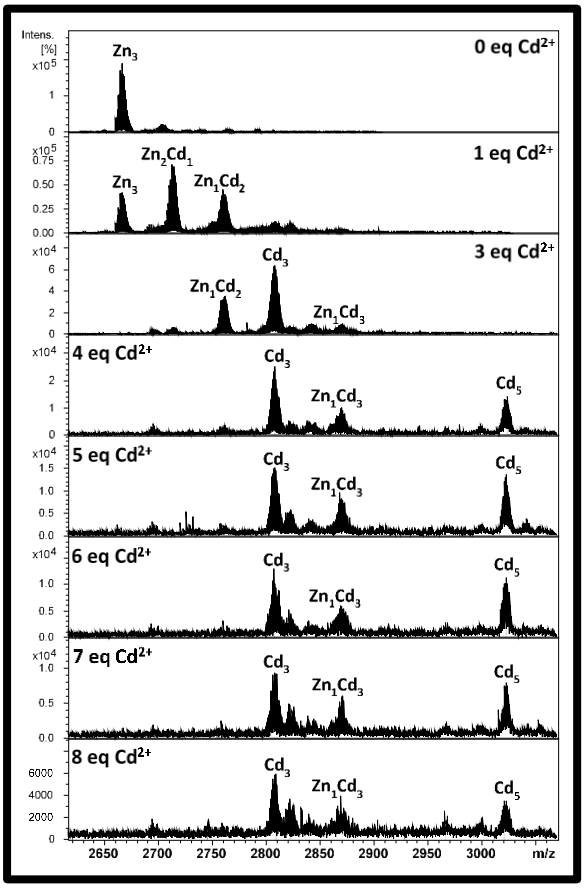

Figure 51. Titration followed by ESI-MS corresponding to the addition of Cd(II) to a solution 14,7 µM of Zn-UrMT at pH 7.0.

The same species Cd_3-UrMT and Cd_5-UrMT are formed in both cases, *in vitro* and *in vivo*, but always with the presence of other complexes with Zn^{2+} or S^{2-}, as the case may be. Consequently, the ESI-MS and CD *in vivo* and *in vitro* of Cu-preparations are similar but with small differences due to the presence of Cd_xS_y-UrMT complexes in the *in vivo* preparation, and Cd_xZn_y-UrMT complexes in the *in vitro* preparation (Figure 52).

8.5.3 UrMT binding Cu(I)

In Cu(I)-enriched media cultures, UrMT is not successfully synthesized. Any concentration of protein was detected by ESI-MS, CD and ICP analysis.

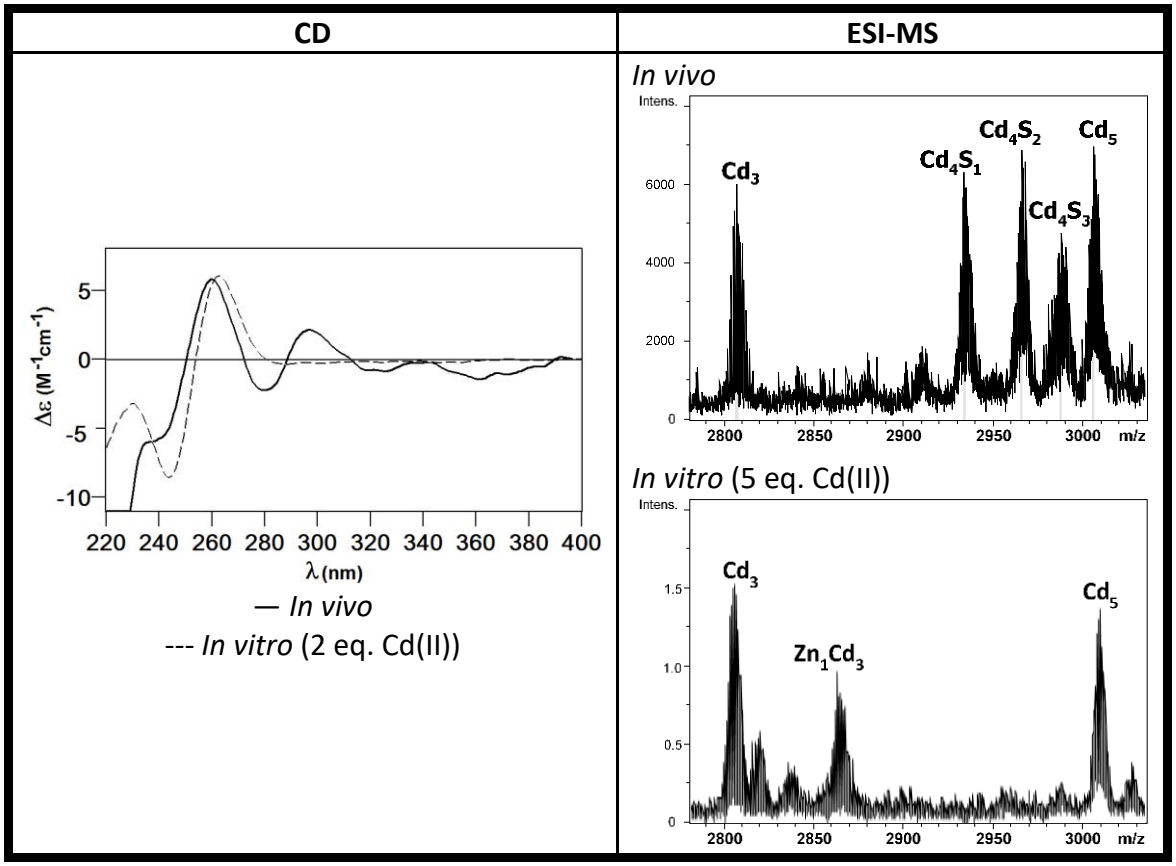

Figure 52. Superposition and comparison of CD and ESI-MS spectra of Cd-UrMT preparation *in vivo* and *in vitro.*

8.6 CipMT1

CipMT1 has a short sequence of 25 amino acids with 8 cysteines (Figure 53A). After recombinant synthesis of this protein in different metal-supplemented cultures, its identity, purity and integrity was confirmed by ESI-MS (pH 2.4). The peak observed for the apo-form was 2442 Da, which resembles with the theoretical MW calculated for CipMT1 2442.7 Da, thus confirming the amino acid sequence (Figure 53B).

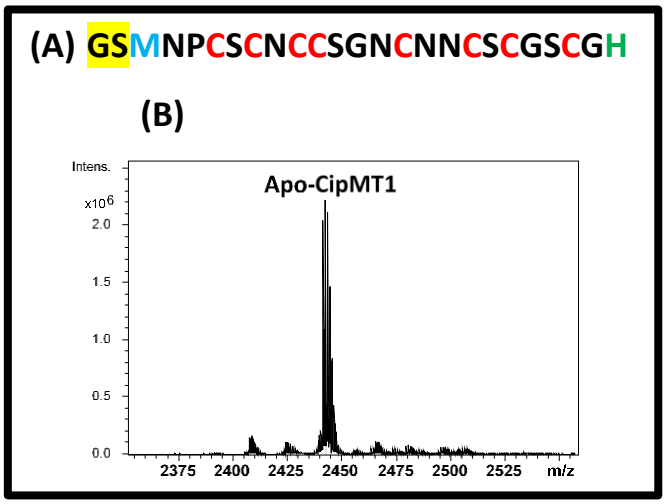

Figure 53. Amino acid sequence of the recombinant CipMT1 isoform and deconvoluted ESI-MS spectrum of the Zn-CipMT1 preparation recorded at pH 2.4, which corresponds to the apo-CipMT1.

Once determined the MT sequence and the corresponding MW, the behaviour of the protein in the presence of Zn(II), Cd(II) and Cu(II) can be studied.

8.6.1 CipMT1 binding Zn(II)

According to the data obtained by ESI-MS (Figure 54A), the synthesis of CipMT1 in Zn(II)-enriched media produces the complex Zn_3-CipMT1 as a single species, result consistent with the value 3.64 Zn(II) per MT obtained in the ICP-AES analysis. On the other hand, the CD analysis indicates that the structuration of the protein about Zn(II) is poor, because of the lack of signals after 240 nm (Figure 54B).

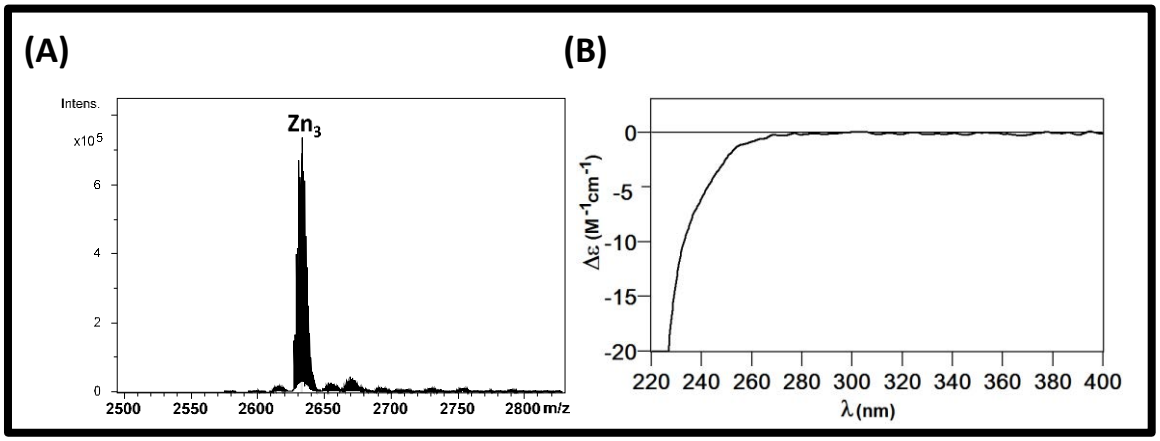

Figure 54. Deconvoluted ESI-MS spectrum of Zn-CipMT1 at pH 7.0 and CD spectrum of the Zn-CipMT1 preparation.

8.6.2 CipMT1 binding Cd(II)

In the case of the synthesis of the protein in Cd(II)-supplemented cultures, the ESI-MS spectrum shows the presence of Cd_4S-CipMT1 as majority specie and other minority species (Figure 55A). The presence of S^{2-} ligands is corroborated by the low Cd-to-S ratio measured by ICP-AES. On the other hand, the CD spectrum shows a Gaussian band at 260 nm, related with the Cd-Cys bond, but characteristic bands of the Cd-S^{2-} bond are not observed due to the low intensity of the spectrum (Figure 55B).

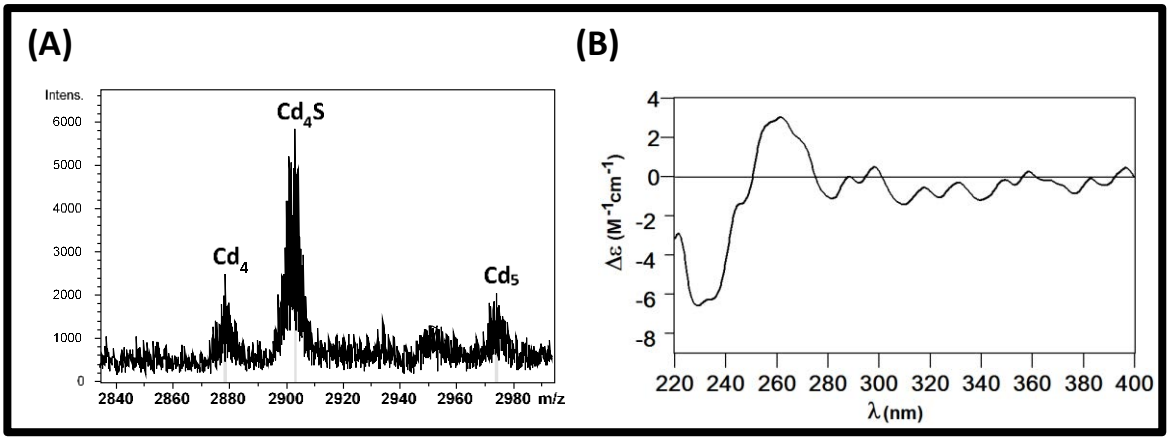

Figure 55. Deconvoluted ESI-MS and CD spectra of the Cd-CipMT1 preparation, recorded both at pH 7.0

The *in vitro* addition of Cd(II) to the Zn-CipMT1 preparation, followed by CD, UV-Vis and ESI-MS, allows observing initially the formation of different heterometallic species Zn_xCd_y-URMT and also the complex Cd_3-CipMT1. The addition of further Cd(II) equivalents provokes the formation of the specie Cd_5-CipMT1 as the majority and unique specie (Figure 56 and 57).

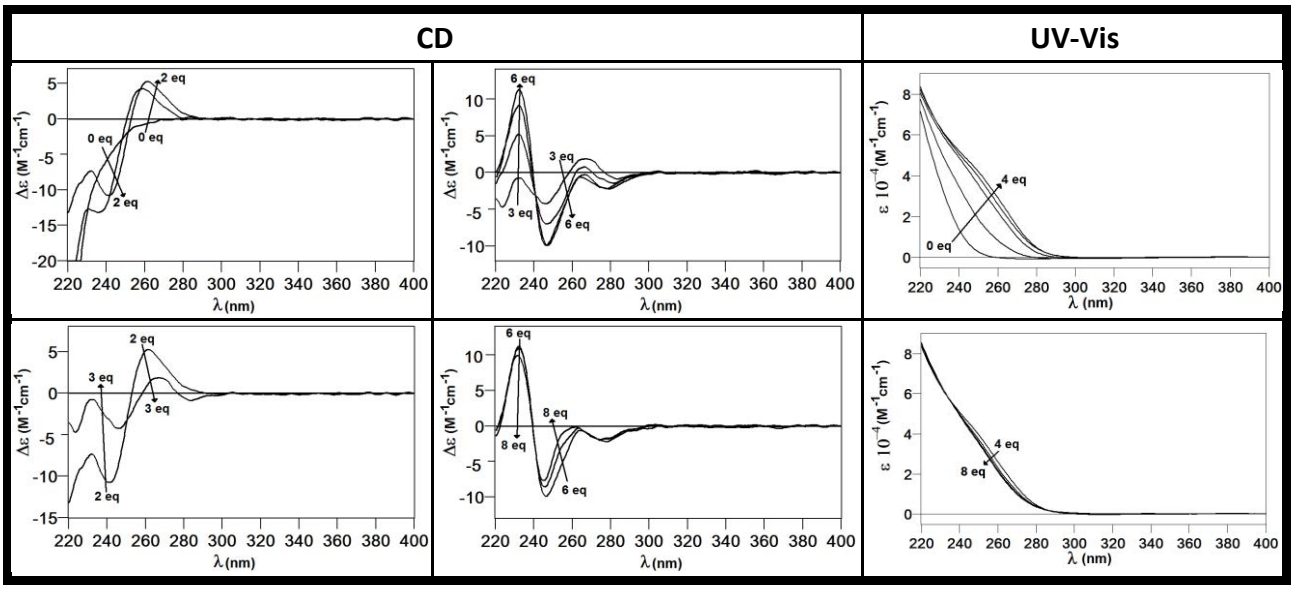

Figure 56. Titration followed by CD and UV-Vis spectroscopies corresponding to the addition of Cd(II) to a solution 15,1 µM of Zn-CipMT1 at pH 7.0 and 25ºC.

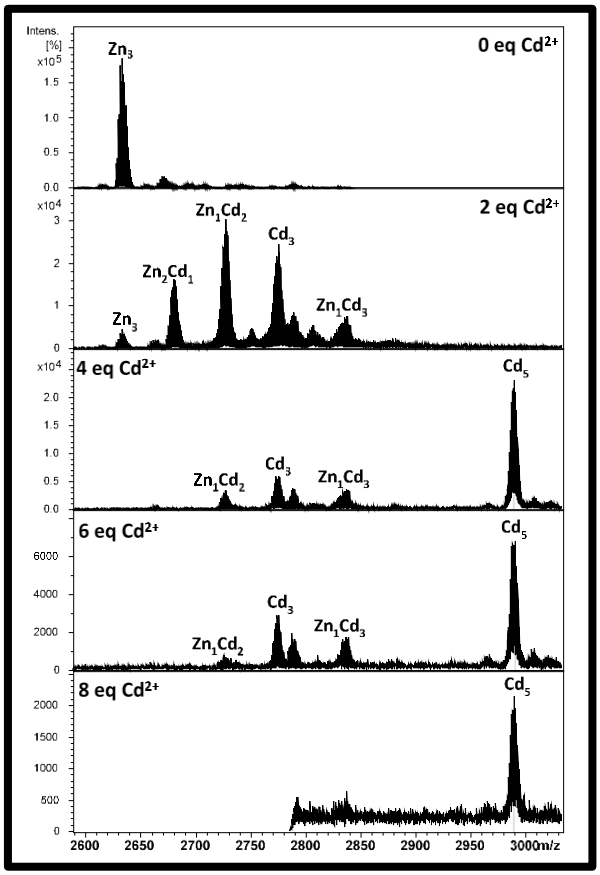

Figure 57. Titration followed by ESI-MS at pH 7.0, corresponding to the addition of Cd(II) to a solution 15.1 µM of Zn-CipMT1.

The same specie Cd_5-CipMT1 is formed in both cases, *in vitro* and *in vivo*, but whereas *in vitro* it is the majority specie formed, *in vivo* is a minority one. This difference is probably due to a considerable affinity and stability of the protein for complexes with S^{2-} which is not produced when Zn(II) is present. Whereas CD spectra of *in vivo* and *in vitro* preparations are very similar, differences important differences between the ESI-MS spectra can be observed by comparing them (Figure 58).

8.6.3 CipMT1 binding Cu(I)

In Cu(I)-enriched media cultures, CipMT1 is not synthesized successfully. Any result was obtained by ESI-MS, DC and ICP analysis.

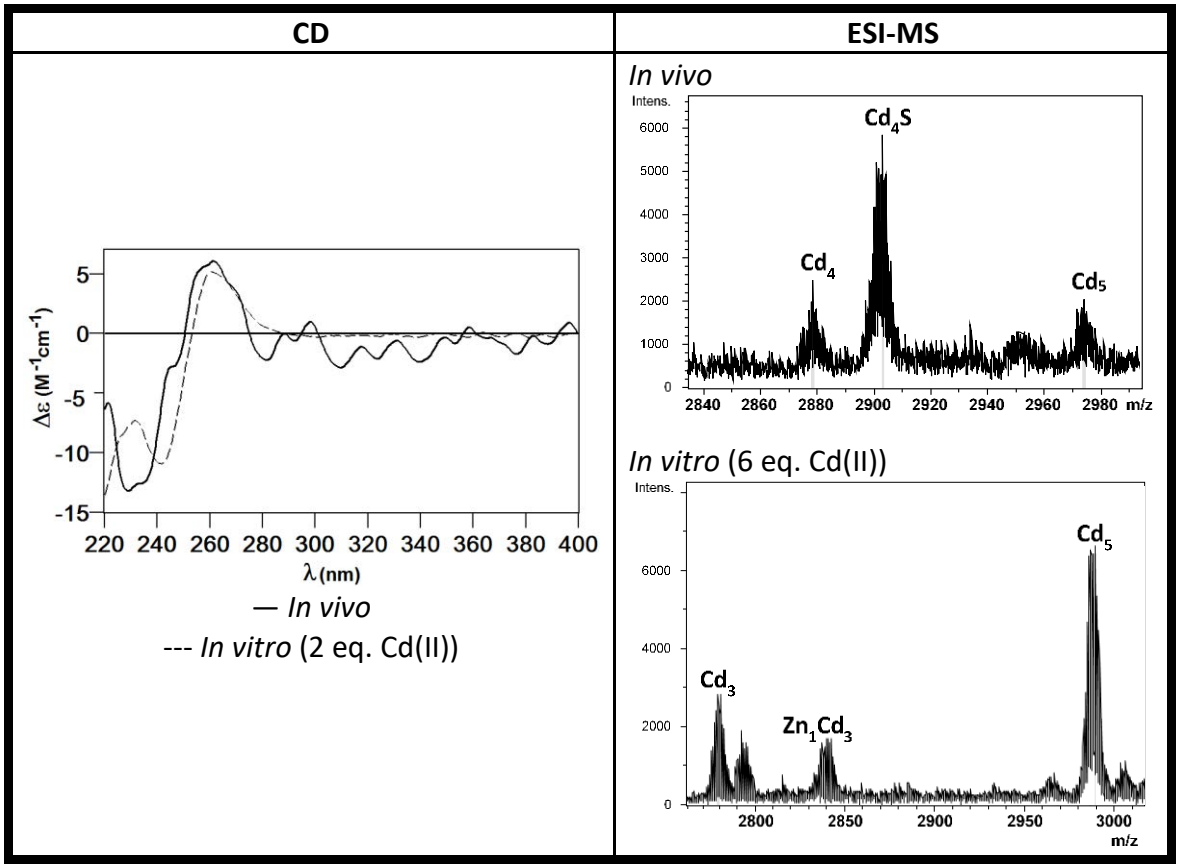

Figure 58. Superposition and comparison of CD and ESI-MS spectra of Cd-CipMT1 preparation *in vivo* and *in vitro*

8.7 Discussion subfamily 1

Within subfamily 1, MTs with 6, 7 and 8 cysteines have been studied. Two of the 7 cysteine MTs, NcMT and FvMT are practically equal. Their sequences are almost homologous, differing only in four amino acids (Figure 59).

NcMT M–GDCGCSGASSCNCGSGCSCSNCGSK

FvMT MAGDCGCSGASSCNCGSSCSCSGCGK

Figure 59. Comparison of the amino acid sequences of NcMT and FvMT.

By comparing the results of the productions *in vivo* of Zn-NcMT and Zn-FvMT is possible to see that the results are the same in both cases. The structuration with this metal ion is weak, and the majority specie formed is Zn_2-MT (Figure 60).

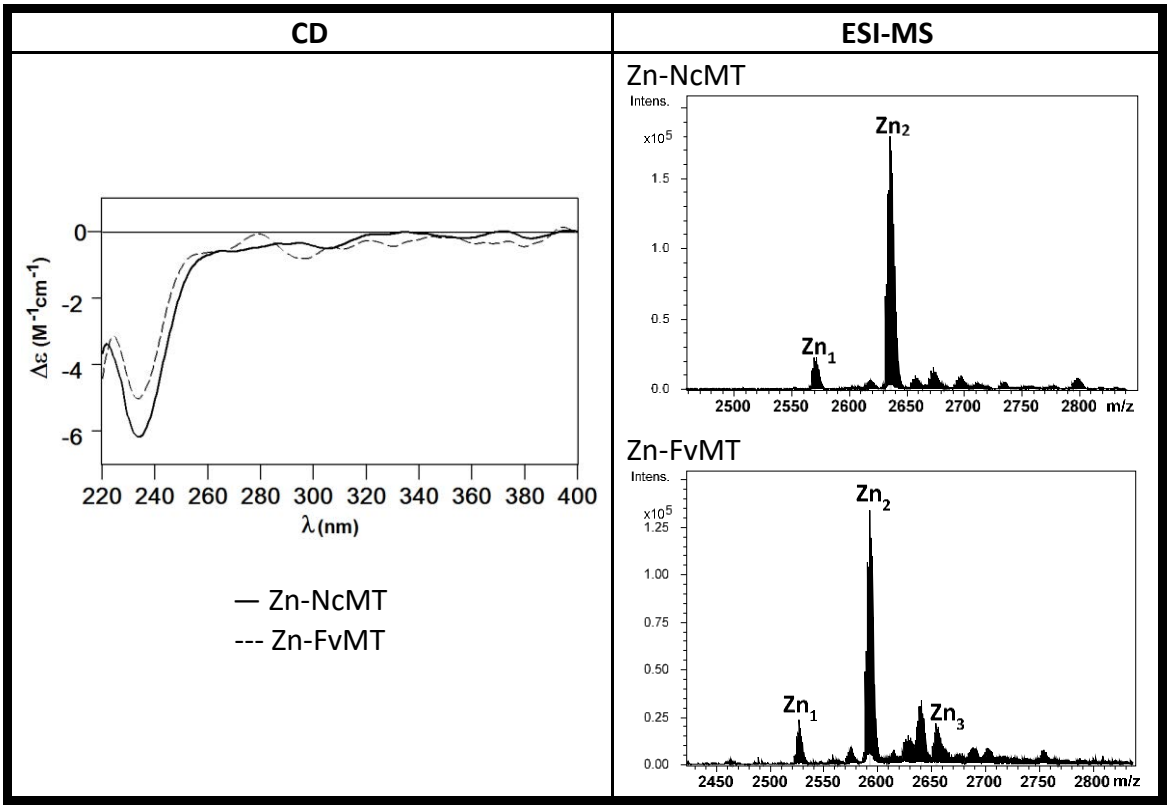

Figure 60. Comparison between CD and deconvoluted ESI-MS spectra of Zn-NcMT and Zn-FvMT.

In the case of the *in vivo* and *in* vitro productions of Cu-NcMT and Cu-FvMT, the species and structuration are also the same (Table 10). These two proteins are able to form a very stable and well-structured cluster with 5 Cu(I) ions. All the spectra show bands at 235, 265 and 300 nm.

NcMT is able to bind traces of Cd(II), but not with high structuration and with heterometallic species always in solution. On the other hand, FvMT is also able to bind traces of Cd(II), but by forming Zn_xS_y-NcMT complexes.

The incapacity of these two MTs to form homometallic species with Cd (II), and the well-structured specie with 5 Cu(I) metal ions formed, evidence the classification of NcMT and FvMT as Cu-thioneins. Despite the sequence differences between them, the behaviour of these two proteins in presence of these metal ions is practically identical. This suggests that their binding abilities proceed from their coordinating amino acids (mainly cysteines) which are perfectly aligned in the two sequences.

	In vivo	*In vitro* (titration)
CD	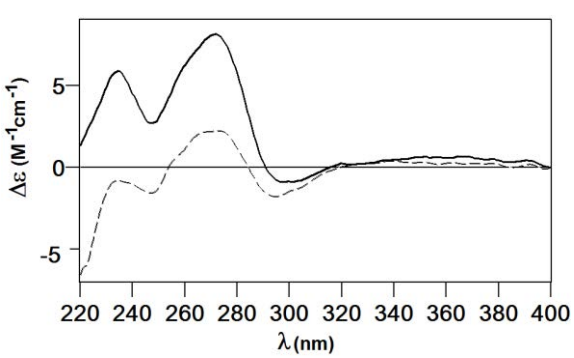 — Cu-NcMT --- Cu-FvMT	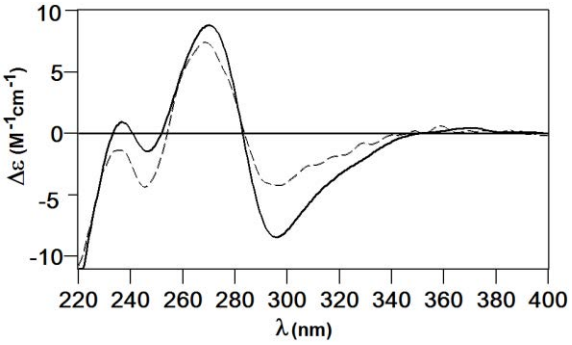 — Cu-NcMT (4 eq. Cu(I)) --- Cu-FvMT (5 eq. Cu(I))
ESI-MS	Cu-NcMT 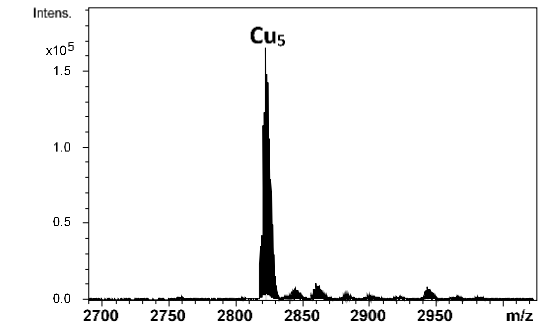 Cu-FvMT 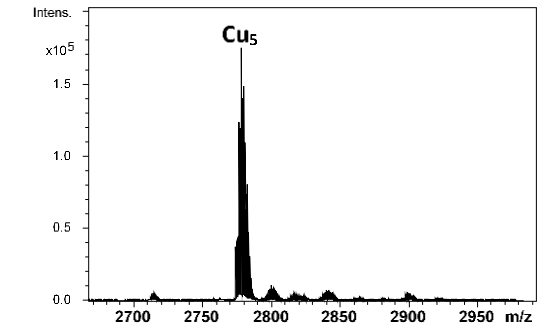	Cu-NcMT 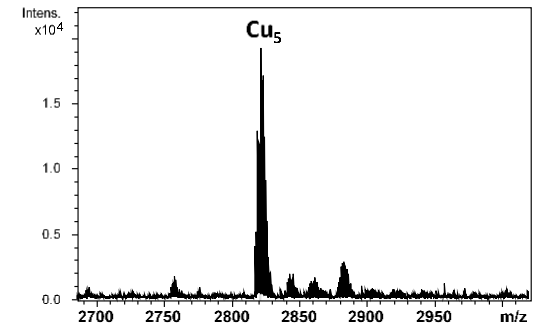 Cu-FvMT 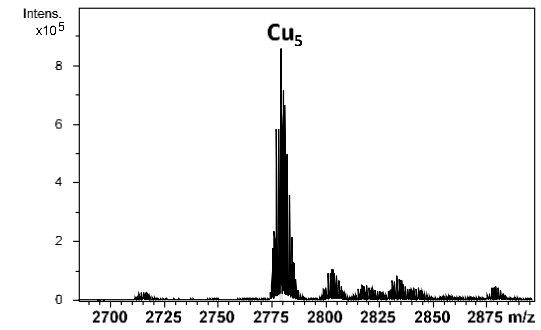

Table 10. Comparison between CD and Deconvoluted ESI-MS spectra of Cu-NcMT and Cu-FvMT *in vivo* and *in vitro*.

The other studied MT with 7 cysteines in the sequence is NcMT2. Despite its 7 cysteines are also perfectly aligned with the 7 ones of NcMT and FvMT (Table 9, section 8), the sequence of NcMT2 is unusually long, consisting in 77 amino acids. The first half of the sequence of this protein does not have any cysteine, focusing all the cysteines in the second half of the sequence. All these produces small changes in the behaviour of this MT against the different metal ions studied.

With Zn(II), NcMT2 is able to form Zn_2-NcMT2 (same specie than NcMT and FvMT), but also the specie Zn_3-NcMT3 more or less with the same importance. With Cu(I) the situation is quite similar. NcMT2 is able to form the Cu_5-NcMT2 cluster, like NcMT and FvMT, but the presence of Cu_6-NcMT2 is

distinguishable, whereas with NcMT and FvMT this specie was not important. Besides, the addition of a high number of Cu(I) equivalents does not produce the unfolding of the Cu_5-NcMT2 cluster, whereas in NcMT and FvMT titrations appeared the Apo-form. Furthermore, with Cd(II), NcMT2 is able to form *in vivo* Cd_3-NcMT2 with considerable stability.

These differences are due to this non-coordinating part of NcMT2 sequence, which confers more stability and allows the protein to form complexes with more metal ions. In addition, despite NcMT2 also can be considered as a Cu-thionein, it seems to have a little more character of Zn-thionein than NcMT and FvMT, due to its capacity to bind divalent metal ions with enough stability.

Therefore, small differences on non-coordinating amino acids are not significant for binding behaviour of MTs, but the addition of a long non-coordinating part in the sequence helps to confer more stable situations and complexes.

On the opposite side, we have CaCup1, a MT with one cysteine less than NcMT, NcMT2 and FvMT. CaCup1 has only 6 cysteines, which are also perfectly aligned with 6 of the 7 cysteines present in the other MT sequences (Table 9, section 8). The lack of this cysteine produces small differences on the behaviour of this MT against the different metal ions studied. With Zn(II) CaCup1 forms the same specie than NcMT and FvMT, Zn_2-CaCup1, but with Cd(II) and Cu(I) the results are significantly different. With Cd(II), unlike NcMT and FvMT, the protein is able to form Cd_xS_y-CaCup1 complexes with considerable structuration and stability. With Cu(I), CaCup1 is not able to form the characteristic cluster with 5 Cu(I) ions. Its 6 cysteines are only capable to bind 4 Cu(I) ions, but not in a very stable situation. Apo-form is present in the *in vivo* productions, and, moreover, the addition of a high number of Cu(I) equivalents *in vitro* produces the unfolding of this Cu_4-CaCup1 specie. Consequently, the presence of 7 cysteines in the sequence seems to be necessary to form the stable cluster Cu_5-MT.

The other two MTs studied from Subfamily 1, UrMT and CipMT1 have 8 cysteines in its sequence. Despite their cysteines have similar patterns than the other studied MTs, the sequences have some differences that produce difficulties to align them with the other ones. One important difference that could be significant is the presence of a motif -CC- in UrMT and CipMT1 sequence.

Between them, there are some differences too. Their cysteines are exactly at the same positions, but the rest of amino acids are slightly different, having UrMT a high quantity of serines (Figure 61).

Figure 61. Comparison of the amino acid sequences of URMT and CipMT1.

The behaviour of both, UrMT and CipMT1 are very similar. With Zn(II) they form the specie Zn_3-MT. Most of the studied MTs with 7 cysteines formed the specie with 2 Zn(II) metal ions as majority specie, so, this extra cysteine and maybe the -CC- motif allows to bind another unity of Zn(II) metal ion with enough stability.

In media cultures with Cu(II) these two proteins are not expressed, which is an important difference with the 7-Cys proteins studied. Probably the position of the cysteines and the -CC- motif produce a poor Cu-thionein character of UrMT and CipMT1, and provide them more affinity for divalent metal ions like Zn(II) or Cd(II).

Their behaviour with Cd could confirm the classification of these two MTs as Zn-thioneins. With this metal ion they form Cd_xS_y-MT complexes, and in the exchange between Zn(II) by Cd(II), heterometallic species Zn_xCd_y-MT are present during almost all the process. This suggests some reluctance for this particular exchange. However, with a big excess of Cd(II), CipMT1 is able to form the homometallic specie Cd_5-CipMT1 as a unique specie in the *in vitro* process. This fact advance considerable higher affinity of CipMT1 for Cd(II) than in the case of UrMT, producing a lower Zn-thionein character of this MT.

Besides the species formed, the CD analysis of UrMT and CipMT1 with the different metal ions are comparable, which helps to confirm the similar behaviour for the two proteins. With Zn(II) they show a plain DC, suggesting a structuration not very high with this metal in the two cases. With cadmium, their spectra are possible to be overlapped, in the case of the *in vivo* and in the exchange *in vitro* (Figure 62).

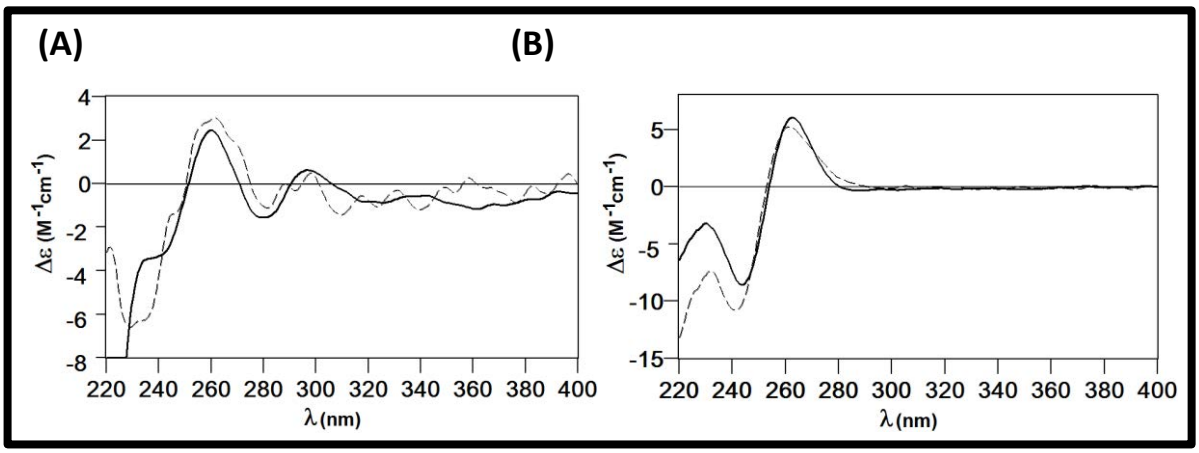

Figure 62. Superposition of Cd-UrMT (black line) and Cd-CipMT1 (dashed line) of both, spectra *in vivo* and *in vitro* (2 equivalents of Cd(II) in the titration).

9. MTs OF SUBFAMILY 2

CipMT2 is the only MT studied from the subfamily 2. It has 9 cysteines in the sequence which are distributed in three motifs -CXC- and a single motif -CXCXXC- already observed on the sequence of the studied MTs from subfamily 1. The cysteines present in the sequence are properly aligned with the cysteines of the 7-Cys MTs studied before, with the lack of the two first ones (Figure 63).

Figure 63. Alignment of the amino acid sequence of CipMT2 with NcMT, one of the 7-Cys MTs studied.

9.1 CipMT2

The sequence of this MT has 34 amino acids and 9 cysteines (Figure 64A). The protein was synthesized recombinantly in Zn-, Cd- and Cu-metal-supplemented cultures, and after its purity and identity was analysed by ESI-MS (pH 2.4). The resultant peak obtained for the apo-form was 3247 Da, value which correlates with the theoretical MW calculated for CipMT2, 3246.7 Da, thus confirming the amino acid sequence (Figure 64B).

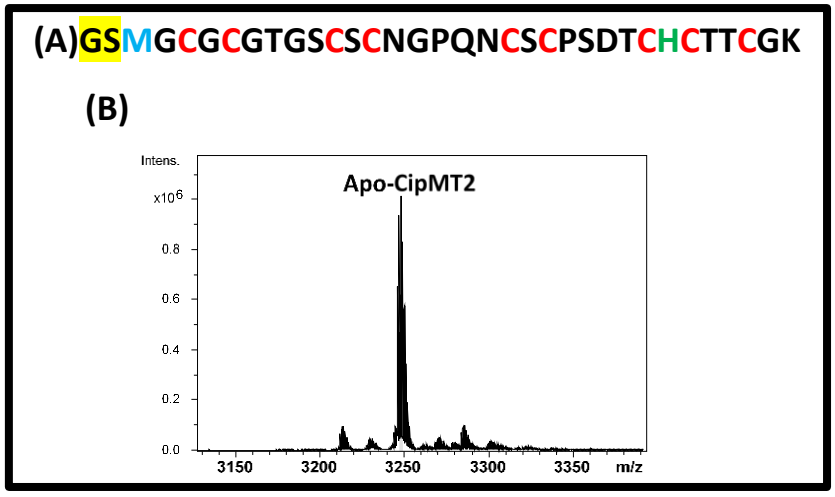

Figure 64. Amino acid sequence of the recombinant CipMT2 isoform and deconvoluted ESI-MS spectrum of the Zn-CipMT2 preparation recorded at pH 2.4, which corresponds to the apo-CipMT2.

Once confirmed the amino acid sequence and the corresponding MW, the behaviour of the protein in the presence of Zn(II), Cd(II) and Cu(II) can be evaluated.

9.1.1 CipMT2 binding Zn(II)

When CipMT2 is synthesized in Zn(II) enriched media, the specie Zn_3-CipMT2 is obtained as a majority specie according to the data obtained by ESI-MS (Figure 65A). This results properly correlates with the value 3.53 Zn(II) metal ions per MT obtained by ICP-AES. In the ESI-MS spectrum, another important peak corresponding to the specie Zn_2Cd_1-CipMT2 is observed, which suggest the presence of contaminant traces of Cd(II) during the production process. This is confirmed by the detection of Cd(II) in ICP-AES analysis, and also by the CD spectrum, which shows an important band at 250 nm, corresponding to the Cd-Cys bond (Figure 65B).

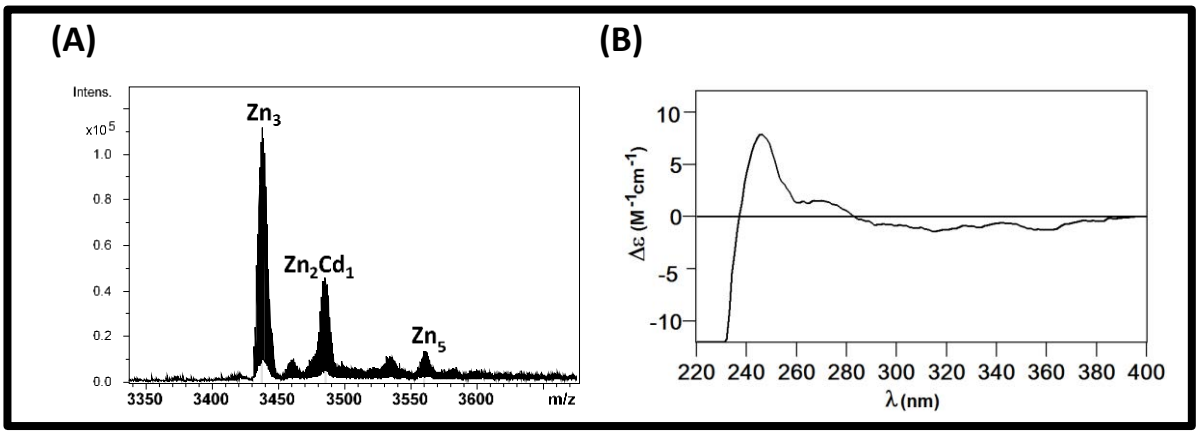

Figure 65. Deconvoluted ESI-MS spectrum of Zn-CipMT2 at pH 7.0 and CD spectrum of the Zn-CipMT2 preparation.

9.1.2 CipMT2 binding Cd(II)

According to the data obtained by ESI-MS (Figure 66A), the biosynthesis of CipMT2 in Cd(II)-enriched media produces the complex Cd_3-CipMT2 as a majority specie. The Cd(II) content was impossible to be confirmed by ICP-AES, because the concentration of the protein was lower than the detection limit for the technique. Conversely, the CD spectrum shows a Gaussian band at 250 nm, characteristic of the Cd-Cys bond. (Figure 66B).

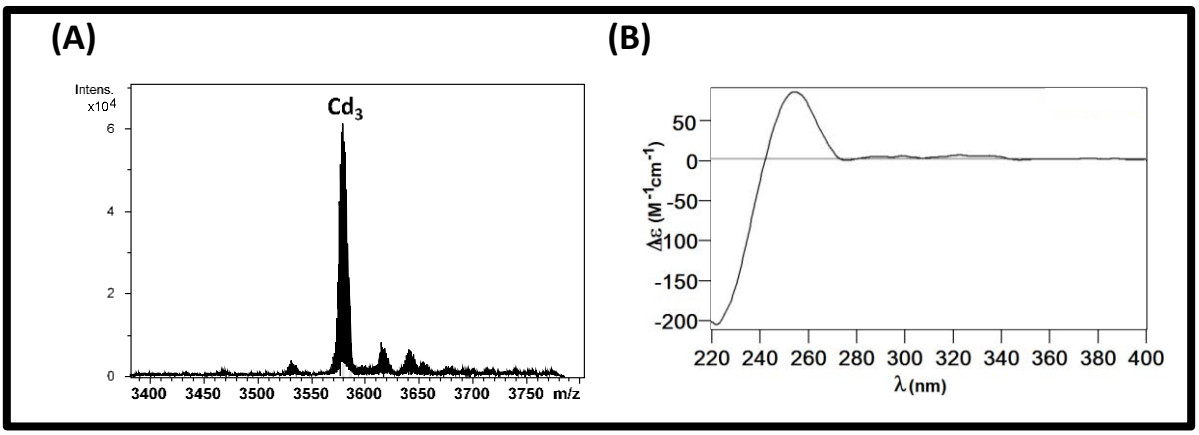

Figure 66. Deconvoluted ESI-MS spectrum of Cd-CipMT2 at pH 7.0 and CD spectrum of the Cd-CipMT2 preparation.

9.1.3 CipMT2 binding Cu(I)

In Cu(II)-enriched media CipMT2 is synthesized forming a mixture of different species, according to the data obtained by ESI-MS (Figure 66). The results at pH 7.0 for cultures at normal and low oxygenation are similar, showing the production of a mixture of species from Cu_4-CipMT2 to Cu_7-CipMT2. However, at pH 2.4 the species Cu_4-CipMT2 and Cu_5-CipMT2 are the most important, observed, together with the Apo-CipMT2 form, suggesting that the protein does not have high affinity for this metal ion. All these results were not possible to be confirmed by ICP-AES and CD, because the concentration of the protein in the solution was under the limit of detection of the techniques.

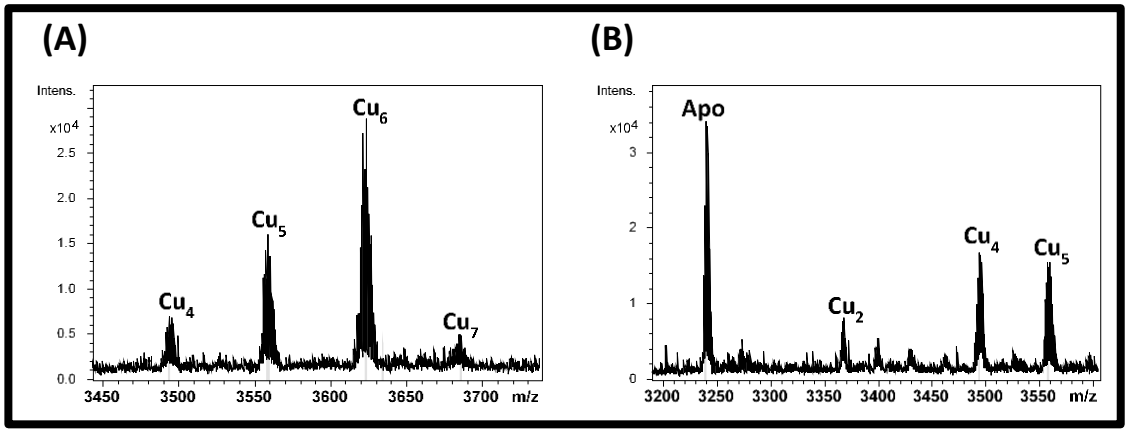

Figure 66. Deconvoluted ESI-MS spectrum of Cu-CipMT2 at pH 7.0 and pH 2.4.

The *in vitro* addition of Cu(I) to a Zn-CipMT2 preparation, followed by CD, UV-Vis and ESI-MS, allows observing the formation of the same species than *in vivo* (Figures 67 and 68). The addition of the first equivalents of Cu(I) to the solution provokes the beginning of the formation of Cu_4-, Cu_5- and Cu_6-CipMT2, but with the Cd(II) contaminant present in the mixture. The addition of further Cu(I) to the solution consolidates Cu_4-, Cu_5- and Cu_6-CipMT2 as majority species, and the apo-form and the Cd(II) contaminant disappear. Finally, the excess of Cu(I) in solution provokes the unfolding of the complexes formed until rendering the apo-specie.

ESI-MS results *in vivo* and *in* vitro are comparable (Figure 69). In both cases the complexes Cu_4-, Cu_5- and Cu_6-CipMT2 are formed as majority species. However, hard conditions like excess of metal, or acidic pH in the case of *in vivo* productions, provoke the unfolding of these complexes by forming the apo-form.

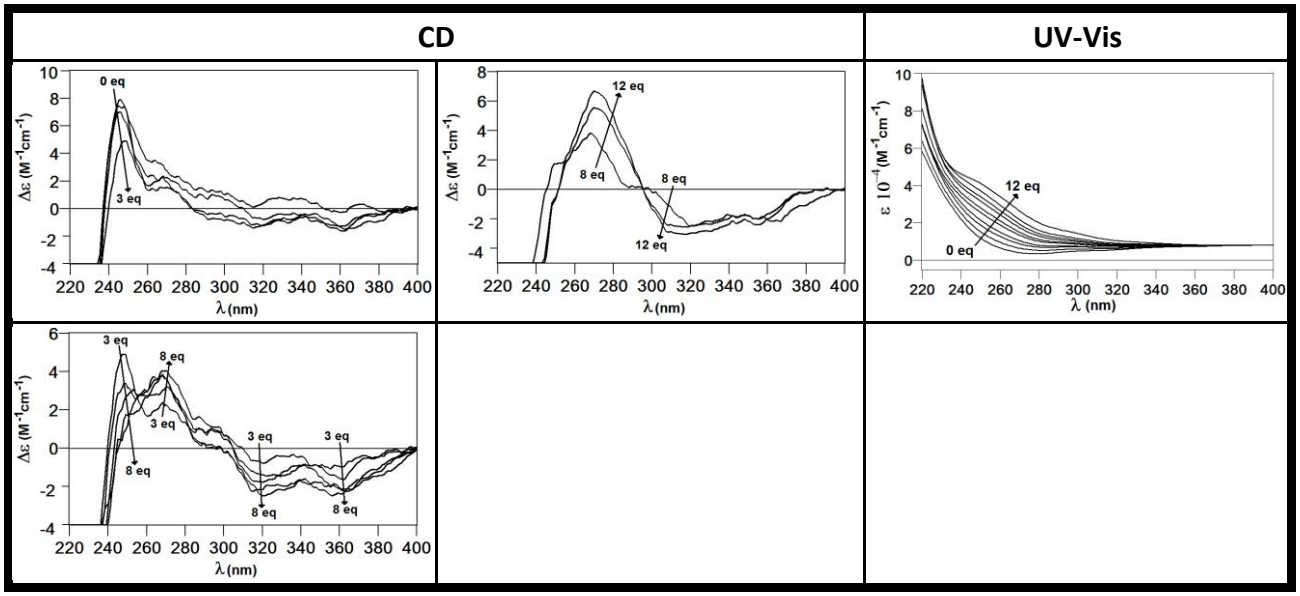

Figure 67. Titration followed by CD and UV-Vis spectroscopies corresponding to the addition of Cu(I) to a solution 4.3 µM of Zn-CipMT2 at pH 7.0 and 25ºC.

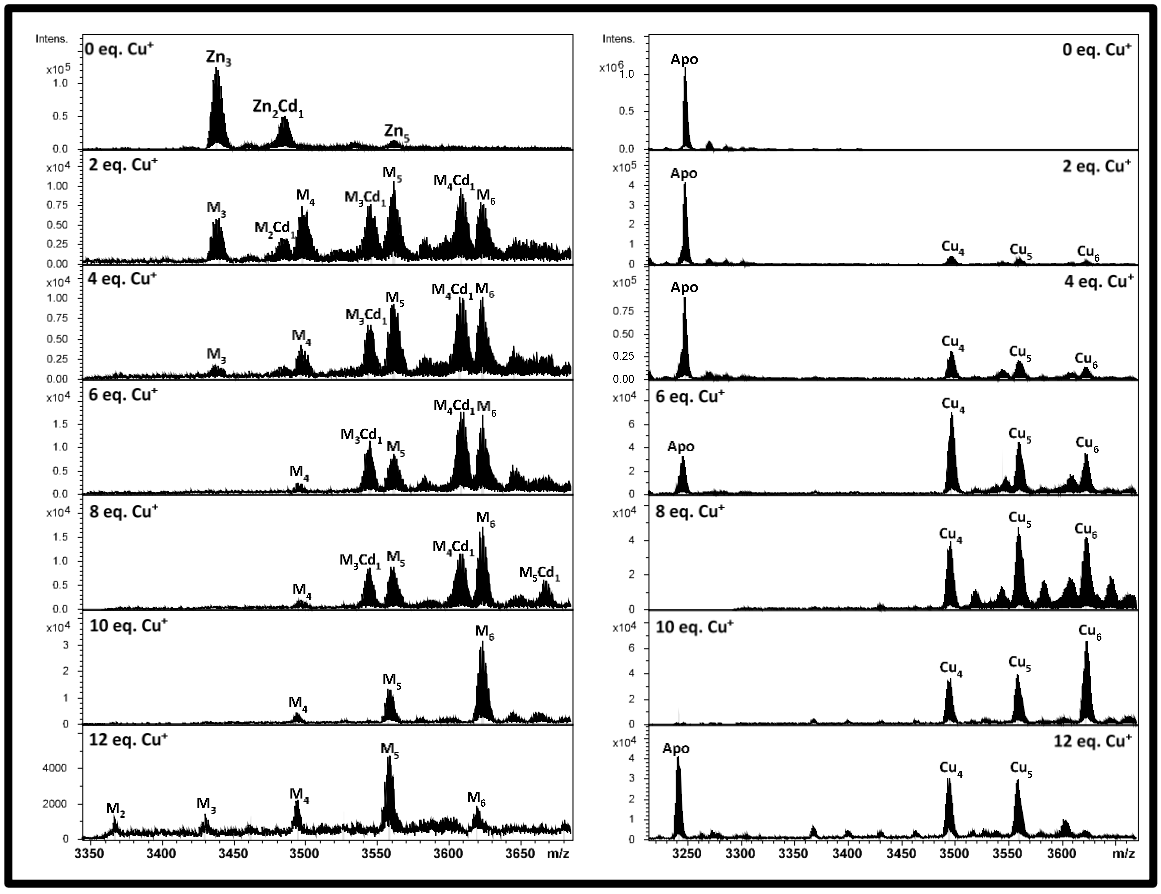

Figure 68. Titration followed by ESI-MS at pH 7.0 and 2.4, corresponding to the addition of Cu(I) to a solution 4.3 µM of Zn-CipMT2.

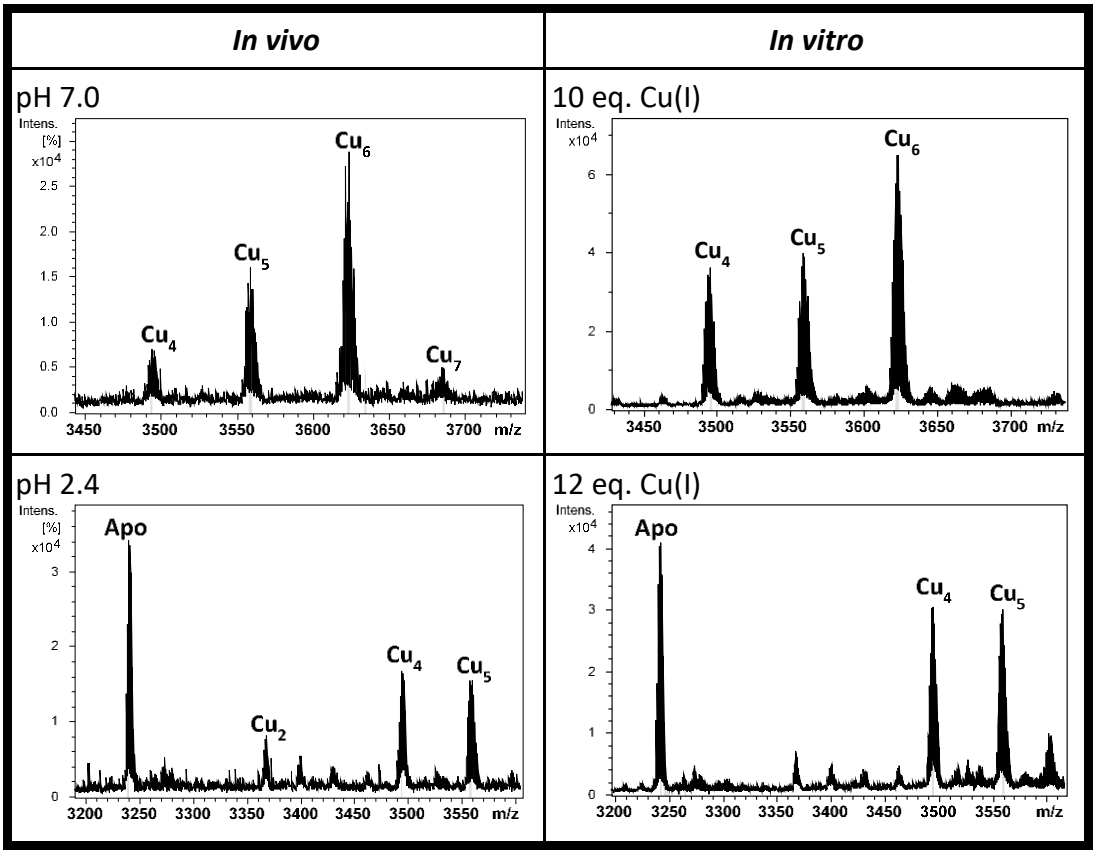

Figure 69. Comparison of ESI-MS spectra of Cu-CipMT2 preparation *in vivo* and *in vitro*

9.2 Discussion subfamily 2

As is explained in section 9, CipMT2 has 9 cysteines, 7 of which are properly aligned with the 7 cysteines of the corresponding 7-Cys MTs from subfamily 1. The similar sequence produces similar properties and similar behaviour against the different metal ions, but the two extra cysteines confer it the capacity to form complexes with more metal ions.

In Zn(II) enriched media, while NcMT and FvMT form Zn_2-MT as majority specie, CipMT2, are able to bind one Zn(II) metal ion more by forming Zn_3-CipMT2, thanks to the two extra cysteines. With Cd(II) the protein forms the complex Cd_3-CipMT2, although not with high concentration. This Cd_3-MT complex is also formed in other Cd cultures of MTs with 7 cysteines, like NcMT and NcMT2. On the other hand, in Cu(II) enriched media, the protein is synthesized by forming different Cu(I) species, being Cu_6-CipMT2 the most important. But, in contrast with the high stable clusters Cu_5-NcMT and Cu_5-FvMT, the species formed with CipMT2 destabilize in hard conditions like acid pH or excess of Cu(I) metal ion. This could mean that the cluster formed between 5 Cu(I) and 7 cysteines are very stable, and the proteins tend to form this kind of cluster. So, the presences of more cysteines or more metal ions do not produce higher stability to the protein.

10. MTs OF SUBFAMILY 3

Four different proteins have been studied from the subfamily 3. Two MTs with 12 cysteines, CaCRD2 and SbMT; and two MTs with 16 cysteines, SaMT and NcMT1. Table 12 summarize the 4 MT sequences with the alignment between their cysteines.

ORGANISM	MT	SEQUENCE	aa	C
Candida albicans	CaCRD2	----------MACSAAQ-CVCAQKSTCSCGKQPALKCNCSKASVENVVPSSNDA CACGKRNKSSCTCGANAICDGTRDGETDFTNLK	78	12
Sporothrix brasiliensis	SbMT	-----MVSSTCCGKGGAECVCAQNATCSCGKQSALHCNCDRAATENNTAGDR- CSCGQRPAGACTCATNPSEVNTANETDFTTRK	81	12
Scedosporium Apiospermum	SaMT	----MSPADTCCRKGEGACVCAQQATCSCGKQSALHCTCDKAAVENTISGPS- CSCGSRPVGQCTCENATVENQKPTGATCGCGARPAGSCTCNNSANETDFTTKK	103	16
Neurospora crassa	NcMT1	MSAPVAKASTCCGKS-AECICAKQATCSCGKQSALHCTCDKANSENAVEGPR- CSCRARPAGQCTCDRASTENQKPTGNACACGTRPADACTCEKAADGGFKPTDLETDFTTKN	114	16

Table 11. Alignment of MT sequences studied from subfamily 3, with the number of amino acids (aa) and cysteines (in red). Also histidines (in green) and methionines (in blue) are marked.

The sequences of SaMT and NcMT1 are very similar, having their cysteines practically at the same positions. SbMT has four cysteines less than the two MTs mentioned above, but its 12 cysteines are also possible to be aligned properly.

These three sequences have an initial doublet -CC- and the rest of cysteines are grouped in motifs -CXC-. This is an important difference with CaCRD2, which has also the cysteines in motifs -CXC- but two cysteines are single at the beginning and at the end of the sequence, instead to be an initial doublet.

10.1 CaCRD2

The sequence of CaCRD2 has 78 amino acids and 12 cysteines (Figure 70A). After the recombinant synthesis of this protein in different metal-supplemented cultures, its purity and identity was analysed by ESI-MS (pH 2.4). The peak obtained for the apo-form was 7890 Da. This value correlates with the theoretical MW calculated for CaCRD2, 7890.9 Da, thus confirming the identity of the amino acid sequence (Figure 70B).

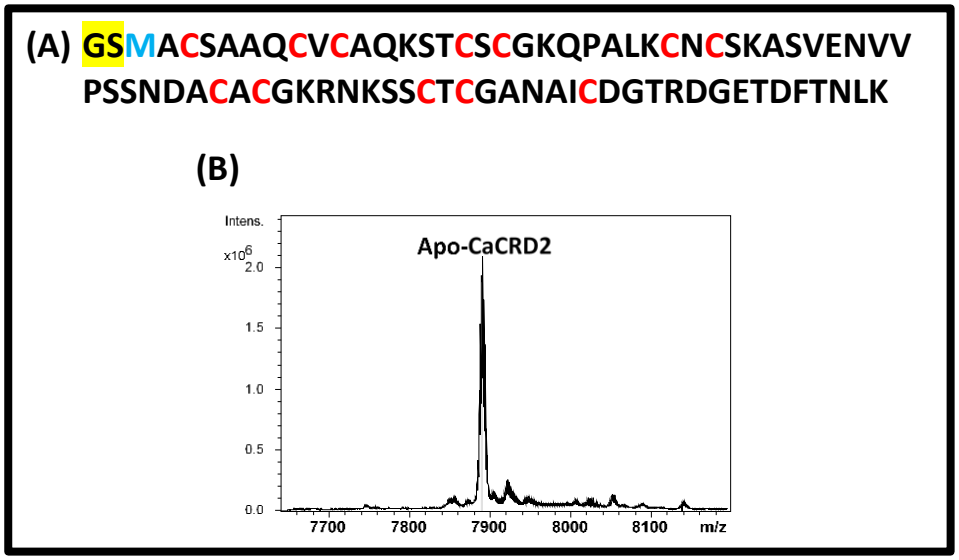

Figure 70. Amino acid sequence of the recombinant CaCRD2 isoform and deconvoluted ESI-MS spectrum of the Zn-CaCRD2 preparation recorded at pH 2.4, which corresponds to the apo-CaCRD2.

Once confirmed the amino acid sequence and the corresponding MW, the behaviour of the protein in the presence of Zn(II), Cd(II) and Cu(II) can be analysed.

10.1.1 CaCRD2 binding Zn(II)

According to the data obtained by ESI-MS (Figure 71), when CaCRD2 is synthesized in Zn(II)-enriched media the complex Zn_3-CaCRD2 is produced as majority specie. This result correlates quite well with the value 2.69 Zn(II) per MT obtained by ICP-AES. The lack of signals after 240 nm in the DC spectrum indicates that the structuration of the protein about Zn(II) is poor (Figure 71B).

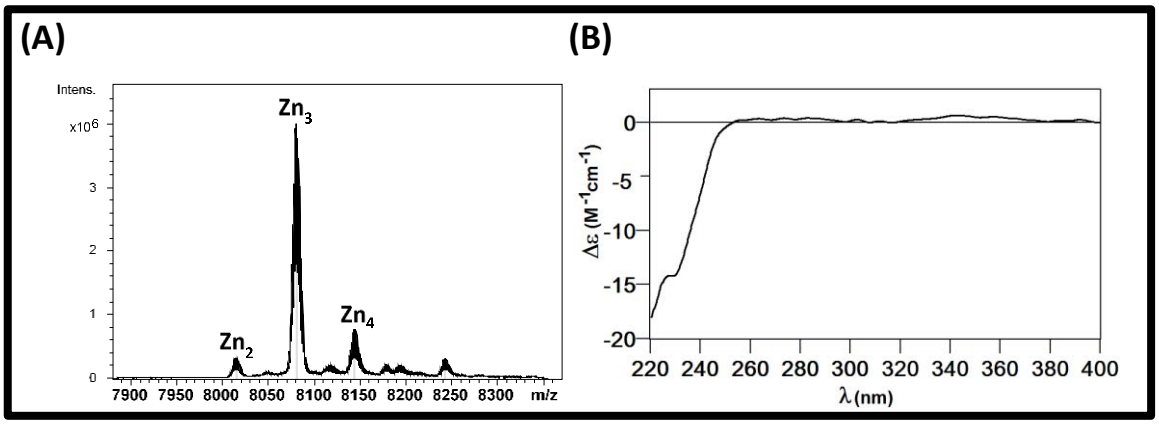

Figure 71. Deconvoluted ESI-MS spectrum of Zn-CaCRD2 at pH 7.0 and CD spectrum of the Zn-CaCRD2 preparation

10.1.2 CaCRD2 binding Cd(II)

When the protein is synthesized in Cd(II)-supplemented cultures, the ESI-MS spectrum shows a mixture formed by the specie Cd_4-CaCRD2 and different Cd_xS_y-CaCRD2 complexes (Figure 72A). The presence of S^{2-} ligands was corroborated by the low Cd-to-S ratio measured by ICP-AES. On the other hand, the CD spectrum shows a Gaussian band at 250 nm, related with the Cd-Cys bond, and bands between 270 to 290 nm, characteristic of the Cd-S^{2-} bond (Figure 72B).

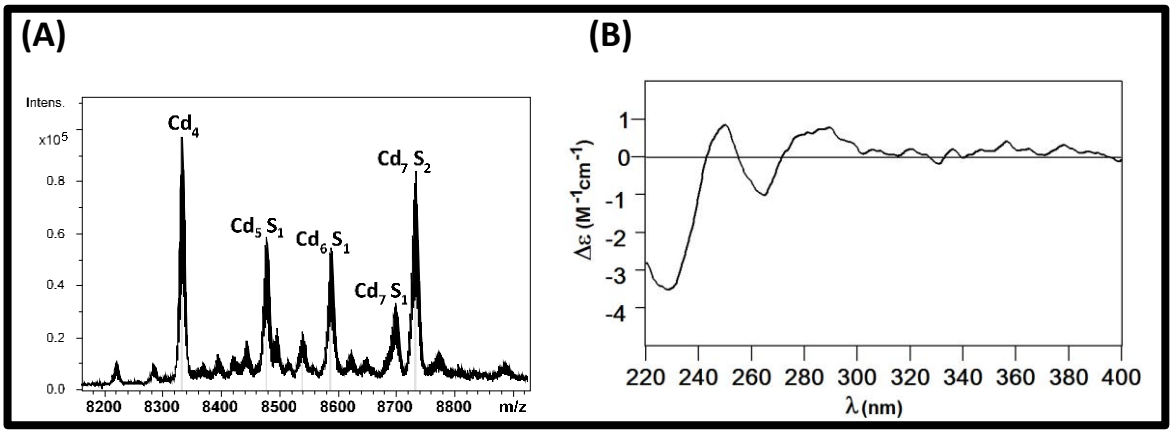

Figure 72. Deconvoluted ESI-MS and CD spectra of the Cd-CaCRD2 preparation, recorded both at pH 7.0

10.1.3 CaCRD2 binding Cu(I)

In Cu(II)-enriched media, the protein is synthesized successfully at normal oxygenation, but unsuccessfully at low oxygenation cultures. Besides, different spectra are obtained at pH7 and pH 2.4. The ESI-MS spectrum for normal oxygenation production at pH 7 shows a mixture of Cu(I) species where the majority specie is Cu_9-CaCRD2. However, at pH 2.4 the protein seems to be less stable and the majority species observed are Cu_4-CaCRD2 and Cu_5-CaCRD2. The ICP analysis indicates a content of 9.84 Cu(I) ions per molecule, which reinforce quite well ESI-MS results. On the other hand, the concentration of the protein is under the detection limit for DC analysis, so any corroboration of the last results was possible with this technique.

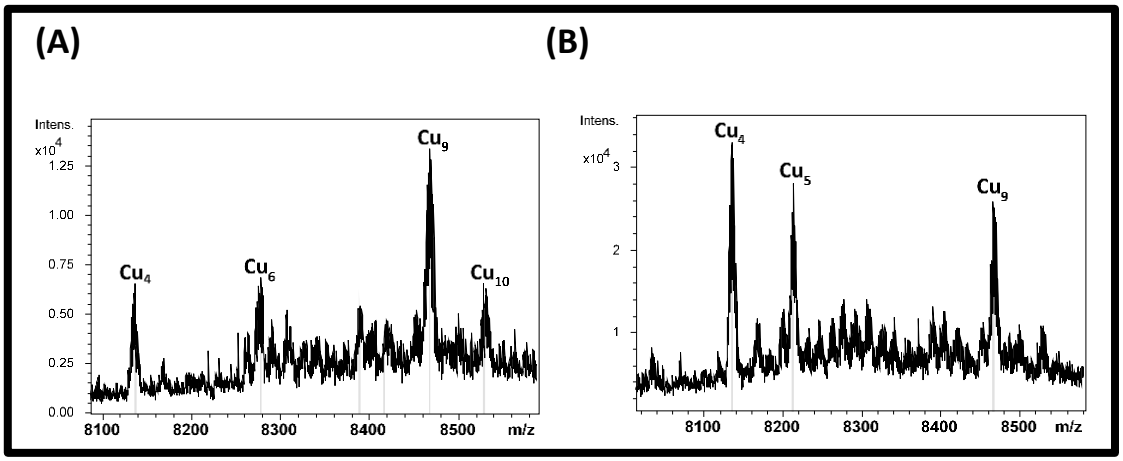

Figure 73. Deconvoluted ESI-MS spectra, recorded at pH 7.0 and 2.4 of Cu-CaCRD2 preparation.

The *in vitro* addition of Cu(I) to the Zn-CaCRD2 preparation, followed by CD, UV-Vis and ESI-MS, allowed observing the formation of a mixture where Cu_4-CaCRD2 and Cu_8-CaCRD2 are the majority species. According to the CD, ESI-MS and UV-Vis data, the addition of further Cu(I) to the solution does not provoke additional binding of Cu but the unfolding of the formed clusters until rendering the apo-species (Figures 74 and 75).

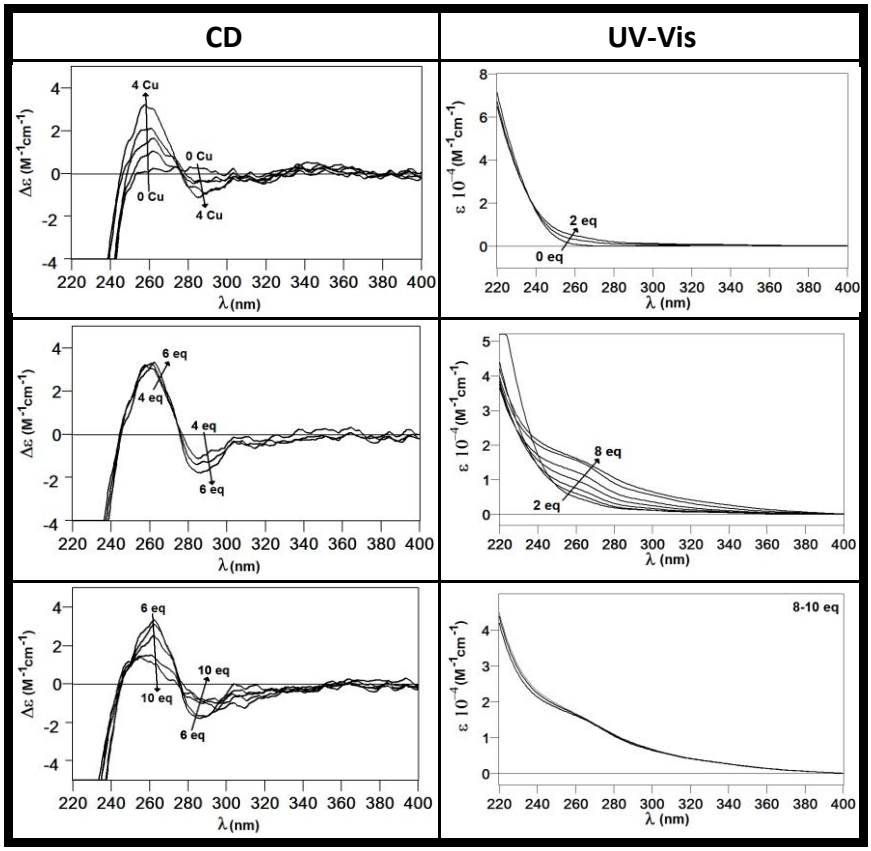

Figure 74. Titration followed by CD and UV-Vis spectroscopies corresponding to the addition of Cu(I) to a solution 20.1 µM of Zn-CaCRD2 at pH 7.0 and 25ºC.

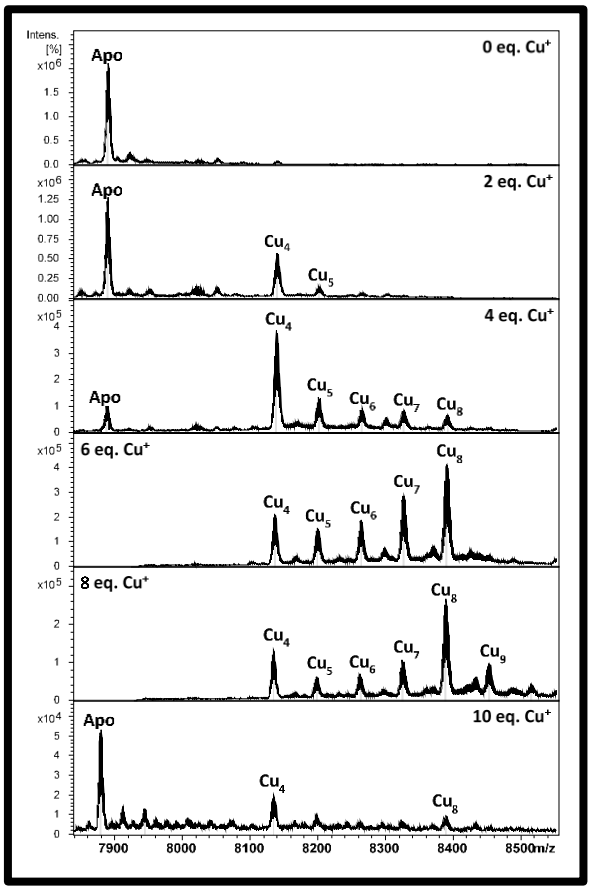

Figure 75. Titration followed by ESI-MS at pH 2.4, corresponding to the addition of Cu(I) to a solution 20.1 µM of Zn-CaCRD2.

The results obtained *in vivo* and *in vitro* are slightly different. *In vitro* the Cu(I) is added slowly and a mixture of species with Cu(I) are formed properly, being Cu_4-CaCRD2 and Cu_8-CaCRD2 the majority ones. *In vivo*, the excess of Cu(I) is present from the beginning, providing a higher availability of the metal. For this reason, in the mixture of species with Cu(I) formed *in vivo*, the prominent specie is Cu_9-CaCRD2, which has one Cu(I) metal ion more than *in vitro* (Figure 76).

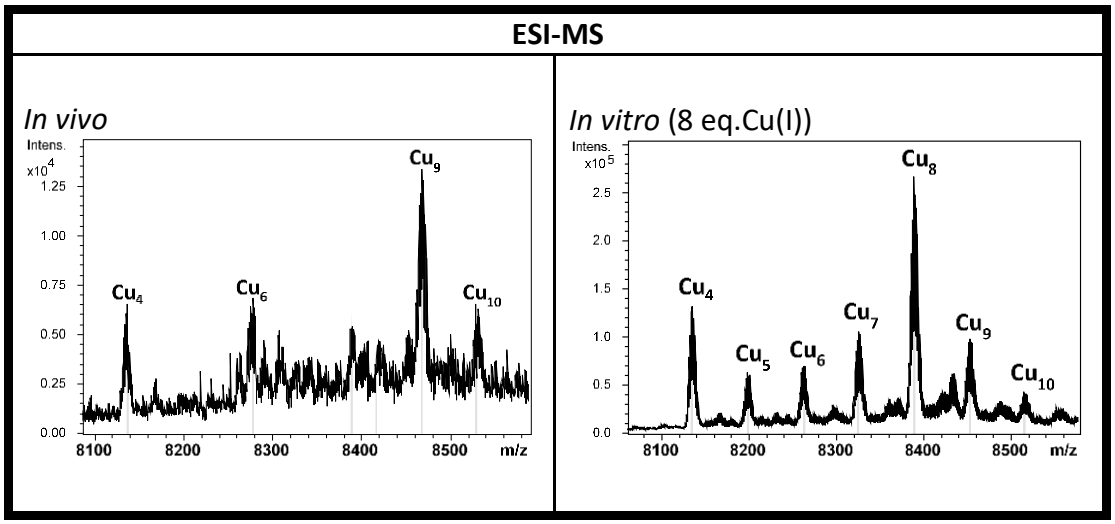

Figure 76. Superposition and comparison of ESI-MS spectra of Cu-CaCRD2 preparation *in vivo* and *in vitro*

10.2 SbMT

The sequence of SbMT has 81 amino acids and 12 cysteines. The protein was synthesized recombinantly in Zn-, Cd- and Cu- metal supplemented cultures, and after its purity and identity was analysed by ESI-MS (pH 2.4). The resultant peak obtained for the apo-form was 8190 Da, value which correlates with the theoretical MW calculated for SbMT, 8189.0 Da, thus confirming the amino acid sequence (Figure 77B).

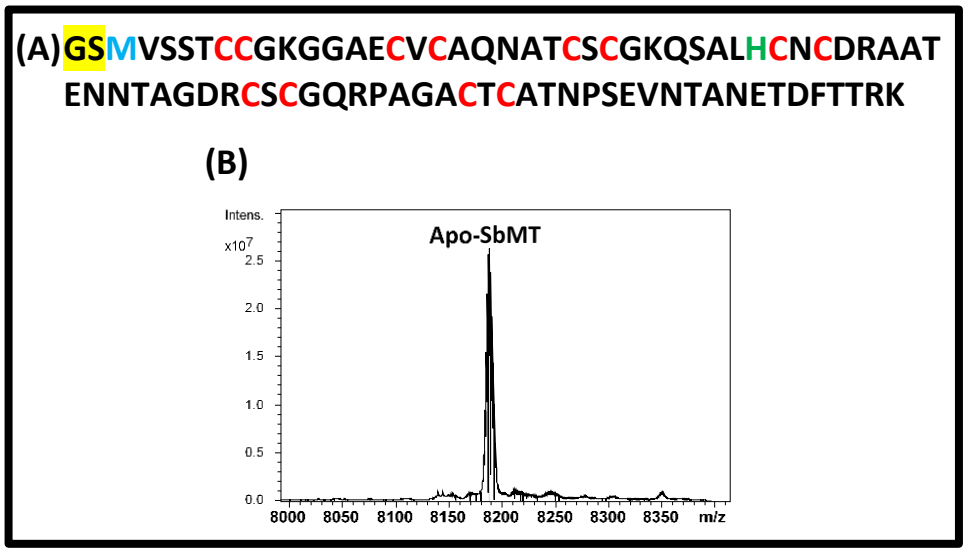

Figure 77. Amino acid sequence of the recombinant SbMT isoform and deconvoluted ESI-MS spectrum of the Zn-SbMT preparation recorded at pH 2.4, which corresponds to the apo-SbMT.

Once confirmed the amino acid sequence and the corresponding MW, the behaviour of the protein in the presence of Zn(II), Cd(II) and Cu(II) can be discussed.

10.2.1 SbMT binding Zn(II)

According to the data obtained by ESI-MS (Figure 78A), when SbMT is synthesized in Zn(II)-enriched media, an almost equimolar mixture of two different complexes Zn_3-SbMT and Zn_4-SbMT is obtained. This result is corroborated by the value 3.2 Zn(II) per MT obtained in ICP-AES analysis. On the other hand, the CD analysis indicates that the structuration of the protein about Zn(II) is poor, because of the lack of signals after 240 nm (Figure 78B).

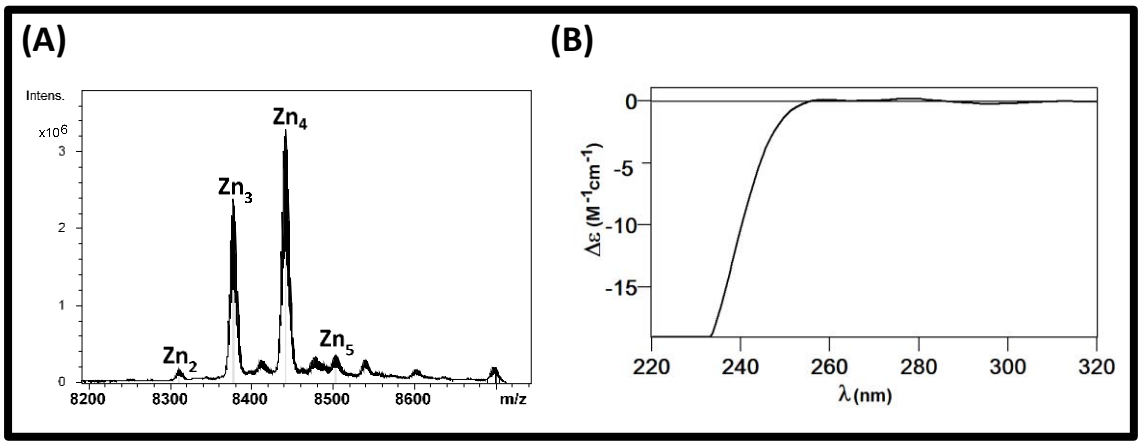

Figure 78. Deconvoluted ESI-MS spectrum of Zn-SbMT at pH 7.0 and CD spectrum of the Zn-SbMT preparation.

10.2.2 SbMT binding Cd(II)

When the protein is synthesized in Cd(II)-supplemented cultures, species Cd_xS_y-SbMT are mainly produced, despite traces of Cd_4-SbMT and Cd_5-SbMT are also present (Figure 79A). The majority species formed in the mixture are Cd_6S_1-SbMT and Cd_5S_1-SbMT. The presence of S^{2-} ligands was corroborated by the low Cd-to-S ratio measured by ICP-AES. On the other hand, the CD spectrum shows a Gaussian band at 250 nm, related with the Cd-Cys bond, and another band at 280 nm, characteristic of the Cd-S^{2-} bond (Figure 79B).

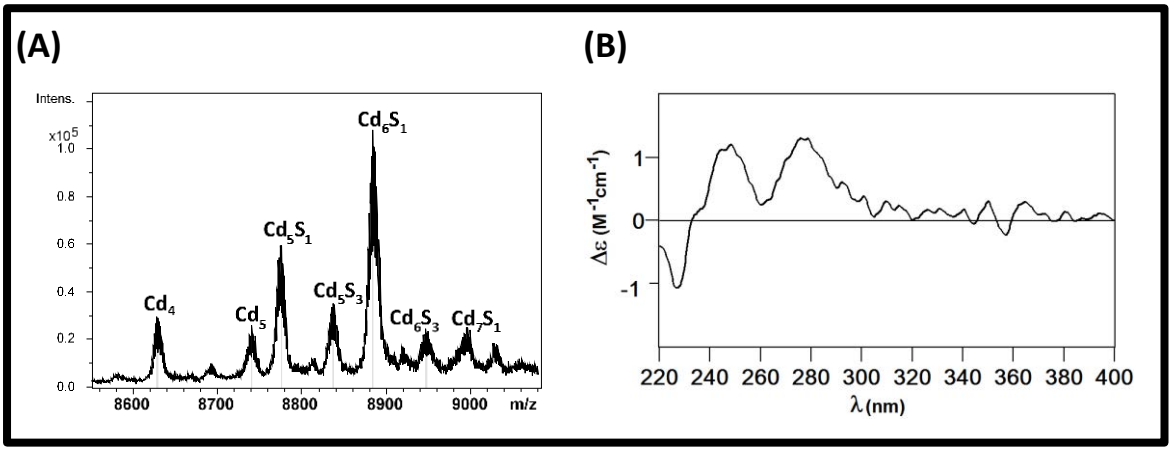

Figure 79. Deconvoluted ESI-MS spectrum of Cd-SbMT at pH 7.0 and CD spectrum of the Cd-SbMT preparation.

10.2.3 SbMT binding Cu(I)

When SbMT is produced in Cu(II)-enriched media, the ESI-MS results obtained for the productions at normal and low oxygenation of the cultures are slightly different (Figure 80A and 80B). At normal oxygenation, a mixture of different species is obtained, where the majority ones are Cu_8-SbMT and Cu_9-SbMT. By contrast, at low oxygenation the majority species are the same, but Cu_8-SbMT is

significantly more prominent. In both productions, the concentration of the protein was lower than the detection limit of CD and ICP-AES analysis, thus impairing to confirm the Cu content.

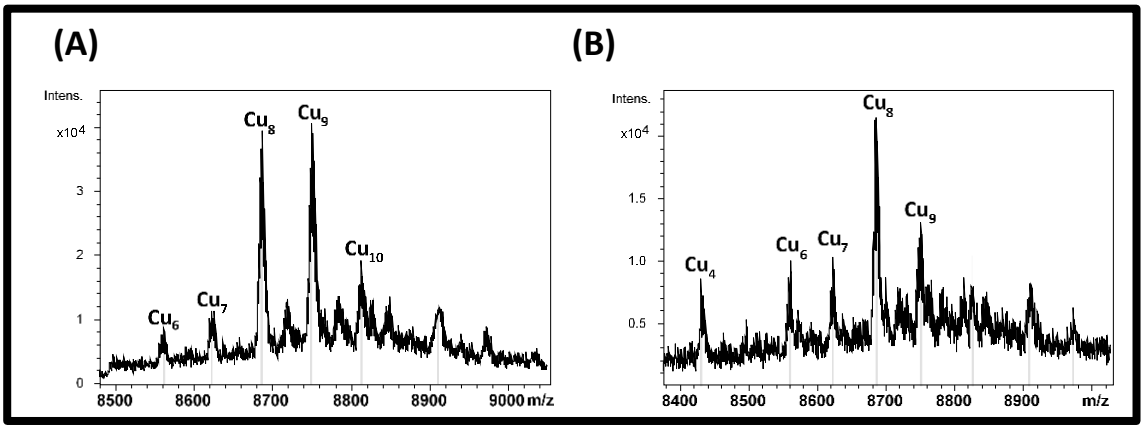

Figure 80. Deconvoluted ESI-MS spectrum of Cu-SbMT at pH 7.0 of normal and low oxygenation cultures.

The *in vitro* addition of Cu(I) to a Zn-SbMT preparation, followed by CD, UV-Vis and ESI-MS, allows observing the formation of a mixture of Cu-species where Cu_8-SbMT and Cu_9-SbMT are the majority ones. According to the CD, ESI-MS and UV-Vis data, the addition of further Cu(I) to the solution do not provoke additional binding of Cu but the unfolding of the formed species (Figures 81 and 82).

The same majority species Cu_8-SbMT and Cu_9-SbMT are formed in both cases, *in vitro* and *in vivo*. Consequently, the ESI-MS *in vivo* spectra of the Cu-preparation can be compared with the *in vitro* spectra, during the stage of the titration where these species are present (Figure 83).

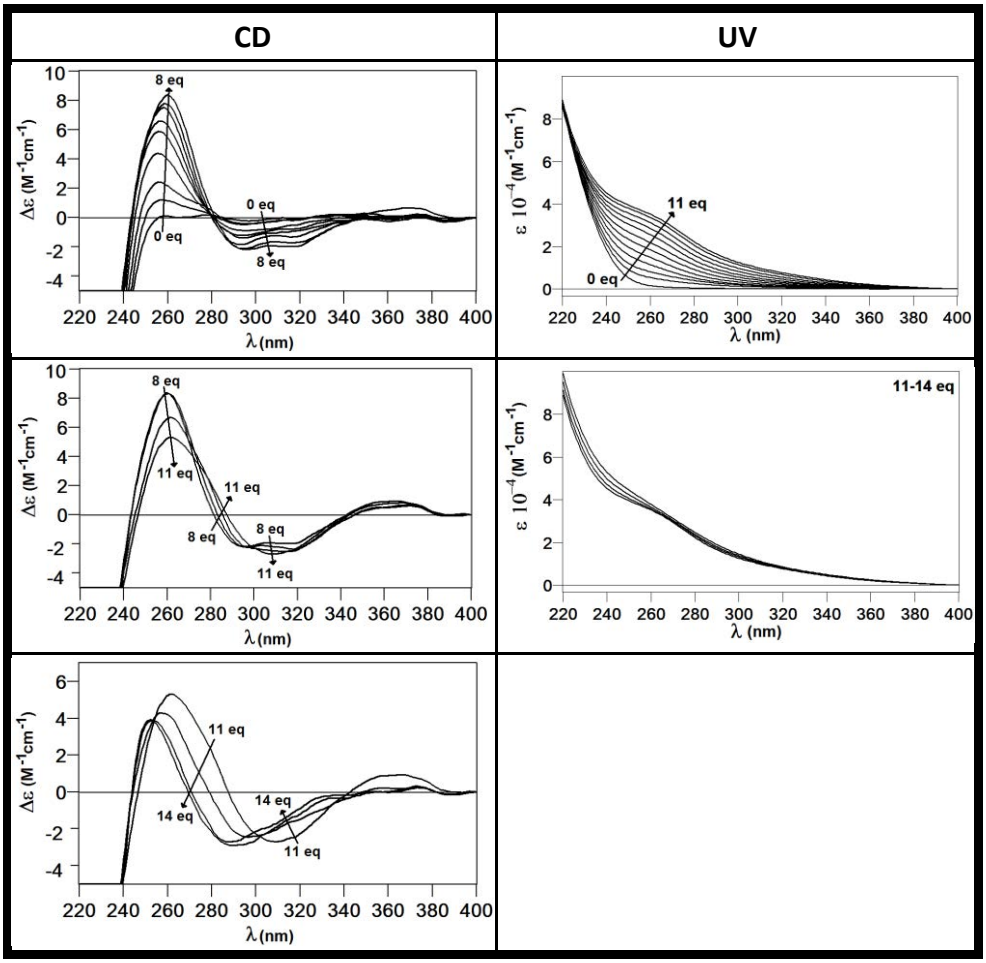

Figure 81. Titration followed by CD and UV-Vis spectroscopies corresponding to the addition of Cu(I) to a solution 17.9 µM of Zn-SbMT at pH 7.0 and 25ºC.

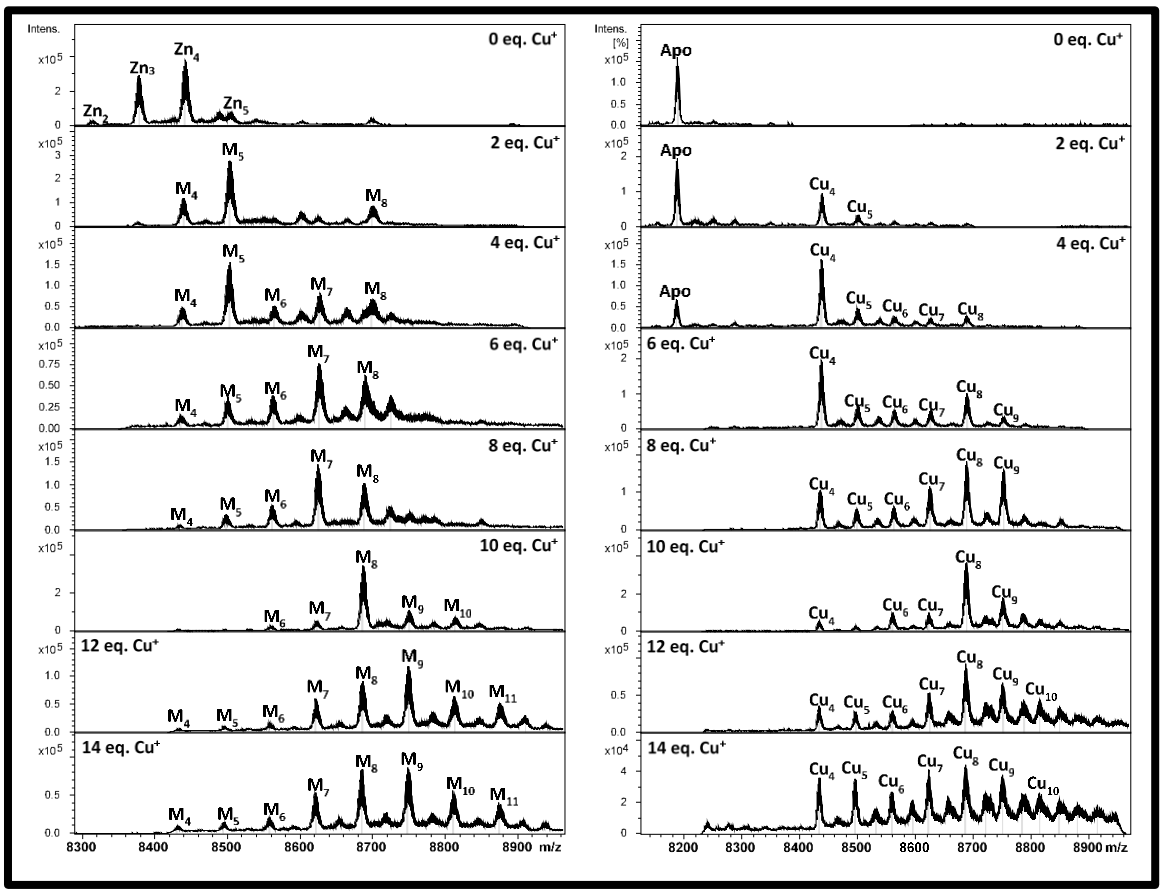

Figure 82. Titration followed by ESI-MS at pH 7 and 2.4 corresponding to the addition of Cu(I) to a solution 17.9 µM of Zn-SbMT.

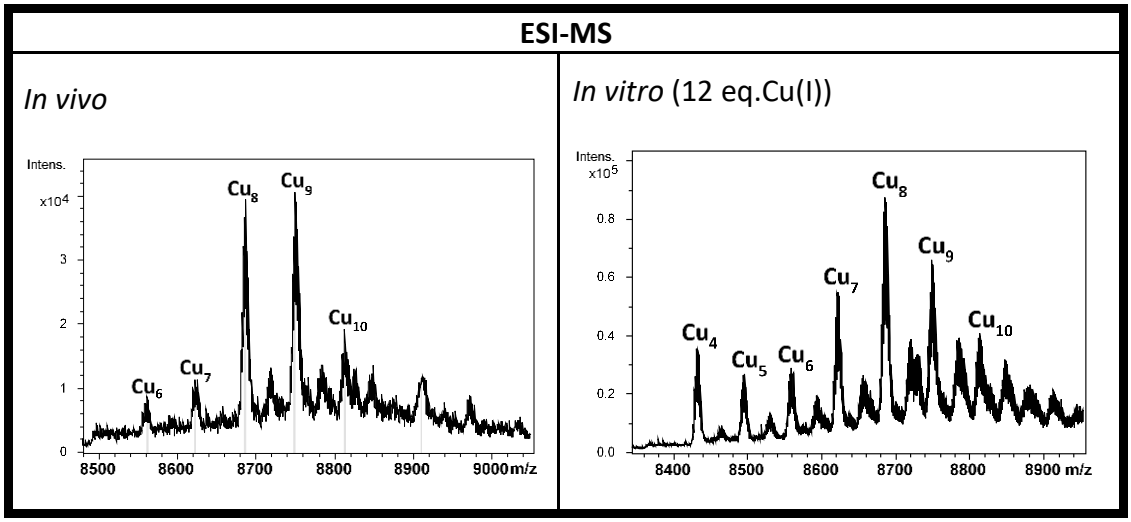

Figure 83. Superposition and comparison of ESI-MS spectra of Cu-SbMT preparation *in vivo* and *in vitro*

10.3 SaMT

The sequence of SaMT has 103 amino acids and 16 cysteines. The protein was synthesized recombinantly in Zn-, Cd- and Cu- metal supplemented cultures, and after its purity and identity was analysed by ESI-MS (pH 2.4). The resultant peak obtained for the apo-form was 10310 Da, value which correlates with the theoretical MW calculated for SaMT, 10310.5 Da, thus confirming the amino acid sequence (Figure 84B).

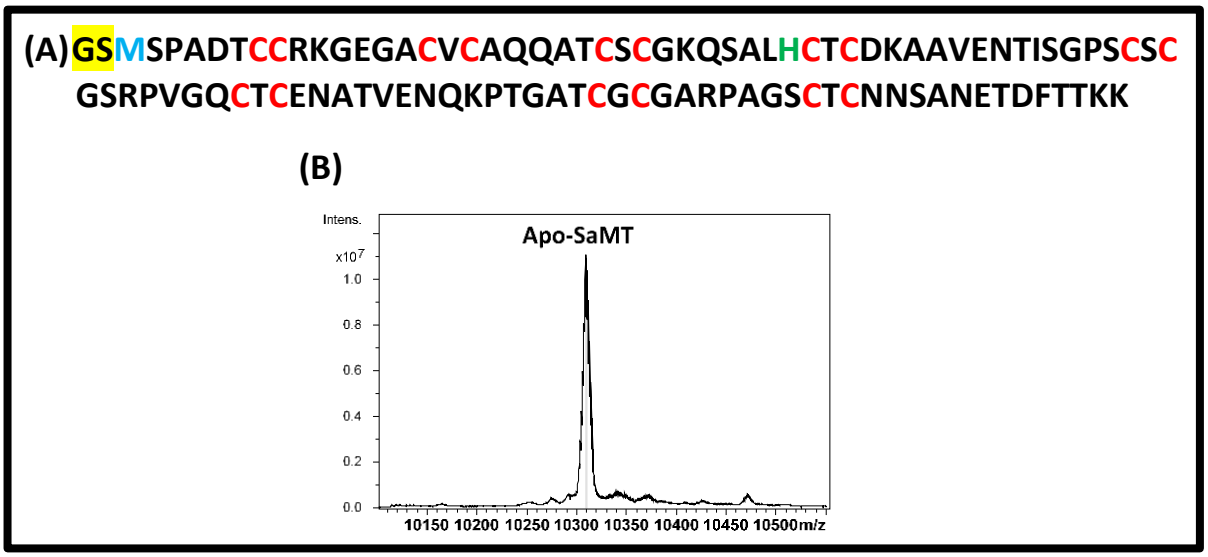

Figure 84. Amino acid sequence of the recombinant SaMT isoform and deconvoluted ESI-MS spectrum of the Zn-SaMT preparation recorded at pH 2.4, which corresponds to the apo-SaMT.

Once confirmed the amino acid sequence and the corresponding MW, the behaviour of the protein in the presence of Zn(II), Cd(II) and Cu(II) can be analysed.

10.3.1 SaMT binding Zn(II)

According to the data obtained by ESI-MS (Figure 85A), when SaMT is synthesized in Zn(II)-enriched media, the majority specie formed is Zn_5-SaMT, also with important presence of Zn_4-SaMT. This result is slightly above the value 3.64 Zn(II) per MT obtained in ICP-AES analysis, probably due to the presence of important species with less Zn(II) content. On the other hand, the CD analysis indicates that the structuration of the protein about Zn(II) is poor, because of the lack of signals after 240 nm (Figure 85B).

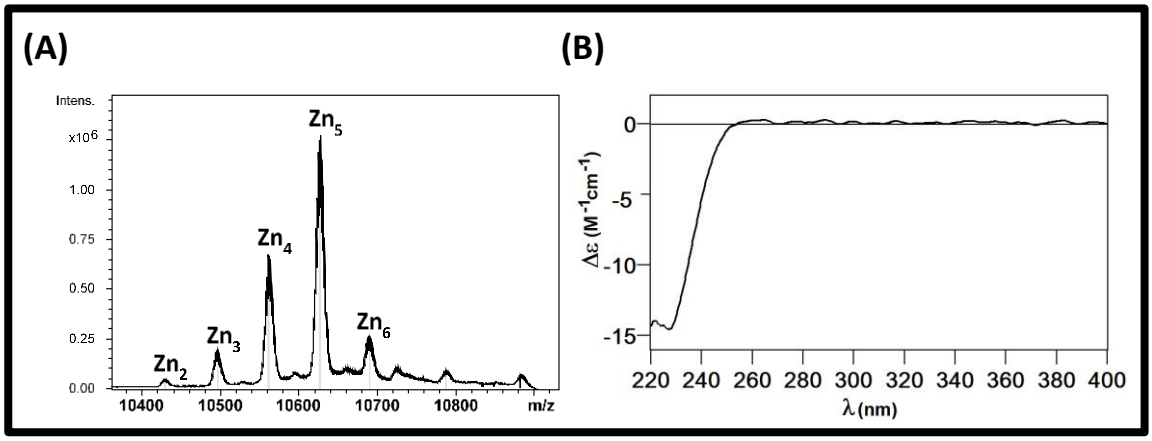

Figure 85. Deconvoluted ESI-MS spectrum of Zn-SaMT at pH 7.0 and CD spectrum of the Zn-SaMT preparation.

10.3.2 SaMT behaviour against Cd(II)

When the protein is synthesized in Cd(II)-supplemented cultures, the complex Cd_8S-SaMT is produced as majority specie (Figure 86A). The presence of S^{2-} ligands is corroborated by the low Cd-to-S ratio measured by ICP-AES. On the other hand, the CD spectrum shows a Gaussian band at 250 nm, related with the Cd-Cys bond, and an exciton coupling at 280 nm, characteristic of the Cd-S^{2-} bond (Figure 86B).

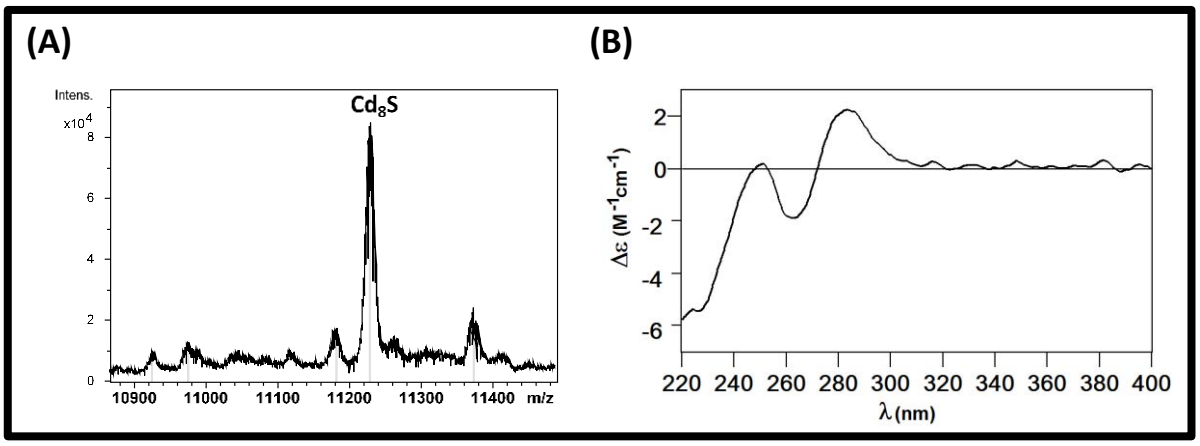

Figure 86. Deconvoluted ESI-MS spectrum of Cd-SaMT at pH 7.0 and CD spectrum of the Cd-SaMT preparation.

10.3.3 SaMT binding Cu(I)

When SaMT is produced in Cu(II)-enriched media, the ESI-MS results obtained for the productions at normal and low oxygenation show the formation of a big mixture of Cu(I) species (Figure 87A and 87B). The mixture formed consists on species with content between 8 to 16 Cu(I) metal ions per MT where the most important specie is Cu_{11}-SaMT. The concentration of the species present is lower than the detection limit of CD and ICP-AES analysis, thus impairing to confirm the Cu content.

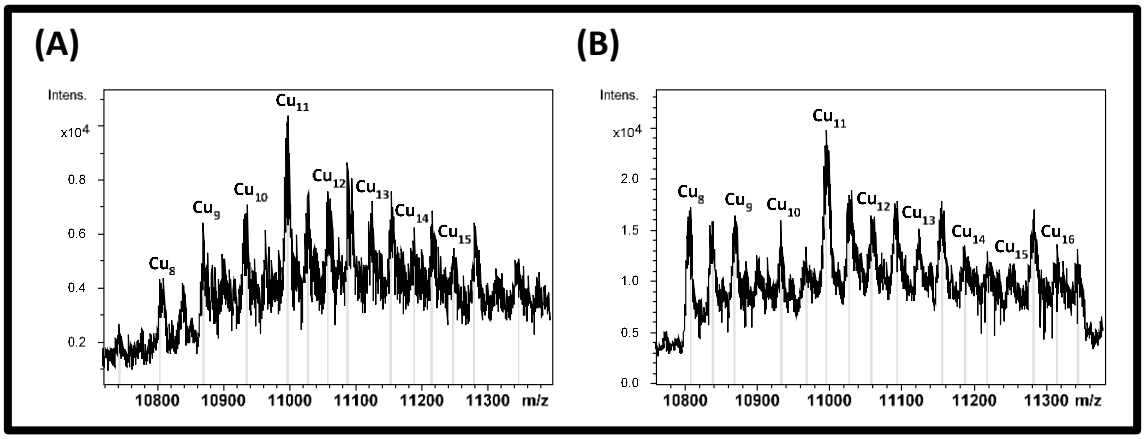

Figure 87. Deconvoluted ESI-MS spectrum of Cu-SaMT at normal and low oxygenation recorded at pH 7.

Due to the necessity to dissolve the Zn-SaMT preparation to avoid the signal saturation in CD analysis, the monitoring of the *in vitro* Cu-SaMT formation by CD, UV-Vis and ESI-MS was impossible. The low concentration of the resultant solution impedes to overcome the detection limit of the techniques.

10.4 NcMT1

The sequence of NcMT1 has 114 amino acids and 16 cysteines. The protein was synthesized recombinantly in Zn-, Cd- and Cu- metal supplemented cultures, and after, its purity and identity was analysed by ESI-MS (pH 2.4). The resultant peak obtained for the apo-form was 11624 Da, value which correlates with the theoretical MW calculated for NcMT1, 11624.0 Da, thus confirming the amino acid sequence (Figure 88B).

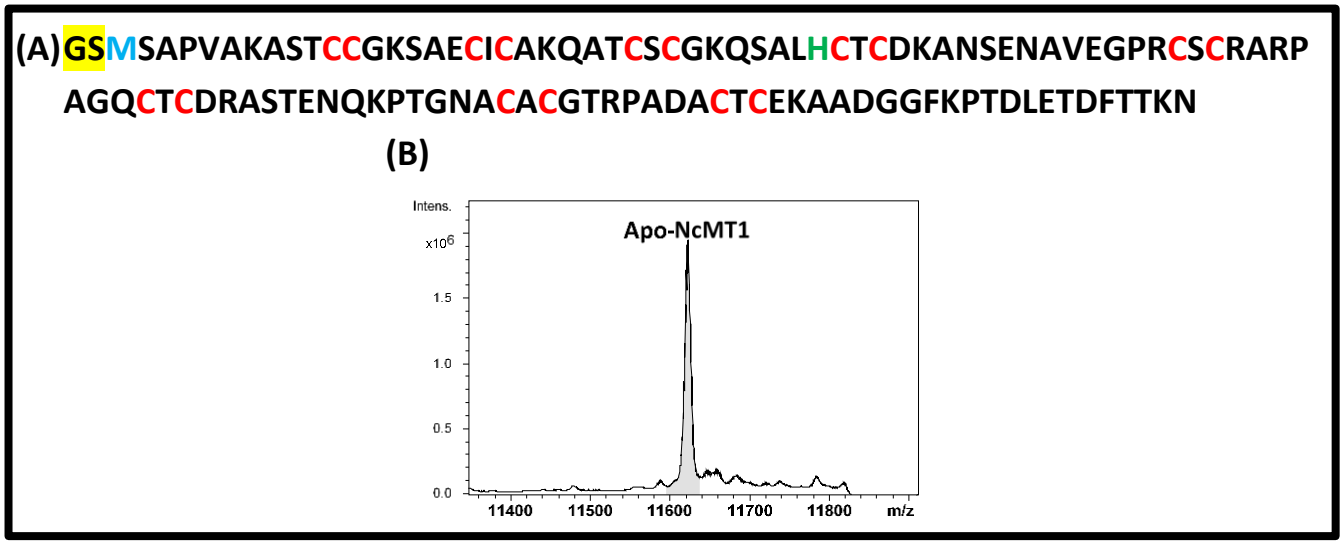

Figure 88. Amino acid sequence of the recombinant NcMT1 isoform and deconvoluted ESI-MS spectrum of the Zn-NcMT1 preparation recorded at pH 2.4, which corresponds to the apo-NcMT1.

Once confirmed the amino acid sequence and the corresponding MW, the behaviour of the protein in the presence Zn(II), Cd(II) and Cu(II) can be analysed.

10.4.1 NcMT1 binding Zn(II)

According to the data obtained by ESI-MS (Figure 89A), when NcMT1 is synthesized in Zn(II)-enriched media, an almost equimolar mixture of the complexes Zn_4-NcMT1 and Zn_5-NcMT1 are formed, together with other Zn(II)-species with less importance. This result is slightly above the value 3.87 Zn(II) per MT obtained in ICP-AES analysis, probably due to the presence of important species with less Zn(II) content. On the other hand, the CD analysis indicates that the structuration of the protein about Zn(II) is poor, because of the lack of signals after 240 nm (Figure 89B).

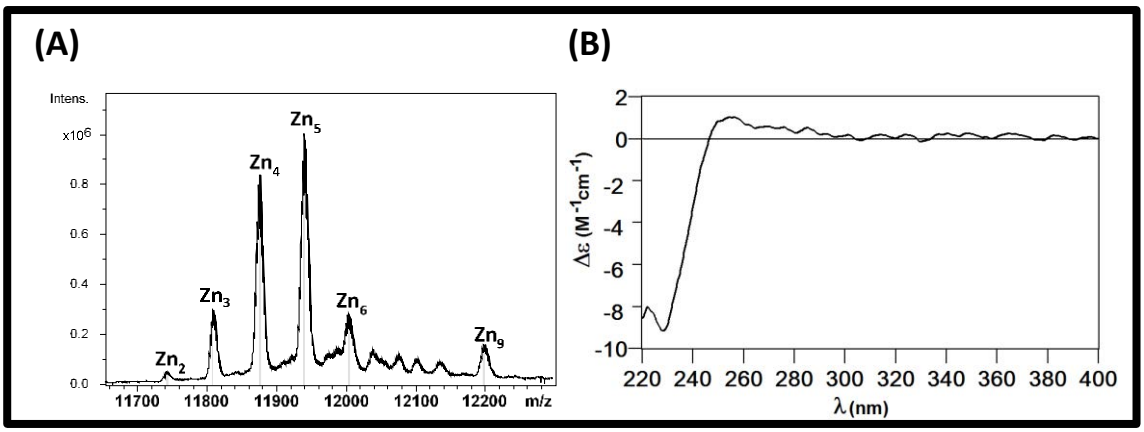

Figure 89. Deconvoluted ESI-MS spectrum of Zn-NcMT1 at pH 7.0 and CD spectrum of the Zn-NcMT1 preparation.

10.4.2 NcMT1 binding Cd(II)

When the protein is synthesized in Cd(II)-supplemented cultures, the complex Cd_8S-NcMT1 is produced as majority specie (Figure 90A). The presence of S^{2-} ligands is corroborated by the low Cd-to-S ratio measured by ICP-AES. On the other hand, the CD spectrum shows a Gaussian band at 250 nm, related with the Cd-Cys bond, and an exciton coupling at 280 nm, characteristic of the Cd-S^{2-} bond (Figure 90B).

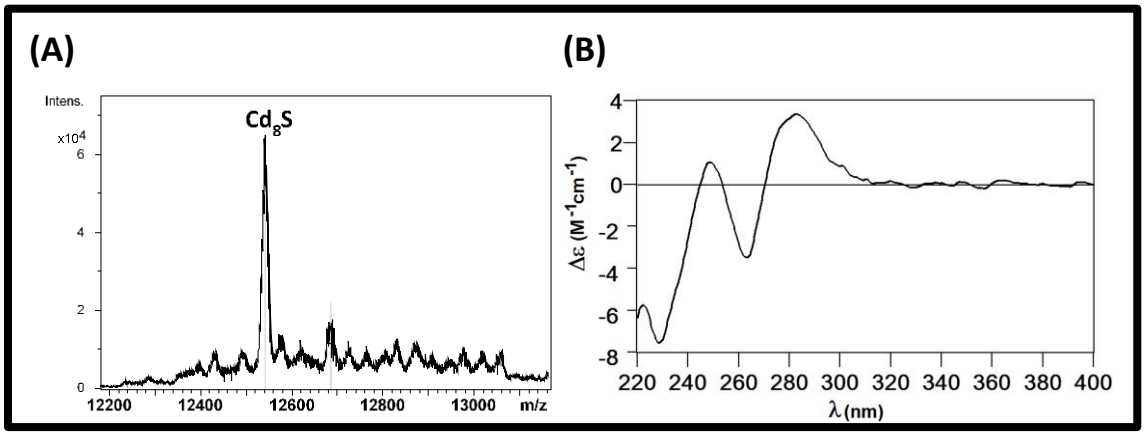

Figure 90. Deconvoluted ESI-MS spectrum of Cd-NcMT1 at pH 7.0 and CD spectrum of the Cd-NcMT1 preparation

10.4.3 NcMT1 binding Cu(I)

When NcMT1 is produced in Cu(II)-enriched media, the ESI-MS results obtained for the productions at normal and low oxygenation show the formation of a mixture of Cu(I) species (Figure 91A and 91B). The mixture formed consists on species with content between 8 to 13 Cu(I) metal ions per MT where the most important specie is Cu_{12}-NcMT1. The concentration of the species present is lower than the detection limit of CD and ICP-AES analysis, thus impairing to confirm the Cu content.

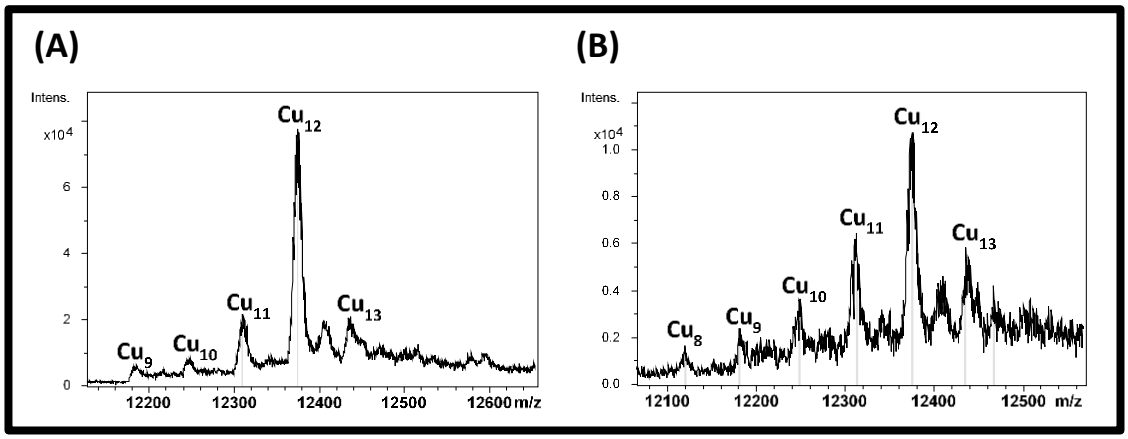

Figure 91. Deconvoluted ESI-MS spectrum of Cu- NcMT1 at normal and low oxygenation recorded at pH 7.

Due to the necessity to dissolve the Zn-NcMT1 preparation to avoid the signal saturation in CD analysis, the monitoring of the *in vitro* Cu-NcMT1 formation by CD, UV-Vis and ESI-MS was impossible. The low concentration of the resultant solution impedes to overcome the detection limit of the techniques.

10.5 Discussion subfamily 3

Within subfamily 3, two MTs with 12 and two with 16 cysteines have been studied. The two MTs with 12 cysteines are CaCRD2, from *Candida albicans*, and SbMT, from *Sporothrix brasiliensis*. Ten of the 12 cysteines of this two MTs are perfectly aligned between them (Figure 92), being structured in motifs -CXC-. The other two cysteines differ between the two sequences. In the case of CaCRD2 the two cysteines are located as a singlet at the beginning and at the end of the sequence, while SbMT has these two cysteines as a doublet -CC- at the beginning.

```
CaCRD2   ----MACSAAQ--CVCAQKSTCSCGKQPALKCNCSKASVENVVPSSNDACACGKRNKSSCTCGANAICDGTRDGETDFTNLK
SbMT     MVSSTCCGKGGAECVCAQNATCSCGKQSALHCNCDRAATENNTAGDR--CSCGQRPAGACTCATNPSEVNTANETDFTTRK
```

Figure 92. Comparison of the amino acid sequences of CaCRD2 and SbMT.

By comparing the results of the productions *in vivo* of Zn-CaCRD2 and Zn-SbMT is possible to see that the results are not exactly the same. In the case of CaCRD2 the majority specie formed was Zn_3-CaCRD2, while in the case of SbMT an equimolar mixture of Zn_3-SbMT and Zn_4-SbMT was produced. The capability of SbMT to bind this extra Zn(II) metal ion could be produced for the presence of the doublet -CC- instead of the two single cysteines of CaCRD2. The CD analysis of the two preparations shows a poor structuration of the proteins about Zn(II) (Figure 93).

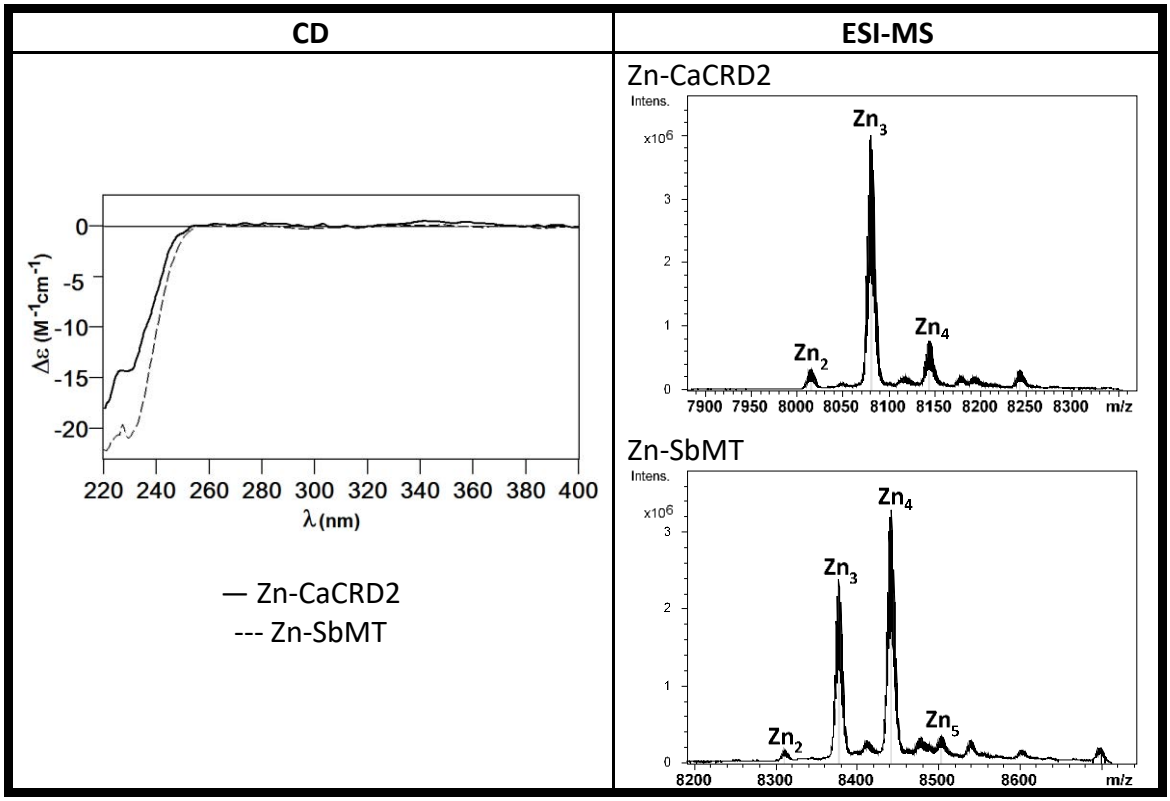

Figure 93. Comparison between CD and deconvoluted ESI-MS spectra of Zn-CaCRD2 and Zn-SbMT.

In the case of the *in vivo* productions of Cd-CaCRD2 and Cd-SbMT, the species formed and the structuration of them are very similar (Figure 61). In both cases, the important species formed are Cd_4-MT and a wide variety of Cd_xS_y-MT complexes. The CD spectra of the two preparations show the same bands at 250 nm, for the Cd-Cys bond, and at 280 nm, characteristic of the Cd-S^{2-} bond (Figure 94).

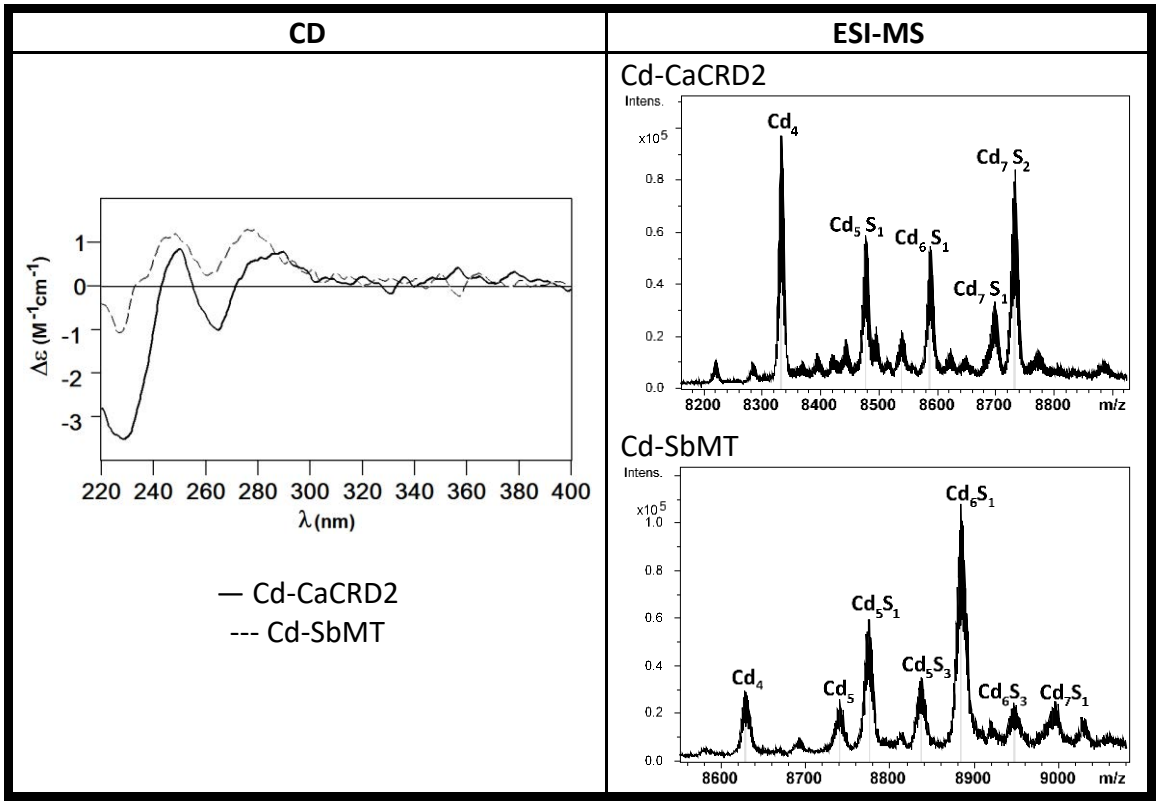

Figure 94. Comparison between CD and deconvoluted ESI-MS spectra of Cd-CaCRD2 and Cd-SbMT.

The productions of Cu-CaCRD2 and Cu-SbMT *in vivo* and *in vitro* are also very similar (Table 12). In the *in vivo* preparations, Cu_9-MT seems to be the prominent specie in both cases, coexisting together with other species. The *in vitro* formation also is practically identical in both cases, especially in the firsts steps of the titration, where is formed the specie Cu_4-MT. However, the end of the titration has small differences, because in the case of CaCRD2 the prominent specie formed is Cu_8-CaCRD2 while in the case of SbMT there is a mixture of Cu_8-SbMT and Cu_9-SbMT. As in the case of Zn-MT, the capability of SbMT to bind this extra metal ion is probably due to the presence of the doublet -CC- instead of the two single cysteines.

	In vivo	*In vitro* (titration)
CD	-	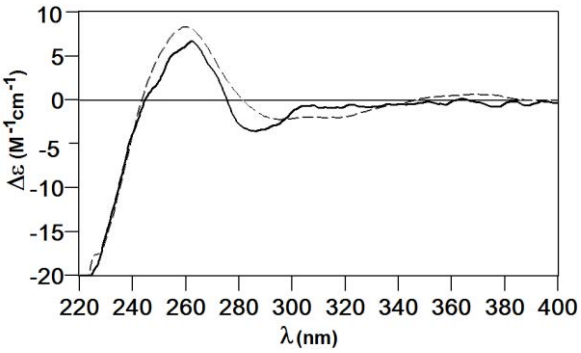 — Cu-CaCRD2 --- Cu-SbMT
ESI-MS	Cu-CaCRD2 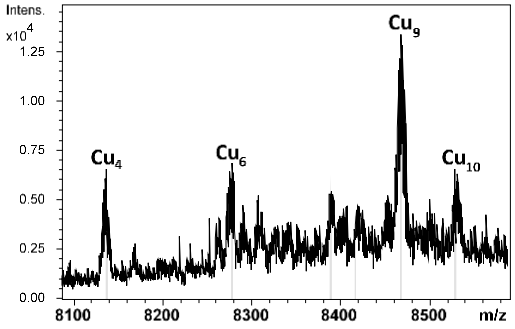 Cu-SbMT 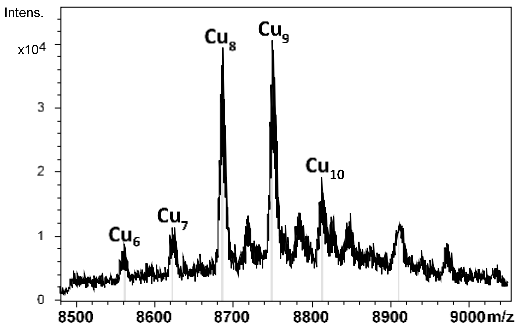	Cu-CaCRD2 (8 eq. Cu(I)) 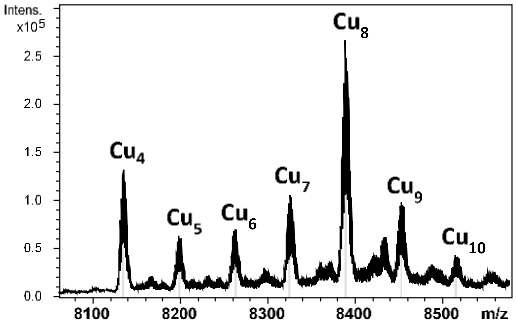 Cu-SbMT (12 eq. Cu(I)) 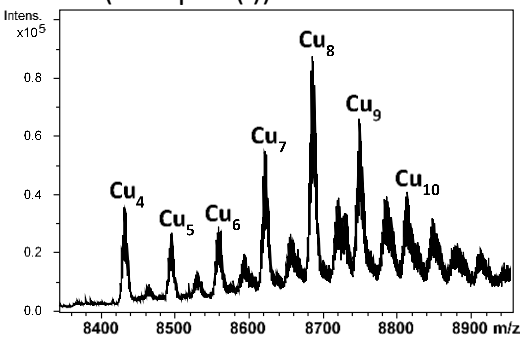

Table 12. Comparison between CD and Deconvoluted ESI-MS spectra of Cu-CaCRD2 and Cu-SbMT *in vivo* and *in vitro*.

The presence of sulphide species in Cd(II) cultures of these two MTs and the formation of complexes rather stable with Cu(I), like Cu_8-MT and Cu_9-MT, suggest the classification of CaCRD2 and SbMT as Cu-thioneins. The length of the two sequences differs only on three amino acids, but the motif with the doublet -CC- present in SbMT confers this MT higher capacity to bind metal ions.

SaMT and NcMT1 can be compared with SbMT. The cysteines of the sequences of these three proteins are perfectly aligned, but SaMT and NcMT1 have an extra sequence fragment which contains two motifs -CXC- more (Figure 95).

```
SbMT    -----MVSSTCCGKGGAECVCAQNATCSCGKQSALHCNCDRAATENNTAGDRCSCGQRPAGACTCATNPSEVNTANETDFTTRK

SaMT    ----MSPADTCCRKGEGACVCAQQATCSCGKQSALHCTCDKAAVENTISGPSCSCGSRPVGQCTCENATVENQKPTGATCGCGA
        RPAGSCTCNNSANETDFTTKK

NcMT1   MSAPVAKASTCCGKSAE-CICAKQATCSCGKQSALHCTCDKANSENAVEGPRCSCRARPAGQCTCDRASTENQKPTGNACACGT
        RPADACTCEKAADGGFKPTDLETDFTTKN
```

Figure 95. Comparison of the amino acid sequences of SbMT, SaMT and NcMT1.

As mentioned above, the cysteines of SaMT and NcM1 are perfectly aligned, which produces results practically homologous in their behaviours in the presence of the different metal ions. With Zn(II), they form an almost equimolar mixture of Zn_4-MT and Zn_5-MT with poor structuration (Figure 96), and with Cd(II) both of them form the complex Cd_8S-MT as single well-structured specie (Figure 97). However, with Cu(I) there is a small difference between the two preparations. In the two cases a mixture of Cu(I) species is formed, but while in the SaMT production the prominent specie is Cu_{11}-SapioMT in the NcMT1 production the prominent specie, Cu_{12}-NcMT1, has one Cu(I) metal ion more. This can be due to the longer amino acid sequence of NcMT1, suggesting some binding role of the non-coordinating amino acids in this case.

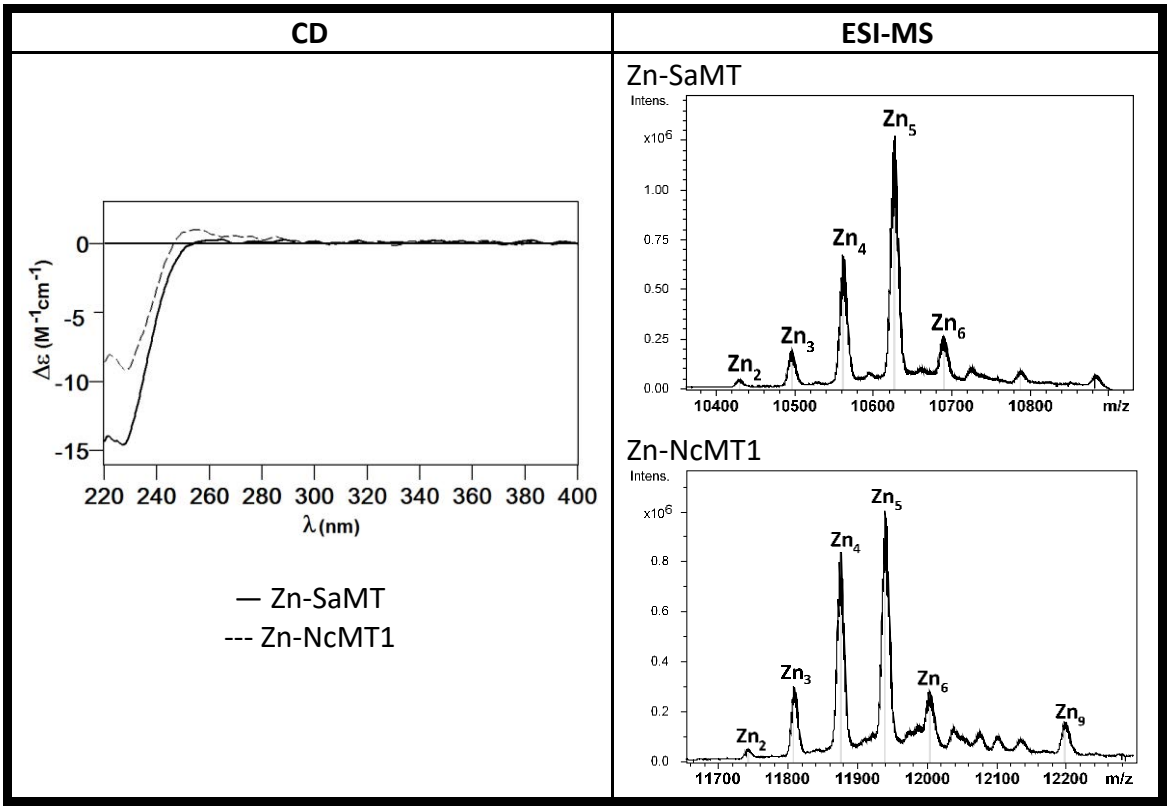

Figure 96. Comparison between CD and deconvoluted ESI-MS spectra of Zn-SaMT and Zn-NcMT1.

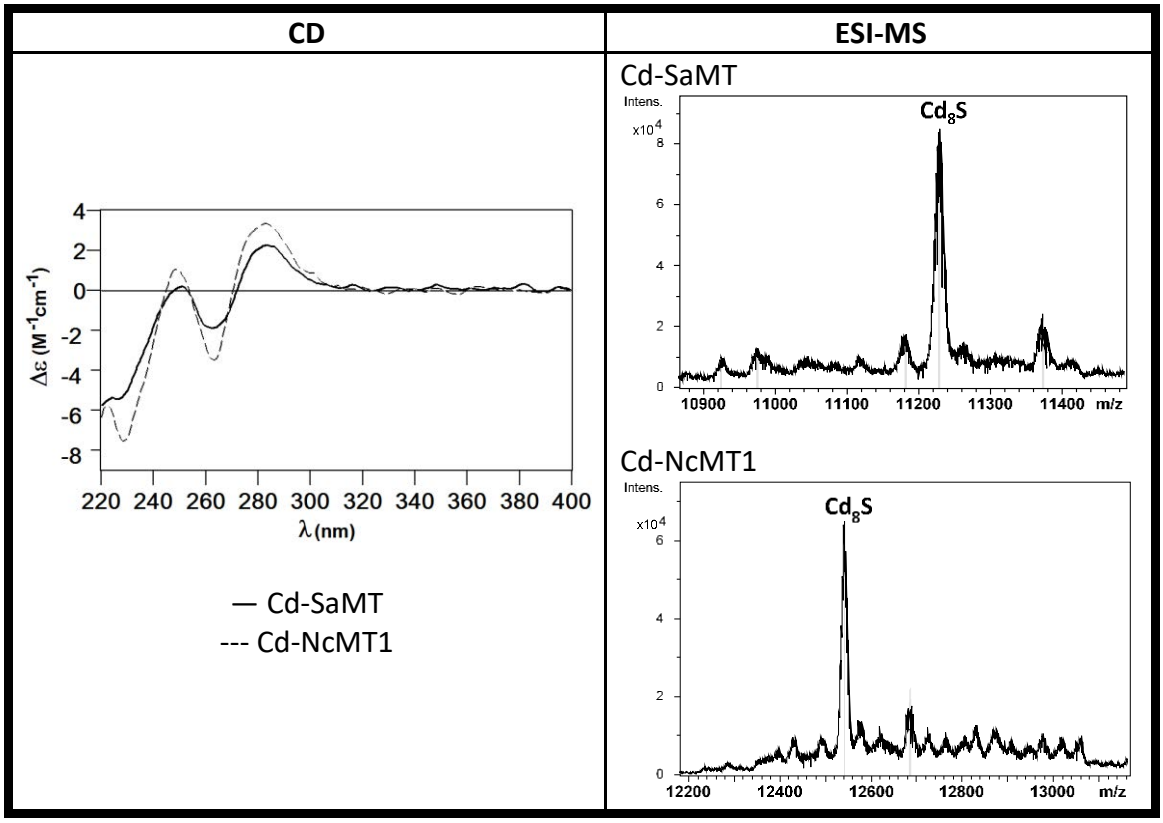

Figure 97. Comparison between CD and deconvoluted ESI-MS spectra of Cd-SaMT and Cd-NcMT1.

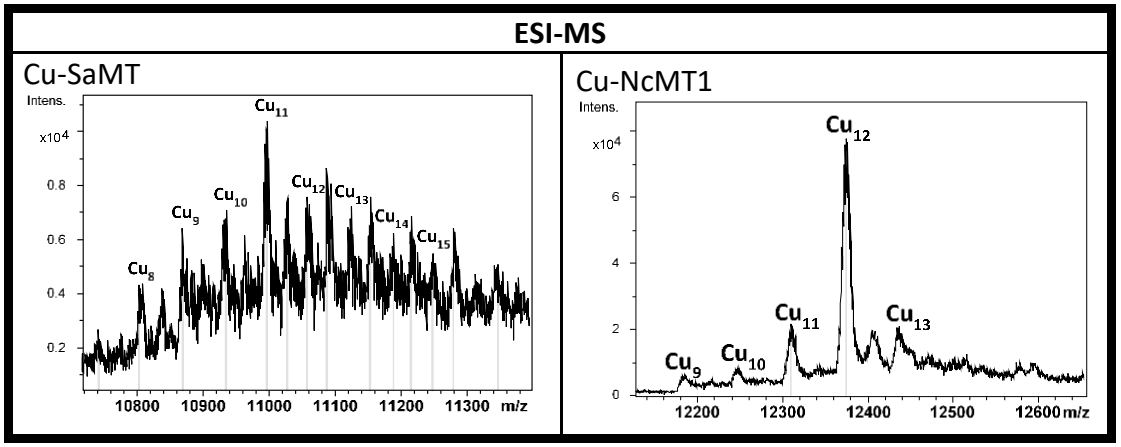

Figure 98. Comparison between deconvoluted ESI-MS spectra of Cu-SaMT and Cu-NcMT1.

By comparing all the ESI-MS and CD results of SaMT and NcMT1 productions with the SbMT ones, is possible to observe clearly that the 4 extra cysteines of these two proteins produce a higher capacity to bind metals and also confer better structuration to the complexes formed.

11. MTs OF SUBFAMILY 4

Three MTs from this subfamily have been studied. Two of them, CnMT1 and CnMT2, belongs to the organism *Cryptococcus neoformans* and the other, TmMT, belongs to the organism *Tremella mesenterica.*

These three MTs are the longest ones described so far, and their principal interest is their peculiar architecture. They exhibit metal-binding abilities compatible with the hypothesis of resulting MTs formation by tandem repetitions of 7-Cys motives, segment homologous to NcMT.

The first manuscript develops the study of the Zn(II)-, and Cu(I)-binding capabilities of several CnMT1 truncated mutants, which help to shed light on the role of non-coordinating amino acids, spacers and also the stability of certain clusters.

The second manuscript approach the extraordinary coordinating capacity of TmMT through the study of their recombinant Zn-, Cd- and Cu-complexes, allowing to discern some modular behaviour of these MT.

11.1 Understanding the 7-Cys module amplification of *C. neoformans* metallothioneins: how high capacity Cu-binding polypeptides are built to neutralize host nutritional immunity

Molecular Microbiology (2015) 98(5), 977–992 ■
doi:10.1111/mmi.13171
First published online 15 September 2015

Understanding the 7-Cys module amplification of *C. neoformans* metallothioneins: how high capacity Cu-binding polypeptides are built to neutralize host nutritional immunity

Anna Espart,[1] Selene Gil-Moreno,[2] Òscar Palacios,[2] Mercè Capdevila[2] and Sílvia Atrian[1]*
[1]*Departament de Genètica, Facultat de Biologia, Universitat de Barcelona, 08028, Barcelona, Spain.*
[2]*Departament de Química, Facultat de Ciències, Universitat Autònoma de Barcelona, 08193, Cerdanyola de Vallès, Spain.*

Summary

Cryptococcus neoformans **metallothioneins (MTs), CnMT1 and CnMT2, have been identified as essential infectivity and virulence factors of this pathogen. Both MTs are unusually long Cu-thioneins, exhibiting protein architecture and metal-binding abilities compatible with the hypothesis of resulting from three and five tandem repetitions of 7-Cys motives, respectively, each of them folding into Cu_5-clusters. Through the study of the Zn(II)- and Cu(I)-binding capabilities of several CnMT1 truncated mutants, we show that a 7-Cys segment of CnMT1 folds into Cu_5-species, of additive capacity when joined in tandem. All the obtained Cu-complexes share practically similar architectural features, if judging by their almost equivalent CD fingerprints, and they also share their capacity to restore copper tolerance in MT-devoid yeast cells. Besides the analysis of the modular composition of these long fungal MTs, we evaluate the features of the Cys-rich stretch spacer and flanking sequences that allow the construction of stable metal clusters by adjacent union of binding modules. Overall, our data support a mechanism by which some microbial MTs may have evolved to enlarge their original metal co-ordination capacity under the specific selective pressure of counteracting the Cu-based immunity mechanisms evolved by the infected hosts.**

Accepted 17 August, 2015. *For correspondence. E-mail satrian@ub.edu; Tel. (+34) 93 4021501; Fax (+34) 934034420.

Introduction

In recent years, metal handling and metabolism have arisen as clear determinants of microbial pathogenicity and virulence (Hodgkinson and Petris, 2012; Samanovic *et al.*, 2012; Staats *et al.*, 2013; Ding *et al.*, 2014), so that research on the so-called *nutritional immunity* is emerging as a key field to unveil both the host defense strategies against bacterial and fungal infections, and the mechanism that these pathogens use to evade them (Skaar and Raffatellu, 2015). The two known host *nutritional immunity* strategies are opposite, but they paradoxically coincide in the need of the pathogens to sequester metal ions to survive: either accumulating essential Zn that the infected organism makes unavailable to them (Wilson *et al.*, 2012) or immobilizing toxic Cu with which the host attempts to kill the invading microorganisms (Ladomersky and Petris, 2015). It becomes evident that metallothioneins (MTs), the ubiquitous, small, Cys-rich, metal-binding proteins that have been identified in all eukaryotes and most prokaryotes (latest reviews in Capdevila *et al.*, 2012; Blindauer, 2014) become the optimum candidates to carry out these vital purposes. In fact, some years ago, the *Mycobacterium tuberculosis* MT (MymT) was already shown to play a critical role for immune Cu-overload neutralization (Gold *et al.*, 2008). Therefore, it is straightforward to assume an equivalent role for pathogenic fungus MTs, since these MTs are known to exhibit a clear preference for Cu-binding (Bofill *et al.*, 2009; Palacios *et al.*, 2011a). However, the paradigmatic fungal Cu-thioneins, such as the yeast (*Saccharomyces cerevisiae*) CUP1 protein and the fungus *Neurospora crassa* and *Agaricus bisporus* MTs, are very small proteins and consequently with rather limited Cu-sequestering capacity (reviewed in Dolderer *et al.*, 2009). In this scenario, it was recently shown that the opportunistic basidiomycete *Cryptococcus neoformans*, responsible for potentially lethal cryptococcosis, senses the Cu ions mobilized by the host macrophages as innate defense and neutralizes their toxic effect using two MT proteins (CnMT1 and CnMT2), which were consequently considered essential virulence factors for host pulmonary colonization and progression of the infection (Ding *et al.*,

Fig. 1. (A) Sequence alignment of the CnMT1 full-length protein and the corresponding segments (Sx) analyzed in this work. Cys residues are in bold, and the spacer segments between 7-Cys boxes are shadowed in gray. All the Sx segments were expressed in the same GST-fusion system as the entire CnMT1 had been (Palacios *et al.*, 2014) and therefore, the corresponding recombinant peptides exhibit a N-terminal *GS* dipeptide, which has been shown not to alter the MT binding properties (Cols *et al.*, 1997). (B) Alignment of the 7-Cys box present in the S1 peptide with the MTs of *Neurospora crassa* and *Agaricus bisporus*.

2013). Outstandingly, *C. neoformans* MTs were characterized as unusually long MTs, CnMT1 consisting of 122 amino acids (cf. Fig. 1A) and CnMT2 with 183 amino acids, this potentially allowing an extraordinary Cu-chelating capacity compatible with the requirements of the fungus to survive the macrophage-generated Cu overload (Ding *et al.*, 2013).

Later, the full evaluation of the metal ion binding abilities of CnMT1 and CnMT2 (Palacios *et al.*, 2014) clearly showed how these polypeptides were optimized to yield well-folded, high-Cu(I) containing complexes, the nature of which reflects the copper concentration of the surrounding medium, as reported before for the *S. cerevisiae* Crs5 MT (Pagani *et al.*, 2007). This entails that, at high-Cu conditions, both isoforms would exert their maximum detoxification abilities, folding into homometallic copper-species. However, most strikingly, we demonstrated how the Zn/Cu replacement on Zn-CnMT1 and Zn-CnMT2 complexes was a cooperative reaction, proceeding by discrete steps of 5 Cu(I) ion incorporations. This prompted us to suggest the formation of unusual Cu_5-building blocks, different to the Cu-clusters so far reported for any MT. Significantly, the modular structure of the CnMT1 and CnMT2 polypeptide sequences, respectively, constituted by three and five 7-Cys regions separated by spacer stretches, further supported the hypothesis that the homometallic Cu-CnMT species folded *in vivo* at high Cu concentrations represent the respective three- and fivefold amplification of basic Cu_5-(7-Cys) clusters (Palacios *et al.*, 2014). Comparison of the CnMT1 and CnMT2 gene and protein sequence features strongly supported the emergence of the long *C. neoformans* MTs by ancient tandem repetitions of a primeval fungal MT unit, precisely comprising seven Cys residues. Hence, the Cys pattern of the *Neurospora* and *Agaricus* MTs (X_2-[CXC]-X_5-[CXC]-X_3-[CXC]-X_2-C-X_3) (Lerch, 1980; Münger and Lerch, 1985; respectively) almost coincided with that of the 7-Cys boxes considered as the building blocks of CnMT1 and CnMT2 (Fig. 1B).

In this scenario, we considered it highly relevant to ascertain if the co-ordination features of these unprecedented Cu_5-(7-Cys) building regions and their putatively additive Cu-binding capacity would support the hypothesis of *C. neoformans* MTs being the result of internal amplifications of such units. To this end, we recombinantly synthesized seven CnMT1 truncated mutants, encompassing one, two or three 7-Cys fragments, and exhibiting different combinations of spacer regions and/or flanking amino acids at their N- and C-terminal ends (Fig. 1). On the one hand, their Zn- and Cu-binding abilities were determined through the characterization of their respective Zn- and Cu-species folded *in vivo* in *Escherichia coli*, and *in vitro* (by Zn/Cu replacement on the corresponding recombinant Zn-species), by means of spectroscopic and spectrometric techniques. Furthermore, their Cu-chelating features, as well as those of the full-length CnMT1 polypeptide, were evaluated by their functional competence to detoxify Cu in yeast MT-knockout cells. Our results confirmed the modular origin of the high Cu-binding capacity of CnMT1 and CnMT2, and the evolutionary relationship that may link these MTs with the other well-studied fungal copper-thioneins (*Neurospora* and *Agaricus*). Additionally, the data provided here shed light on the role of the MT regions other than Cys-motifs, i.e. spacer linkers and

Table 1. Experimental molecular masses of the recombinant Sx apo-peptides. The corresponding ESI-MS spectra are shown in Supplementary Figs S1 to S7.

Peptide	Experimental MM	Calculated MM[a]
S1	2333	2333.6
S2	3261	3260.8
S3	3191	3191.6
S4	3899	3899.3
S5	3847	3847.4
S6	5349	5350.1
S7	8983	8984.1

a. Calculated mean molecular mass for neutral species.

flanking amino acids, which determine the stability of a given metal-MT complex, and therefore the ability of an MT to optimally bind that metal ion. Overall, we propose and analyze an evolution strategy by which some pathogenic fungi may have enlarged their MT metal co-ordination capacities under the specific selective pressure of counteracting the Cu-based immunity mechanisms evolved by the infected hosts.

Results and discussion

Cloning and recombinant synthesis of the CnMT1:Sx peptides

For the sake of brevity, the different CnMT1:Sx (x from 1 to 7, cf. Fig. 1) segments will be referred to as Sx throughout this work. Once the pGEX constructs coding for the Sx peptides had been confirmed by DNA sequencing, preliminary protein expression assays allowed the identification of their respective apo-forms by electrospray ionization mass spectrometry (ESI-MS) through the acidification to pH 2.4 of the corresponding Zn-Sx preparations (Table 1). These results confirmed not only the identity but also the integrity of the obtained peptides.

Zn(II) binding abilities of the CnMT1:Sx peptides and comparison with the full-length CnMT1 protein

The species formed when the *C. neoformans* full-length MTs co-ordinate Zn(II) were Zn_7- and Zn_8-CnMT1, and Zn_{11}-CnMT2 (Palacios *et al.*, 2014). Taking into account the composition of three 7-Cys boxes for CnMT1 and five for CnMT2, these results suggest that each 7-Cys box would be able to optimally bind 2 Zn(II), whereas the flanking Cys residues would account for the co-ordination of the additional Zn(II) ions of the complexes. This assumption was fully corroborated by the behavior of the CnMT1 truncated mutants studied in this work (Table 2). Hence, all the peptides consisting in one 7-Cys box and without extra Cys (i.e. S1, S2 and S3) yielded Zn_2-complexes as major products when biosynthesized in Zn-enriched cultures. In the case of the S4 peptide, the Zn(II) content of the recovered complexes was slightly increased up to a major Zn_3 and a very minor Zn_4 species, in good concordance with the presence of two flanking Cys residues at its C-terminal end. It is worth noting that the 3 Zn:9 Cys ratio observed for S4 precisely coincides with the well-know stoichiometry reported for the mammalian MT ß domain, from the first characterization of its metal binding features from native sources (Otvos and Armitage, 1980) and later corroborated by recombinantly prepared complexes (Capdevila *et al.*, 1997). This ratio was thereafter corroborated for other nine Cys MT domains, such as the C-terminal echinodermata (*Strongylocentrotus purpuratus*) MT moiety (Wang *et al.*, 1995; Tomas *et al.*, 2013), or both moieties of the crustacean (*Homarus americanus* and other) MTs (Valls *et al.*, 2001). No Zn-complex could be detected by ESI-MS for S5, which is attributable to a marked instability of the Zn-S5 association and not to the lack of protein synthesis – since the apo-S5 peptide was clearly identified (Table 1 and Fig. S5) – or to the lack of metal, as a comparable amount of Zn(II) to that of S4 was detected by ICP (Table 2). In S6, the presence of two 7-Cys

Table 2. Analytical characterization of the recombinant Zn(II)-Sx complexes. For comparative purposes, data for the full-length CnMT1 are included (Palacios *et al.*, 2014).

Peptide	ICP-AES[a]	Neutral ESI-MS[b]	Experimental MM[c]	Calculated MM[d]
S1	0.68	**Zn_2-S1**	2460	2460.4
(7 Cys)		Zn_1-S1	2396	2397.1
S2	1.87	**Zn_2-S2**	3387	3387.5
(7 Cys)		Zn_1-S2	3323	3324.2
S3	1.19	**Zn_2-S3**	3317	3318.4
(7 Cys)		Zn_3-S3	3380	3381.8
		Zn_4-S3	3442	3445.1
		Zn_1-S3	3251	3255.0
		apo-S3	3187	3191.6
S4	3.52	**Zn_3-S4**	4088	4089.5
(9 Cys)		Zn_4-S4	4150	4152.9
S5	3.30	–	–	–
(9 Cys)				
S6	3.39	**Zn_4-S6**	5604	5603.7
(14 Cys)		Zn_5-S6	5666	5667.1
		Zn_3-S6	5540	5540.0
S7	6.09	**Zn_7-S7**	9427	9427.8
(21 Cys)		Zn_8-S7	9489	9491.2
		Zn_6-S7	9362	9364.4
CnMT1	7.88	**Zn_8-MT1**	Palacios *et al.*	Palacios *et al.*
(25 Cys)		Zn_7-MT1	(2014)	(2014)

a. Zn(II)-to-peptide ratio calculated from S and Zn content (ICP-AES data).**b.** The deduced Zn(II)-species were calculated from the mass difference between the holo- and apo-peptides. The major species are indicated in bold.**c.** Experimental molecular masses corresponding to the detected Zn(II)-Sx complexes. The corresponding ESI-MS spectra are shown in Fig. 4, Fig. 5 and Supplementary Figs S1 to S7.**d.** Theoretical molecular masses corresponding to the Zn(II)-Sx complexes.(–) means non-detected.

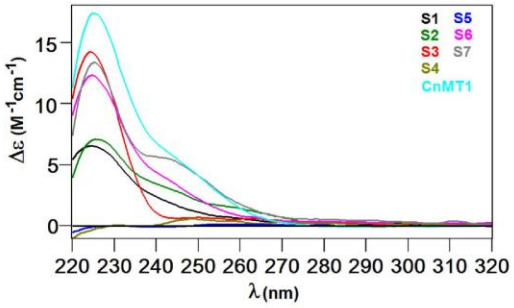

Fig. 2. Comparison of the circular dichroism spectra of the recombinant Zn-Sx preparations as well as that obtained for the CnMT1 protein, which has been normalized to a lower intensity for comparison purposes (Palacios *et al.*, 2014).

blocks automatically doubled the Zn(II) content of the major complexes, resulting in a major Zn_4-S6. Finally, the S7 peptide (three 7-Cys segments) yielded a mixture of major Zn_7-S7 and minor Zn_8-S7 plus Zn_6-S7 complexes, which again is concordant with 2 Zn(II) per 7-Cys box, and some extra Zn(II) possibly contributed by some terminal-to-bridging Zn-SCys bond conversion.

Comparison of this collection of Zn-complexes allows some considerations to be made on the role of the Cys residues positioned outside the 7-Cys blocks and of the spacer and flanking regions devoid of Cys residues. No differences could be detected between S1 and S2, and therefore no significant role has to be assumed for the presence of the N-terminal spacer in S2. Contrarily, the C-terminal spacer of S3 slightly increased the Zn binding capacity of the 7-Cys box, because minor Zn_3- and Zn_4-species were detected, which could be explained by the presence of one glutamic acid in this stretch. Further information is obtained from the comparison between S7 and the full-length CnMT1. Unexpectedly, the fact that CnMT1 has four more Cys than S7 does not considerably enlarge its Zn-binding capacity, as the only difference is that CnMT1 folds into major Zn_8- and minor Zn_7-complexes, whereas for S7, the Zn_7-species predominates. This suggests a function of the two flanking spacers plus the two outside Cys-X-Cys pairs (cf. Fig. 1) more associated with a stabilizing (or *closing*) role of the metal cluster than to an increase of Zn-coordination capacity.

It is worth noting that the CD fingerprints (Fig. 2) of all the analyzed Zn-Sx preparations are very similar among them, except for those of S4 and S5. Hence, S1, S2, S6 and S7 draw a clear Gaussian band centered at *ca.* 240 nm, characteristic of the absorptions of the $Zn(Cys)_4$ chromophores superimposed to the 220–230 nm absorptions contributed by the peptide bonds, and which are coincident in shape, although far less intense, to that of the entire Zn-CnMT1 complex (Fig. 2). The observed lack of chirality at 240 nm of S3 could be attributed to the mixture of Zn-complexes rendered by this peptide. A poor chirality/degree of folding of the major Zn_3-S4 complex could explain the silent nature of its CD spectrum. Finally, the lack of MS-detectable Zn-S5 species is corroborated by its CD spectrum that resembles that on an apo-peptide.

Cu(I) binding abilities of the CnMT1:Sx peptides and comparison with the full-length CnMT1 protein

A first glance at the results of the syntheses of all the Sx peptides in Cu-enriched bacterial cultures readily showed the extreme Cu-thionein character of the one and two 7-Cys boxes segments – except for S5, *vide infra*-, since all them rendered equivalent results at both culture aeration conditions (Table 3 and Fig. 3), and there were no traces of Zn presence in any of the corresponding Cu-complexes. It is well established that culture oxygenation determine the amount of Cu available in host cells for recombinant MT to form the corresponding complexes; the lower the aeration, the higher the intracellular Cu levels (Pagani *et al.*, 2007). Hence, a Cu-thionein will be able to render homometallic Cu-complexes even at regular aeration, when Cu in not specially abundant inside the cell; however, at the contrary, a Zn/Cd-thionein will yield heterometallic Zn,Cu-complexes at the same conditions, and only produce homometallic Cu-species when obtained from cells grown under low aeration (i.e. high intracellular Cu) (Bofill *et al.*, 2009). Contrarily S7, the three 7-Cys boxes segment, behaved as the full-length CnMT1, because the complexes formed at regular aeration (i.e. regular intracellular Cu content) were heterometallic (2.5 Zn:8.7 Cu mean ratio for S7; and 4.2 Zn:5.0 Cu, for CnMT1), but both rendered homometallic Cu-MT complexes when synthesized at low aeration conditions. This indicates that long MTs are more prone than shorter peptides to form Zn,Cu-heterometallic complexes when not synthesized under high Cu concentrations.

All the Sx segments encompassing one 7-Cys box (i.e. S1, S2, S3 and S4) yielded major Cu_5-Sx species (Table 3 and Fig. 4), except for S5 for which no Cu-S5 species could be recovered at any culture condition, in agreement with the unsuccessful Zn-S5 synthesis (Tables 2 and 3). Further consideration of the minor species of each synthesis revealed significantly different Cu(I)-binding features of the Sx species. Hence, the presence of an N-term (S2) or a C-term (S3 and S4) flanking spacer (in relation with its absence in S1) conferred stability to the corresponding Cu_5 clusters, as unique Cu_5-Sx (x = 2, 3 and 4) were obtained while a minor Cu_4-S1 was detected for the spacer-devoid S1 peptide. Unexpectedly, the presence of two additional Cys in the final peptide tail of S4 does not apparently enhance the Cu(I)-binding capacity of its 7-Cys core. The results afforded by S6 allowed analyzing

Table 3. Analytical characterization of the recombinant Cu(I)-Sx complexes. Normal aeration (na) or low aeration (la) (i.e. high intracellular Cu) is indicated only for those syntheses yielding different results under both conditions. For comparative purposes, data for the full-length CnMT1 are included (Palacios *et al.*, 2014).

		Neutral			Acidic		
	ICP-AES[a]	ESI-MS[b]	MM_{Exp}[c]	MM_{Theor}[d]	ESI-MS[b]	MM_{Exp}[c]	MM_{Theor}[d]
S1	0.0 Zn	**Cu_5-S1**	2646	2646.4	**Cu_5-S1**	2646	2646.4
(7 Cys)	3.2 Cu	Cu_4-S1	2582	2583.8	Cu_4-S1	2582	2583.8
S2	0.0 Zn	**Cu_5-S2**	3573	3573.5	**Cu_5-S2**	3573	3573.5
(7 Cys)	5.7 Cu						
S3	0.0 Zn	**Cu_5-S3**	3505	3504.3	**Cu_5-S3**	3504	3504.3
(7 Cys)	4.9 Cu						
S4	0.0 Zn	**Cu_5-S4**	4210	4212.1	**Cu_5-S4**	4210	4212.1
(9 Cys)	5.2 Cu						
S5	–	–	–	–	–	–	–
(9 Cys)							
S6	0.0 Zn	**Cu_5-S6**	5661	5662.9	**Cu_5-S6**	5660	5662.9
(14 Cys)	4.8 Cu	Cu_6-S6	5724	5725.4	apo-S6	5348	5350.1
		Cu_9-S6	5912	5913.1	Cu_4-S6	5597	5600.3
		Cu_4-S6	5598	5600.3	Cu_9-S6	5911	5913.1
					Cu_{10}-S6	5974	5975.8
$S7_{na}$	2.5 Zn	**M_{10}-S7**	9608	9609.6	**Cu_9-S7**	9546	9547.1
(21 Cys)	8.7 Cu	**M_9-S7**	9546	9547.1	Cu_5-S7	9294	9296.9
		M_{11}-S7	9796	9797.3	Cu_{10}-S7	9610	9609.6
		M_{13}-S7	9670	9672.2			
$S7_{la}$	0.0 Zn	–	–	–	**Cu_9-S7**	9545	9547.1
(21 Cys)	11.1 Cu				Cu_{14}-S7	9862	9859.1
					Cu_{12}-S7	9798	9796.7
$CnMT1_{na}$	4.2 Zn	**M_{11}-CnMT1**	Palacios *et al.*	Palacios *et al.*	**Cu_5-CnMT1**	Palacios *et al.*	Palacios *et al.*
(25 Cys)	5.0 Cu	M_8-CnMT1	(2014)	(2014)		(2014)	(2014)
		M_9-CnMT1					
$CnMT1_{la}$	0.0 Zn	**Cu_{16}-CnMT1**	Palacios *et al.*	Palacios *et al.*	**Cu_{15}-CnMT1**	Palacios *et al.*	Palacios *et al.*
(25 Cys)	15.8 Cu		(2014)	(2014)	Cu_{16}-CnMT1	(2014)	(2014)
					Cu_{17}-CnMT1		
					Cu_{14}-CnMT1		

a. Zn(II) and Cu(I)-to-peptide ratio calculated from S, Zn and Cu content (ICP-AES data).**b.** The deduced species (M = Zn or Cu) were calculated from the mass difference between the holo- and the respective apo-peptides. The major species are indicated in bold.**c.** Experimental molecular masses corresponding to the detected complexes. The corresponding ESI-MS spectra are shown in Figs 4 and 5.**d.** Theoretical molecular masses corresponding to the metal-Sx complexes.(–) means non-detected.

the behavior of two 7-Cys-boxes connected by a linker. Significantly, although Cu_5-S6 was the major species produced, Cu_9- and Cu_{10}-S6 could be also detected among the minor species produced at both aeration conditions (Table 3 and Fig. 5), this indicating that at least a subpopulation of S6 could fill its two 7-Cys boxes with Cu(I). However, the fact that Cu_5-, Cu_4- and even apo-S6 was detected by the acid ESI-MS of the same sample points to a marked instability of Cu_9- and Cu_{10}-S6 if compared with the major Cu_5-S6 complexes. This can be readily explained if assuming that only one of the two 7-Cys boxes of S6 is able to fold into a compact and robust Cu_5-cluster. Finally S7, the three 7-Cys box fragments devoid of N- and C-terminal spacers and adjacent CXC motifs were the unique CnMT1 truncated mutant that yielded different metal complexes if synthesized in regular or low-aerated Cu-supplemented cultures, as the entire CnMT1 and CnMT2 do (Palacios *et al.*, 2014). Hence, at regular oxygenation, heterometallic Zn,Cu-complexes were recovered, as shown by the ICP-AES results and by the different speciation observed after neutral (major M_{10}- and M_9- and minor M_{11}- and M_{13}-S7, M = Zn or Cu) or acid (major Cu_9- and minor Cu_5- and Cu_{10}-S7) ESI-MS (Table 3 and Fig. 5). Contrarily, only homometallic Cu-complexes were recovered from low-aerated synthesis: major Cu_9- and minor Cu_{14}- and Cu_{12}-S7 according to acidic ESI-MS data (Table 3). These results suggest that when Cu is not particularly high, two of the three 7-Cys boxes in S7 can fold into one or two Cu_{4-5}-clusters (Cu_9-, Cu_{10}-S7 species), which will additionally include some Zn(II) ions. Contrarily, at high copper concentrations, the Cu load of two 7-Cys boxes is completed and accompanied in some cases with a partial load of the third box [up to 14 Cu(I)], although through the formation of complexes of probably very low stability in view of the low yield of the production, the impossibility of recording ESI-MS data at pH 7, and the low intensity of the ESI-MS spectrum at acid pH (data not shown). It is worth remarking here that both S5 and S7, the two peptides that have Cys as their C-termini, exhibit a similarly misbehavior when rendering Cu-complexes, as

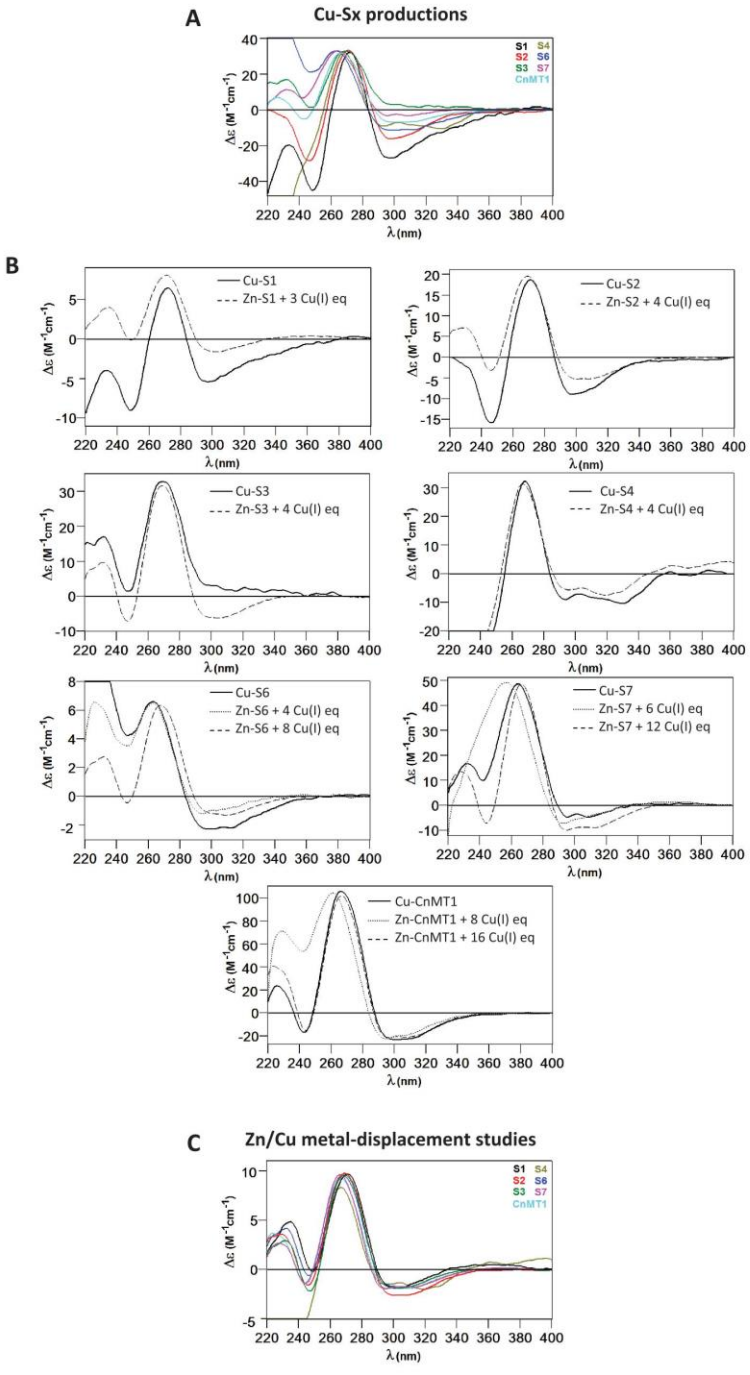

Fig. 3. Comparison of (A) the normalized CD spectra recorded for the recombinant Cu-Sx productions, (B) the circular dichroism spectra corresponding to the recombinant Cu-Sx preparations (solid lines correspond to both types of productions – normal and low aeration conditions), and those recorded in the corresponding Zn/Cu metal-displacement studies on Zn-Sx (dashed) – when necessary, the spectra in dashed line were normalized in intensity in order to allow comparisons – and (C) after the *in vitro* addition of several Cu(I) equivalents to the corresponding Zn-Sx preparations. The spectra corresponding to the entire protein, CnMT1, have also been included for comparison.

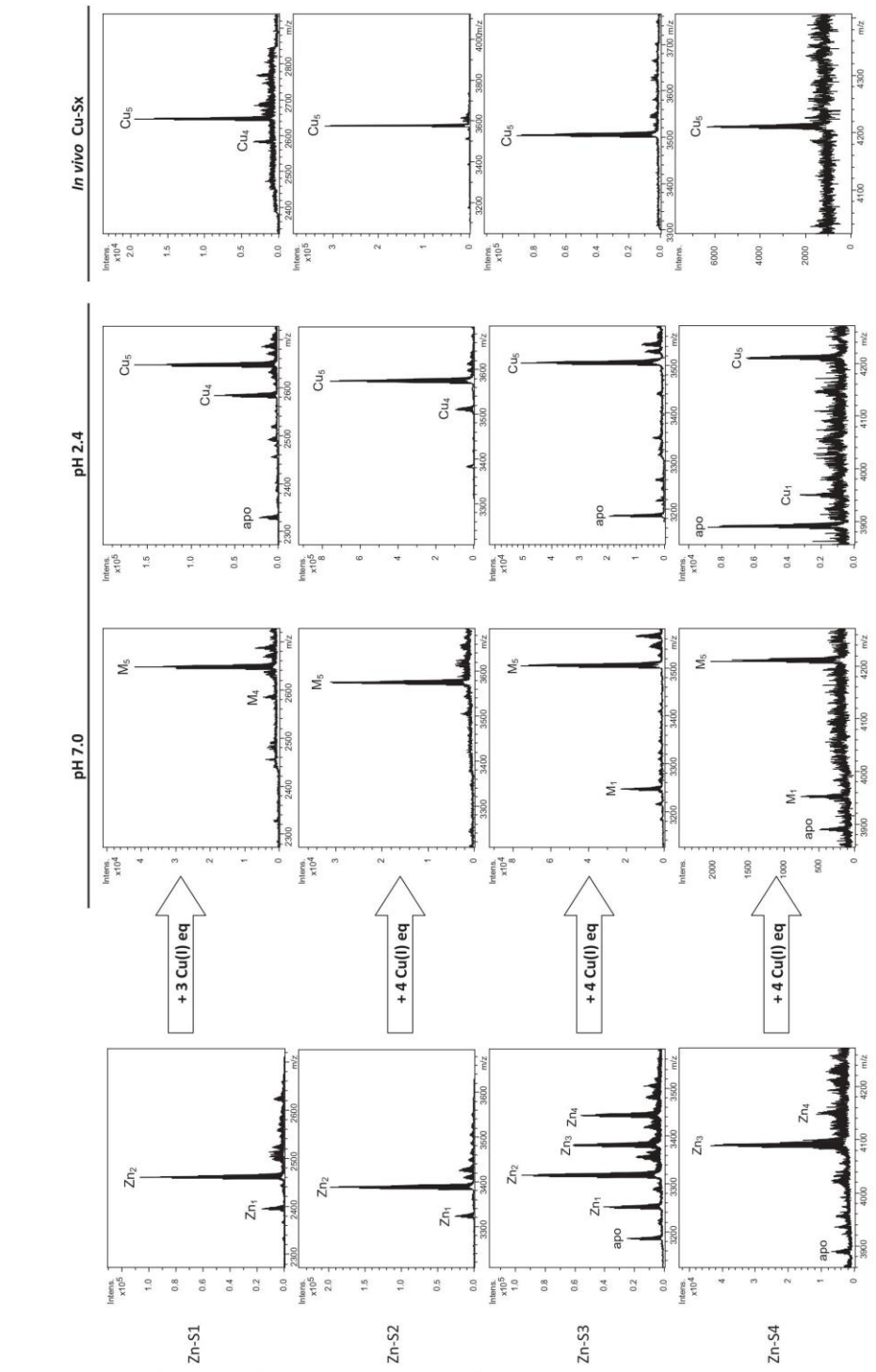

Fig. 4. Deconvoluted ESI-MS spectra recorded, at neutral and acidic pH (central columns), after the addition of the indicated number of Cu(I) equivalents to the corresponding Zn-Sx preparations, x = 1, 2, 3 and 4 (first column). No data are included for S5 due to the lack of metal complexes detected by ESI-MS in all the cases. The ESI-MS spectra of the *in vivo* obtained Cu-Sx preparations are included (last column) for comparison purposes, those at pH 7 and pH 2.4 being identical.

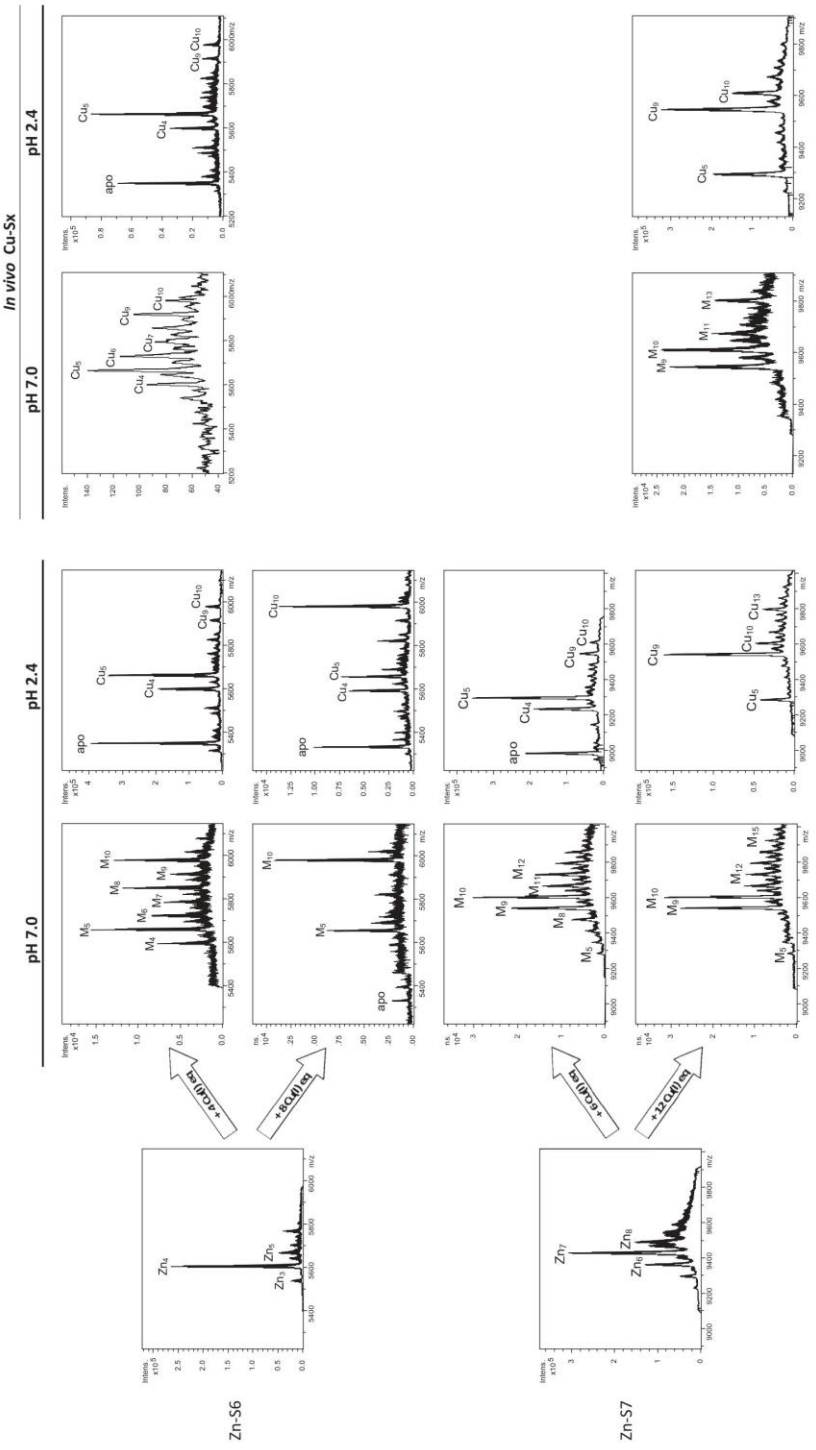

Fig. 5. Deconvoluted ESI-MS spectra recorded, at neutral and acidic pH (central columns), after the addition of the indicated number of Cu(I) equivalents to the corresponding Zn-S6 and Zn-S7 preparations (first column). The ESI-MS spectra at pH 7 and pH 2.4 of the *in vivo* obtained Cu-S6 (regular and low aeration conditions rendering identical spectra) and Cu-S7 (only spectra of the regular aeration conditions shown) preparations are included (two last columns) for comparison purposes.

the only 7-Cys box constituting S5 is totally unable to fold into metallated species, and S7 (three 7-Cys regions) only fills satisfactorily two of them. These results point to a marked unsuitability of Sx peptides with C-terminal Cys to constitute stable Cu-clusters and thus to the need of *closing* residues, as it would be otherwise confirmed by the ability of S6 (with two C-terminal residues after the last Cys), to fully fill its two 7-Cys segments. Comparison with the results of the full-length CnMT1 leads to the hypothesis that in the first case (no Cu surplus), the recovered heterometallic Zn,Cu-CnMT1 complexes exhibit a higher Zn(II) content than the corresponding Zn,Cu-S7, so that it could be assumed that the flanking spacers plus CXC stretches of CnMT1 stabilize the Zn(II) ions co-ordinated to the Cu-cores. However, in the second case, if Cu is abundant, CnMT1 is also able to fully load its three 7-Cys boxes (major $Cu_{15\text{-}16}$-CnMT1 species, Table 3), this suggesting that the presence of the flanking regions missing in S7 are necessary to *close* the 3-Cu_5 cluster structure.

Globally, the CD spectra of all the Cu-Sx productions except that of S5, which rendered no product, were highly coincident in shape (Fig. 3A), drawing a CD fingerprint with the typical absorptions of the Cu-MT complexes (maximum *ca.* 270 nm and minima at *ca.* 250 and 300 nm), and which are also very similar, although markedly less intense, to that of the entire Cu-CnMT1 complex (included in Fig. 3 for comparative purposes). Further details are discussed in the next section.

Zn(II)/Cu(I) replacement reactions of the CnMT1:Sx peptides and comparison with the full-length CnMT1 protein

Very informative results about the Cu(I)-binding abilities of the Sx segments were obtained from the addition of Cu(I) to the respective Zn-Sx recombinant preparations (i.e. the study of the species constituted *in vitro* by Zn/Cu exchange). The metal substitution process was followed by ESI-MS analysis, and CD and UV-vis spectrophotometry. For each metal-replacement reaction, the CD spectrum most similar to that of the recombinant Cu-Sx preparation is shown in Fig. 3B and C, and the species detected by ESI-MS at those titration steps are included in Figs 4 and 5; the complete sets of data being available as Supplementary Material (Figs S1 to S7).

All the Zn-complexes of the peptides containing only one 7-Cys box (S1, S2 and S3) followed a similar behavior when titrated with Cu(I), being those of S2 and S3, the two segments with N- or C-terminal flankers, the more similar among them, whereas S1 showed higher complexity associated with the already observed lack of stabilization of the Cu_5-S1 complexes. The behavior of the three peptides is clearly suggestive of an almost complete cooperative loading of 5 Cu(I) – a small amount of Cu_4-Sx is also detected – concomitant to the displacement of all the initial Zn(II). This is shown by the isodichroic points observed in the evolution of the corresponding CD spectra, and nicely illustrated by the cooperative formation of M_5-Sx complexes, which are mainly Cu_5-Sx, even for the mixture of Zn_x-S3 species, ranging from the apo-peptide to Zn_4-S3 (Fig. S3). Similarly, the addition of an excess of Cu(I) after the formation of Cu_5-Sx species inevitably provokes a collapse of the CD fingerprints that reveals the unfolding of the complexes, concomitantly to the detection of major peaks corresponding to the apo-peptides by analysis at acidic ESI-MS. The different sequences of S1, S2 and S3 may be associated with the small differences observed in their Zn/Cu exchange processes. Hence, the presence of an N-term spacer in S2 or C-term in S3 (in relation to S1) suggests that the Cu_5-S2 and Cu_5-S3 complexes are almost unique at the step of the titration yielding the species with the highest nuclearity, and before cluster unfolding; while for S1, a clear coexistence of major Cu_5- and minor Cu_4-S1 is detected. These results are fully concordant with those of the corresponding Cu-Sx recombinant syntheses (Fig. 4 and Table 3), and altogether, they indicate that the flanking spacer is essential for the stabilization of the 5th Cu(I) in the cluster.

For the two nine-Cys fragments (7-Cys box plus + 2 adjacent Cys), only the titration of Zn-S4 was somewhat successful, ending in M_5-S4, mainly constituted by a Cu_5-S4 complex, despite the noise of the corresponding ESI-MS spectra. Although no product other than the apo-peptide could be retrieved from the Zn-S5 synthesis, the Cu(I) titration was equally assayed with this preparation. The reaction was clearly unsuccessful, according to the poor CD spectra and the noise of the ESI-MS spectra, data, which is also concordant with the unproductive synthesis of S5 in Cu-supplemented cultures.

The Zn/Cu displacement in Zn-S6 (two 7-Cys boxes) and Zn-S7 (three 7-Cys boxes), both without flanking spacers, clearly differs from that described for S1, S2 and S3, as it takes place in three successive stages (Fig. 5 and Figs S6 and S7). During the first steps of adding Cu(I) (until 4 and 6 Cu(I) eq, respectively, for S6 and S7), a mixture of heterometallic species containing major Cu_5- and minor Cu_4-cores is formed, this process generating clear isodichroic points in the corresponding CD spectra. These species are replaced by major Cu_{10}-S6 and Cu_9-S7 complexes in the second stage of the metal replacement (when 8 or 12 Cu(I) eq had been respectively added), also yielding an isodichroic evolution of the respective CD fingerprints of the mixtures. The third stage in both cases corresponds to the, again, isodichroic unfolding of the formed Cu-complexes into Cu_5-, Cu_4-cores and apo-forms indicating that they do not resist further Cu(I) additions. While this behavior is totally understandable for S6 (two 7-Cys boxes), a further stage corresponding to the filling

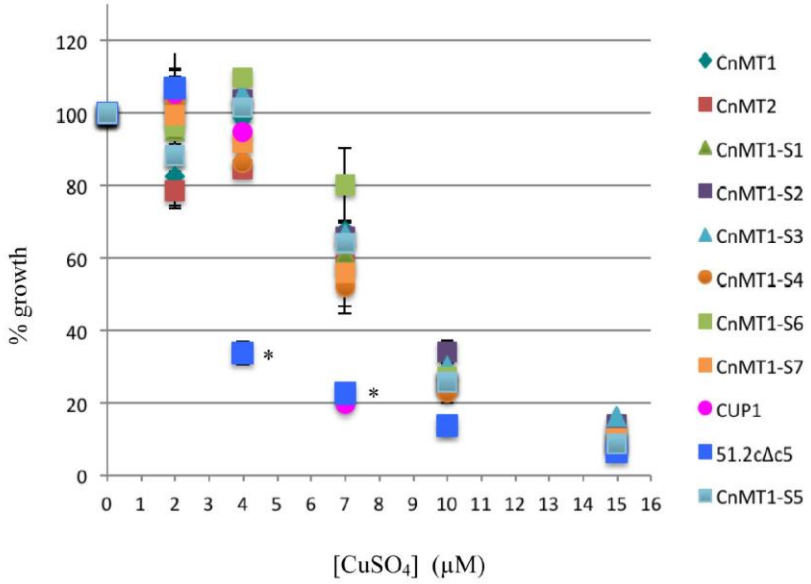

Fig. 6. Scatterplot of the tolerance to copper conferred to *S. cerevisiae* cells by *C. neoformans* MTs and CnMT1 truncated mutants. 51.2cΔc5 (an MT null yeast strain) cells were transformed with the corresponding MT or MT-construct coding regions cloned into the constitutive expression vector p424. Growth was evaluated in liquid cultures, and it is represented as the percentage of the growth rate attained in a non-Cu supplemented medium. Controls were the non-transformed yeast strain and the CUP1 (yeast MT) transformants. Each value is the mean of at least two replicates, and vertical lines represent standard deviations. Asterisks show the strains yielding significant different results than the rest at the corresponding Cu concentrations. For more details, see the *Experimental procedures* section.

of its third 7-Cys box would have been expected for S7. This is not observed, although some minor species of higher nuclearity (M_{15}- and Cu_{13}-S7) are detected for 12 Cu(I) eq added. Interestingly, these results nicely reproduce those obtained for the recombinant Cu-S6 and Cu-S7 preparations, those of S6 matching the end of the first stage of the metal replacement pathway, while those of S7 at normal aeration coincide with the results of the second stage of the titration (Fig. 5). It is surprising that while for S6, the Cu(I) filling of its two 7-Cys boxes is achievable (at least *in vitro*, if not *in vivo*) with further Cu(I) additions, for S7 only two of the three 7-Cys boxes are able to fold into Cu_5-cores, and only traces of the loading of the third box are weakly observed at high (12) amounts of Cu(I) added, before unfolding to Cu_5. Hence, the comparison of the S7 and CnMT1 Zn/Cu replacement reactions suggests that the presence of the terminal spacers plus adjacent CXC regions (or at least one of them) may be required to fill up and maintain a third Cu_5-cluster, as occurs for CnMT1, because in this case a clear Cu_{15}-CnMT1 species is detected in the corresponding metal exchange experiment.

Another point worth highlighting is that there is not only a good concordance between the CD spectra of all the *in vivo* preparations with those recorded after the addition of the number of Cu(I) eq indicated in Figs 4 and 5 to the corresponding Zn-Sx preparations (Fig. 3B), but also among all the CD fingerprints recorded *in vitro* for the final stages of the Cu(I) additions preceding the unfolding of the complexes and of these with that of Cu-CnMT1 (Fig. 3C). This observation gives support to the modular architecture of the entire protein as well as to that of those mutant peptides that contain more than one 7-Cys box.

Cu tolerance tests by a yeast complementation assay

To analyze the effect on Cu tolerance in *S. cerevisiae* of the heterologous expression of all the analyzed Sx peptides, a resistance experiment was performed using a yeast strain devoid of its two MTs (CUP1 and CRS5). Hence, the cDNAs encoding the Sx segments, as well as the *CUP1* cDNA for comparative purposes, were subcloned in the episomic plasmid p424-GDP. 51-2c-Δc5 yeast cells were transformed with either one of these constructs or with non-recombinant p424 as a control. The ability of these transformants to grow in media supplemented with increasing copper concentrations was tested by OD_{600} measurements of liquid cultures (Fig. 6) and by

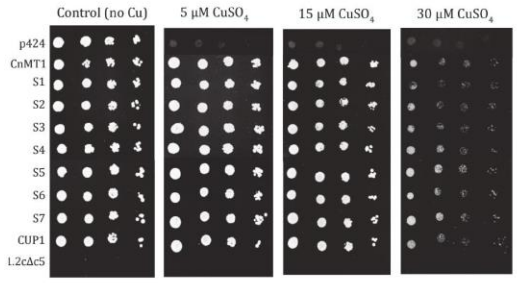

Fig. 7. Effect of the heterologous expression of the *C. neoformans* CnMTs and its truncated mutants in *S. cerevisiae* cell growth under Cu supplementation. 51.2cΔc5 (an MT null yeast strain) was transformed with the constitutive expression vector p424 (void) or the corresponding MT or MT constructs cloned into p424. Cultures were grown in SC-Trp-Ura-Leu medium overnight at 30°C, were diluted to OD_{600} 0.5 and spotted into SC-Trp-Ura-Leu agar plates supplemented with $CuSO_4$ at different concentrations. Plates were allowed to grow at 30°C during 3 days. For control growth purposes, non-transformed 51.2cΔc5 cells and cells transformed with the p424-CUP1 construct were also included in the assay. The results at 50 μM $CuSO_4$ supplementation are not included, because no growth was seen for any transformant.

standard dot assays (Fig. 7). The corresponding results clearly show that all the tested peptides are able to restore copper tolerance as efficiently as the yeast CUP1 MT, as growth was impaired beyond the first dilution for the control cells, whereas those overexpressing CUP1, CnMT1 or any Sx segment yielded colonies even at the fourth dilution range (Fig. 7). Results from the liquid cultures exactly reproduce the similarity of restoring copper tolerance for all the assayed peptides, as they exhibit similar growth rates in Cu-rich cultures, which are equivalent or higher than that of the CUP1-transformed cells, and definitely different to that of the MT-devoid strain. It is worth noting that at 7 μM $CuSO_4$ (the maximum concentration allowing a growth higher than 50% in liquid cultures, all the Sx segments yield higher resistance than CUP1, an effect that is consistent with the slightly impaired growth of the corresponding transformant in agar plates (cf. Fig. 7). The fact that all the Sx constructs appear to be better or as good as the native yeast Cu-thionein in restoring growth at high copper concentrations correlates well with the fact that all of them fold into Cu_5-clusters of similar features (i.e. similar CD fingerprints), which suggests that Cu-tolerance would be more related to the capacity of an MT polypeptide to fold into clusters that remain stable inside the cell than to their mere Cu(I) chelating capacity. In fact, such a conclusion was reached some time ago, when showing that different constructs of the *Quercus suber* QsMT2 MT with the same co-ordination capacity, but different architecture, conferred dissimilar Cd tolerance when assayed in yeast cells (Domenech *et al.*, 2007).

Conclusions

After the characterization of the two *C. neoformans* metallothioneins (CnMT1 and CnMT2) as infection and virulence factors (Ding *et al.*, 2013), it has been shown that their increased Cu-binding capacity was derived from their extraordinary length, if compared with the most well-known fungal Cu-thioneins (Palacios *et al.*, 2014). We then proposed that the CnMT proteins had a modular structure built by the repetition of three (CnMT1) or five (CnMT2) 7-Cys unit, separated by spacer regions devoid of Cys residues, plus Cys doublets flanking the whole sequence. This was concordant with each of these 7-Cys boxes forming independent Cu_5-clusters, which would be cooperatively filled with Cu(I) ions. This was an appealing hypothesis, but it remained to be proved, especially because the *N. crassa* MT, with a sequence completely alignable to the 7-Cys boxes of the *C. neoformans* MTs (Fig. 1), had been shown to form Cu_6-complexes (Cobine *et al.*, 2004). Therefore, a study of the metal-binding behavior of different truncated mutants of CnMT1 was compulsory to shed light on the proposed modular architecture of these MTs, and additionally, to the role of spacers and flanking amino acid sequences when modulating the co-ordination abilities of the Cys regions in proteins, which are determinant factors for MT preference on monovalent or divalent metal ions (Palacios *et al.*, 2011b).

Consideration of our current results fully supports our previous hypothesis about the modular, independent metal-binding behavior of the *C. neoformans* MT 7-Cys boxes. Strikingly, the influence of elements other than the co-ordinating Cys is different for Zn(II) and Cu(I) co-ordination. Hence, each 7-Cys stretch co-ordinates 2 Zn(II) ions, which is clearly reflected by the Zn_2-complexes yielded by S1, S2 and S3 and the Zn_4-complexes of S6. Noteworthy, the S3 folding about Zn(II) renders a collection of minor species, which is attributable to its C-term spacer. As Zn_3- and Zn_4-species are detected, it may be possible that the Glu residue, a well-known Zn(II)-coordinating amino acid, contributes to the final complexes. Also, the basic 2 Zn: 7 Cys relationship is enlarged by the presence of two extra flanking Cys (CXC motif) in the S4 C-terminal tail to yield up to Zn_3- and Zn_4-complexes. Finally, the higher Zn(II) binding capacity of S7 (major Zn_7-complex) in relation to the six Zn(II) theoretically bound by the three 7-Cys boxes, is also attributable the glutamic acid present in its N-term spacer region.

In the case of Cu(I) co-ordination, all the segments consisting of a 7-Cys box invariably render a unique Cu_5-cluster, where one of the Cu(I) ions appears quite unstable if the segment is devoid of a flanking spacer (i.e. S1). No effect is seen for the two extra Cys in S4. When several 7-Cys boxes are tandemly combined (two in S6 and three in S7), always one of them seems unable to remain filled

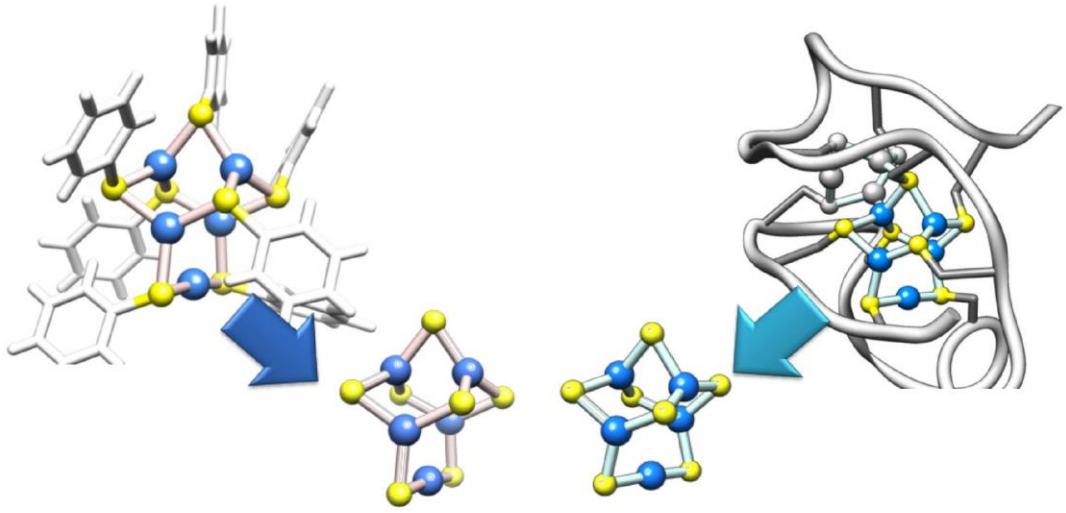

Fig. 8. Comparison of the 3D crystal structures of the $[Cu5(SPh)7]2^-$ complex (left) and the Cu8-Cup1 species (right) in which the Cu5S7 clusters have been colored and represented separately (center) to illustrate their high similarity (i.e. same metal and sulfur co-ordination environments). The inorganic complex data have been retrieved from the Cambridge Structural Database (entry MITWAO) and those for the protein from the Protein Data Bank (entry 1rju). They have been both treated with the Chimera software (Pettersen *et al.*, 2004).

with Cu(I), although the presence of high Cu(I) (i.e. in low aeration Cu-synthesis or Zn/Cu replacement experiments) enhances its capability to render higher nuclearity Cu-complexes. Therefore, the presence of flanking amino acids is revealed necessary to endow the Cu_5-clusters with enough stability in cell environments. Finally, it can be observed that the higher the number of 7-Cys boxes in these modular MTs, the higher the difference between the species rendered when synthesized in normal or high Cu cultures. The trend is that at normal aeration (regular Cu cell content), heterometallic Zn,Cu-complexes are recovered, while from poorly aerated cultures, homometallic Cu-species are purified, as occurs for S7 and the full-length CnMTs. A comparison between S7 and CnMT1 suggests that the two CXC motives present in CnMT1 and absent in S7 favor the co-ordination of Zn(II), if Cu(I) is not specially high. Therefore, if the main influence of spacer and flanking regions for Zn(II) co-ordination is the increase in the metal content of the afforded complexes, for Cu(I) co-ordination, it would be the stabilization of the final Cu_5-clusters, this sometimes contributed by additional Zn(II) co-ordination.

Overall, all the data presented in this study fully support the initial hypothesis that each 7-Cys segment constituting the basic unit of *C. neoformans* MTs folds into very favored Cu_5-clusters. The interest of deepening in the architecture of these novel Cu(I)-MT clusters promoted a revision of the model structures reported for inorganic Cu(I) thiolates (Dance, 1986; Henkel and Krebs, 2004), as well as of the unique X-ray diffraction-solved Cu-MT structure (Cu_8-Cup1) (Calderone *et al.*, 2005). According to all the knowledge gathered for inorganic metal thiolates, there is a unique model structure for a $Cu_5(SR)_7$ complex, which can be considered an extension of the $Cu_4(SR)_6$ complexes. It contains four metal ions in trigonal-planar and one in linear co-ordination, and was first observed in $[Cu_5(SPh)_7]^{2-}$ (Dance, 1978). Interestingly, this is the model structure that has been quoted in bioinorganic studies related to Cu-proteins, such as precisely MTs (Maiti *et al.*, 2007) and Cu-chaperones (Pushie *et al.*, 2012) illustrating the flexibility of the Cu(I) thiolates and the facile interconversion of Cu_4-, Cu_5- and Cu_6 clusters as features explaining their biological function. Finally, a modification of the structure of Cu_8-Cup1 consisting in the deletion of three Cys residues and three Cu(I) ions has rendered a 'biological model' that exactly matches the inorganic model, which is shown in Fig. 8. Furthermore, the sequence, and significantly the Cys motifs of the 7-Cys boxes are, as stated in the *Introduction*, fully alignable with those of *N. crassa MT* (Fig. 1), which discordantly has been reported to yield Cu_6-NcMT complexes (Cobine *et al.*, 2004). To tackle this apparent paradox, we have already performed experiments consisting of the recombinant synthesis of NcMT in Cu-supplemented media, by following the same rationale used in this work. They have unambiguously shown formation of a unique Cu_5-NcMT species (manuscript in preparation), which led us to consider as an unavoidable aim the reso-

lution of the 3D structure and the corresponding Cu-thiolate connectivities of these until nowadays unreported Cu-protein clusters.

With this work, we have shown how the pressure to cope with high copper concentrations may have positively selected the natural amplification of a small primeval fungal copper-chelating peptide by adjacently joining metal co-ordinating modules through adequate spacer sequences that led to the construction of 'high capacity' Cu-MTs. This supposes a newly reported mechanism by which fungal MTs – typically very short in size – can increase their Cu-sequestration capacity for detoxification purposes, besides gene number amplification (long known for the *S. cerevisiae* CUP1 MT) and gene transcription enhancement (as described in some *Aspergillus* species, Fedorova *et al.*, 2008). Therefore, we propose that amplified MTs should be taken into account when seeking for and studying pathogenic fungus virulence factors, and precisely those strategies used to escape Cu surplus-associated host nutritional immunity.

Experimental procedures

Construction of CnMT1 fragments and E. coli *expression vectors*

The cDNAs encoding the seven Sx segments of CnMT1 analyzed in this work (Fig. 1) were obtained by specific PCR amplification using as template, the complete CnMT1 cDNA sequence (GenBank: AFR98878.2) subcloned in the pGEX-4T-1 (GE Healthcare) *E. coli* expression vector (Palacios *et al.*, 2014), and as primers the oligonucleotides shown in Table S1 (Supplementary material). These oligonucleotides served to introduce the *BamH*I/*Xho*I sites for pGEX-4T-1 insertion, as well as a translation stop codon at the end of each coding sequence. 30-cycle PCR amplification reactions were performed with thermo-resistant Taq DNA polymerase (Expand High Fidelity PCR System, Roche) under the following conditions: 2 min at 94°C (initial denaturation), 15 s at 94°C (denaturation), 30 s at 57°C (annealing) and 30 s at 72°C (elongation). The final products were analyzed in 2% agarose gel and the expected bands were excised (Genelute™ Gel Extraction Kit, Sigma Aldrich). pGEX-4T-1 and the amplified inserts were digested with *BamH*I/*Xho*I and subsequently ligated (DNA Ligation Kit 2.1, Takara Bio). The recombinant plasmids were transformed into the *E. coli* MachI strain for DNA sequencing, using the Big Dye Terminator 3.1 Cycle Sequencing Kit in an ABIPRISM 310 Automatic Sequencer (Applied Biosystems). Positive clones were transformed into the *E. coli* BL21 protease deficient strain for protein synthesis.

Synthesis and purification of the recombinant Zn- and Cu-complexes of the CnMT1:Sx peptides

The GST-Sx fusion proteins were biosynthesized in 5 l Luria–Bertani (LB) cultures of transformed *E. coli* BL21 cells. Gene expression was induced with 100 μM (final concentration) of isopropyl β-D-thiogalactopyranoside (IPTG); after 30 min of induction, cultures were supplemented with 300 μM $ZnCl_2$ or 500 μM $CuSO_4$ (final concentration), and they were allowed to grow for a further 2.5 h for the synthesis of the respective metal complexes. In the case of Cu-supplementation, cultures were grown either under normal aeration conditions (1 l medium in a 2 l Erlenmeyer flask, at 250 r.p.m.), or under low oxygen conditions (1.5 l medium in a 2 l Erlenmeyer flask at 150 r.p.m.), as culture aeration determine the amount of intracellular copper available for recombinant MTs in the host cells (Pagani *et al.*, 2006).

After growth, cells were harvested by centrifugation, resuspended in ice-cold PBS (1.4 M NaCl, 27 mM KCl, 101 mM Na_2HPO_4, 18 mM KH_2PO_4) with 0.5% v/v β-mercaptoethanol and subsequently disrupted by sonication (20 s pulses for 5 min). To prevent metal-MT complex oxidation pure grade argon was invariably bubbled in all the steps of the purification and also in the PBS buffer stock. The sample was the centrifuged at 12 000 *g* for 30 min, and the recovered supernatant was incubated (gentle agitation for 60 min at room temperature) with Glutathione-Sepharone 4B (GE Healthcare) to allow batch affinity purification of the GST-Sx polypeptides. After three PBS washes of the Glutathione-Sepharone matrix, the Sx portion was recovered by thrombin cleavage (10 u per mg of fusion protein at 17°C overnight), so that the cleaved metal-Sx complexes remained in solution. This was concentrated by Centriprep Microcon 3 (Amicon, cut-off of 3 kDa) centrifugation, and the metal complexes were finally purified through FPLC in a Superdex75 column (GE Healthcare) equilibrated with 50 mM Tris-HCl, pH 7.0 and run at 0.8 ml min^{-1}. Fractions were collected and analyzed for protein content by their absorbance at 254 and 280 nm. Further details of the synthesis and purification steps are described in Cols *et al.* (1997) and Capdevila *et al.* (1997).

Zn(II)/Cu(I) replacement reactions on the CnMT1:Sx peptides

The *in vitro*-constituted Cu(I)-Sx complexes were prepared *via* metal replacement by adding a Cu(I) standard solution to each recombinant Zn-Sx preparation. These reactions were performed at pH 7.0 following the procedure previously reported for mammalian MTs (Bofill *et al.*, 1999). Characterization of the *in vitro* complexes was performed by UV–Vis and CD spectroscopies, as well as ESI-MS analysis, as explained below. All assays were carried out in an argon atmosphere, and the pH remained constant throughout all the experiments, without the addition of any other reagent, such as buffers or reductants.

Spectroscopic analyses (ICP-AES and CD) of the Zn- and Cu-complexes rendered by the CnMT1:Sx peptides

The S, Zn and Cu content of all the Sx preparations was analyzed by means of Inductively Coupled Plasma Atomic Emission Spectroscopy (ICP-AES) in a Polyscan 61E (Thermo Jarrel Ash) spectrometer, measuring S at 182.040 nm, Zn at 213.856 nm and Cu at 324.803. Samples were treated as in Bongers *et al.* (1988), but they were alter-

natively incubated in 1 M HNO_3 at 65°C for 10 min prior to measurements in order to eliminate possible traces of labile sulfide ions (Capdevila *et al.*, 2005). Protein concentrations were calculated from the acid ICP-AES sulfur measurements, assuming that all S atoms were contributed by the Sx peptides.

A Jasco spectropolarimeter (Model J-715) interfaced to a computer (J700 software) was used for CD measurements at a constant temperature of 25°C maintained using a Peltier PTC-351S equipment. Electronic absorption measurements were performed on an HP-8453 Diode array UV-visible spectrophotometer (GMI, Ramsey, MN, USA). All spectra were recorded with 1 cm capped quartz cuvettes, corrected for the dilution effects and processed using the GRAMS 32 software (Thermo Fisher Scientific, Waltham, MA, USA).

Electrospray ionization time-of-flight mass spectrometry (ESI-TOF MS) of the Zn- and Cu-Sx complexes

MW determinations were performed by electrospray ionization time-of-flight mass spectrometry (ESI-TOF MS) on a Micro TOF-Q instrument (Bruker) interfaced with a Series 1200 HPLC Agilent pump, equipped with an autosampler, all of which were controlled by the Compass Software. Calibration was attained with ESI-L Low Concentration Tuning Mix (Agilent Technologies). Samples containing Zn-Sx complexes were analyzed under the following conditions: 20 µl of protein solution injected through a PEEK (polyether heteroketone) tubing (1.5 m × 0.18 mm i.d.) at 40 µl min^{-1}; capillary counter-electrode voltage 5 kV; desolvation temperature 90–110°C; dry gas 6 l min^{-1}; spectra collection range 800–2500 m z^{-1}. The carrier buffer was a 5:95 mixture of acetonitrile : ammonium acetate (15 mM, pH 7.0). Alternatively, the corresponding Cu-complexes were analyzed as follows: 20 µl of protein solution injected at 40 µl min^{-1}; capillary counter-electrode voltage 3.5 kV; lens counter-electrode voltage 4 kV; dry temperature 80°C; dry gas 6 l min^{-1}. Here, the carrier was a 10:90 mixture of acetonitrile : ammonium acetate, 15 mM, pH 7.0. For the analysis of the apo-peptides and Cu-Sx complexes at acidic pH, 20 µl of the corresponding sample were injected under the same conditions described previously, but using a 5:95 mixture of acetonitrile : formic acid pH 2.4, as liquid carrier, which caused the complete demetalation of the peptides loaded with Zn, but kept the Cu ions bound to the peptide. Under all the conditions assayed, the error associated with the mass measurements was always lower than 0.1%. Masses for the holo-species were calculated as previously described (Fabris *et al.*, 1996).

Metal tolerance complementation assays in transformed yeast MT-knockout cells

The *S. cerevisiae* 51.2cΔc5 strain (*MAT*a, *trp*1-1, *ura*3-52, *ade*-, *his*-, *CAN*^{R}, *gal*1, *leu2-3*, *112 met13*, *cup1*Δ::*URA*3 *crs5*Δ::*LEU2*), derived from VC-sp6 (Culotta *et al.*, 1994), was used for copper tolerance complementation assays. The cDNAs coding for the full size CnMT1 and its derived constructed segments (Sx) were ligated into the *BamH*I/*Xho*I sites of the yeast vector p424-GPD (ATCC), whereas the CnMT2 cDNA had to be cloned into its *EcoR*I/*Xho*I sites due to an internal *BamH*I restriction site. ATG and STOP codons were suitably inserted into the coding sequences for proper translation when amplified by PCR using the oligonucleotides shown in Table S2. The p424-GPD vector contains TRP1 as a selection marker, the constitutive glyceraldehyde-3-phosphate dehydrogenase (GPD) promoter for gene expression, and the cytochrome *c* oxidase (CYC1) transcriptional terminator (Mumberg *et al.*, 1995). The recombinant p424 plasmids were introduced into the 51.2cΔc5 cells using the LiAc/SS-DNA/PEG procedure (Gietz and Woods, 2002). Transformed cells were selected according to their capacity to grow in synthetic complete medium (SC) without Trp, Leu and Ura. The construction p424-CUP1, encoding for the yeast Cu-thionein CUP1, was used as control. For copper tolerance tests, transformed yeast cells were initially grown in selective SC-Trp-Ura medium at 30°C and 220 r.p.m. until saturation. These cells were then diluted to OD_{600} 0.01 and used to re-inoculate tubes with 3 ml of fresh medium supplemented with $CuSO_4$ added at 0, 2, 4, 7, 10 and 15 µM final concentrations. These cultures were allowed to grow for 18 h, and the final OD_{600} was recorded and plotted as a percentage of the OD_{600} reached by the culture grown without metal supplement. Two replicates were run for each concentration, and each kind of transformation. Data were analyzed by a Principal Component algorithm, due to the complexity of including 11 strains and 4 Cu concentrations.

Alternatively, cell cultures were grown in SC-Trp-Ura liquid medium at 30°C until an OD600 of 0.5, and from them, three or four 10-fold dilutions were performed, so that 3 µl of each dilution were spotted on SC plates and on SC supplemented with copper at 0, 5, 15, 30 and 50 µM final concentrations. Plates were incubated for 3 days at 30°C and then photographed.

Acknowledgements

This work was supported by the Spanish Ministerio de Economía y Competitividad (MINECO), grants BIO2012-39682-C02-01 (to SA) and -02 (to MC), which are co-financed by the European Union through the FEDER program. Authors are members of the 2014SGR-423 *Grup de Recerca de la Generalitat de Catalunya*. AE was the recipient of a predoctoral grant from the MINECO (BES-2010–036553). SGM received a predoctoral fellowship from the *Departament de Química, Universitat Autònoma de Barcelona*. We thank Jordi Espín and Nerea Rovellada, who performed some experimental work, and the *Centres Científics i Tecnològics (CCiT) de la Universitat de Barcelona* (ICP-AES, DNA sequencing) and the *Servei d'Anàlisi Química (SAQ) de la Universitat Autònoma de Barcelona* (CD, UV-vis, ESI-MS) for allocating instrument time. Finally, we are deeply indebted to Prof. D. Thiele (Duke University, NC, USA) for introducing us to the fascinating world of fungal MTs and for his continuous support.

References

Blindauer, C.A. (2014) Metallothioneins. In *RSC Metallobiology Series No.2: Binding, Transport and Storage of Metal Ions in Biological Cells*. Maret, W., and Wedd, A. (eds). Cambridge, UK: RSC Publishing, pp. 594–653.

Bofill, R., Palacios, O., Capdevila, M., Cols, N., González-Duarte, R., Atrian, S., and González-Duarte, P. (1999) A new insight into the Ag^{+} and Cu^{+} binding sites in the metallothionein β domain. *J Inorg Biochem* **73:** 57–64.

Bofill, R., Capdevila, M., and Atrian, S. (2009) Independent metal-binding features of recombinant metallothioneins convergently draw a step gradation between Zn- and Cu-thioneins. *Metallomics* **1:** 229–234.

Bongers, J., Walton, C.D., Richardson, D.E., and Bell, J.U. (1988) Micromolar protein concentrations and metalloprotein stoichiometries obtained by inductively coupled plasma. Atomic emission spectrometric determination of sulfur. *Anal Chem* **60:** 2683–2686.

Calderone, V., Dolderer, B., Hartmann, H.-J., Echner, H., Luchinat, C., Del Bianco, C., *et al.* (2005) The crystal structure of yeast copper thioneins: the solution of a long-lasting enigma. *Proc Natl Acad Sci USA* **102:** 51–56.

Capdevila, M., Cols, N., Romero-Isart, N., Gonzalez-Duarte, R., Atrian, S., and Gonzalez-Duarte, P. (1997) Recombinant synthesis of mouse Zn_3-β and Zn_4-α metallothionein 1 domains and characterization of their cadmium(II) binding capacity. *Cell Mol Life Sci* **53:** 681–688.

Capdevila, M., Domenech, J., Pagani, A., Tio, L., Villarreal, L., and Atrian, S. (2005) Zn- and Cd-metallothionein recombinant species from the most diverse phyla may contain sulfide (S^{2-}) ligands. *Angew Chem Int Ed Engl* **44:** 4618–4622.

Capdevila, M., Bofill, R., Palacios, O., and Atrian, S. (2012) State-of-the-art of metallothioneins at the beginning of the 21st century. *Coord Chem Rev* **256:** 46–62.

Cobine, P., McKay, R.T., Zangger, K., Dameron, C., and Armitage, I.M. (2004) Solution structure of Cu_6 metallothionein from the fungus *Neurospora crassa*. *Eur J Biochem* **271:** 4213–4221.

Cols, N., Romero-Isart, N., Capdevila, M., Oliva, B., Gonzalez-Duarte, P., Gonzalez-Duarte, R., and Atrian, S. (1997) Binding of excess cadmium(II) to Cd_7-metallothionein from recombinant mouse Zn_7-metallothionein 1. UV-VIS absorption and circular dichroism studies and theoretical location approach by surface accessibility analysis. *J Inorg Biochem* **68:** 157–166.

Culotta, V.C., Howard, W.R., and Liu, X.F. (1994) CRS5 encodes a metallothionein-like protein in *Saccharomyces cerevisiae*. *J Biol Chem* **269:** 25295–25302.

Dance, I.G. (1978) The hepta(μ-benzenethiolato) pentametallate(I) dianions of copper and silver: formation and crystal structures. *Aust J Chem* **31:** 2195–2206.

Dance, I.G. (1986) The structural chemistry of metal thiolate complexes. *Polyhedron* **5:** 1037–1104.

Ding, C., Festa, R.A., Chen, Y.-L., Espart, A., Palacios, O., Espín, J., *et al.* (2013) *Cryptococcus neoformans* copper detoxification machinery is critical for fungal virulence. *Cell Host Microbe* **13:** 265–276.

Ding, C., Festa, R.A., Sun, T.-S., and Wang, Z.-Y. (2014) Iron and copper as virulence modulators in human fungal pathogens. *Mol Microbiol* **93:** 10–23.

Dolderer, B., Hartmann, H.J., and Weser, U. (2009) Metallothioneins in Yeast and Fungi. In *Metal Ions in Life Sciences, vol. 5: Metallothioneins and Related Chelators: Metallothioneins in Yeasts and Fungi*. Sigel, A., Sigel, H., and Sigel, R.K.O. (eds). Cambridge, UK: RSC Publishing, pp. 83–106.

Domenech, J., Orihuela, R., Mir, G., Molinas, M., Atrian, S., and Capdevila, M. (2007) The Cd^{II}-binding abilities of recombinant *Quercus suber* metallothionein: bridging the gap between phytochelatins and metallothioneins. *J Biol Inorg Chem* **12:** 867–882.

Fabris, D., Zaia, J., Hathout, Y., and Fenselau, C. (1996) Retention of thiol protons in two classes of protein zinc ion coordination centers. *J Am Chem Soc* **118:** 12242–12243.

Fedorova, N.D., Khaldi, N., Joardar, V.S., Maiti, R., Amedeo, P., Anderson, M.J., *et al.* (2008) Genomic islands in the pathogenic filamentous fungus *Aspergillus fumigatus*. *PLoS Genet* **4:** e1000046.

Gietz, R.D., and Woods, R.A. (2002) Transformation of yeast by lithium acetate/single-stranded carrier DNA/polyethylene glycol method. *Methods Enzymol* **350:** 87–96.

Gold, B., Deng, H., Bryk, R., Vargas, D., Eliezer, D., Roberts, J., *et al.* (2008) Identification of a copper-binding metallothionein in pathogenic mycobacteria. *Nat Chem Biol* **4:** 609–616.

Henkel, G., and Krebs, B. (2004) Metallothioneins: zinc, cadmium, mercury, and copper thiolates and selenolates mimicking protein active site features – structural aspects and biological implications. *Chem Rev* **104:** 801–824.

Hodgkinson, V., and Petris, M.J. (2012) Copper homeostasis at the host-pathogen interface. *J Biol Chem* **287:** 13549–13555.

Ladomersky, E., and Petris, M.J. (2015) Copper tolerance and virulence in bacteria. *Metallomics* **7:** 957–964.

Lerch, K. (1980) Copper metallothionein, a copper-binding protein from *Neurospora crassa*. *Nature* **284:** 368–370.

Maiti, B.K., Pal, K., and Sabyasachi, S. (2007) Flexible Cu^{I}-thiolate clusters with relevance to metallothioneins. *Eur J Inorg Chem* **2007:** 5548–5555.

Mumberg, D., Müller, R., and Funk, M. (1995) Yeast vectors for the controlled expression of heterologous proteins in different genetic backgrounds. *Gene* **156:** 119–122.

Münger, K., and Lerch, K. (1985) Copper metallothionein from the fungus *Agaricus bisporus*: chemical and spectroscopic properties. *Biochemistry* **24:** 6751–6756.

Otvos, J.D., and Armitage, I.M. (1980) Structure of the metal clusters in rabbit liver metallothionein. *Proc Natl Acad Sci USA* **77:** 7094–7098.

Pagani, A., Villarreal, L., Capdevila, M., and Atrian, S. (2007) The *Saccharomyces cerevisiae* Crs5 metallothionein metal-binding abilities and its role in the response to zinc overload. *Mol Microbiol* **63:** 256–269.

Palacios, O., Atrian, S., and Capdevila, M. (2011a) Zn- and Cu-thioneins: a functional classification for metallothioneins? *J Biol Inorg Chem* **16:** 991–1009.

Palacios, O., Pagani, A., Perez-Rafael, S., Egg, M., Höckner, M., Brandstätter, A., *et al.* (2011b) Shaping mechanisms of metal specificity in a family of metazoan metallothioneins: evolutionary differentiation of mollusc metallothioneins. *BMC Biol* **9:** 4.

Palacios, O., Espart, A., Espín, J., Ding, C., Thiele, D.J., Atrian, S., and Capdevila, M. (2014) Full characterization of the Cu-, Zn- and Cd-binding properties of CnMT1 and CnMT2, two metallothioneins of the pathogenic fungus

Cryptococcus neoformans acting as virulence factors. *Metallomics* **6:** 279–291.
Pettersen, E.F., Goddard, T.D., Huang, C.C., Couch, G.S., Greenblatt, D.M., Meng, E.C., and Ferrin, T.E. (2004) UCSF Chimera – a visualization system for exploratory research and analysis. *J Comput Chem* **25:** 1605–1612.
Pushie, M.J., Zhang, L., Pickering, I.J., and George, G.N. (2012) The fictile coordination chemistry of cuprous-thiolate sites in copper chaperones. *Biochim Biophys Acta* **1817:** 938–947.
Samanovic, M.I., Ding, C., Thiele, D.J., and Darwin, H. (2012) Copper in microbial pathogenesis: meddling with the metal. *Cell Host Microbe* **11:** 106–115.
Skaar, E.P., and Raffatellu, M. (2015) Metals in infectious diseases and nutritional immunity. *Metallomics* **7:** 926–928.
Staats, C.C., Kmetzsch, L., Schrank, A., and Vainstein, M.H. (2013) Fungal zinc metabolism and its connections to virulence. *Front Cell Infect Microbiol* **3:** 1–7.
Tomas, M., Domenech, J., Capdevila, M., Bofill, R., and Atrian, S. (2013) The sea urchin metallothionein system: comparative evaluation of the SpMTA and SpMTB metal-binding preferences. *FEBS Open Bio* **3:** 89–100.
Valls, M., Bofill, R., Gonzalez-Duarte, R., Gonzalez-Duarte, P., Capdevila, M., and Atrian, S. (2001) A new insight into metallothionein (MT) classification and evolution. The *in vivo* and *in vitro* metal binding features of *Homarus americanus* recombinant MT. *J Biol Chem* **276:** 32835–32843.
Wang, Y., Mackay, E.A., Zerbe, O., Hess, D., Hunziker, P.E., Vašák, M., and Kägi, J.H.R. (1995) Characterization and sequential localization of the metal clusters in sea urchin metallothionein. *Biochemistry* **34:** 7460–7467.
Wilson, D., Citiulo, F., and Hube, B. (2012) Zinc exploitation by pathogenic fungi. *PLoS Pathog* **8:** e1003034.

Supporting information

Additional supporting information may be found in the online version of this article at the publisher's web-site.

11.2 The Fungus *Tremella mesenterica* Encodes the Longest Metallothionein Currently Known: Gene, Protein and Metal Binding Characterization

PLOS | ONE

RESEARCH ARTICLE

The Fungus *Tremella mesenterica* Encodes the Longest Metallothionein Currently Known: Gene, Protein and Metal Binding Characterization

Paul Iturbe-Espinoza[1☯], Selene Gil-Moreno[2☯], Weiyu Lin[1], Sara Calatayud[1], Òscar Palacios[2], Mercè Capdevila[2], Sílvia Atrian[1]*

1 Departament de Genètica, Facultat de Biologia, Universitat de Barcelona, Barcelona, Spain, **2** Departament de Química, Facultat de Ciències, Universitat Autònoma de Barcelona, Cerdanyola del Vallès, Barcelona, Spain

☯ These authors contributed equally to this work.
* satrian@ub.edu

OPEN ACCESS

Citation: Iturbe-Espinoza P, Gil-Moreno S, Lin W, Calatayud S, Palacios Ò, Capdevila M, et al. (2016) The Fungus *Tremella mesenterica* Encodes the Longest Metallothionein Currently Known: Gene, Protein and Metal Binding Characterization. PLoS ONE 11(2): e0148651. doi:10.1371/journal.pone.0148651

Editor: Yong-Sun Bahn, Yonsei University, REPUBLIC OF KOREA

Received: October 19, 2015

Accepted: January 21, 2016

Published: February 16, 2016

Data Availability Statement: GenBank: KM244758.1 GenBank: AJK28606.1.

Funding: This work was supported by the Spanish Ministerio de Economía y Competitividad (MINECO), grants BIO2012-39682-C02-01 (to SA) and -02 (to MC), which are co-financed by the European Union through the FEDER program. Authors are members of the 2014SGR-423 Grup de Recerca de la Generalitat de Catalunya.

Abstract

Fungal Cu-thioneins, and among them, the paradigmatic *Neurospora crassa* metallothionein (MT) (26 residues), were once considered as the shortest MTs -the ubiquitous, versatile metal-binding proteins- among all organisms, and thus representatives of their primeval forms. Nowadays, fungal MTs of diverse lengths and sequence features are known, following the huge heterogeneity of the Kingdom of Fungi. At the opposite end of *N. crassa* MT, the recently reported *Cryptococcus neoformans* CnMT1 and CnMT2 (122 and 186 aa) constitute the longest reported fungal MTs, having been identified as virulence factors of this pathogen. CnMTs are high-capacity Cu-thioneins that appear to be built by tandem amplification of a basic unit, a 7-Cys segment homologous to *N. crassa* MT. Here, we report the *in silico*, *in vivo* and *in vitro* study of a still longer fungal MT, belonging to *Tremella mesenterica* (TmMT), a saprophytic ascomycete. The *TmMT* gene has 10 exons, and it yields a 779-bp mature transcript that encodes a 257 residue-long protein. This MT is also built by repeated fragments, but of variable number of Cys: six units of the 7-Cys building blocks-$CXCX_3CSCPPGXCXCAXCP$-, two fragments of six Cys, plus three Cys at the N-terminus. TmMT metal binding abilities have been analyzed through the spectrophotometric and spectrometric characterization of its recombinant Zn-, Cd- and Cu-complexes. Results allow it to be unambiguous classified as a Cu-thionein, also of extraordinary coordinating capacity. According to this feature, when the TmMT cDNA is expressed in MT-devoid yeast cells, it is capable of restoring a high Cu tolerance level. Since it is not obvious that *T. mesenterica* shares the same physiological needs for a high capacity Cu-binding protein with *C. neoformans*, the existence of this peculiar MT might be better explained on the basis of a possible role in Cu-handling for the Cu-enzymes responsible in lignin degradation pathways.

Competing Interests: The authors have declared that no competing interests exist.

Introduction

Metallothioneins (MTs) constitute a heterogeneous superfamily of ubiquitously occurring, low molecular weight, cysteine rich proteins that natively coordinate divalent (Zn^{2+}, Cd^{2+}) or monovalent (Cu^{+}) metal ions through metal-thiolate bonds, which imposes a definite polypeptide folding (see [1,2,3] for recent MT reviews). No single biological role has been assigned to these peptides, but, instead, several functions have been proposed [4], ranging from physiological metal handling to toxic metal protection. MTs are highly polymorphic proteins exhibiting a low degree of sequence similarity, so that in fact they can be considered different homology groups along the Tree of Life [5]. It is precisely this sequence heterogeneity what explains why different classification criteria have emerged during the progressive discovery and characterization of new MTs. Binz and Kägi, in the late nineties [6], proposed a taxonomy-based MT classification, in which essentially each MT group (so-called *family*) included the MTs of a taxonomic group of organisms, this ensuring their homology. In contrast to this *sequence-based* criterion, we proposed a MTs *function-based* classification that assigns a Zn-/Cd (*i.e.* divalent metal ion) or Cu-thionein (*i.e.* monovalent metal ion) character to each peptide, according to its metal-binding preference [7], a classification that was latter modulated as a step gradation between these two extreme metal preferences [8,9]. Thereafter, we showed that a unique, energetically optimized complex results when a MT polypeptide folds about its cognate metal ions, while with non-cognate metal ions, it renders a mixture of species, none of them specially favored [10].

The Kingdom of Fungi is an extremely large and heterogeneous group of organisms, comprising between 1.5 million to 5 million species. This same heterogeneity applies to their MTs, because as for no other taxon fungal MTs are distributed in 6 different families (from Family #8 to #13) in the Binz and Kägi classification [6] (Table 1). At the time of such proposal, the fungal non-yeast MTs (Family #8) were restricted to those of the ascomycete *Neurospora crassa* [11] and the basidiomycete *Agaricus bisporus* (the edible champignon or white mushroom) [12]. Both were the shortest MTs reported (26 amino acids, encompassing 7 Cys residues), and shared with Cup1 (the yeast *Saccharomyces cerevisiae* MT [13,14]) its definite Cu-thionein character. From these results, the idea that fungal non-yeast MTs were representative of short, archetypical MTs, which would have evolved to yield the higher invertebrate and vertebrate forms by domain duplication and specialization towards divalent metal ion binding, gained full support [15].

This picture was completely turned over when the two MTs of the human pathogenic fungus *Cryptococcus neoformans* (CnMT1 and CnMT2) were recently reported as infection, virulence, and pathogenicity factors [16]. CnMT1 and CnMT2 counteract the Cu(I) ions diffused by macrophages in the infected tissues through the extraordinary Cu-binding capacity derived from their unusual length: 122 (CnMT1) and 183 amino acids (CnMT2) [17]. These two MTs revealed an unexpected modular structure, being respectively constituted by three and five

Table 1. Families of the Binz & Kägi MT classification that include the fungal MTs.

Family	Group	Example	Sequence	UniProtKB
8	**Fungal 1**	*N. crassa* MT	MGDCGCSGASSCNCGSGCSCSNCGSK	P02807
9	**Fungal 2**	*C. glabrata* MT1	MANDCKCPNGCSCPNCANGGCQCGDKCECKKQSCHGCGEQCKCGSHGSSCHGSCGCGDKCECK	P15113
10	**Fungal 3**	*C. glabrata* MT2	MPEQVNCQYDCHCSNCACENTCNCCAKPACACTNSASNECSCQTCKCQTCKC	P15114
11	**Fungal 4**	*Y. lipolytica* MT3	MEFTTAMLGASLISTTSTQSKHNLVNNCCCSSSTSESSMPASCACTKCGCKTCKC	Q9HFD0
12	**Fungal 5**	*S. cerevisiae* Cup1	MFSELINFQNEGHECQCQCGSCKNNEQCQKSCSCPTGCNSDDKCPCGNKSEETKKSCCSGK	P0CX80
13	**Fungal 6**	*S. cerevisiae* Crs5	MTVKICDCEGECCKDSCHCGSTCLPSCSGGEKCKCDHSTGSPQCKSCGEKCKCETTCTCEKSKCNCEKC	P41902

doi:10.1371/journal.pone.0148651.t001

A)

```
C. neoformans   -MACNCPP-QKNTACCSTSEAQDKCTCQKGNCECKACPNSTKTSESGGKASTCNCGGSGE 58
T. mesenterica  GEECSCPPGQCSCANCPAKEKKDACSCSEG-CSCPPGQCACANCPHKDKAKGCSCG---E 56
                   *.*** * . * *.:.* :* *:*.:* *.* .   :  ..   .**. *.**   *
C. neoformans   ACTCPPGQCACDKCPKKAKSVSTCGCGGSGAACSCPPGKCACDNCPKQAQEKVSSCACSG 118
T. mesenterica  SCSCPPGECKCANCPKKSEPAKACACG---DECSCPPGQCGCADCP----GKTSS----- 104
                :*:****:* * :****::...:*.**     ******:*.* :**     *.**
C. neoformans   SGAA 122
T. mesenterica  ----
```

B)

```
AGATGTGGAGAAGAATGTTCATGCCCCCCCGGACAATGTTCTTGTGCCAATTGTCCCGCTAAAGAGAAGAAAGATGCTTGCAGGTATGTCTTTC
GCCCTCTTCTTGTCACATCTCCCGTCTTGAATGACGGGACGCGTAGTATCGTGACACTCGTATTTGTCATCAGAGGAACGACGCCCGACATCTT
GCATTTGATTGACAGGCGGACGCGAGATATGCGGTGTGAGAAATGCTGCATTTAGCAGGGGTTCAACACTGCAGTATGAGAAGAGGGCTGATAT
CAAAGCTGCTCTGAAGGGTGTTCTTGCCCTCCTGGTCAATGCGCATGCGCCAACTGTCCGCACAAGGACGAAGCGAAGGGGTGCAGGTGAGCTA
TGTTGTCCTTGACCTCATTCCTAACCCTGCTTGTCAAGTTGTCACGTTCTGATGACTGATAGTGTAACCTGATTTTGAGACAAACGCTGATGAT
AGCTGCGGCGAGTCATGTTCATGCCCACCTGGAGAATGTAAATGTGCGAACTGCCCCAAGAAAACCGAACCTGCCAAAGCCTGCGCGTGAGTGG
CTCCTTCCCTCAGTCTGCAACCTTTCCCCTCTCGACTACGCTTGAAGACATGACGTTCTCTCCCTACTATAGAAGTATAGAGCGGGGAGAGGGA
AGTTAGAAAAGATGTTGACCAATAGTTGCGGTGACGAATGTTCTTGTCCTCCTGGACAGTGCGGATGTGCGGATTGTCCAGGGAAGACTTCATC
TTGATTGGCACCTTGAGCACGGATGAACCTCAGCAAAATTCCCGACACCACAATGACCCCAA
```

Fig 1. Partial *T. mesenterica* MT protein and cDNA sequences retrieved from data banks. (A) Clustal W2 alignment of the *C. neoformans* CnMT2 protein sequence and that retrieved from the *T. mesenterica* NCBI EIW70699 ORF annotation. (B) cDNA corresponding to the sequence coding for the protein shown in (A) localized in the TREMEscaffold_3 (access code JH711530.1) of the *T. mesenterica* genome. The putative exons are shown in yellow and the conventional splicing donor/acceptor sites in gray.

doi:10.1371/journal.pone.0148651.g001

7-Cys regions separated by spacer stretches. Therefore, their origin was hypothesized to be the result of ancient tandem repetitions of a primeval fungal MT unit comprising seven Cys residues, with the same Cys pattern of the *Neurospora* and *Agaricus* MTs (X_2-[CXC]-X_5-[CXC]-X_3-[CXC]-X_2-C-X_3) ([11,12], respectively) [16]. The analysis of the Cu-binding features of CnMT1 and CnMT2 further supported this hypothesis, because the homometallic Cu-CnMT species folded *in vivo* at high Cu concentrations could be readily explained by the respective three- and five-fold presence of basic Cu_5-(7-Cys) clusters [17]. The other known "long MTs" are the five MT isoforms present in the ciliate *Tetrahymena* species, thus another unicellular eukaryote, with lengths ranging between 96 and 181 amino acids, most of them also with modular primary structures [18].

During the study of *C. neoformans CnMT1* and *CnMT2*, there was evidence that both genes had been wrongly annotated [17]. Miss annotation of MTs or MT-like's often occurs as the result of automatic analysis of raw genome sequences, due to the common short exon length of the *MT* genes, and the Cys repetition in MT proteins. In this scenario, we aimed at examining the ensemble of available fungus genomes, transcript and EST databases, in order to identify other putative long-length MTs, and to analyze their putative modular structure and metal binding abilities. Among all the retrieved hits, a partial cDNA from *Tremella mesenterica*, devoid of translation starting codon, and annotated as coding a hypothetical protein (Fig 1) attracted our attention. This sequence showed a Cys pattern characteristic of MT polypeptides, it aligned well with the *C. neoformans* MTs, and it belonged to a fungus genus also member of the Tremellales order [19]. *T. mesenterica* is typically considered as a saprophytic fungus, but it has also been reported as parasitic to other fungi. Hence, starting from the partial and

unassigned sequence, we were able to define, both bioinformatically and experimentally, the whole polypeptide coding sequence, showing that it had all the requirements to be considered as an MT protein, which in fact turned out to be the longest MT ever reported (257 amino acids), and it also exhibited a modular structure. The *T. mesenterica* MT (TmMT) was then recombinantly synthesized as Zn-, Cd- and Cu-complexes, which were spectroscopically and spectrometrically characterized. The results showed that TmMT was also a Cu-thionein, with an extremely high Cu coordination capacity. This is in concordance with the high tolerance exhibited by this fungus to Cu. Our results open the possibility to ascertain the biological significance that this protein may exhibit in the *T. mesenterica* physiology, but most significantly, they show how tandem amplification of basic MT units seem to be a common trait in the evolution of several MTs in the Tremellales fungi.

Materials and Methods

Bioinformatic methods for identification of MT genes in the *Tremella mesenterica* genome

DNA and protein sequences were retrieved, analyzed and compared using the online versions of BLAST (at www.ncbi.nim.nih.gov) and Clustal Omega2 (W2) (at http://www.ebi.ac.uk). Screened databases were NCBI (National Center for Biotechnology Information, at www.ncbi.nim.nih.gov) the JCI (Joint Genome Institute of the USA Department of Energy (at genomeportal.jgi.doe.gov) [20].

Tremella mesenterica cultures

Tremella mesenterica strain was obtained from PYCC® (Portuguese Yeast Culture Collection, ref # PYCC 5472). Liquid cultures were performed at 25°C in YM (Yeast Mold) medium (yeast extract 3 g/L, malt extract 3 g/L, peptone 5 g/L, and glucose 10 g/L) [21], supplemented with copper salt when necessary ($CuSO_4$, at concentrations ranging from 0.1 mM to 5 mM, as indicated in each experiment). For plate cultures, YPD (2% glucose, 1% yeast extract, 2% peptone and 2% agar) was used and supplemented with $CuSO_4$ when necessary.

Tremella mesenterica RNA isolation and retrotranscription

Total RNA was extracted from *T. mesenterica* 10-mL YM cultures, following an adaptation of yeast RNA isolation rationale [22]. All the used material was sterilized and treated to be RNAase free. 1-mL aliquots of grown cultures were centrifuged in Eppendorf tubes for 3 min at 2500 rpm, frozen in liquid N_2 and re-suspended in 0.5 mL of LETS buffer (0.1 mM LiCl, 0.01 mM EDTA, 0.01 mM Tris, 2% SDS, pH 4.3). Further 0.5 mL of Tris-HCl saturated phenol (pH 4.3) and 0.5 mL of glass beads (425–600 μm diameter) were added to each Eppendorf and cells were disrupted in a TissueLyser® (Qiagen) by two 30-s series of 30 pulse/s. A mixture of phenol:chlorophorm:isoamyl alcohol (25:24:1) was added 1:1 v:v to the supernatant of a 15-min centrifugation at 12000 rpm for a first extraction. A second extraction was performed from the previous supernatant with 24:1 chlorophorm:isoamyl alcohol, and samples were precipitated with 5 M LiCl and kept at -80°C for at least 3 h. After centrifugation at 12000 rpm for 15 min, the pellet was washed with 200 μL of 70% ethanol per Eppendorf, and re-precipitated. Finally, the RNA was re-suspended in 30 μL of milliQ water per Eppendorf and its concentration assessed by A_{260} in a NanoQuant® (Tecan) equipment, and by agarose gel electrophoresis (1% agarose in TAE (40 mM Tris, 20 mM acetic acid, 1 mM EDTA) buffer. The isolated RNA was treated with RQ1® RNAse-Free DNAse (Promega) to avoid DNA contamination (digestion with 1 u/μL of the enzyme at 37°C for 30 min) and stored at -80°C until needed. Total RNA

was retrotranscribed using the Transcriptor First Strand cDNA Synthesis® kit (Roche), which includes oligo dT and random hexamer primers. 1 ng of total RNA was denatured for 5 min at 65°C, and then RT buffer (8 mM $MgCl_2$), RNAse inhibitor, RT enzyme and the oligonucleotide mix were added in a 20-μL final volume. The sample was incubated for 10 min at 25°C, and retrotranscription was allowed for 30 min at 55°C and finally stopped by a 5-min incubation at 85°C. The obtained cDNA was quantified by A_{260} measurement in a NanoQuant® (Tecan).

RACE amplification of the *Tremella mesenterica* mRNA

To obtain the full *T. mesenterica* MT cDNA 5' end sequence, the RACE (Rapid Amplification of cDNA Ends) strategy was applied, through the 5' RACE v12® kit from Roche. To this end, three antisense primers were designed from the already known TmMT sequence: R1 (5' TCAA GATGAAGTCTTCCCTG 3'), R2 (5' GACAATCCGCACATCCGCAC 3') and R3 (5' ACATT CGTCACCGCAAGCGC 3'). RACE reactions were performed following the supplier instructions, starting from 2 μg of the total *T. mesenterica* RNA preparation (147.5 μg RNA/μL) obtained from fresh fungus cultures in YM medium. The products of the nested PCR of the RACE steps were followed by agarose gel electrophoresis, and the final product was directly sequenced.

Synthesis of the *Tremella mesenterica* cDNA and cloning in the *E. coli* expression vector

cDNA cloning procedures were performed essentially as described previously in detail for the *C. neoformans* [17] and *Amphioxus* [23] MTs. Hence, the complete TmMT cDNA was amplified by PCR from the total *T. mesenterica* cDNA preparation obtained as previously described. The reaction was performed in a final volume of 25 μL, using the Expand High Fidelity PCR system® (Roche), and the specific primers: 5' 5'AAAAGGATCCATGTCTGCTCCTGTCGA AAC 3' (upstream) and 5'AAAACTCGAGGATTTGACGTTAGAGCAACC 3' (downstream), to respectively add the *BamHI*/*Xho*I sites necessary for in-frame cloning into the *E. coli* pGEX-4T-1® expression vector (GE Healthcare). Expression from this system yields GST-fusion proteins, from which the MT portion is isolated by thrombin cleavage [24]. The 35-cycle amplification reaction was performed under the following conditions: 15 s at 94°C (denaturation), 50 s at 55°C (annealing), and 50 s at 72°C (elongation). The final product was analyzed by 2% agarose gel electrophoresis/ethidium bromide staining, and directly purified from the PCR reaction with the Illustra DNA Purification Kit® (GE Healthcare). The amplified DNA and the pGEX-4T-1 vector were digested with *BamH*I and *Xho*I (Fast Digest®, Thermo Scientific), and ligated using the DNA Ligation Kit 2.1® (Takara Bio Inc.). Finally, the recombinant plasmids were transformed into *E. coli* Mach I strain for sequencing, which was attained using the Big Dye Terminator 3.1 Cycle Sequencing Kit® (Applied Biosystems) and the pGEX-4T-1 5' and 3' primers, in a automatic sequencer (ABIPRISM 310, Applied Biosystems) of the CCiTUB (Genomics Services of the University of Barcelona). The correct recombinant plasmids (pGEX-TmMT) were then transformed into the *E. coli* BL21 protease deficient strain (GE Healthcare) for protein synthesis.

Cloning of the *Tremella mesenterica* cDNA in yeast expression vector and complementation assays

The *Saccharomyces cerevisiae* 51.2cΔc5 strain (*MAT*a, *trp*1-1, *ura*3-52, *ade*-, *his*-, CAN^R, *gal*1, *leu2-3*, *112 met13*, *cup1*Δ::*URA*3 *crs5*Δ::*LEU2*), derived from VC-sp6 [25] was used for copper tolerance assays as described in detail previously for the CnMT1-derived peptides [26]. The TmMT cDNA was inserted into the *BamHI*/*Xho*I sites of the yeast vector p424-GPD, which

contains TRP1 as a selection marker, the constitutive glyceraldehyde-3-phosphate dehydrogenase (GPD) promoter for gene expression, and the cytochrome-c-oxidase (CYC1) transcriptional terminator [27]. The recombinant TmMT-p424 plasmid was transformed into 51.2cΔc5 cells using the LiAc/SS-DNA/PEG procedure [28], and positive transformants were selected by their capacity to grow in synthetic complete medium (SC) devoid of Trp, Leu, and Ura. For comparative purposes, yeast transformants with CUP1-p424 and mMT1-p424, encoding for the yeast CUP1 MT and the mouse MT1 isoform respectively, and with the void p424 plasmid, were also assayed. For copper tolerance tests, the transformants were initially grown in selective SC-Trp-Ura medium at 30°C and 220 rpm until saturation, and then a cell suspension of OD_{600} = 0.01 was used to inoculate 3-mL fresh cultures supplemented with $CuSO_4$ at 0, 2, 4, 7, 10, 15, 20, and 30 μM final concentrations. After 18 h of growth, the final OD_{600} was measured and plotted as a percentage of the OD_{600} reached by the culture grown without Cu. Three replicates were run for each Cu concentration, and for each transformant.

Preparation of recombinant and *in vitro*-constituted metal-TmMT complexes

5-L LB (Luria-Bertani) cultures of pGEX-TmMT transformed BL21 cells were induced with 100 μM (final concentration) of IPTG (isopropyl β-D-thiogalactopyranoside), and after 30-min growth, they were supplemented with 300 μM $ZnCl_2$, 300 μM $CdCl_2$ or 500 μM $CuSO_4$ (final concentrations) to respectively allow the synthesis of the Zn-, Cd- or Cu-TmMT complexes, and further grown for additional 2.5 h. Cu-supplemented cultures were performed at two aeration conditions: regular (*i.e.* 1-L of LB media in a 2-L Erlenmeyer flask, at 250 rpm) or low (1.5-L of LB media in a 2-L Erlenmeyer flask, at 150 rpm), since available oxygen determines the intracellular copper levels in the host cells, as described in [29]. To prevent oxidation of the metal–TmMT complexes, argon was bubbled in all the steps of the purification protocol. Cells recovered from the bacterial cultures by centrifugation were resuspended in ice-cold PBS (1.4 M NaCl, 27 mM KCl, 101 mM Na_2HPO_4, 18 mM KH_2PO_4)-0.5% v/v β-mercaptoethanol and disrupted by sonication in a Sonifier® ultrasonic cell disruptor (8 min, at 0.6 pulse/s). The total protein extract was centrifuged at 12,000 x*g*, 40 min, and the supernatant was incubated with Glutathione-Sepharose 4B® (GE Healthcare) beads at gentle agitation for 1 h, room temperature. After three washes in cold PBS, the matrix-bound GST-MT protein was split by thrombin digestion (10 u per mg of fusion protein, overnight at 17°C). The solution containing the metal-TmMT complexes, which had consequently been released from the matrix, was concentrated using Ultracel® YM-3 (Millipore) filters, and finally fractionated through a Superdex-75 FPLC column (GE Healthcare) equilibrated with 20 mM Tris-HCl, pH 7.0, and run at 0.8 mL min^{-1}. The protein-containing fractions, identified by their absorbance at 254 and 280 nm, were later analyzed in 15% SDS-PAGE gels stained with Coomassie Blue, and they were pooled and stored at -80°C until further use. Due to the pGEX vector cloning specificities, the recombinant TmMT exhibited two additional N-term residues (Gly-Ser), but they have been shown to have no effect on the MT metal-binding features [30]. Further details about the synthesis and purification procedures can be found in previous publications [17,23,26].

The so-called "*in vitro* complexes" were those prepared *via* metal replacement by adding the corresponding metal ions (Cd(II) or Cu(I)) to the recombinant Zn-TmMT samples. These reactions were performed at pH 7.0 using $CdCl_2$ or $[Cu(CH_3CN)_4]ClO_4$ solutions, respectively, as described earlier in detail for mammalian MTs [24,31]. During all the experiments, strict oxygen-free conditions were maintained by saturating the solutions with argon. All the *in vitro*-obtained metal-MT samples were analyzed following the same rationale as for the recombinant samples.

Characterization of the metal-TmMT complexes

ICP-AES (inductively coupled plasma atomic emission spectroscopy) analysis of the purified metal-TmMT complexes was essentially performed as previously described for other MTs [17,23,26]. S, Zn, Cd and Cu contents were measured in a Polyscan 61E (Thermo Jarrell Ash) spectrometer, reading S at 182.040 nm, Zn at 213.856 nm, Cd at 228.802 and Cu at 324.803 nm. Samples were treated as in [32], and were also alternatively incubated in 1 M HCl at 65°C for 15 min (acid ICP conditions) to eliminate any labile sulfide ions, as described in [33]. Protein concentration was calculated from the acid ICP-AES sulfur content, assuming that the measured S atoms were contributed by the MT peptide. CD spectra were recorded in a Jasco spectropolarimeter (model J-715) interfaced to a computer (J700 software) at a constant temperature of 25°C, maintained by a Peltier PTC-351S apparatus. Electronic absorption was measured in a HP-8453 Diode array UV–visible spectrophotometer. All spectra were recorded using 1-cm capped quartz cuvettes, corrected for the dilution effects and processed using the GRAMS 32 program.

ESI-MS (electrospray ionization mass spectrometry) analyses of the metal-TmMT complexes

Electrospray ionization time-of-flight mass spectrometry (ESI-TOF MS) conditions for the analysis of the metal-TmMT complexes were adapted from those reported in detail in [17] and [26]. The equipment used was a Micro TOF-Q (Bruker) interfaced with a Series 1200 HPLC Agilent pump and an autosampler, all of them controlled by the Compass Software. The mass spectrophotometer was calibrated with ESI-L Low Concentration Tuning Mix (Agilent Technologies). The Zn- and Cd-TmMT samples were analyzed under the following conditions: 20 μL of protein solution injected through PEEK (polyether heteroketone) tubing (1.5 m x 0.18 mm i.d.) at 40 μL min^{-1}; capillary counter-electrode voltage 5 kV; desolvation temperature 90–110°C; dry gas 6 L min^{-1}; spectra collection range 800–2500 m/z. The carrier buffer was a 5:95 mixture of acetonitrile:ammonium acetate (15 mM, pH 7.0). The Cu-TmMT samples were analyzed by injecting 20 μL of protein solution at 40 μL min^{-1}; capillary counter-electrode voltage 3.5 kV; lens counter-electrode voltage 4 kV; dry temperature 80°C; dry gas 6 L min^{-1}. Here, the carrier was a 10:90 mixture of acetonitrile:ammonium acetate, 15 mM, pH 7.0. Acidic-MS conditions, which cause the release of the divalent metal ions from the MT complexes, but keeps the Cu(I) ions, were used to generate apo-TmMT forms and to analyze the Cu-containing samples. To this end, 20 μL of the preparation were injected under the same conditions described previously, but using a 5:95 mixture of acetonitrile:formic acid, pH 2.4, as liquid carrier. For all the ESI-MS results, the error associated with the mass measurements was always inferior to 0.1%. Masses for the holo-species were calculated as described in [34].

Results and Discussion

Identification and analysis of MT coding sequences in *Tremella mesenterica* databases

The discovery of the *C. neoformans* long MTs [16] and their relevance in pathogenesis, prompted us to analyze several fungal genomes for the presence of unusually lengthy MTs. Among all the retrieved BLAST matches using *C. neoformans* CnMT1 and CnMT2 as queries in the NCBI databases, the sequence derived from the *T. mesenterica* NCBI EIW70699 ORF (Fig 1A) was the clearest MT-like candidate, as 25% of its 104 residues were cysteine and it contained no aromatic amino acids. Nevertheless, since it constituted an incomplete protein sequence in view of its lack of a N-terminal initial methionine, the *T. mesenterica* genome was

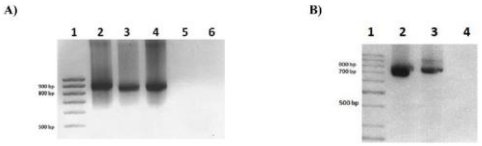

Fig 2. (A) PCR products of the TmMT 5' RACE reaction. Lanes are: (1) DNA size markers, (2) first RACE amplification reaction, (3) second RACE amplification reaction 1:20 dilution, (4) second RACE amplification reaction, (5 and 6) negative control RACE reactions (no template DNA included). **(B) PCR products of the RT PCR and 5' RACE TmMT amplification reactions.** Lanes are: (1) DNA size markers, (2) the PCR product of the RT-PCR reaction using TmMT specific primers, (3) final product of the RACE amplification, (4) negative control PCR reaction (no template DNA included).

doi:10.1371/journal.pone.0148651.g002

searched in the JCI BioProject (PRJNA32829), and its encoding sequence was localized in the TREMEscaffold_3 (access code JH711530.1). This 750 bp-long sequence was located between positions 1234899 and 1235652 in this scaffold and it included unambiguous exon/intron limits, according to the canonical splicing signals (GT/AG). In concordance with the protein sequence, this gene fragment did not show any ATG starting codon in frame, but it exhibited a stop codon (TGA) after the last serine triplet. All these observations were indicative of a 5'-truncated gene and cDNA in the *T. mesenterica* genome annotation, so it was necessary to further investigate the *TmMT* cDNA start.

Determination of the full-length *T. mesenterica* MT cDNA and gene

The full TmMT transcript 5' sequence was determined by RACE. Sequencing of the final RACE product (Fig 2) allowed to unambiguously identify the *TmMT* ATG start codon nearly 1200 bp upstream from the start of the truncated sequence initially retrieved (Fig 1B) from the *T. mesenterica* genome, and also revealed the presence of a 69- bp 5' UTR region in the corresponding cDNA (Fig 3).

Analysis of the *T. mesenterica* MT gene, cDNA and protein sequences

The full-length *T. mesenterica* MT protein and cDNA sequences (Fig 3) were submitted to GenBank, and are available under the accession numbers: AJK28606.1 and KM244758.1, respectively. The TmMT cDNA coding portion (from the ATG to the STOP codons) encompasses 774 bp, and encodes a 257 aa-long protein with a molecular weight of 25.37 kDa, including 57 Cys (23% of the polypeptide) and 1 His (Fig 4A). A RT-PCR reaction on total *T. mesenterica* cDNA (retrotranscribed from total RNA preparation) corroborated that it was not a cloning or amplification artifact. The result of this reaction (Fig 2B) yielded a unique band of the expected size (approximately 834 bp), the sequence of which matched those of the corresponding regions in the genomic DNA database (Fig 3A). Therefore, it was established that *TmMT* was a *real* coding gene, with a sequence split into 10 exons interrupted by 9 introns (Fig 3B). The cDNA 5' UTR had 69 bp, and an *in silico* analysis of 1500 bp of the scaffold sequence upstream the *TmMT* translation start site revealed the presence of a putative TATA box at -38 bp, an also a putative MRE at -1457 bp. It is worth noting that when the retro-PCR was carried out using RNA preparations obtained from cells grown in Cu-enriched cultures, no difference was observed in the intensity of the TmMT product, which indirectly suggests a rather constitutive gene expression pattern (data not shown).

The isolated TmMT cDNA presented ten site variations regarding the sequence in the JH11530.1 scaffold, five of which represented a missense mutation, involving the following substitutions: N22S, S35P, T48I, K201E and S207T, neither of them altering the expected metal

A)

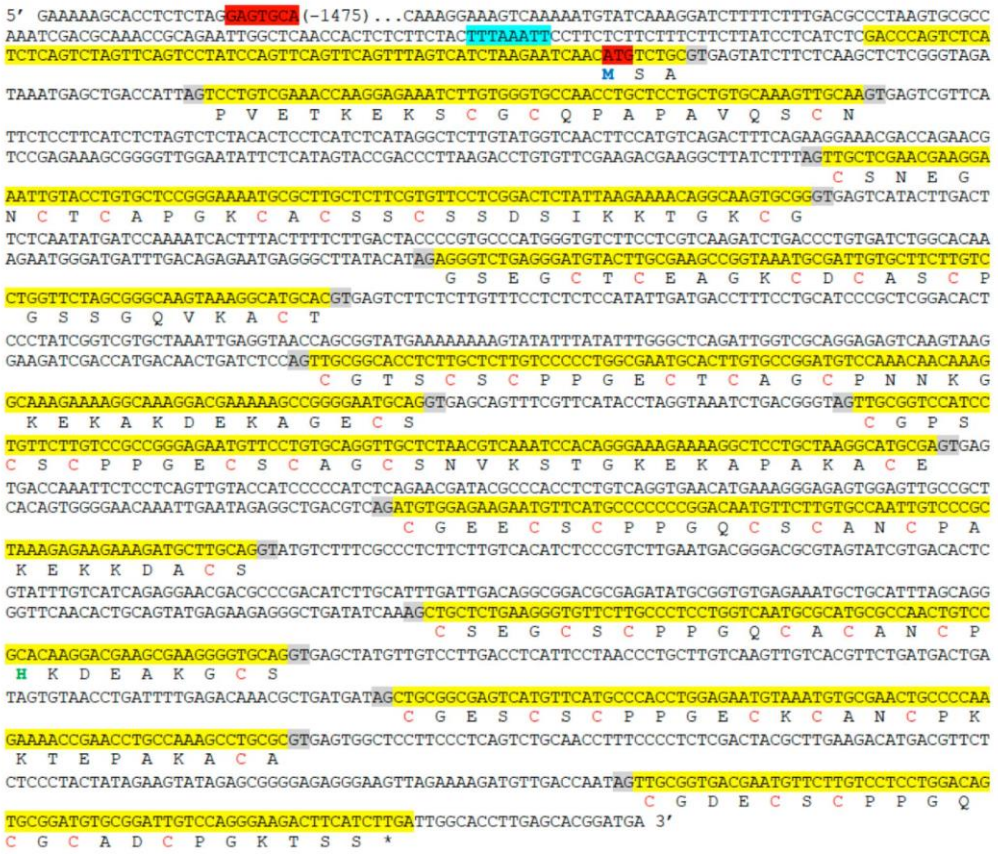

B)

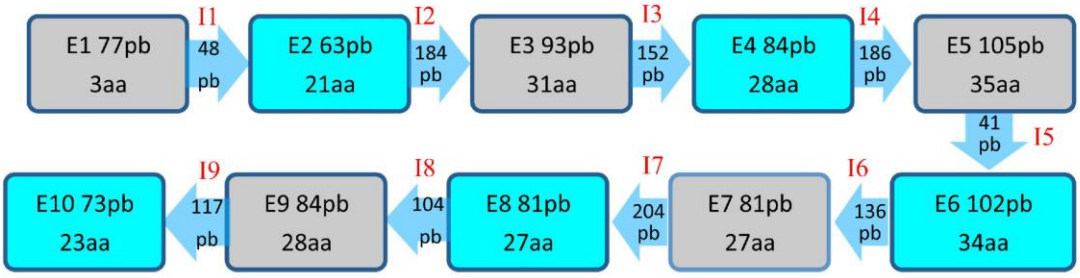

Fig 3. (A) Complete TmMT cDNA and protein sequence. The TmMT cDNA sequence obtained from the RACE reactions has been localized into the *T. mesenterica* genomic sequence (BioProject PRJNA32829, access code # JH711530.1), and the corresponding gene and protein significant elements have been localized. Exons are shown in yellow and the corresponding splicing donor/acceptor sites in gray, and the translational initiation codon is in red. A putative TATA is boxed in blue and a putative MRE in red. In the protein sequence, Cys are in red, His in green and Met in blue. **(B)** Scheme showing the *TmMT* gene structure (exon and intron sizes). This sequence has been submitted to GenBank and has the accession number TPA: BK008867.

doi:10.1371/journal.pone.0148651.g003

Fig 4. (A) Protein sequence of TmMT and (B) proposed modular structure of TmMT. The alignment with one 7-Cys segment of *C. neoformans* CnMT2 and *N. crassa* MT is also displayed.

doi:10.1371/journal.pone.0148651.g004

ion coordination properties of a MT polypeptide. Overall, these substitutions (representing a 1.25% of the total coding sequence) were fully compatible with a natural polymorphism between the *T. mesenterica* strain used in this work and that used for genomic sequencing an annotation in the JCI project. TmMT, with 257 amino acids and 57 Cys, is the longest MT protein ever reported, longer than the *C. neoformans* CnMT2 isoform (183 aa), the *Tetrahymena thermophila* MTT1 isoform (162 aa) and the *Paramecium sp*. PMCd1 protein (203 aa, [35]), all of them belonging to unicellular eukaryotes. Forty-eight of its 57 Cys are organized in CXC motifs, the most extended arrangement of the Cys residues in the MT sequences, but furthermore, the analysis of TmMT readily revealed an internal repetition pattern (Fig 4B), which suggests that it was originated by a modular amplification process, as shown for *Cryptococcus neoformans* [16,17] *and Tetrahymena* [18,36] MTs. In the case of TmMT, the most obvious delimitation of hypothetical internal repetitions involves six units with a -CXCX$_3$CSCPPGXCXCAXCP- sequence including 7 Cys in an arrangement alignable to that of the paradigmatic *Neurospora* MT, two units with six Cys, and a N-terminal segment with only three Cys. Other sequence features also support the homology between the TmMT building blocks and those proposed for the *C. neoformans* MTs, such as the occurrence of a proline doublet after the second CXC motif, a single proline after the last Cys of the segment, and the high similarity of the Cys interspersed amino acids, with a clear predominance of small residues (glycine, alanine), and the conservation of charged residues in key positions (lysine).

The recombinant synthesis of the TmMT protein

DNA sequencing of several pGEX-TmMT constructs confirmed that they included no nucleotide substitutions, and that the cDNA was cloned in correct frame after the GST coding

sequence. Protein extracts of small-scale (3 mL) cultures of pGEX-*TmMT*-transformed BL21 cells yielded an exclusive band a *ca.* 51 kDa, concordantly with the size of the expected fusion protein (*ca.* 26 kDa of the GST plus *ca.* 25 kDa of TmMT) (data not shown). Consequently, synthesis of TmMT was then performed in large scale cultures (5-L) supplemented with Zn (II), Cd(II) or Cu(II). Aliquots of the complexes purified from Zn- and Cd-enriched cultures (Zn-TmMT and Cd-TmMT, respectively) were first analyzed by acid (pH 2.4) ESI-MS, which revealed an almost unique peak of 25377.0 Da (Fig 5A) corresponding well with the TmMT MW of 25377.62 Da theoretically calculated for the recombinant peptide, including N-terminal Gly and Ser residues derived from the GST-fusion construct. Thus, the identity, purity and integrity of the recombinant TmMT were fully confirmed.

The divalent metal ion (Zn(II) and Cd(II)) binding abilities of TmMT

The recombinant synthesis of TmMT in cells grown under Zn-supplementation yielded a mixture of Zn-complexes of different stoichiometries, with Zn_{17}- to Zn_{21}-TmMT as major species (Table 2 and S1 Table, and Fig 5B). This matched well with the Zn-per-protein mean content calculated by ICP-AES, which gave values between 14.0 and 20.1 (Table 2). The CD spectra of the three samples preparations were practically identical, exhibiting a Gaussian band centered at *ca.* 240 nm typical of the Zn-Cys chromophores (Fig 5B).

The biosynthesis of TmMT in Cd-supplemented cultures revealed its poor ability for coordination of this metal ion, even lower than for Zn(II). The synthesis was repeated several times, and practically always it was impossible to discriminate individual peaks (Table 2 and S1 Table, and Fig 5C). The only data that can be suggested from the ESI-MS spectra was that most probably the major complexes were those including between 23 and 25 Cd(II), this coinciding with results of ICP-AES that yielded an average content of 24.2 to 24.5 Cd(II) per TmMT (Table 2). The CD spectrum showed the typical fingerprint attributable to tetrahedral $Cd(SCys)_4$ chromophores absorbing at *ca.* 250 nm, and a slight absorption in the region of 280–300 nm, probably contributed by the presence of some Cd-S^{2-} chromophores (Fig 5C). Overall, all the previous results lead to the conclusion that TmMT is far from exhibiting a binding preference for divalent (Zn(II) or Cd(II) [8]). This is reflected in the formation of a continuum of species, none of them energetically favored, with both Zn(II) and Cd(II) ions, and also accounts for the lack of reproducibility of the recombinant syntheses, which is patent in this work for the Zn-complexes, and which has been observed also before, among others, for the *Tetrahymena pyriformis* MT1 [37] and *C. neoformans* MT1 isoforms [17]. The presence of S^{2-} ligands in the Cd-TmMT complexes also corroborates this inability [33].

Cu-binding abilities of TmMT

TmMT was recombinantly synthesized in Cu(II)-supplemented cultures grown under normal and low aeration, because this modulates the amount of Cu available inside the host cells for recombinant Cu-MT complex formation [29]. Hence, when TmMT was synthesized in normally aerated cultures, it yielded a mixture of Zn,Cu-TmMT species ranging from M_8- to M_{19}-TmMT (M = Zn+Cu), with those from M_{12}- to M_{17}-TmMT as major products, as shown by ESI-MS at neutral pH (Table 2 and S2 Table, and Fig 6A). ESI-MS at pH 2.4 revealed that this continuum was formed by heterometallic complexes with Cu(I) contents showing a peculiar periodicity: multiple of 4, and multiple of 4 plus one, that is: Cu_4 and Cu_5, Cu_8 and Cu_9, and Cu_{12} and Cu_{13} (*cf.* Table 2 and S2 Table, and Fig 6A). In contrast, low aeration yielded a mixture of homometallic Cu-TmMT species -since ICP-AES measurements only detected this metal-, which ranged between Cu_{36}- and Cu_{45}-TmMT, with major species being Cu_{42}- and Cu_{41}-TmMT (Table 2 and S2 Table, Fig 6B). Acid ESI-MS of this sample revealed a similar

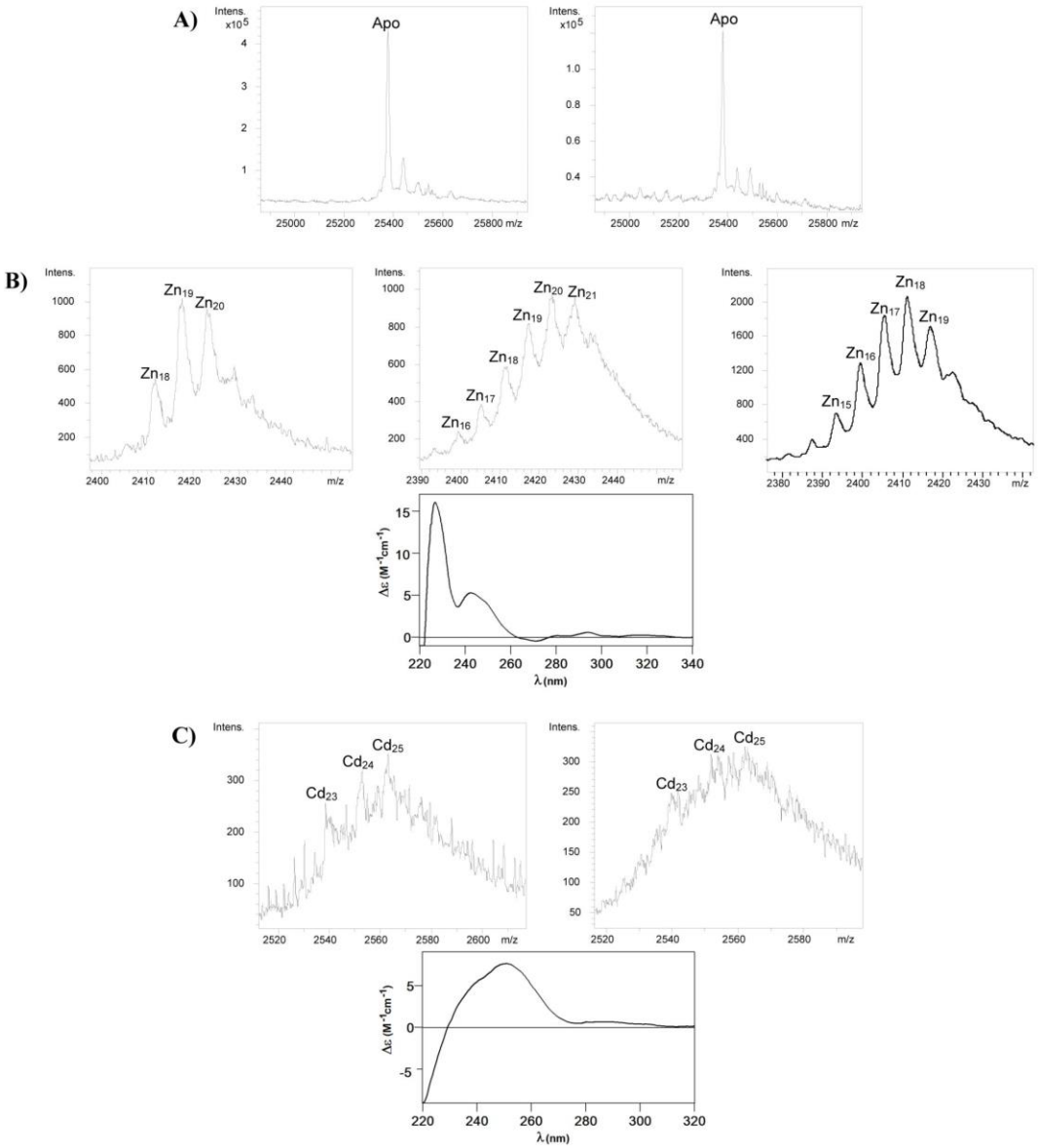

Fig 5. Spectroscopic and spectrometric analyses of the Zn- and Cd-TmMT preparations. (A) Deconvoluted ESI-MS spectra of the recombinant Zn- and Cd-TmMT samples, run at acid pH (2.4). A practically unique peak, corresponding to the expected molecular weight of the protein is observed in each spectrum. (B) ESI-MS spectra of three different Zn-TmMT syntheses (at the +11 charge state) recorded at neutral pH. The CD spectra corresponding to Zn-$TmMT_2$ is included, those for Zn-$TmMT_1$ and Zn-$TmMT_3$ being completely similar. (C) ESI-MS spectra of two different Cd-TmMT syntheses (at the +11 charge state) recorded at neutral pH. The CD spectra corresponding to the Cd-$TmMT_2$ is included; that for Cd-$TmMT_1$ being completely similar.

doi:10.1371/journal.pone.0148651.g005

distribution of species, of slightly lower stoichiometry (Cu_{29} and Cu_{38}) probably attributable to some loosely bound Cu(I) ions. Interestingly, both types of preparations rendered well defined and closely related CD spectra (Fig 6A and 6B). The CD fingerprint of the sample purified

Table 2. Recombinant synthesis yield and metal-to-protein ratios of the purified Zn-, Cd- and Cu-TmMT complexes, according to neutral ICP-AES and ESI-MS measurements.

Metal-TmMT syntheses[a]	[TmMT] (10^{-4} M)	ICP-AES[b]			Neutral ESI-MS[c]				Acid ESI-MS[c]
		Zn/MT	Cd/MT	Cu/MT	Zn species	Cd species	Zn/Cu species	Cu species	Cu species
Zn-TmMT$_1$	0.71	20.1			Zn_{21}				
					Zn_{20}				
					Zn_{19}				
					Zn_{18}				
Zn-TmMT$_2$	0.74	14.0			**Zn_{21}**				
					Zn_{20}				
					Zn_{19}				
					Zn_{18}				
					Zn_{17}				
					Zn_{16}				
Zn-TmMT$_3$	0.94	16.8			Zn_{19}				
					Zn_{18}				
					Zn_{17}				
					Zn_{16}				
					Zn_{15}				
Cd-TmMT$_1$	0.54		24.2			**Cd_{25}**			
						Cd_{24}			
						Cd_{23}			
						multiple			
Cd-TmMT$_2$	0.62		24.5			**Cd_{25}**			
						Cd_{24}			
						Cd_{23}			
						multiple			
Cu-TmMT (normal aeration)	0.55	6.6		5.8			**M_{15}**		Cu_{12}
							M_{19}-M_8		Cu_{10}
									Cu_9
									Cu_8
									Cu_6
									Cu_5
									Cu_4
									Apo
Cu-TmMT (low aeration)	0.05			40.0				**Cu_{42}**	**Cu_{38}**
								Cu_{41}	**Cu_{36}**
								Cu_{45}-Cu_{38}	Cu_{38}-Cu_{29}

[a] Several syntheses were performed in each metal supplemented medium, which are numbered by subscripts.

[b] In all cases, the Zn, Cd, Cu and S content was measured by ICP-AES, but only the detectable contents are shown. Protein concentration was calculated from the S content in normal ICP-AES measurements.

[c] Stoichiometries were calculated from the mass difference between the holo- and apo-proteins. Major species are in bold. M = Zn or Cu which have a molecular mass indiscernible by ESI-MS. *Multiple* means that a continuum of peaks are observed between the indicated values.

doi:10.1371/journal.pone.0148651.t002

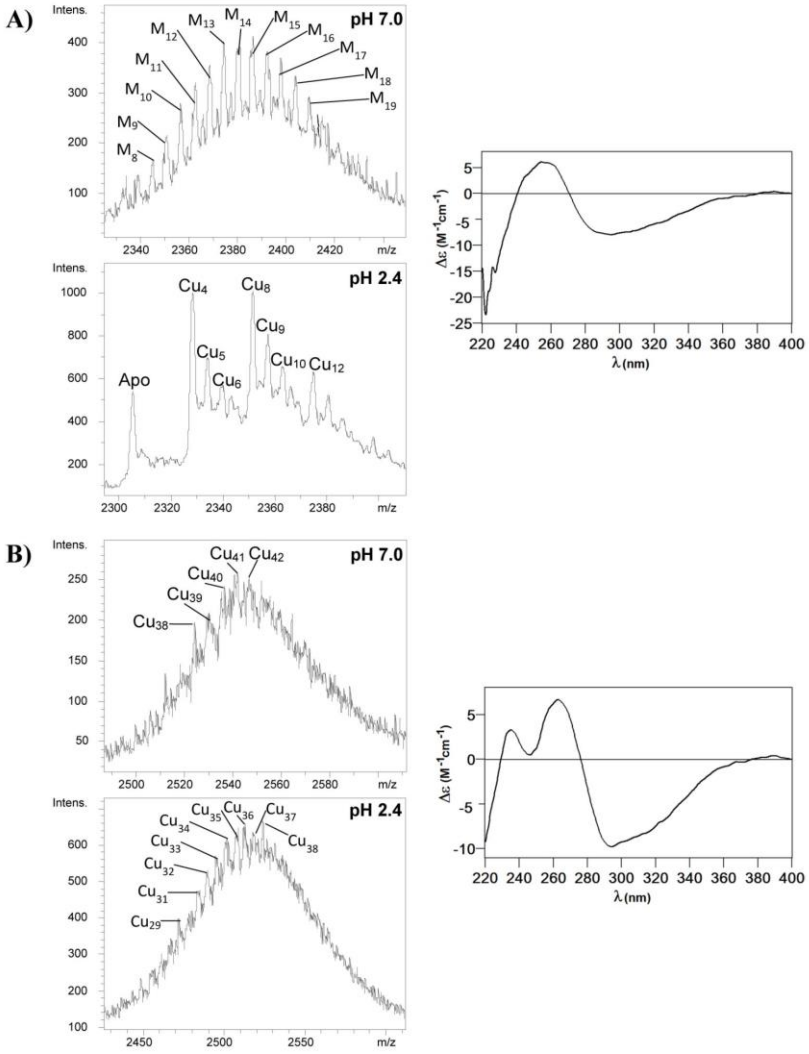

Fig 6. Spectroscopic and spectrometric analyses of the Cu-TmMT preparations. (A) ESI-MS spectra of the recombinant Cu-TmMT synthesized in normally-aerated cultures (at the +11 charge state), run at neutral pH (7.0) and acid pH (2.4), and CD spectrum of the same sample. (B) ESI-MS spectra of the Cu-TmMT synthesized in low-aerated cultures (at the +11 charge state), run at neutral pH (7.0) and acid pH (2.4), and CD spectrum of the same sample.

doi:10.1371/journal.pone.0148651.g006

from normally aerated bacteria showed a wide absorption between 240 and 270 nm, while that of the low-aerated productions precisely showed two maxima with no absorption at 240 nm, which reinforces the presence of Zn(II) ions in the former.

Most informative results about TmMT Cu(I) binding abilities came from the study of the species constituted *in vitro* by Zn/Cu exchange. Nevertheless, these experiments revealed an

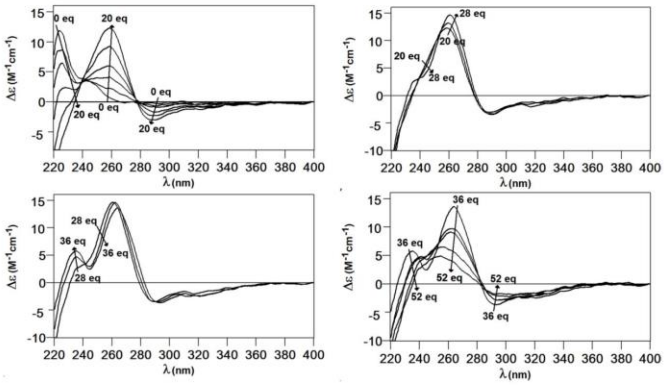

Fig 7. CD spectrum of the Zn/Cu exchange reaction in Zn-TmMT. The CD spectra were recorded every 4 Cu(I) eq added to a 3 μM solution of Zn-TmMT.

doi:10.1371/journal.pone.0148651.g007

unprecedented feature regarding the standard methodological procedure used [31], because spectroscopic (CD, UV-vis) and spectrometric (ESI-MS) measurements could not be performed on the same sample due to incompatible concentration requirements. Thus the CD and UV-vis data was collected on a 3 μM solution of Zn-TmMT with additions of 4 Cu(I) eq each to avoid detector saturation (Fig 7) and the ESI-MS data on a *ca*. 100 μM solution, which enabled the detection of the high number of species present in solution (Fig 8). The CD spectra of the successive reaction steps draw very neat isodichroic points, which strongly suggested a cooperative copper loading and zinc displacement process. These isodichroic points arise by the decrease of the *ca*. 230 nm band and the increase of the 260(+) and 290(-) nm CD absorptions, owing to the creation of Cu-SCys chromophores from 0 to 28 Cu(I) eq added. After a small rearrangement between 28 and 36 Cu(I) eq, further additions provoke the collapse of the CD signal.

It is evident that, from the beginning, the addition of Cu(I) enhances the already high complexity of the initial Zn-TmMT sample, generating a larger number of species in solution (Fig 8). The heterometallic species formed increase in nuclearity up to a maximum of M_{38}-TmMT (M = Zn or Cu), after the addition of 30 Cu(I) eq, which is the step yielding one of the most intense CD spectra (Fig 7). However, the most remarkable hints about the replacement reaction are revealed by the acid ESI-MS analyses, because they suggest how TmMT builds its copper complexes. Hence, the addition of just 4 Cu(I) eq at the beginning of the experiment already gave rise to a predominant Cu_4-core, accompanied by a minor Cu_5-cluster, and species of higher nuclearity which will become significant later. Thence, at the following step, Cu_4- and Cu_5-TmMT are still significant, but the doublet Cu_8- and Cu_9- is almost as important. In the next step, Cu_4-, Cu_5- and Cu_6- Cu_8- have practically disappeared, and the predominant cores are the Cu_{12}- and Cu_{13}-clusters. From this point on (*i.e.* 10 Cu(I) eq added), the complexity of the Cu(I)-containing species is very high, with a continuum of Cu(I)-cores, the Cu(I) content of which increases until approximately 40. It is worthwhile noting that the addition of 25 Cu(I) eq was necessary to totally displace the Zn(II) initially bound to TmMT. Finally, in the presence of an excess of copper beyond 30 Cu(I) eq added, the Cu-TmMT complexes become unstable, so that the Cu(I) nuclearity of the detected species decreases, and at the end of the reaction (Cu overload conditions) only the apo-TmMT peptide is detected, which has been reported also for other Cu-thioneins [38,39]. From these data, a certain periodicity of the predominant Cu(I)

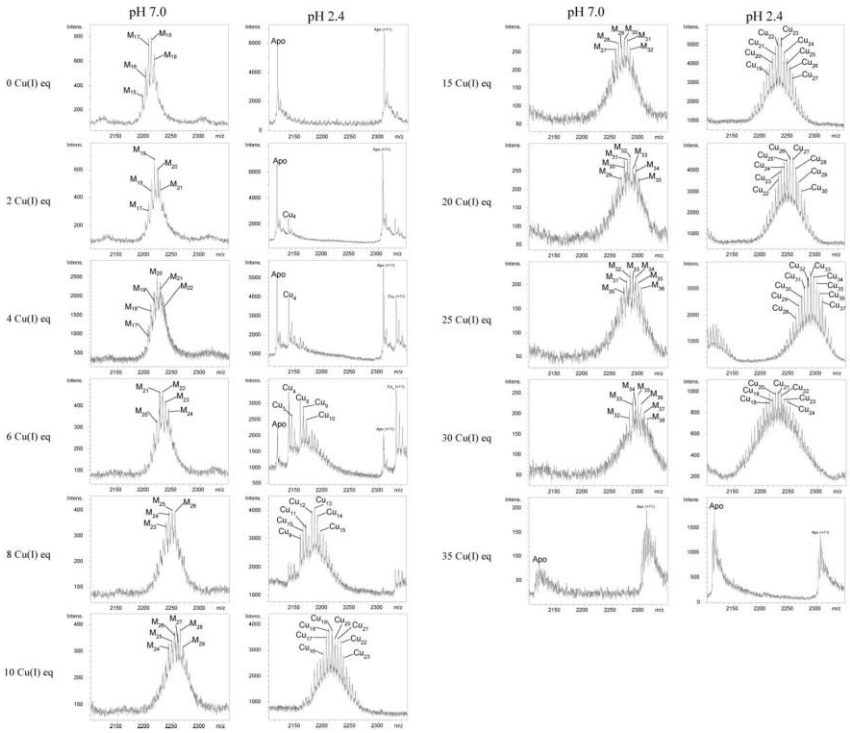

Fig 8. ESI-MS spectra of the Zn/Cu exchange reaction in Zn-TmMT. The ESI-MS spectra were measured, both at pH 7.0 and pH 2.4, on aliquots of a 94 μM solution of TmMT every 2 Cu(I) eq added at the beginning of the reaction and every 5 Cu(I) between 10 and 35 equivalents added.

doi:10.1371/journal.pone.0148651.g008

clusters can be deduced, so that in the two first steps, they were Cu_4-units always accompanied by a more or less important peak with an additional Cu(I) (*i.e.* Cu_4- and Cu_5-, and then Cu_8- and Cu_9), and from here onwards, the following predominant peaks result from adding 5 Cu(I) to the previous species (*i.e.* Cu_{12}- and Cu_{13}-; Cu_{17}- and Cu_{18}-; Cu_{22}- and Cu_{23}-; Cu_{27}- and Cu_{28}- and Cu_{33}-TmMT). Although a strict cooperative process for the Zn/Cu displacement in Zn-TmMT has to be ruled out owing to the many different species coexisting during the experiment, a clear periodicity for the major Cu(I) content of created species is observed, which can be related to the modular structure of the TmMT polypeptide (*cf.* Fig 4). Characterization of the Cu-binding abilities of the also modular *C. neoformans* CnMTs showed that their 7-Cys boxes render Cu_5-clusters of additive behavior [16,17,26], and coincidently the TmMT results suggest that its 7-Cys stretches may exhibit a similar behavior. Additionally, TmMT has two 6-Cys boxes, which can be assumed to optimally bind 4 Cu(I) ions. The remaining 3 Cys would also contribute to bind extra Cu(I) ions. This will explain the series observed for the Cu(I)-core composition in the Zn/Cu exchange reaction. Precisely, both $[Cu_4S_6]$ and $[Cu_5S_7]$ clusters were characterized by classic inorganic chemistry model studies as the most relevant flexible cores in relation to Cu-MT complexes [40,41,42].

Finally, it is worth noting that, also as first noticed for the yeast Crs5 MT [29] and later reported for other Cu-thioneins, the results of TmMT synthesis in Cu-supplemented media at both assayed aerations is reproduced in two different steps of the Zn/Cu exchange process, at

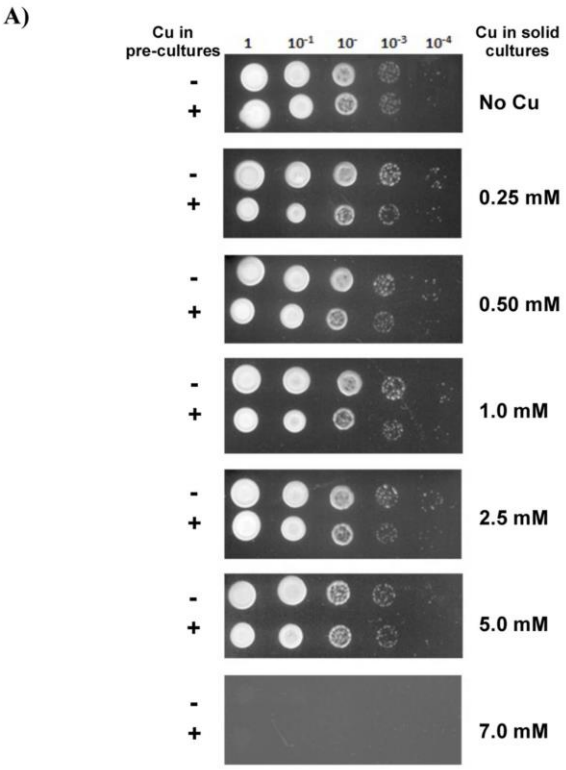

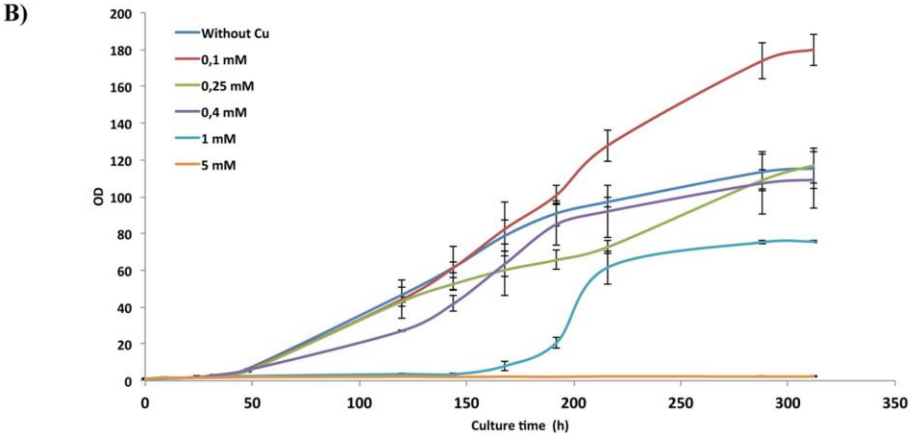

Fig 9. *Tremella mesenterica* growth under Cu supplementation conditions. (A) *T. mesenterica* solid cultures. Pre-cultures were grown in YPD liquid medium overnight at 25°C (first row in each condition without added Cu and second row, with 0.1 mM Cu added), then diluted to OD_{600} 0.5 and spotted into the YPD agar plates at 4 serial dilutions. Plates were allowed to grow at 30°C for 3 days. For more details, see the Experimental Procedures section. (B)

Growth curve representing the normalized mean values of the OD_{600} exhibited by the liquid cultures grown in MY medium supplemented with the indicated Cu concentrations. Results represent the mean and standard deviation (vertical bars) of at least three replicates.

doi:10.1371/journal.pone.0148651.g009

least in relation to the Cu(I) cores present. Hence, the results of the Cu-TmMT production in regularly aerated cultures correspond to the Zn-TmMT+6 Cu(I) eq added stage (*cf.* CD features and ESI-MS spectra in Figs 6, 7 and 8), while the results from low aerated syntheses correspond to the last steps of the titration, just before the unfolding of the Cu-TmMT complexes caused by an excess of Cu(I) ions (*cf.* CD features and ESI-MS spectra in Figs 6, 7 and 8). This indicates that the results of these recombinant syntheses effectively correspond to two different situations of Cu-availability.

Copper tolerance of native *Tremella mesenterica* and *Saccharomyces cerevisiae* cells transformed with TmMT

T. mesenterica copper tolerance assayed in solid cultures revealed a rather unaltered growth up to 5.0 mM Cu, and at 7.0 mM Cu cells were unable to grow. In this experiment, each Cu concentration was assayed in two conditions, depending on whether the pre-culture spotted on the plates had been supplemented with Cu (0.1 mM) or not (Fig 9A). No significant differences could be observed. When Cu tolerance was measured in liquid cultures, two different phases were observed in long-term cultures (up to 300 h), taking into account that this fungus exhibits a slow growth, and a clear increase in the OD_{600} was not observed until 50 h after inoculation (Fig 9B). Hence, until 150 h growth, all the cultures grew at an equivalent rate, except those supplemented with 1 mM Cu, which exhibited a lengthened lag phase in concordance with the stress imposed by the excess of Cu. All these results confirm a high Cu tolerance for this fungus, comparable to that of the CUP1 multicopy *S. cerevisiae* strains [43], considering that only one copy of the *TmMT* gene was detected in the genome by the *in silico* screening. However, it has to be noted that this increased tolerance is manifested in lasting cultures, maybe in relation to the slow *T. mesenterica* growth dynamics. Noteworthy, the culture supplemented with 0.1 mM Cu exhibited a maintained increased growth in relation to all other conditions, so that it could be hypothesized that the optimal growth of *T. mesenterica* depends on the presence of this metal ion in its natural environment.

To confirm the ability of the *TmMT* to confer high-Cu resistance, the effect of its heterologous expression in the *S. cerevisiae* 51-2c-Δc5 strain, which lacks its two MT genes (*CUP1* and *CRS5*) was assayed. The ability of the cells transformed with *TmMT*-p424, to grow in liquid media supplemented with increasing copper concentrations was represented as percentage of the growth exhibited in cultures with no Cu supplementation (Fig 10). For comparative purposes, the *CUP1*-p424 and *mMT1*-p424 constructs, containing respectively the *S. cerevisiae* and the mouse MT1 isoforms, as well as the void p424 plasmids were also assayed. The results unambiguously show the extraordinary tolerance to Cu conferred by the expression of *TmMT* in yeast cells, in all the assayed Cu concentrations, up to 30 μM. What is more, it allows cell survival, and at considerable levels, beyond 10 μM Cu, when expression of either *CUP1* or *mMT1* fails to maintain cell growth (Fig 10).

Conclusions

One gene encoding a metallothionein polypeptide is present in the *Tremella mesenterica* genome, hereinafter called, *TmMT*. It has been identified *in silico* from a partial protein sequence found in a *T. mesenterica* data bank as starting query, and also from total mRNA retrotranscription and specific amplification, which has confirmed that the predicted *TmMT*

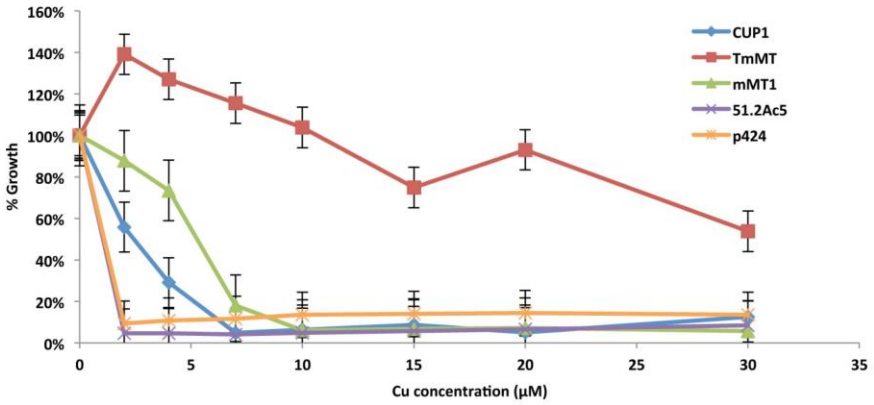

Fig 10. Effect of the heterologous expression of the *T. mesenterica* TmMT in *S. cerevisiae* 51.2cΔc5 MT-null strain. Yeast cells were transformed with the different p424-MT constructs. Besides p424-TmMT, cells transformed with the void p424, and the p424-CUP1 (the yeast MT) and p424-mMT1 (the mammalian isoform MT1) plasmids were also included in the assay for comparative purposes. 3-mL cultures grown overnight at 30°C were diluted to OD_{600} 0.1 in 3-mL fresh SC-Trp-Ura medium supplemented with 0, 2, 4, 7, 10, 15, 20, and 30 μM $CuSO_4$ and grown for 18h at 30°C. The growth of the host 51.2cΔc5 strain cultured in complete medium was also assayed. Growth was evaluated in liquid cultures and it is represented as the percentage of the growth rate attained in a non-Cu supplemented medium. All the experiments were carried out at least by triplicate and the plotted points represent the mean value for each condition associated to its corresponding error bar. The data unambiguously show the extraordinary copper tolerance conferred by TmMT. For more details, see the Experimental Procedures section.

doi:10.1371/journal.pone.0148651.g010

ORF was a *real* coding sequence of uncommon length for a *MT* gene. The *TmMT* gene covers more than 2 kb of DNA, and its coding sequence is separated in 10 small exons -sizes from 63 bp to 105 bp-, interrupted by 9 introns, from 48 bp to 204 bp. The 5' UTR of this cDNA is 69-bp long, and in the upstream gene sequence, a putative TATA box and an MRE element have been identified. The cDNA coding portion encompasses 774 bp, and the resulting protein has 257 amino acids, 57 of which are Cys distributed in CXXC motifs as corresponding to the common hallmarks of Metallothioneins. Therefore, this is the longest MT polypeptide reported up to now, beyond the *Paramecium sp*. PMCd1 protein (203 aa) the fungal *C. neoformans* CnMT2 (183 aa) and CnMT1 (122 aa) isoforms. Coincidently with the *C. neoformans* MTs, the TmMT polypeptide exhibits clear internal repetition patterns, which suggests that modular amplification processes of a primeval fungal MT -represented by the paradigmatic short MTs reported in the *Neurospora* or *Agaricus* genus- would be in the bases of the genesis of long MTs in the Tremellales order of Ascomycota fungi. In the case of TmMT, the most obvious arrangement of hypothetical internal repetitions is the alignment shown in Fig 4B, for which six of the units depict a -$CXCX_3$CSCPPGXCXCAXCP- motif including 7 Cys, as for paradigmatic fungal MTs (*i.e. Neurospora* MT), and includes two units with 6 Cys and a N-terminal segment with only 3 Cys.

The analysis of the metal binding abilities of TmMT confirmed that it exhibits all the features of a high-capacity Cu-thionein. Hence, when TmMT coordinates Zn(II) ions, it renders a mixture of species of different stoichiometries, which is also the case for Cd(II) coordination. This patent inability for divalent metal ion coordination is accompanied by a clear behavior of Cu-thionein, although its large size entails that when synthesized in regular Cu concentrations, the obtained complexes are heterometallic (Zn, Cu) species, just as the *C. neoformans* CnMT1 and CnMT2 were. However, at high Cu concentrations (*i.e.* produced in host cells grown under poor aeration), TmMT is able to render homometallic complexes of as high nuclearity as 45 Cu(I), with the major species being Cu_{40} to Cu_{42}-TmMT. The modular composition

reported for the *C. neoformans* Cu-CnMT complexes is probably also re-encountered in Cu-TmMT, since its polypeptide sequence is easily dissected in alignable stretches: six 7-Cys boxes, two 6-Cys boxes, and three N-terminal Cys. This assumption would also explain the Cu contents of the most favored Cu-species. Strong similarity is also observed for some residues located between the coordinating Cys (*i.e.* the proline doublet after the second CXC motif, a single proline after the last Cys of the segment, a clear predominance of small (glycine, alanine) residues, and the conservation of charged residues in other key positions (lysine)). Thus, it is tempting to associate these features, not only to the evolutionary origin and conservation of this protein pattern, but also to their optimization for Cu(I) coordination geometry.

Of course, the most interesting question raised by these results concerns the physiological role that this MT protein may play in its native surrounding. A first approach is to consider the natural habitat where *Tremella* grows, mainly decaying wood, suggests that Cu-handling may be of the utmost importance to provide active lignin-metabolizing enzymes, such as laccases and peroxidases, which are well-known Cu-containing oxidases. This would be in concordance with the constitutive, rather than inducible, *TmMT* pattern expression, since it could be considered a housekeeping gene functionality. Appealingly, this hypothesis might, in the end, link the biological function of TmMT with that proposed for the Cu-MTs of the pulmonate snails, which are supposed to serve as storage/chaperones of Cu for the hemocyanins, the respiratory O_2 carriers of these organisms [44].

Supporting Information

S1 Table. Experimental molecular masses (ESI-MS results) and calculated molecular masses for Zn-TmMT and Cd-TmMT species. Subindexes describe different syntheses. Major species are in bold.
(PDF)

S2 Table. Experimental molecular masses (ESI-MS results) and calculated molecular masses for Cu-TmMT species synthesized in regular and low-aerated *E. coli* cultures. Major species are in bold. M = Zn or Cu.
(PDF)

Acknowledgments

Technical advise of Dra. E. Jimenez and Dra. A. Espart and experiment support of M. Sebastian Artime are greatly appreciated. We thank the Centres Científics i Tecnològics (CCiT) de la Universitat de Barcelona (ICP-AES, DNA sequencing) and the Servei d'Anàlisi Química (SAQ) de la Universitat Autònoma de Barcelona (CD, UV-vis, ESI-MS) for allocating instrument time.

Author Contributions

Conceived and designed the experiments: MC SA. Performed the experiments: PIE SGM WL SC OP. Analyzed the data: OP MC SA. Wrote the paper: OP MC SA.

References

1. Sigel A, Sigel H, Sigel RKO. Metal ions in Life Sciences; vol. 5: Metallothioneins and Related Chelators. 1st ed. Cambridge: The Royal Society of Chemistry; 2009.
2. Capdevila M, Bofill R, Palacios O, Atrian S. State-of-the-art of metallothioneins at the beginning of the 21st century. Coord Chem Rev. 2012; 256: 46–62.

3. Blindauer C. Binding, Transport and Storage of Metal Ions in Biological Cells. In: Maret W, Wedd A, editors.) Metallothioneins. (RSC Metallobiology Series 2). Cambridge: The Royal Society of Chemistry; 2014. pp. 594–653.
4. Vasak M, Hasler DW. Metallothioneins: new functional and structural insights. Curr Opin Chem Biol. 2000; 4: 177–183. PMID: 10742189
5. Capdevila M, Atrian S. Metallothionein protein evolution: a miniassay. J Biol Inorg Chem. 2011; 16: 977–989. doi: 10.1007/s00775-011-0798-3 PMID: 21633816
6. Binz PA, Kägi JHR. () Metallothionein: Molecular evolution and classification. In: Klaassen C, editor. Metallothionein IV. Basel: Birkhäuser Verlag; 1999. pp.7–13.
7. Valls M, Bofill R, Gonzalez-Duarte R, Gonzalez-Duarte P, Capdevila M, Atrian S. A New Insight into Metallothionein (MT) Classification and Evolution. J Biol Chem. 2001; 276: 32835–32843. PMID: 11413132
8. Bofill R, Capdevila M, Atrian S. Independent metal-binding features of recombinant metallothioneins convergently draw a step gradation between Zn- and Cu-thioneins. Metallomics 2009; 1: 229–234. doi: 10.1039/b904953c PMID: 21305119
9. Palacios O, Atrian S, Capdevila M. Zn- and Cu-thioneins: a functional classification for metallothioneins?. J Biol Inorg Chem. 2011; 16: 991–1009. doi: 10.1007/s00775-011-0827-2 PMID: 21823038
10. Palacios O, Pagani A, Pérez-Rafael S, Egg M, Höckner M, Brandstätter A, et al. How Metazoan Metallothioneins achieved Metal Specificity: Evolutionary Differentiation in the Mollusc MT Gene Families. BMC Biol. 2011; 9: 4.
11. Lerch K. Copper metallothionein, a copper-binding protein from *Neurospora crassa*. Nature. 1980; 284: 368–370. PMID: 6444697
12. Munger K, Lerch K. Copper metallothionein from the fungus *Agaricus bisporus*: chemical and spectroscopic properties. Biochemistry. 1985; 24: 6751–6756.
13. Prinz R, Weser U. A naturally occurring Cu-thionein in *Saccharomyces cerevisiae*. Hoppe Seylers Z Physiol Chem. 1975; 356: 767–776. PMID: 1102411
14. Winge DR, Nielson KB, Gray WR, Hamer DH. Yeast metallothionein. Sequence and metal-binding properties. J Biol Chem. 1985; 260: 14464–14470. PMID: 3902832
15. Nemer M, Wilkinson DG, Travaglini EC, Sternberg EJ, Butt TR. Sea urchin metallothionein sequence: Key to an evolutionary diversity. Proc Natl Acad Sci USA. 1985; 82: 4992–4994. PMID: 3860837
16. Ding C, Festa RA, Chen Y- L, Espart A, Palacios O, Espín J, et al. *Cryptococcus neoformans* copper detoxification machinery is critical for fungal virulence. Cell Host Microbe. 2013; 13: 265–276. doi: 10.1016/j.chom.2013.02.002 PMID: 23498952
17. Palacios O, Espart A, Espín J, Ding C, Thiele DJ, Atrian S, et al. Full characterization of the Cu-, Zn- and Cd-binding properties of CnMT1 and CnMT2, two metallothioneins of the pathogenic fungus *Cryptococcus neoformans* acting as virulence factors. Metallomics. (2014; 6: 279–291. doi: 10.1039/c3mt00266g PMID: 24317230
18. Espart A, Marín M, Gil-Moreno S, Palacios P, Amaro F, Martín-González A, et al. Hints for Metal-Preference Protein Sequence Determinants: Different Metal Binding Features of the Five *Tetrahymena thermophila* Metallothioneins. Int J Biol Sci. 2015; 11: 456–471. doi: 10.7150/ijbs.11060 PMID: 25798065
19. Findley K, Rodriguez-Carres M, Metin B, Kroiss J, Fonseca A, Vilgalys R, et al. Phylogeny and phenotypic characterization of pathogenic *Cryptococcus* species and closely related saprobic taxa in the Tremellales. Eukariot Cell. 2009; 8: 353–361.
20. Grigoriev IV, Nordberg H, Shabalov I, Aerts A, Cantor M, Goodstein D et al. The Genome Portal of the Department of Energy Joint Genome Institute. Nucleic Acids Res. 2012; 40: D26–D32. doi: 10.1093/nar/gkr947 PMID: 22110030
21. Wickerman L. Taxonomy of yeasts. Dept Agric Tech Bull. 2012; 1029: 1–56.
22. Sherman F, Fink GF, Hicks J. Techniques and protocols: 6. Yeast RNA Isolation. In: Kaiser C, Michaelis S, Mitchell A, editors. Methods in Yeast Genetics. A Cold Spring Harbor Laboratory Course Manual, 1994 edition. New York: Cold Spring Harbor Laboratory Press; 1994. pp. 151–155.
23. Guirola M, Perez-Rafael S, Capdevila M, Palacios O, Atrian S. Metal Dealing at the Origin of the Chordata Phylum: The Metallothionein System and Metal Overload Response in *Amphioxus*. PLoS ONE 2012; 7: e43299. doi: 10.1371/journal.pone.0043299 PMID: 22905252
24. Capdevila M, Cols N, Romero-Isart N, González-Duarte R, Atrian S, González-Duarte P. Recombinant synthesis of mouse Zn_3-ß and Zn_4-α metallothionein 1 domains and characterization of their cadmium (II) binding capacity. Cell Mol Life Sci. 1997; 53: 681–688. PMID: 9351472
25. Culotta VC, Howard WR, Liu XF. CRS5 encodes a metallothionein-like protein in *Saccharomyces cerevisiae*. J Biol Chem. 1994; 269: 25295–25302. PMID: 7929222

26. Espart A, Gil-Moreno S, Palacios P, Capdevila M, Atrian S. Understanding the internal architecture of long metallothioneins: 7-Cys building blocks in fungal (*C. neoformans*) MTs. Mol Microbiol. 2015; 98: 977–992. doi: 10.1111/mmi.13171 PMID: 26287377

27. Mumberg D, Müller R, Funk M. Yeast vectors for the controlled expression of heterologous proteins in different genetic backgrounds. Gene. 1995; 156: 119–122. PMID: 7737504

28. Gietz RD, Woods RA. Transformation of yeast by lithium acetate/single-stranded carrier DNA/polyethylene glycol method. Methods Enzymol. 2002; 350: 87–96. PMID: 12073338

29. Pagani A, Villarreal L, Capdevila M, Atrian S. The *Saccharomyces cerevisiae* Crs5 metallothionein metal-binding abilities and its role in the response to zinc overload. Mol Microbiol. 2007; 63: 256–269. PMID: 17163970

30. Cols N, Romero-Isart N, Capdevila M, Oliva B, Gonzàlez-Duarte P, Gonzàlez-Duarte R, et al. Binding of excess cadmium(II) to Cd_7-metallothionein from recombinant mouse Zn_7-metallothionein 1. UV-VIS absorption and circular dichroism studies and theoretical location approach by surface accessibility analysis. J Inorg Biochem. 1997; 68: 157–166. PMID: 9352652

31. Bofill R, Palacios O, Capdevila M, Cols N, Gonzalez-Duarte R, Atrian S, et al. A new insight into the Ag^+ and Cu^+ binding sites in the metallothionein beta domain. J Inorg Biochem. 1999; 73: 57–64. PMID: 10212995

32. Bongers J, Walton CD, Richardson DE, Bell JU. Micromolar protein concentrations and metalloprotein stoichiometries obtained by inductively coupled plasma atomic emission spectrometric determination of sulfur. Anal Chem. 1988; 60: 2683–2686. PMID: 3245594

33. Capdevila M, Domenech J, Pagani A, Tio L, Villarreal L, Atrian S. Zn- and Cd-metallothionein recombinant species from the most diverse phyla may contain sulfide (S^{2-}) ligands. Angew Chem Int Ed Engl. 2005; 44: 4618–4622. PMID: 15991200

34. Fabris D, Zaia J, Hatout Y, Fenselau C. Retention of thiol protons in two classes of protein zinc coordination centers. J Am Chem Soc. 1996; 118: 12242–12243.

35. Shuja RN, Shakoori AR. Identification and cloning of first cadmium metallothionein like gene from locally isolated ciliate, *Paramecium* sp. Mol Biol Rep. 2009; 36: 549–560. doi: 10.1007/s11033-008-9213-8 PMID: 18273691

36. Diaz S, Amaro F, Rico D, Campos V, Benitez L, Martín-González A, et al. *Tetrahymena* metallothioneins fall into two discrete subfamilies. PLoS ONE. 2007; 3: e291.

37. Domenech J, Bofill R, Tinti A, Torreggiani A, Atrian S, Capdevila M. Comparative insight into the Zn(II)-, Cd(II)- and Cu(I)-binding features of the protozoan *Tetrahymena pyriformis* MT1 metallothionein. Biochim Biophys Acta. 2008; 1784: 693–704. doi: 10.1016/j.bbapap.2008.01.008 PMID: 18280816

38. Perez-Rafael S, Kurz A, Guirola M, Capdevila M, Palacios O, Atrian S.X Is MtnE, the fifth *Drosophila metallothionein*, functionally distinct from the other members of this polymorphic protein family? Metallomics. 2008; 4: 342–349.

39. Artells E, Palacios O, Capdevila M, Atrian S. In vivo-folded metal-MT3 complexes reveal the Cu- rather than Zn-thionein character of this brain-specific mammalian metallothionein. Metallomics. 2013; 5: 1397–1410. doi: 10.1039/c3mt00123g PMID: 23925449

40. Winge D, Dameron CT, George GN, Pickering IJ, Dance IG. Cuprous-thiolate polymetallic clusters in biology. In: Karin KD, Tyeklar Z, editors. Bioinorganic Chemistry of Copper. New York: Chapman & Hall; 1994. pp. 110–122.

41. Maiti BK, Pal K, Sarkar S. Flexible Cu^I-thiolate clusters with relevance to Metallothioneins. Eur J Inor Chem. 2007; 2007: 5548–5555.

42. Pushie MJ, Zhang L, Pickering IJ, George GN. The fictile coordination chemistry of cuprous-thiolate sites in copper chaperones. Biochim Biophys Acta. 2012; 1817: 938–947. doi: 10.1016/j.bbabio.2011.10.004 PMID: 22056518

43. Adamo GM, Lotti M, Tamas MJ, Brocca S. Amplification of the *CUP1* gene is associated with evolution of copper tolerance in *Saccharomyces cerevisiae*. Microbiol. 2012; 158: 2325–2335.

44. Dallinger R, Chabicovsky M, Hödl E, Prem C, Hunziker P, Manzl C. Copper in *Helix pomatia* (Gastropoda) is regulated by one single cell type: differently responsive metal pools in rhogocytes. Am J Physiol. 2005; 189: R1185–R1195.

CONCLUSIONS

12. CONCLUSIONS

From the presented and discussed results of this Thesis work, there are several conclusions that can be drawn:

The amino acid sequence including 7 cysteines is very common in a lot of fungal MTs, as is possible to observe by the huge number of members classified in subfamily 1 containing this number of cysteines in their sequence. According to all the discussed results, the conclusion that these particular MTs with 7 cysteines have distinguishing features is possible to be affirmed.

The most important features are their construction by motifs -CXC- and -CXCXXC-, their ability for bind optimally 2 Zn(II) metal ions and their notable Cu-thionein character. This last feature is reinforced by the formation of very stable Cu_5-MT complexes in all the 7-Cys MT cases studied. However, these defined features become modified as a result of various factors.

The presence of additional flanking Cys residues in the sequence, observed for example in CipMT2, provokes the coordination of further metal ions. Nevertheless, a very high stability is shown by the complexes Cu_5-MT formed, and these situations with excess of cysteines do not helps to confer more stability to the complexes with additional metal ions formed.

By contrast, the lack of cysteines in the 7-Cys sequences produces a lower number of coordinated metal ions and a lower stability of the complexes Cys-metal formed. This fact is possible to be observed in CaCup1, which only have 6 cysteine residues and is unable to bind 5 Cu(I) ions with stability.

When the sequences of 7 cysteines are flanked by fragments of non-coordinating amino acids enough long, the coordination of additional metal ions is also possible in some cases, as is observed for example in the formation of Zn_3-NcMT2 or Cu_6-NcMT2. Besides, the presence of these fragments seems to confer more stability to the cluster Cu_5-MT formed, allowing them to resist hard situations without unfolding.

Apart from the number of cysteines, the position of the cysteines inside the sequence is also important for the binding features of MTs. When the cysteines are located by forming part of -CC- motifs, MTs seems to have less Cu-thionein character, thus their affinity by divalent metal ions is higher. This is the case of UrMT and CipMT1, unable to bind Cu(I) successfully, but able to form Zn-MT and Cd-MT stable complexes.

However, the presence of cysteines in -CC- motifs seems to confer to MTs more capability to bind metal ions than the presence of single cysteines. This is clearly observed by the different binding abilities of SbMT and CaCRD2.

Apart from all that, by studying extremely long MTs, several interested features are also observed. Cysteines in long MTs are not randomly located, they are in well-known sequences. The characteristic 7-Cys sequence is observed several times in CnMTs and TmMT, allowing fragments of their sequence to be aligned with the short 7-Cys MTs know, like NcMT. The study of the binding abilities of these fragments separately allows concluding

that they can form stable complexes by themselves. Besides, the contribution on the stabilization of complexes thanks to the spacers is also evidenced, as is possible to observe by the different mutants of CnMT1 analysed. Then, the association of the 7-Cys fragments, with the inclusion of spacers between them grant the possibility to form large MTs with extremely elevated coordinating capacities.

Consequently, the existence of these long MTs formed by 7-Cys fragments suggest that peptides can suffer evolution and amplification by joining metal-coordinating modules in order to increase their coordinating abilities and cope against high metal concentrations.

EXPERIMENTAL PROCEDURES

13. EXPERIMENTAL PROCEDURES

13.1 Synthesis and purification of recombinant and in vitro-constituted metal-MT complexes[A]

Luria-Bertani (LB) cultures of the transformed BL21 *E. coli* strains were the source of recombinant metal-MT complexes. Gene induction was switched on with 100 µM (final concentration) of isopropyl β-D-thiogalactopyranoside (IPTG) 30 min before the addition of the suitable metal supplement (300 µM $ZnCl_2$, 300 µM $CdCl_2$ or 500 µM $CuSO_4$, final concentrations) to allow the synthesis of the corresponding metal complex. The cultures grew for 3 h, and in the case of Cu-supplementation, cultures were aerated to obtain either a normal oxygenation (1-l of LB media in a 2-l Erlenmeyer flask at 250 rpm) or a low oxygenation (1.5-l of LB media in a 2-l Erlenmeyer flask at 150 rpm), since this condition highly determines the level of intracellular copper in the host cells. It is worth noting that to prevent oxidation of the metal-MT complexes, argon was bubbled in all the subsequent steps of the purification protocol. The cultures were centrifuged and the recovered cell mass was resuspended in ice-cold Phosphate Buffered Saline (PBS, 1.4 M NaCl, 27 mM KCl, 101 mM Na_2HPO_4, 18 mM KH_2PO_4)-0.5% v/v 2-mercaptoethanol, and disrupted by sonication. The total protein extract was obtained in the supernatant of a 12,000 x g, 30 min centrifugation, which was then incubated with Glutathione-Sepharose 4B (GE Healthcare) beads at gentle agitation for 1 h at room temperature, for GST-MT purification by batch affinity chromatography. After three washes in PBS, the GST-MT proteins were digested with thrombin (10 u per mg of fusion protein, overnight at 17 °C) to separate the metal-MT complexes from the GST fragment, which remains bound to the gel matrix. The recovered solution was concentrated using Centriprep 3 kDa cut-off Microcons (Amicon) and finally fractionated through a Superdex-75 FPLC column equilibrated with 50 mM Tris-HCl, pH 7.0, and run at 0.8 ml min^{-1}. Aliquots of the protein-containing fractions were identified by their absorbance at 254 and 280 nm, and later analysed in 15% SDS-PAGE gels stained with Coomassie Blue. MT-containing samples were pooled and stored at -80 °C until further use. Due to the pGEX recombinant expression system specificities, the synthesized MTs contained two additional residues (Gly-Ser) as their N-termini, but these amino acids have been shown not to alter the MT metal-binding features. The so-called “in vitro complexes”, to differentiate them from the “in vivo” recombinantly synthesized complexes, were prepared via metal replacement by adding the corresponding metal ions (Cd^{2+} or Cu^{+}) to the recombinant Zn-MT samples. Characterization of the in vitro complexes was performed by UV-Vis and CD spectroscopies, as well as ESI-MS analysis, as explained below for the recombinant complexes. All assays were carried out in an Ar atmosphere, and the pH remained constant throughout all the experiments, without the addition of any extra buffers.

[A] Process of synthesis performed by the Biology and Genetics Group of *Universitat de Barcelona*

13.2 Spectroscopic characterization of the metal-MT complexes

The S, Zn, Cd and Cu content of all the metal-MT preparations was analysed by Inductively Coupled Plasma Atomic Emission Spectroscopy (ICP-AES), using a Polyscan 61E (Thermo Jarrell Ash) spectrometer, measuring S at 182.040 nm, Zn at 213.856 nm, Cd at 228.802 nm, and Cu at 324.803 nm. Their incubation in 1 M HCl at 65 °C for 15 min prior to analyses allowed the elimination of labile sulfide ions. Protein concentrations were calculated from the ICP-AES sulfur measurement, assuming that all S atoms were contributed by the MT peptides.[B] CD spectra were recorded in a Jasco spectropolarimeter (Model J-715) interfaced to a computer (J700 software), where a 25 °C temperature was maintained constant by a Peltier PTC-351S equipment. Electronic absorptions measurements were performed on an HP-8453 Diode array UV-visible spectrophotometer. 1-cm capped quartz cuvettes were used to record all the spectra, which were corrected for the dilution effects and processed using the GRAMS 32 program.

13.3 ElectroSpray ionization mass spectrometry (ESI-MS) analysis of the metal-MT complexes[C]

Electrospray ionization time-of-flight mass spectrometry (ESI-TOF MS) was performed on a Micro TOF-Q instrument (Bruker) interfaced with a Series 1200 HPLC Agilent pump, equipped with an autosampler, all of which controlled by the Compass Software. The ESI-L Low Concentration Tuning Mix (Agilent Technologies) was used for equipment calibration. For the analysis of Zn- and Cd-MT complexes, samples were run under the following conditions: 20 µl of protein solution injected through a polyether heteroketone (PEEK) tubing (1.5 m x 0.18 mm i.d.) at 40 µl min^{-1}; capillary counter-electrode voltage 5 kV; desolvation temperature 90-110 °C; dry gas 6 l min^{-1}; spectra collection range 800-2500 m/z. The carrier buffer was a 5:95 mixture of acetonitrile:ammonium acetate (15 mM, pH 7.0). Instead, the Cu-MTT samples were analysed as follows: 20 µl of protein solution injected at 40 µl min^{-1}; capillary counter-electrode voltage 3.5 kV; lens counter-electrode voltage 4 kV; dry temperature 80 °C; dry gas 6 l min^{-1}. Here, the carrier was a 10:90 mixture of acetonitrile:ammonium acetate, 15 mM, pH 7.0. Acidic-MS conditions, which causes the demetalation of the peptides loaded with divalent metal ions, but keeps the Cu^{+} ions bound to the protein, were used to generate the apo-MT forms and to analyse the Cu-containing MT samples. For it, 20 µl of the preparation were injected under the same conditions described previously, but using a 5:95 mixture of acetonitrile:formic acid, pH 2.4, as liquid carrier. For all the ESI-MS results, the error associated with the mass measurements was always inferior to 0.1%.

[B] ICP-AES analysis performed by the *Servei d'Anàlisi Química* of *Universitat Autònoma de Barcelona*

[C] Analysis done with the help of the techniques of *Servei d'Anàlisi Química* of *Universitat Autònoma de Barcelona*

BIBLIOGRAPHY

14. BIBLIOGRAPHY

1. Linneo, C. (1735). Systema naturæ, sive regna tria naturæ systematice proposita per classes, ordines, genera, & species (1st ed.). Leiden: *Theodorum Haak*.
2. Haeckel, E. H. P. A. (1966). Generelle morphologie der organismen (2nd ed.). Berlin: *G. Reimer.*
3. Chatton, E. (1925). Pansporella perplexa: amœbien à spores protégées parasite des daphnies: réflexions sur la biologie et la phylogénie des protozoaires. *Ann. Sci. Nat. Zool.* VII:1-84
4. Chatton, E. (1937). Titres et travaux scientifiques (1906-1937). Sète, France: *Impr E. Sottano*.
5. Copeland, H. F. (1938). The kingdoms of organisms. *Quarterly Review of Biology. 13: 383–420.*
6. Copeland, H. F. (1956). The classification of lower organisms. Palo Alto, Calif.: *Pacific Books*.
7. Whittaker, R. H. (1969). New concepts of kingdoms of organisms. *Science*, 163(3863), 150–160.
8. Balch, W. E., Magrum, L. J., Fox, G. E., Wolfe, R. S., & Woese, C. R. (1977). An ancient divergence among the bacteria. *Journal of Molecular Evolution*, 9(4), 305–311.
9. Woese, C. R., & Fox, G. E. (1977). Phylogenetic structure of the prokaryotic domain: the primary kingdoms. *Proceedings of the National Academy of Sciences of the United States of America*, 74(11), 5088–90.
10. Woese, C. R., Kandler, O., & Wheelis, M. L. (1990). Towards a natural system of organisms: proposal for the domains Archaea, Bacteria, and Eucarya. *Proceedings of the National Academy of Sciences of the United States of America*, 87(12), 4576–9.
11. Cavalier-Smith, T. (1981). Eukaryote kingdoms: seven or nine? *Bio Systems*, 14(3–4), 461–81.
12. Cavalier-Smith, T. (1992). Origins of secondary metabolism. *Ciba Foundation Symposium*, 171, 64-80–7.
13. Cavalier-Smith, T. (1993). Kingdom protozoa and its 18 phyla. *Microbiological Reviews*, 57(4), 953–94.
14. Cavalier-Smith, T. (1998). A revised six-kingdom system of life. *Biological Reviews of the Cambridge Philosophical Society*, 73(3), 203–66.

15. Cavalier-Smith, T. (2004). Only six kingdoms of life. *Proceedings. Biological Sciences*, 271(1545), 1251–62.
16. Cavalier-Smith, T. (2010). Kingdoms Protozoa and Chromista and the eozoan root of the eukaryotic tree. *Biology Letters*, 6(3), 342–345.
17. Ruggiero, M. A., Gordon, D. P., Orrell, T. M., Bailly, N., Bourgoin, T., Brusca, R. C., & Kirk, P. M. (2015). A Higher Level Classification of All Living Organisms. *PLOS ONE*, 10(4).
18. Alexopoulos, C. J., Mims, C. W., & Blackwell, M. (1996). Introductory mycology (4th ed.). *Wiley*.
19. Held, A. A., & Webster, J. (1972). Introduction to Fungi. *Mycologia*, 64(1), 226.
20. Cole, G. T., & Hoch, H. C. (1991). The fungal spore and disease initiation in plants and animals. New York: *Plenum Press*.
21. Dugan, F. M., & American Phytopathological Society (2008). Fungi in the ancient world: how mushrooms, mildews, molds, and yeast shaped the early civilizations of Europe, the Mediterranean, and the Near East. St, Paul, Minn: *APS Press*.
22. Karlson-Stiber, C., & Persson, H. (2003). Cytotoxic fungi—an overview. *Toxicon*, 42(4), 339–349.
23. Deshpande, M. V. (1999). Mycopesticide Production by Fermentation: Potential and Challenges. *Critical Reviews in Microbiology*, 25(3), 229–243.
24. Hube, B. (2004). From commensal to pathogen: stage- and tissue-specific gene expression of *Candida albicans*. *Current Opinion in Microbiology*, 7(4), 336–341.
25. Nielsen, K., & Heitman, J. (2007). Sex and Virulence of Human Pathogenic Fungi. *Advances in Genetics*, 57, 143–173.
26. Brakhage, A. A. (2005). Systemic fungal infections caused by *Aspergillus* species: epidemiology, infection process and virulence determinants. *Current Drug Targets*, 6(8), 875–86.
27. Blackwell, M. (2011). The fungi: 1, 2, 3 ... 5.1 million species? *American Journal of Botany*, 98(3), 426–38.
28. Kirk, P. M., Cannon, P. F., Minter, D. W., & Stalpers, J. A. (2008). Dictionary of the Fungi (10th ed.). Wallingford, UK: *CAB International*.
29. Hawksworth, D. L. (2001). The magnitude of fungal diversity: the 1.5 million species estimate revisited. *Mycological Research*, 105(12), 1422–1432.
30. Webster, J., & Weber, R. (2007). Introduction to fungi. New York: *Cambridge University Press*.

31. Hibbett, D. S., Binder, M., Bischoff, J. F., Blackwell, M., Cannon, P. F., Eriksson, O. E., & Zhang, N. (2007). A higher-level phylogenetic classification of the Fungi. *Mycological Research*, 111(5), 509–547.

32. Longcore, J. E., Simmons, D. R., Longcore, J. E., & Simmons, D. R. (2012). Blastocladiomycota. Chichester, UK: *John Wiley & Sons, Ltd*.

33. Perotto, S., Angelini, P., Bianciotto, V., Bonfante, P., Girlanda, M., Kull, T., & Selosse, M. A. (2013). Interactions of fungi with other organisms. *Plant Biosystems - An International Journal Dealing with All Aspects of Plant Biology*, 147(1), 208–218.

34. Gonzalez-Fernandez, R., & Jorrin-Novo, J. V. (2012). Contribution of Proteomics to the Study of Plant Pathogenic Fungi. *Journal of Proteome Research*, 11(1), 3–16.

35. Dean, R., Van Kan, J. A. L., Pretorius, Z. A., Hammond-Kosack, K. E., Di Pietro, A., Spanu, P. D., & Foster, G. D. (2012). The Top 10 fungal pathogens in molecular plant pathology. *Molecular Plant Pathology*, 13(4), 414–430.

36. Brown, G. D., Denning, D. W., Gow, N. A. R., Levitz, S. M., Netea, M. G., & White, T. C. (2012). Hidden killers: human fungal infections. *Science Translational Medicine*, 4(165), 165rv13.

37. Roberts, G. D., & Rippon, J. W. (1988). Medical Mycology: The Pathogenic Fungi and the Pathogenic *Actinomycetes*. *Mayo Clinic Proceedings*, 63(10), 1061–1062.

38. Ochiai, E-I. (1987). General Principles of Biochemistry of the Elements. *Plenum Press*.

39. Gadd G. M., & Griffiths A. J. (1978). Microorganisms and heavy metal toxicity. *Microbial Ecology*, 4, 303-317.

40. Mehlhorn R. J. (1986). The Interaction of Inorganic Species with Biomembranes. In Bernhard, M., Brinckman, F. E., Sadler P. J. eds. The Importance of Chemical “Speciation” in Environmental Processes. Dahlem Workshop Reports (Life Sciences Research Report). *Springer*, 33.

41. Greco, M. A., Hrab, D. I., Magner, W., & Kosman, D. J. (1990). Cu,Zn superoxide dismutase and copper deprivation and toxicity in *Saccharomyces cerevisiae*. *Journal of Bacteriology*, 172(1), 317–25.

42. Brown, M. T., & Hall, I. R. (1990). Metal tolerance in fungi. In Shaw, J., ed. Heavy metal tolerance in plants: evolutionary aspects. Boca Raton: *CRC Press*, 95-104.

43. Gadd, G. M., & White, C. (1989). Heavy metal and radionuclide accumulation and toxicity in fungi and yeasts. In Poole, R. K., & Gadd, G. M., eds. Metal-microbe interactions. Oxford: *IRL Press*, 19-38.

44. Ross, I.S. (1975). Some effects of heavy metals on fungal cells. *Transactions of the British Mycological Society*, 64, 175-193.

45. Margoshes, M., & Vallee, B. L. (1957). A cadmium protein from equine kidney cortex. *Journal of the American Chemical Society*, 79(17), 4813–4814.

46. Kagi, J. H., & Valle, B. L. (1960). Metallothionein: a cadmium- and zinc-containing protein from equine renal cortex. *The Journal of Biological Chemistry*, 235, 3460–5.

47. Gold, B., Deng, H., Bryk, R., Vargas, D., Eliezer, D., Roberts, J., & Nathan, C. (2008). Identification of a copper-binding metallothionein in pathogenic mycobacteria. *Nature Chemical Biology*, 4(10), 609–16.

48. Capdevila, M., Bofill, R., Palacios, Ò., & Atrian, S. (2012). State-of-the-art of metallothioneins at the beginning of the 21st century. *Coordination Chemistry Reviews*, 256(1-2), 46–62.

49. Stillman, M. J. (1995). Metallothioneins. *Coordination Chemistry Reviews*, 144, 461–511.

50. Riordan, J. F., & Vallee, B. L. (1991). Metallothionein and related molecules. In Methods in enzymology, vol. 205, Metallobiochemistry, part B. San Diego: *Academic Press*.

51. Kull, F. J., Reed, M. F., Elgren, T. E., Ciardelli, T. L., & Wilcox, D. E. (1990). Solid-phase peptide synthesis of the α and β domains of human liver metallothionein 2 and the metallothionein of Neurospora crassa. *Journal of the American Chemical Society*, 112(6), 2291–2298.

52. Nishiyama, Y., Nakayama, S., Okada, Y., Min, K. S., Onosaka, S., & Tanaka, K. (1990). Amino acids and peptides. XXVI. Synthesis of *Agaricus bisporus* metallothionein and related peptides and examination of their heavy metal-binding properties. *Chemical & Pharmaceutical Bulletin*, 38(8), 2112–7.

53. Okada, Y., Ohta, N., Iguchi, S., Tsuda, Y., Sasaki, H., Kitagawa, T., & Tanaka, K. (1986). Amino acids and peptides. XIII. Synthesis of a nonacosapeptide corresponding to the N-terminal sequence 1-29 (beta-fragment) of human liver metallothionein II (hMT II) and its heavy metal-binding properties. *Chemical & Pharmaceutical Bulletin*, 34(3), 986–98.

54. Hartmann, H. J., Li, Y. J., & Weser, U. (1992). Analogous copper(I) coordination in metallothionein from yeast and the separate domains of the mammalian protein. *Biometals: An International Journal on the Role of Metal Ions in Biology, Biochemistry, and Medicine*, 5(3), 187–91.

55. Sewell, A. K., Jensen, L. T., Erickson, J. C., Palmiter, R. D., & Winge, D. R. (1995). Bioactivity of metallothionein-3 correlates with its novel beta domain sequence rather than metal binding properties. *Biochemistry*, 34(14), 4740–7.

56. Cols, N. (1996). *PhD thesis*, Department of Genetics, *Universitat de Barcelona*.

57. Capdevila, M., Cols, N., Romero-Isart, N., González-Duarte, R., Atrian, S., & González-Duarte, P. (1997). Recombinant synthesis of mouse Zn_3-β and Zn_4-α metallothionein 1 domains and characterization of their cadmium(II) binding capacity. *Cellular and Molecular Life Sciences (CMLS)*, 53(8), 681–688.

58. Atrian S., Capdevila M., Cols N., González-Duarte R., González-Duarte P., Romero N., Stillman M. J. (1995). Metal binding properties of recombinant metallothioneins and related peptides. *Journal of Inorganic Biochemistry*, 59 (2), 103.

59. Schultze, P., Wörgötter, E., Braun, W., Wagner, G., Vasák, M., Kägi, J. H. R. & Wüthrich, K. (1988). Conformation of [Cd_7]-metallothionein-2 from rat liver in aqueous solution determined by nuclear magnetic resonance spectroscopy. *J. Mol. Biol.*, 203, 251-268.

60. Arseniev, A., Schultze, P., Worgotter, E., Braun, W., Wagner, G., Vasdk, M., Kagi, J. H. R. & Wfthrich, K. (1988). Three-dimensional structure of rabbit liver [Cd_7]-metallothionein-2a in aqueous solution determined by nuclear magnetic resonance. *J. Mol. Biol.*, 201, 637-657.

61. Messerle, B., Schiffer, A., Vakik, M., Kigi, J. H. R. & Wuthrich, K. (1990). Comparison of the NMR solution structure and the X-ray crystal structure of rat metallothionein-2. *J. Mol. Biol.*, 214, 765-779.

62. Robbins, A. H., McRee, D. E., Williamson, M., Collett, S. A., Xoung, N. H., Furey, W. F., Wang, B. C. & Stout, C. D. (1991). Refined crystal structure of Cd, Zn metallothionein at 2.0 A resolution. *J. Mol. Biol.*, 221, 1269-1293.

63. Zangger, K., Oz, G., Otvos, J. D., & Armitage, I. M. (1999). Three-dimensional solution structure of mouse [Cd_7]-metallothionein-1 by homonuclear and heteronuclear NMR spectroscopy. *Protein Science: A Publication of the Protein Society*, 8(12), 2630–8.

64. Oz, G., Zangger, K., & Armitage, I. M. (2001). Three-dimensional structure and dynamics of a brain specific growth inhibitory factor: metallothionein-3. *Biochemistry*, 40(38), 11433–41.

65. Capasso, C., Carginale, V., Crescenzi, O., Di Maro, D., Parisi, E., Spadaccini, R., & Temussi, P. A. (2003). Solution structure of MT_nc, a novel metallothionein from the Antarctic fish *Notothenia coriiceps*. *Structure*, 11(4), 435–43.

66. Narula, S. S., Brouwer, M., Hua, Y., & Armitage, I. M. (1995). Three-dimensional solution structure of *Callinectes sapidus* metallothionein-1 determined by homonuclear and heteronuclear magnetic resonance spectroscopy. *Biochemistry*, 34(2), 620–31.

67. Muñoz, A., Försterling, H. F., Shaw, F. C., & Petering, D. H. (2002). Structure of the $^{113}Cd_3\beta$ domains from *Homarus americanus* metallothionein-1: hydrogen bonding and solvent accessibility of sulfur atoms. *Journal of Biological Inorganic Chemistry*, 7(7–8), 713–724.

68. Riek, R., Prêcheur, B., Wang, Y., Mackay, E. A., Wider, G., Güntert, P., & Wüthrich, K. (1999). NMR Structure of the Sea Urchin (*Strongylocentrotus purpuratus*) Metallothionein MTA. *Journal of Molecular Biology*, 291(2), 417–428.

69. Bertini, I., Hartmann, H. J., Klein, T., Liu, G., Luchinat, C., & Weser, U. (2000). High resolution solution structure of the protein part of Cu_7 metallothionein. *European Journal of Biochemistry*, 267(4), 1008–18.

70. Peterson, C. W., Narula, S. S., & Armitage, I. M. (1996). 3D solution structure of copper and silver-substituted yeast metallothioneins. *FEBS Letters*, 379(1), 85–93.

71. Calderone, V., Dolderer, B., Hartmann, H.-J., Echner, H., Luchinat, C., Del Bianco, C., & Weser, U. (2005). The crystal structure of yeast copper thionein: The solution of a long-lasting enigma. *Proceedings of the National Academy of Sciences*, 102(1), 51–56.

72. Blindauer, C. A., Harrison, M. D., Parkinson, J. A., Robinson, A. K., Cavet, J. S., Robinson, N. J., & Sadler, P. J. (2001). A metallothionein containing a zinc finger within a four-metal cluster protects a bacterium from zinc toxicity. *Proceedings of the National Academy of Sciences*, 98(17), 9593–9598.

73. Cobine, P. A., McKay, R. T., Zangger, K., Dameron, C. T., & Armitage, I. M. (2004). Solution structure of Cu_6 metallothionein from the fungus *Neurospora crassa*. *European Journal of Biochemistry / FEBS*, 271(21), 4213–21.

74. Peroza, E. A., Schmucki, R., Güntert, P., Freisinger, E., & Zerbe, O. (2009). The βE-Domain of wheat Ec-1 Metallothionein: A Metal-Binding Domain with a Distinctive Structure. *Journal of Molecular Biology*, 387(1), 207–218.

75. Romero-Isart, N., & Vasák, M. (2002). Advances in the structure and chemistry of metallothioneins. *Journal of Inorganic Biochemistry,* 88(3–4), 388–96.

76. Vašak, M., & Romero-Isart, N. (2005). Encyclopedia of Inorganic Chemistry (2nd ed.). New York: *Jhon Wiley & Sons.*

77. Dolderer, B., Hartmann, H. J., Weser, U. (2009). Metallothioneins in Yeast and Fungi. In Sigel, A., Sigel, H., Sigel, R. K. O., eds. Metal Ions in Life Sciences: Metallothioneins and Related Chelators, Vol. 5. Cambridge, UK: *RSC Publishing*, pp. 83–106.

78. Smith, T. A., Lerch, K., & Hodgson, K. O. (1986). Structural study of the Cu sites in metallothionein from *Neurospora crassa*. *Inorg. Chem*, 25, 4677-4680.

79. Maret, W., Heffron, G., Hill, H. A. O., Djuricic, D., Jiang, L.-J., & Vallee, B. L. (2002). The ATP/metallothionein interaction: NMR and STM. *Biochemistry*, 41(5), 1689–94.

80. Domenech, J., Palacios, O., Villarreal, L., González-Duarte, P., Capdevila, M., & Atrian, S. (2003). MTO: the second member of a *Drosophila* dual copper-thionein system. *FEBS Letters*, 533(1–3), 72–8.

81. Tío, L., Villarreal, L., Atrian, S., & Capdevila, M. (2006). The Zn- and Cd-clusters of recombinant mammalian MT1 and MT4 metallothionein domains include sulfide ligands. *Experimental Biology and Medicine*, 231(9), 1522–7.

82. Reese, R. N., Mehra, R. K., Tarbet, E. B., & Winge, D. R. (1988). Studies on the gamma-glutamyl Cu-binding peptide from *Schizosaccharomyces pombe*. *The Journal of Biological Chemistry*, 263(9), 4186–92.

83. Reese, R. N., & Winge, D. R. (1988). Sulfide stabilization of the cadmium-gamma-glutamyl peptide complex of *Schizosaccharomyces pombe*. The Journal of Biological Chemistry, 263(26), 12832–5.

84. Dameron, C. T., & Winge, D. R. (1990). Characterization of peptide-coated cadmium-sulfide crystallites. *Inorganic Chemistry*, 29(7), 1343–1348.

85. Mir, G., Domènech, J., Huguet, G., Guo, W.-J., Goldsbrough, P., Atrian, S., & Molinas, M. (2004). A plant type 2 metallothionein (MT) from cork tissue responds to oxidative stress. *Journal of Experimental Botany*, 55(408), 2483–2493.

86. Capdevila, M., Domènech, J., Pagani, A., Tío, L., Villarreal, L., & Atrian, S. (2005). Zn- and Cd-Metallothionein Recombinant Species from the Most Diverse Phyla May Contain Sulfide (S^{2-}) Ligands. *Angewandte Chemie International Edition*, 44(29), 4618–4622.

87. Orihuela, R., Monteiro, F., Pagani, A., Capdevila, M., & Atrian, S. (2010). Evidence of Native Metal-S^{2-}-Metallothionein Complexes Confirmed by the Analysis of Cup1 Divalent-Metal-Ion Binding Properties. *Chemistry - A European Journal*, 16(41), 12363–12372.

88. Park, T. J., Lee, S. Y., Heo, N. S., & Seo, T. S. (2010). In Vivo Synthesis of Diverse Metal Nanoparticles by Recombinant *Escherichia coli*. *Angewandte Chemie International Edition*, 49(39), 7019–7024.

89. Fowler, B. A., Hildebrand, C. E., Kojima, Y., & Webb, M. (1987). Nomenclature of metallothionein. *Experientia. Supplementum*, 52, 19–22.

90. Kägi, J. H., & Schäffer, A. (1988). Biochemistry of metallothionein. *Biochemistry*, 27(23), 8509–15.

91. Binz, P.-A., & Kägi, J. H. R. (1999). Metallothionein: Molecular evolution and classification. In Metallothionein IV (pp. 7–13). Basel: *Birkhäuser Basel*.

92. Pagani, A., Villarreal, L., Capdevila, M., & Atrian, S. (2007). The *Saccharomyces cerevisiae* Crs5 Metallothionein metal-binding abilities and its role in the response to zinc overload. *Molecular Microbiology*, 63(1), 256–269.

93. Bofill, R., Capdevila, M., & Atrian, S. (2009). Independent metal-binding features of recombinant metallothioneins convergently draw a step gradation between Zn- and Cu-thioneins. *Metallomics*, 1(3), 229.

94. Capdevila, M., Palacios, O., & Atrian, S. (2010). The zn- or cu-thionein character of a metallothionein determines its metal load when synthesized in physiological (metal-unsupplemented) conditions. *Bioinorganic Chemistry and Applications*, 2010, 1-6.

95. Palacios, Ò., Atrian, S., & Capdevila, M. (2011). Zn- and Cu-thioneins: a functional classification for metallothioneins? *JBIC Journal of Biological Inorganic Chemistry*, 16(7), 991–1009.

96. Orihuela, R. (2008). *PhD thesis*, Department of Chemistry, *Universitat Autònoma de Barcelona*.

97. Villarreal, L., Tio, L., Capdevila, M., & Atrian, S. (2006). Comparative metal binding and genomic analysis of the avian (chicken) and mammalian metallothionein. *FEBS Journal*, 273(3), 523–535.

98. Beach, L. R., & Palmiter, R. D. (1981). Amplification of the metallothionein-I gene in cadmium-resistant mouse cells. *Proceedings of the National Academy of Sciences of the United States of America*, 78(4), 2110–4.

99. Crawford, B. D., Enger, M. D., Griffith, B. B., Griffith, J. K., Hanners, J. L., Longmire, J. L., Munk, A. C., Stallings, R. L., Tesmer, J. G., & Walters, R. A. (1985). Coordinate amplification of metallothionein I and II genes in cadmium-resistant Chinese hamster cells: implications for mechanisms regulating metallothionein gene expression. *Molecular and Cellular Biology*, 5(2), 320–9.

100. Hamer, D. H. (1986). Metallothionein. *Annual Review of Biochemistry*, 55(1), 913–951.

101. Udom, A. O., & Brady, F. O. (1980). Reactivation in vitro of zinc-requiring apo-enzymes by rat liver zinc-thionein. *The Biochemical Journal*, 187(2), 329–35.

102. Beltramini, M., & Lerch, K. (1982). Copper transfer between Neurospora copper metallothionein and type 3 copper apoproteins. *FEBS Letters*, 142(2), 219–22.

103. Viarengo, A., Burlando, B., Ceratto, N., & Panfoli, I. (2000). Antioxidant role of metallothioneins: a comparative overview. *Cellular and Molecular Biology*, 46(2), 407–17.

104. Quesada, A. R., Byrnes, R. W., Krezoski, S. O., & Petering, D. H. (1996). Direct Reaction of H_2O_2 with Sulfhydryl Groups in HL-60 Cells: Zinc-Metallothionein and Other Sites. *Archives of Biochemistry and Biophysics*, 334(2), 241–250.

105. Lazo, J. S., Kondo, Y., Dellapiazza, D., Michalska, A. E., Choo, K. H., & Pitt, B. R. (1995). Enhanced sensitivity to oxidative stress in cultured embryonic cells from transgenic mice deficient in metallothionein I and II genes. *The Journal of Biological Chemistry*, 270(10), 5506–10.

106. Formigari, A., Santon, A., & Irato, P. (2007). Efficacy of zinc treatment against iron-induced toxicity in rat hepatoma cell line H4-II-E-C3. *Liver International*, 27(1), 120–7.

107. Winge, D. R., Jensen, L. T., & Srinivasan, C. (1998). Metal-ion regulation of gene expression in yeast. *Current Opinion in Chemical Biology*, 2(2), 216–221.

108. Beattie, J. H., Wood, A. M., Newman, A. M., Bremner, I., Choo, K. H., Michalska, A. E., & Trayhurn, P. (1998). Obesity and hyperleptinemia in metallothionein (-I and -II) null mice. *Proceedings of the National Academy of Sciences of the United States of America*, 95(1), 358–63.

109. Kondo, Y., Rusnak, J. M., Hoyt, D. G., Settineri, C. E., Pitt, B. R., & Lazo, J. S. (1997). Enhanced apoptosis in metallothionein null cells. *Molecular Pharmacology*, 52(2), 195–201.

110. Pedersen, M. Ø., Jensen, R., Pedersen, D. S., Skjolding, A. D., Hempel, C., Maretty, L., & Penkowa, M. (2009). Metallothionein-I+II in neuroprotection. *BioFactors*, 35(4), 315–325.

111. Meloni, G., Sonois, V., Delaine, T., Guilloreau, L., Gillet, A., Teissié, J., & Vašák, M. (2008). Metal swap between Zn_7-metallothionein-3 and amyloid-β–Cu protects against amyloid-β toxicity. *Nature Chemical Biology*, 4(6), 366–372.

112. Irie, Y., & Keung, W. M. (2001). Metallothionein-III Antagonizes the Neurotoxic and Neurotrophic Effects of Amyloid β Peptides. *Biochemical and Biophysical Research Communications*, 282(2), 416–420.

113. Quaife, C. J., Findley, S. D., Erickson, J. C., Froelick, G. J., Kelly, E. J., Zambrowicz, B. P., & Palmiter, R. D. (1994). Induction of a new metallothionein isoform (MT-IV) occurs during differentiation of stratified squamous epithelia. *Biochemistry*, 33(23), 7250–9.

114. Liang, L., Fu, K., Lee, D. K., Sobieski, R. J., Dalton, T., & Andrews, G. K. (1996). Activation of the complete mouse metallothionein gene locus in the maternal deciduum. *Molecular Reproduction and Development*, 43(1), 25–37.

115. Egli, D., Domènech, J., Selvaraj, A., Balamurugan, K., Hua, H., Capdevila, M., & Atrian, S. (2006). The four members of the *Drosophila* metallothionein family exhibit distinct yet

overlapping roles in heavy metal homeostasis and detoxification. *Genes to Cells*, 11(6), 647–658.

116. Valls, M., Bofill, R., Gonzalez-Duarte, R., Gonzalez-Duarte, P., Capdevila, M., & Atrian, S. (2001). A New Insight into Metallothionein (MT) Classification and Evolution: The in vivo and in vitro metal binding features of *Homarus americanus* recombinant MT. *Journal of Biological Chemistry*, 276(35), 32835–32843.
117. Lerch, K., Ammer, D., & Olafson, R. W. (1982). Crab metallothionein. Primary structures of metallothioneins 1 and 2. *The Journal of Biological Chemistry*, 257(5), 2420–6.
118. Ceratto, N., Dondero, F., van de Loo, J. W., Burlando, B., & Viarengo, A. (2002). Cloning and sequencing of a novel metallothionein gene in *Mytilus galloprovincialis* Lam. Comparative Biochemistry and Physiology. *Toxicology & Pharmacology: CBP*, 131(3), 217–22.
119. Liao, V. H.-C., Dong, J., & Freedman, J. H. (2002). Molecular Characterization of a Novel, Cadmium-inducible Gene from the Nematode *Caenorhabditis elegans*: A new gene that contributes to the resistance to cadmium toxicity. *Journal of Biological Chemistry*, 277(44), 42049–42059.
120. Maruyama, K., Hori, R., Nishihara, T., & Kondo, M. (1986). Isolation and characterization of metallothionein from nematode (*Caenorhabditis elegans*). *Eisei Kagaku*, 32(1), 22–27.
121. Amiard, J., Amiard-Triquet, C., Barka, S., Pellerin, J., & Rainbow, P. (2006). Metallothioneins in aquatic invertebrates: Their role in metal detoxification and their use as biomarkers. *Aquatic Toxicology*, 76(2), 160–202.
122. Lane, B., Kajioka, R., & Kennedy, T. (1987). The wheat-germ E_c protein is a zinc-containing metallothionein. *Biochemistry and Cell Biology*, 65(11), 1001–1005.
123. Van Hoof, N. A., Hassinen, V. H., Hakvoort, H. W., Ballintijn, K. F., Schat, H., Verkleij, J. A., & Tervahauta, A. I. (2001). Enhanced copper tolerance in *Silene vulgaris* (Moench) Garcke populations from copper mines is associated with increased transcript levels of a 2b-type metallothionein gene. *Plant Physiology*, 126(4), 1519–26.
124. Kojima, Y. (1991). Definitions and nomenclature of metallothioneins. *Methods in Enzymology*, 205, 8–10.
125. Kojima, Y., Binz, P.-A., & Kägi, J. H. R. (1999). Nomenclature of metallothionein: Proposal for a revision. In Metallothionein IV (pp. 3–6). Basel: *Birkhäuser Basel*.
126. Prinz, R., & Weser, U. (1975). A naturally occurring Cu-thionein in *Saccharomyces cerevisiae*. *Hoppe-Seyler's Zeitschrift Für Physiologische Chemie*, 356(6), 767–76.

127. Winge, D. R., Nielson, K. B., Gray, W. R., & Hamer, D. H. (1985). Yeast metallothionein. Sequence and metal-binding properties. *The Journal of Biological Chemistry*, 260(27), 14464–70.

128. Culotta, V. C., Howard, W. R., & Liu, X. F. (1994). CRS5 encodes a metallothionein-like protein in *Saccharomyces cerevisiae*. *The Journal of Biological Chemistry*, 269(41), 25295–302.

129. Jensen, L. T., Howard, W. R., Strain, J. J., Winge, D. R., & Culotta, V. C. (1996). Enhanced Effectiveness of Copper Ion Buffering by CUP1 Metallothionein Compared with CRS5 Metallothionein *in Saccharomyces cerevisiae*. *The Journal of Biological Chemistry*, 271(31), 18514–18519.

130. Mehra, R. K., Tarbet, E. B., Gray, W. R., & Winge, D. R. (1988). Metal-specific synthesis of two metallothioneins and gamma-glutamyl peptides in *Candida glabrata*. *Proceedings of the National Academy of Sciences of the United States of America*, 85(23), 8815–9.

131. Mehra, R. K., Garey, J. R., Butt, T. R., Gray, W. R., & Winge, D. R. (1989). *Candida glabrata* metallothioneins. Cloning and sequence of the genes and characterization of proteins. *The Journal of Biological Chemistry*, 264(33), 19747–53.

132. Lachke, S. A., Srikantha, T., Tsai, L. K., Daniels, K., & Soll, D. R. (2000). Phenotypic switching in *Candida glabrata* involves phase-specific regulation of the metallothionein gene MT-II and the newly discovered hemolysin gene HLP. *Infection and Immunity*, 68(2), 884–95.

133. García, S., Prado, M., Dégano, R., & Domínguez, A. (2002). A copper-responsive transcription factor, CRF1, mediates copper and cadmium resistance in *Yarrowia lipolytica*. *The Journal of Biological Chemistry*, 277(40), 37359–68.

134. Borrelly, G. P. M., Harrison, M. D., Robinson, A. K., Cox, S. G., Robinson, N. J., & Whitehall, S. K. (2002). Surplus Zinc Is Handled by Zym1 Metallothionein and Zhf Endoplasmic Reticulum Transporter in *Schizosaccharomyces pombe*. *Journal of Biological Chemistry*, 277(33), 30394–30400.

135. Lerch, K. (1980). Copper metallothionein, a copper-binding protein from *Neurospora crassa*. *Nature*, 284(5754), 368–70.

136. Münger, K., Germann, U. A., & Lerch, K. (1985). Isolation and structural organization of the *Neurospora crassa* copper metallothionein gene. *The EMBO Journal*, 4(10), 2665–8.

137. Beltramini, M., & Lerch, K. (1983). Spectroscopic studies on *Neurospora* copper metallothionein. *Biochemistry*, 22(9), 2043–2048.

138. Beltramini, M., Lerch, K., & Vasak, M. (1984). Metal substitution of *Neurospora* copper metallothionein. *Biochemistry*, 23(15), 3422–3427.

139. Malikayil, J. A., Lerch, K., & Armitage, I. M. (1989). Proton NMR studies of a metallothionein from Neurospora crassa: sequence-specific assignments by NOE measurements in the rotating frame. *Biochemistry*, 28(7), 2991–5.

140. Muenger, K., & Lerch, K. (1985). Copper metallothionein from the fungus Agaricus bisporus: chemical and spectroscopic properties. *Biochemistry*, 24(24), 6751–6756.

141. Sácký, J., Leonhardt, T., Borovička, J., Gryndler, M., Briksí, A., & Kotrba, P. (2014). Intracellular sequestration of zinc, cadmium and silver in *Hebeloma mesophaeum* and characterization of its metallothionein genes. *Fungal Genetics and Biology*, 67, 3–14.

142. Ramesh, G., Podila, G. K., Gay, G., Marmeisse, R., & Reddy, M. S. (2009). Different Patterns of Regulation for the Copper and Cadmium Metallothioneins of the Ectomycorrhizal Fungus *Hebeloma cylindrosporum*. *Applied and Environmental Microbiology*, 75(8), 2266–2274.

143. Bellion, M., Courbot, M., Jacob, C., Guinet, F., Blaudez, D., & Chalot, M. (2007). Metal induction of a *Paxillus involutus* metallothionein and its heterologous expression in *Hebeloma cylindrosporum*. *New Phytologist*, 174(1), 151–158.

144. Lanfranco, L., Bolchi, A., Ros, E. C., Ottonello, S., & Bonfante, P. (2002). Differential expression of a metallothionein gene during the presymbiotic versus the symbiotic phase of an arbuscular mycorrhizal fungus. *Plant Physiology*, 130(1), 58–67.

145. Leonhardt, T., Sácký, J., Šimek, P., Šantrůček, J., Kotrba, P., Bellion, M., & Capdevila, M. (2014). Metallothionein-like peptides involved in sequestration of Zn in the Zn-accumulating ectomycorrhizal fungus *Russula atropurpurea*. *Metallomics*, 6(9), 1693.

146. Osobová, M., Urban, V., Jedelský, P. L., Borovička, J., Gryndler, M., Ruml, T., & Kotrba, P. (2011). Three metallothionein isoforms and sequestration of intracellular silver in the hyperaccumulator *Amanita strobiliformis*. *New Phytologist*, 190(4), 916–926.

147. González-Guerrero, M., Cano, C., Azcón-Aguilar, C., & Ferrol, N. (2007). GintMT1 encodes a functional metallothionein in *Glomus intraradices* that responds to oxidative stress. *Mycorrhiza*, 17(4), 327–335.

148. Kameo, S., Iwahashi, H., Kojima, Y., & Satoh, H. (2000). Induction of metallothioneins in the heavy metal resistant fungus *Beauveria bassiana* exposed to copper or cadmium. *Analusis*, 28(5), 382–385.

149. Loebus, J., Leitenmaier, B., Meissner, D., Braha, B., Krauss, G.-J., Dobritzsch, D., & Freisinger, E. (2013). The major function of a metallothionein from the aquatic fungus *Heliscus lugdunensis* is cadmium detoxification. *Journal of Inorganic Biochemistry*, 127, 253–260.

150. Jaeckel, P., Krauss, G.-J., & Krauss, G. (2005). Cadmium and zinc response of the fungi *Heliscus lugdunensis* and *Verticillium cf. alboatrum* isolated from highly polluted water. *Science of The Total Environment* (Vol. 346).

151. Friesen, T. L., Zhang, Z., Solomon, P. S., Oliver, R. P., & Faris, J. D. (2008). Characterization of the interaction of a novel *Stagonospora nodorum* host-selective toxin with a wheat susceptibility gene. *Plant Physiology*, 146(2), 682–93.

152. Hane, J. K., Lowe, R. G. T., Solomon, P. S., Tan, K.-C., Schoch, C. L., Spatafora, J. W., & Oliver, R. P. (2007). *Dothideomycete* Plant Interactions Illuminated by Genome Sequencing and EST Analysis of the Wheat Pathogen *Stagonospora nodorum*. *The Plant Cell*, 19(11), 3347–3368.

153. Hwang, C. S., Flaishman, M. A., & Kolattukudy, P. E. (1995). Cloning of a gene expressed during appressorium formation by *Colletotrichum gloeosporioides* and a marked decrease in virulence by disruption of this gene. *The Plant Cell*, 7(2), 183–93.

154. Averbeck, N. B., Borghouts, C., Hamann, A., Specke, V., & Osiewacz, H. D. (2001). Molecular control of copper homeostasis in filamentous fungi: increased expression of a metallothionein gene during aging of *Podospora anserina*. *Molecular & General Genetics* : MGG, 264(5), 604–12.

155. Weissman, Z., Berdicevsky, I., Cavari, B. Z., & Kornitzer, D. (2000). The high copper tolerance of *Candida albicans* is mediated by a P-type ATPase. *Proceedings of the National Academy of Sciences of the United States of America*, 97(7), 3520–5.

156. Riggle, P. J., & Kumamoto, C. A. (2000). Role of a *Candida albicans* P1-Type ATPase in Resistance to Copper and Silver Ion Toxicity. *Journal of Bacteriology*, 182(17), 4899–4905.

157. Voiblet, C., Duplessis, S., Encelot, N., & Martin, F. (2008). Identification of symbiosis-regulated genes in *Eucalyptus globulus-Pisolithus tinctorius* ectomycorrhiza by differential hybridization of arrayed cDNAs. *The Plant Journal*, 25(2), 181–191.

158. Courbot, M., Diez, L., Ruotolo, R., Chalot, M., & Leroy, P. (2004). Cadmium-responsive thiols in the ectomycorrhizal fungus *Paxillus involutus*. *Applied and Environmental Microbiology*, 70(12), 7413–7.

159. Kwan, H.-S., & Xu, H.-L. (2002). Construction of a genetic linkage map of shiitake mushroom *Lentinula edodes* strain L-54. *Journal of Biochemistry and Molecular Biology*, 35(5), 465–71.

160. Sácký, J., Leonhardt, T., & Kotrba, P. (2016). Functional analysis of two genes coding for distinct cation diffusion facilitators of the ectomycorrhizal Zn-accumulating fungus *Russula atropurpurea*. *Biometals : An International Journal on the Role of Metal Ions in Biology, Biochemistry, and Medicine*, 29(2), 349–63.

161. Reddy, M. S., Prasanna, L., Marmeisse, R., & Fraissinet-Tachet, L. (2014). Differential expression of metallothioneins in response to heavy metals and their involvement in metal tolerance in the symbiotic basidiomycete *Laccaria bicolor*. *Microbiology* (Reading, England), 160(Pt 10), 2235–42.

162. Tucker, S. L., Thornton, C. R., Tasker, K., Jacob, C., Giles, G., Egan, M., & Talbot, N. J. (2004). A fungal metallothionein is required for pathogenicity of *Magnaporthe grisea*. *The Plant Cell*, *16*(6), 1575–88.

163. Ding, C., Yin, J., Tovar, E. M. M., Fitzpatrick, D. A., Higgins, D. G., & Thiele, D. J. (2011). The copper regulon of the human fungal pathogen *Cryptococcus neoformans* H99. *Molecular Microbiology*, *81*(6), 1560–1576.

164. Ding, C., Festa, R. A., Chen, Y.-L., Espart, A., Palacios, Ò., Espín, J., & Thiele, D. J. (2013). *Cryptococcus neoformans* Copper Detoxification Machinery Is Critical for Fungal Virulence. *Cell Host & Microbe*, *13*(3), 265–276.

165. Palacios, Ò., Espart, A., Espín, J., Ding, C., Thiele, D. J., Atrian, S., & Capdevila, M. (2014). Full characterization of the Cu-, Zn-, and Cd-binding properties of CnMT1 and CnMT2, two metallothioneins of the pathogenic fungus *Cryptococcus neoformans* acting as virulence factors. *Metallomics : Integrated Biometal Science*, *6*(2), 279–91.

166. Wagner, D., Maser, J., Lai, B., Cai, Z., Barry, C. E., Höner Zu Bentrup, K., & Bermudez, L. E. (2005). Elemental analysis of Mycobacterium avium-, Mycobacterium tuberculosis-, and Mycobacterium smegmatis-containing phagosomes indicates pathogen-induced microenvironments within the host cell's endosomal system. *Journal of Immunology (Baltimore, Md. : 1950)*, *174*(3), 1491–500.

167. Espart, A. (2015). *PhD thesis*, Department of Genetics, *Universitat de Barcelona*.

168. Shear, C. L., & Dodge B. O. (1927). Life histories and heterothallism of the red bread-mold fungi of the *Monilia sitophilia* group. *J. Agric. Res.*, 34:1019-1049.

169. Lindegren, C. C. (1936). A six-point map of the sex chromosome of *Neurospora crassa*. *J. Genet.*, 32:243-256.

170. Beadle, G. W., & Tatum, E. L. (1941). Genetic Control of Biochemical Reactions in *Neurospora*. *Proceedings of the National Academy of Sciences*, *27*(11), 499–506.

171. Nelson, P. E., Dignani, M. C., & Anaissie, E. J. (1994). Taxonomy, biology, and clinical aspects of *Fusarium* species. *Clinical Microbiology Reviews*, 7(4), 479–504.

172. Evans, J., Levesque, D., de Lahunta, A., & Jensen, H. E. (2004). Intracranial Fusariosis: A Novel Cause of Fungal Meningoencephalitis in a Dog. *Veterinary Pathology*, 41(5), 510–514.

173. Nucci, M., & Anaissie, E. (2002). Cutaneous Infection by *Fusarium* Species in Healthy and Immunocompromised Hosts: Implications for Diagnosis and Management. *Clinical Infectious Diseases*, 35(8), 909–920.

174. Kriek, N. P., Kellerman, T. S., & Marasas, W. F. (1981). A comparative study of the toxicity of *Fusarium verticillioides* (= *F. moniliforme*) to horses, primates, pigs, sheep and rats. *The Onderstepoort Journal of Veterinary Research*, 48(2), 129–31.

175. Erdogan, A., & Rao, S. S. C. (2015). Small Intestinal Fungal Overgrowth. *Current Gastroenterology Reports*, 17(4), 16.

176. Martins, N., Ferreira, I. C. F. R., Barros, L., Silva, S., & Henriques, M. (2014). Candidiasis: Predisposing Factors, Prevention, Diagnosis and Alternative Treatment. *Mycopathologia*, 177(5–6), 223–240.

177. Mukherjee, P. K., Sendid, B., Hoarau, G., Colombel, J.-F., Poulain, D., & Ghannoum, M. A. (2014). Mycobiota in gastrointestinal diseases. *Nature Reviews Gastroenterology & Hepatology*, 12(2), 77–87.

178. Hector, R. F., & Laniado-Laborin, R. (2005). Coccidioidomycosis - a fungal disease of the Americas. *PLoS Medicine*, 2(1), e2.

179. Binnicker, M. J., Buckwalter, S. P., Eisberner, J. J., Stewart, R. A., McCullough, A. E., Wohlfiel, S. L., & Wengenack, N. L. (2007). Detection of *Coccidioides* species in clinical specimens by real-time PCR. *Journal of Clinical Microbiology*, 45(1), 173–8.

180. Viriyakosol, S., Fierer, J., Brown, G. D., & Kirkland, T. N. (2005). Innate Immunity to the Pathogenic Fungus *Coccidioides posadasii* Is Dependent on Toll-Like Receptor 2 and Dectin-1. *Infection and Immunity*, 73(3), 1553–1560.

181. Mirbod-Donovan, F., Schaller, R., Hung, C.-Y., Xue, J., Reichard, U., & Cole, G. T. (2006). Urease produced by *Coccidioides posadasii* contributes to the virulence of this respiratory pathogen. Infection and Immunity, 74(1), 504–15.

182. Arsura, E. L., & Hospenthal, D.R. (2005). Coccidioidomycosis (infectious diseases). In: *Medicine, Ob/Gyn, Psychiatry, and Surgery*. *eMedicine Online Textbook, eMedicine World Medical Library*, www.emedicine.com.

183. Bowman, B. H., White, T. J., & Taylor, J. W. (1996). Human pathogenic fungi and their close nonpathogenic relatives. *Mol. Phylogenet. Evol.*, 6:89–96.

184. Koufopanou, V., Burt, A., Szaro, T., & Taylor, J. W. (2001). Gene genealogies, cryptic species, and molecular evolution in the human pathogen *Coccidioides immitis* and relatives (*Ascomycota, Onygenales*). *Mol. Biol. Evol.*, 18:1246– 1258.

185. Pan, S., Sigler, L., & Cole, G. T. (1994). Evidence for a phylogenetic connection between *Coccidioides* immitis and *Uncinocarpus reesii* (Onygenaceae). *Microbiology*, 140:1481–1494.

186. Yu, J.-J., Kirkland, T. N., Hall, L. K., Wopschall, J., Smith, R. C., Hung, C.-Y., & Cole, G. T. (2005). Characterization of a Serodiagnostic Complement Fixation Antigen of *Coccidioides posadasii* Expressed in the Nonpathogenic Fungus *Uncinocarpus reesii*. *Journal of Clinical Microbiology*, 43(11), 5462–5469.

187. Oliveira, M. M. E., Almeida-Paes, R., Gutierrez-Galhardo, M. C., & Zancope-Oliveira, R. M. (2014). Molecular identification of the *Sporothrix schenckii* complex. *Revista Iberoamericana de Micología*, 31(1), 2–6.

188. De Hoog, G. S. (1974). The genera *Blastobotrys*, *Sporothrix*, *Calcarisporium* and *Calcarisporiella* gen. nov. *Studies in Mycology*, 7, 1–84.

189. Fernandes, G. F., dos Santos, P. O., Rodrigues, A. M., Sasaki, A. A., Burger, E., & de Camargo, Z. P. (2013). Characterization of virulence profile, protein secretion and immunogenicity of different *Sporothrix schenckii sensu stricto* isolates compared with *S. globosa* and *S. brasiliensis* species. *Virulence*, 4, 241–249.

190. Lopes-Bezerra, L. M., Schubach, A., & Costa, R. O. (2006). *Sporothrix schenckii* and sporotrichosis. *An. Acad. Bras. Cienc.*, 78, 293–308.

191. Marimon, R., Cano, J., Gené, J., Sutton D. A., Kawasaki, M., Guarro, J. (2007). *Sporothrix brasiliensis*, *S. globosa*, and *S. mexicana*, three new *Sporothrix* species of clinical interest. *J. Clin. Microbiol.*, 45, 3198–3206.

192. Marimon, R., Gené, J., Cano, J., Guarro, J. (2008). *Sporothrix luriei*: a rare fungus from clinical origin. *Med. Mycol.*, 46, 621–625.

193. Marimon, R., Serena, C., Gené, J., Cano, J., & Guarro, J. (2008). In vitro antifungal susceptibilities of five species of *Sporothrix*. *Antimicrob. Agents. Chemother.*, 52, 732–734.

194. Romeo, O., Criseo, G. (2013). What lies beyond genetic diversity in *Sporothrix schenckii* species complex? New insights into virulence profiles, immunogenicity and protein secretion in *S. schenckii sensu stricto* isolates. *Virulence*, 4, 203–206.

195. Arrillaga-Moncrieff, I., Capilla, J., Mayayo, E., Marimon, R., Marine, M., Genis, J., & Guarro, J. (2009). Different virulence levels of the species of Sporothrix in a murine model. *Clinical Microbiology and Infection*, 15(7), 651–655.

196. Howden, B. P., Slavin, M. A., Schwarer, A. P., & Mijch, A. M. (2003). Successful control of disseminated *Scedosporium prolificans* infection with a combination of voriconazole and terbinafine. *European Journal of Clinical Microbiology & Infectious Diseases: Official Publication of the European Society of Clinical Microbiology*, 22(2), 111–3.

197. Solé, A., & Salavert, M. (2009). Fungal infections after lung transplantation. *Current Opinion in Pulmonary Medicine*, 15(3), 243–253.

198. Solé, A., & Salavert, M. (2007). Voriconazol como terapia de las micosis en receptores de Trasplantes de Órganos Sólidos. *Revista Iberoamericana de Micología*, 24(3), 217–222.

199. Cortez, K. J., Roilides, E., Quiroz-Telles, F., Meletiadis, J., Antachopoulos, C., Knudsen, T., & Walsh, T. J. (2008). Infections caused by *Scedosporium* spp. *Clinical Microbiology Reviews*, 21(1), 157–97.

200. Husain, S., Munoz, P., Forrest, G., Alexander, B. D., Somani, J., Brennan, K., & Singh, N. (2005). Infections Due to *Scedosporium apiospermum* and *Scedosporium prolificans* in Transplant Recipients: Clinical Characteristics and Impact of Antifungal Agent Therapy on Outcome. *Clinical Infectious Diseases*, 40(1), 89–99.

201. Troke, P., Aguirrebengoa, K., Arteaga, C., Ellis, D., Heath, C. H., Lutsar, I., & Global Scedosporium Study Group. (2008). Treatment of Scedosporiosis with Voriconazole: Clinical Experience with 107 Patients. *Antimicrobial Agents and Chemotherapy*, *52*(5), 1743–1750.

202. Ingavale, S. S., Chang, Y. C., Lee, H., McClelland, C. M., Leong, M. L., & Kwon-Chung, K. J. (2008). Importance of mitochondria in survival of *Cryptococcus neoformans* under low oxygen conditions and tolerance to cobalt chloride. *PLoS Pathogens*, 4(9), e1000155.

203. Tripathi, K., Mor, V., Bairwa, N. K., Del Poeta, M., & Mohanty, B. K. (2012). Hydroxyurea treatment inhibits proliferation of *Cryptococcus neoformans* in mice. *Frontiers in Microbiology*, 3, 187.

204. Buchanan, K., & Murphy, J. W. (1998). What Makes *Cryptococcus neoformans* a Pathogen? *Emerging Infectious Diseases*, 4(1), 71–83.

205. Alvarez, M., Burns, T., Luo, Y., Pirofski, L., & Casadevall, A. (2009). The outcome of *Cryptococcus neoformans* intracellular pathogenesis in human monocytes. *BMC Microbiology*, 9(1), 51.

206. Charlier, C., Nielsen, K., Daou, S., Brigitte, M., Chretien, F., & Dromer, F. (2009). Evidence of a Role for Monocytes in Dissemination and Brain Invasion by *Cryptococcus neoformans*. *Infection and Immunity*, 77(1), 120–127.

207. Sabiiti, W., Robertson, E., Beale, M. A., Johnston, S. A., Brouwer, A. E., Loyse, A., & Bicanic, T. (2014). Efficient phagocytosis and laccase activity affect the outcome of HIV-associated cryptococcosis. *Journal of Clinical Investigation*, 124(5), 2000–2008.

208. Velagapudi, R., Hsueh, Y.-P., Geunes-Boyer, S., Wright, J. R., & Heitman, J. (2009). Spores as infectious propagules of *Cryptococcus neoformans*. *Infection and Immunity*, 77(10), 4345–55.

209. Fan, W., Kraus, P. R., Boily, M.-J., & Heitman, J. (2005). *Cryptococcus neoformans* Gene Expression during Murine Macrophage Infection. *Eukaryotic Cell*, 4(8), 1420–1433.

210. Alspaugh, J. A., & Granger, D. L. (1991). Inhibition of *Cryptococcus neoformans* replication by nitrogen oxides supports the role of these molecules as effectors of macrophage-mediated cytostasis. *Infection and Immunity*, 59(7), 2291–6.

211. Zugmaier, W., Bauer, R., & Oberwinkler, F. (1994). Mycoparasitism of Some *Tremella* Species. *Mycologia*, 86(1), 49.

212. Vinogradov, E., Petersen, B. O., Duus, J. Ø., & Wasser, S. (2004). The structure of the glucuronoxylomannan produced by culinary-medicinal yellow brain mushroom (*Tremella mesenterica* Ritz.: Fr. (Heterobasidiomycetes) grown as one cell biomass in submerged culture. *Carbohydrate Research*, 339(8), 1483–1489.

213. Wasser, S. P., Elisashvili, V., & Tan, K.-K. (2002). Hypoglycemic, Interferonogenous, and Immunomodulatory Activity of Tremellastin from the Submerged Culture of *Tremella mesenterica* Ritz.: Fr. (Heterobasidiomycetes). *International Journal of Medicinal Mushrooms*, 4(3), 13.

214. Vinogradov, E., Petersen, B. O., Duus, J. O., & Wasser, S. P. (2004). The Isolation, Structure, and Applications of the Exocellular Heteropolysaccharide Glucuronoxylomannan Produced by Yellow Brain Mushroom *Tremella mesenterica* Ritz.: Fr. (Heterobasidiomycetes). *International Journal of Medicinal Mushrooms*, 6(4), 335–346.

ANNEX

15. ANNEX

(OTHER PUBLISHED ARTICLES ABOUT NON-FUNGAL MTs)

A set of papers are presented below in the annex. I have participated widely in these projects which have allowed me to acquire the necessary learning and fluency to work in the field of MTs. It is important to note that these papers have not been included in the primary part of the thesis because it is mainly based on the study of a set of MTs from fungi organisms. The vast amount of results obtained for fungi MTs have allowed completing an extensive thesis work. Nevertheless, there are still some results from both fungi and non-fungi MTs, which will probably be published in a near future by completing and corroborating the current results.

IVYSPRING INTERNATIONAL PUBLISHER

International Journal of Biological Sciences

2015; 11(4): 456-471. doi: 10.7150/ijbs.11060

Research Paper

Hints for Metal-Preference Protein Sequence Determinants: Different Metal Binding Features of the Five Tetrahymena thermophila Metallothioneins

Anna Espart[1], Maribel Marín[2], Selene Gil-Moreno[2], Òscar Palacios[2], Francisco Amaro[3], Ana Martín-González[3], Juan C. Gutiérrez[3], Mercè Capdevila[2] and Sílvia Atrian[1]✉

1. Departament de Genètica, Facultat de Biologia, Universitat de Barcelona, 08028-Barcelona, Spain;
2. Departament de Química, Facultat de Ciències, Universitat Autònoma de Barcelona, 08193-Cerdanyola del Vallès (Barcelona), Spain;
3. Departamento de Microbiología-III, Facultad de Biología, Universidad Complutense, 28040-Madrid, Spain.

✉ Corresponding author: Departament de Genètica, Facultat de Biologia, Universitat de Barcelona, Av. Diagonal 643, 08028-Barcelona, Spain, Phone: +34 934021501, FAX: +34 934034420, E-mail: satrian@ub.edu

Received: 2014.11.14; Accepted: 2015.01.21; Published: 2015.03.18

Abstract

The metal binding preference of metallothioneins (MTs) groups them in two extreme subsets, the Zn/Cd- and the Cu-thioneins. Ciliates harbor the largest MT gene/protein family reported so far, including 5 paralogs that exhibit relatively low sequence similarity, excepting MTT2 and MTT4. In *Tetrahymena thermophila*, three MTs (MTT1, MTT3 and MTT5) were considered Cd-thioneins and two (MTT2 and MTT4) Cu-thioneins, according to gene expression inducibility and phylogenetic analysis. In this study, the metal-binding abilities of the five MTT proteins were characterized, to obtain information about the folding and stability of their cognate- and non-cognate metal complexes, and to characterize the *T. thermophila* MT system at protein level. Hence, the five MTTs were recombinantly synthesized as Zn^{2+}-, Cd^{2+}- or Cu^{+}-complexes, which were analyzed by electrospray mass spectrometry (ESI-MS), circular dichroism (CD), and UV-vis spectrophotometry. Among the Cd-thioneins, MTT1 and MTT5 were optimal for Cd^{2+} coordination, yielding unique Cd_{17}- and Cd_8- complexes, respectively. When binding Zn^{2+}, they rendered a mixture of Zn-species. Only MTT5 was capable to coordinate Cu^{+}, although yielding heteronuclear Zn-, Cu-species or highly unstable Cu-homometallic species. MTT3 exhibited poor binding abilities both for Cd^{2+} and for Cu^{+}, and although not optimally, it yielded the best result when coordinating Zn^{2+}. The two Cu-thioneins, MTT2 and MTT4 isoforms formed homometallic Cu-complexes (major Cu_{20}-MTT) upon synthesis in Cu-supplemented hosts. Contrarily, they were unable to fold into stable Cd-complexes, while Zn-MTT species were only recovered for MTT4 (major Zn_{10}-MTT4). Thus, the metal binding preferences of the five *T. thermophila* MTs correlate well with their previous classification as Cd- and Cu-thioneins, and globally, they can be classified from Zn/Cd- to Cu-thioneins according to the gradation: MTT1>MTT5>MTT3>MTT4>MTT2. The main mechanisms underlying the evolution and specialization of the MTT metal binding preferences may have been internal tandem duplications, presence of doublet and triplet Cys patterns in Zn/Cd-thioneins, and optimization of site specific amino acid determinants (Lys for Zn/Cd- and Asn for Cu-coordination).

Key words: Metallothionein, Functional Differentiation, Metal specificity, Zinc, Copper, *Tetrahymena thermophila*.

Introduction

The massive explosion of Genome and Proteome projects in the last decades demonstrated the wide existence of gene/protein families, instead of single-copy elements, in all types of genomes along the tree of life. A broadly accepted Molecular Evolution principle considers gene duplication events and subsequent specialization of paralogs as the optimal scenario for the acquisition of novel and differentiated

functions, from the unicellular Eukaryote organisms and first Metazoa ([1,2]) up to the Chordates/Vertebrates ([3]). Consequently, the characterization of the protein structure/function relationships in any polymorphic gene/protein system, and precisely the features of the specialized paralogous forms, should shed light to determine the evolutionary determinants that had caused the differentiation of the initially identical duplicates. Unfortunately, in many gene/protein families this basis for paralogous differentiation cannot be analyzed because even the function of every family member is unknown.

Metallothioneins (MTs) are small, ubiquitous, proteins exhibiting an extraordinary Cys content (*ca.* 30 %), which allows them the coordination of heavy-metal ions through the corresponding metal-thiolate bonds ([4,5]). They are polymorphic in practically all the organisms (plants and animals) studied up to now. It is supposed that the diversification of MT isoforms had its origin in successive gene duplication events ([6,7]) occurred independently in different taxa, where they constitute different homology groups. In each case, the MT function may have evolved to serve different molecular metal-related functions, such as essential metal ion homeostasis (Zn^{2+} or Cu^{+}), the defense in front of toxic metal ions (*i.e.* Cd^{2+}, Pb^{2+} or Hg^{2+}), the scavenging of free radicals and ROS, and a wide range of cell stresses ([8,9]). Therefore, MTs are a very useful model to study function (in this case, *metal-binding*) differentiation and specificity. MT isoforms in a given organism exhibit either equivalent or opposite preferences for divalent (Zn^{2+} and Cd^{2+}) *vs.* monovalent (Cu^{+}) metal ion coordination ([5,10]), independently of the degree of their similarity at protein sequence level. At present, there is no clear clue about the molecular determinants of this specificity, a question that is framed in the more global subject of protein/metal interaction specificity in living systems ([11,12]). Sequence/function relationship evolution is best investigated in gene/protein families that simultaneously include highly differentiated members. In the case of MTs, this assumes the coexistence in the same organism of MTs optimized for Zn/Cd-binding (Zn/Cd-thioneins) and for Cu-binding (Cu-thioneins). Significantly, our recent thorough analysis of the MT system in pulmonate gastropod Molluscs (the *Helix pomatia* and *Cantareus aspersus* snails), which consists of highly similar MT paralogs with extreme opposite metal ion binding specialization (Cd *vs.* Cu), revealed that this "metal specificity" lies in their protein sequence attributes and not in other possible factors, such as gene expression inducibility, metal availability, or cell environment ([13]). Precisely, the specific constraints imposed by the coordination geometry of each metal ion should be in accordance with the number and disposition of ligands (*i.e.* thiolate groups or alternative amino acid side chains) in the MT polypeptide sequences. As a consequence, the MT protein synthesis and folding about their cognate metal ions results in a unique, energetically optimized complex, while when taking place about non-cognate metal ions, a mixture of species is produced, none of them representing an energy well conformation, but principally reflecting the amount of metal ions available in its molecular environment ([14]).

The first studies of function and structure in metallothioneins took for granted that the most primitive eukaryotic MTs might have been extremely short peptides of Cu-thionein character, represented nowadays by the fungal *N. crassa* and *A. bisporus* MTs, which evolved to produce all the ß-like domains of MTs in higher Eukaryotes, including Vertebrates ([15]). Since then, this hypothesis has been superseded by multiple experimental evidence, among which the molecular characterization of the *Tetrahymena* (Ciliophora, Protozoa) MT system in several species of the genus offers a most striking example. In fact, *Tetrahymena* MTs are among the longer MTs reported (up to 191 amino acids) and include MTs classified both as Cd-thioneins (Family 7a in the Kägi's classification ([16])), and as Cu-thioneins (Family 7b) ([17,18]), while the evolutionary origin of Ciliates has been proposed for around 10^9 years ago, thus, notably before the emergence of fungi and other major eukaryotic lineages ([19]). These features triggered a more extensive study of the MT system in different *Tetrahymena* species in terms of molecular evolution and differentiation (*T. thermophila* ([20,21,22,23,24]), *T. pigmentosa* ([20,25,26,27,28]), *T. pyriformis* ([25,29,30,31]), *T. rostrata* ([32]), *T. tropicalis lahorensis* ([33,34,35]) and lately *T. hegewischi, T. malaccensis* and *T. mobilis* ([36])), all of them exhibiting a high degree of polymorphism. At this point, it is worth remembering that the classification of a given MT peptide as Zn/Cd- or Cu-thionein can be performed according to three different criteria, that logically converge in their results: gene expression inducibility, protein sequence similarity, and protein metal-binding behavior ([37]). The wealth of information gathered from the above mentioned literature refers almost exclusively to the first two criteria. Hence, on the one hand, all the reported *Tetrahymena* MTs have been so far classified according to the type of metal ion that provokes or enhances the expression of its gene, and the promoter response to different metals and stresses has been deeply characterized, also in view of biotechnological applications ([38,39,40,41,42]). On the other hand, the origin, relationships and evolution of the corresponding protein sequences has been the object of deep and

thorough analyses that have revealed close internal relationships in the Cd- and Cu-thioneins clades, as well as an interesting modular organization of the MT Cd-thionein sequences showing their more than probable origin from tandem duplications of primeval amino acid stretches ([17,18]). However, it is striking that studies on the third criterion, *i.e.* metal binding behavior or metal preference, are almost absent. Hence, only the metal ion binding features of the *T. pyriformis* MT1 isoform were shown in full concordance with its Cd-thionein character ([43]), and a partial attempt to compare the *T. thermophila* MTT1 and MTT2 isoforms has been recently published ([44]).

Thus, to fill the gap of protein functional studies on *Tetrahymena* MTs, we present here the full characterization of the Zn-, Cd- and Cu-binding abilities of the five *T. thermophila* MT isoforms (named MTT1 to MTT5 ([17]), *cf.* Figure 1 for polypeptide features). The MTT1, MTT3 and MTT5 Cd-thioneins exhibit Cys patterns typical of MTs (XCCX, CXC, XXCXX), and also some atypical Cys arrangements, such as CCC, CXCC, and CXCXC, while the MTT2 and MTT4 isoforms only enclose typical CXC motifs. Comprehensive interpretation of our results, obtained from the spectrometric and spectroscopic analyses of the recombinantly synthesized, as well as *in vitro*-reconstituted, metal-MTT complexes confirm that the MTT1 and MTT5 isoforms are optimized for divalent metal binding, MTT2 and MTT4 forms behave as clear Cu-thioneins and MTT3 shows an undefined behavior. However, clear differences can be defined among the coordination abilities of the five isoforms. This allows some relationships between the metal preference traits and the amino acid composition of the *Tetrahymena* MTs to be proposed, which will contribute to the understanding of the factors determining metal preference in proteins. Finally, the correspondence of a modular sequence structure, as proposed for the Cd-isoforms, and the metal clusters formed, is examined. Overall, it remains clear that from the first steps of the eukaryotic world, two complementary forces have driven the evolution of metallothioneins: a qualitative one, for metal specificity; and a quantitative one, to enlarge the metal binding capacity of a basic peptide fragment. This resulted in protein lengthening by internal tandem repeats (as the case of *Tetrahymena*, or the recently reported fungal MTs (*cf. C. neoformans* Cu-thioneins ([45,46])), or in entire gene duplication events, as is reported for *S. cerevisiae* Cup1 ([47]).

A

```
MTT2  GSMDT-----------------------------------QTQTKVTVGCSCNPCKCQPLCKCGTTAACNCQPCEN-------------
MTT4  GSMDT-----------------------------------QTQTKVTVGCSCNPCKCQPLCKCGTTAACNCQPCEN-------------
MTT5  GSMDKIS----GESTKICSKTEEKWCCCPSETQNCCNSDDKQCCVGSGEGCIYVCCKCCK-----------------------------
MTT1  GSMDKVNSCCCGVNAKPCCTDPNSGCCCVSKTDNCCKSDTKECCTGTGEGCKCVNCKCCKPQANCCCGVNAKPCCFDPNSGCCCVSKTNN
MTT3  GSMEKINNSCCGENTKICCTDLNRQCNCACKTDNCCKPETNECCTDTLEGCKCVDCKCCKSHVTCCHGVNVKSSCLDPNSGYQCASKTDN

MTT2  CDPCSCNPCKCGATESCGCNPCKCAE-----CKCGSHTE-----KTSACKCNPCACNPCNCGSTSNCKCNPCKCAECKC
MTT4  CDPCSCNPCKCGATESCGCNPCKCAE-----CKCGSHTE-----KTSACKCNPCACNPCKCGSTSNCKCNPCKCAECKC
MTT5  --------------------------VQAECKCGPNAKYCCIDPNTGNCCVCKTKFCSKSDSKECCPGGSC
MTT1  CCKSDTKECCTGTGEGCKCTSCQCCKPVQQGCCCGDKAKACCTDPNSGCCCSNKANKCCDATSKQECQTCQCCK
MTT3  CCKSDTKECCTGTQEGCKCTNCQCYKQAQQGCCCGDKAKACCTDPNSGCCCSNKANKCCDATSKKECQVCQCCK
```

B

	subfamily	NCBI reference sequence	length	Cys	Met	His	Cys triplets	Cys doublets	Single Cys
MTT1	7a (Cd-thionein)	XP_001024888.1	162 aa	48	1	0	6	11	8 (7 in CXC motives)
MTT3	7a (Cd-thionein)	XP_001024889.1	162 aa	42	1	2	2	11	14 (11 in CXC motives)
MTT5	7a (Cd-thionein)	XP_001020086.1	99 aa	24	1	0	1	7	7 (3 in CXC motives)
MTT2	7b (Cu-thionein)	AAQ55281.1	108 aa	32	1	1	0	0	32 (30 in CXC motives)
MTT4	7b (Cu-thionein)	XP_001011379.1	108 aa	32	1	1	0	0	32 (30 in CXC motives)

Figure 1. (A) Multiple sequence alignment (Clustal Omega) of the five *Tetrahymena thermophila* MT isoforms. The Cys residues are in grey. The unique amino acid substitution between MTT2 and MTT4 is marked in bold. The Glu (Q) residues encoded by mutated codons are marked in bold italics. The initial GS residues (in italics) result from the recombinant synthesis rationale. (B) Comparison of the main sequence features of the five *Tetrahymena thermophila* MT isoforms.

Materials and Methods

Construction of MTT cDNAs and *E.coli* expression vectors.

The cDNAs corresponding to the five *T. thermophila* MT isoforms were obtained by mRNA retrotranscription, from cultures previously treated with Cd^{2+} (27 μM), Zn^{2+} (870 μM) or Cu^{2+} (80 μM) for 1h, and subcloned in PCR2.1-TOPO-TA vectors (Invitrogen), as previously reported ([17]). Since in *Tetrahymena* nuclear genes, the TAA and TAG triplets encode a glutamine instead of being stop codons (as in the Universal Gene Code) ([48]), the cDNAs of the MTT1, MTT3 and MTT5 isoforms had to be site-directed-mutated before cloning in the bacterial expression plasmid (pGEX-4T1). MTT2 and MTT4 cDNAs include no TAA or TAG codons, thus they could be directly subcloned. Two different site-directed-mutagenesis methods were used, owing to the different location of the bases to be mutated inside the cDNA length; hence the MTT1 and MTT5 cDNAs were mutated through Megaprimer PCR reactions ([49]) and the QuickChange Lightning Multi Site-Directed Mutagenesis Kit (Agilent Technologies) was used for the MTT3 cDNA mutagenesis. In all cases the T position of the TAA and TAG codons was changed to C, the CAA and CAG codons encoding Gln in the Universal Genetic Code.

In the MTT1 cDNA, four TAA (encoding Gln110, Gln116, Gln117 and Gln159) and one TAG (encoding Gln156) triplets were present. The first PCR amplified a MTT1 cDNA fragment which included the five target codons, by using as primer oligonucleotides: 5′AAATGTACAAGTTGCCAATGCTGCAAACCTGT TCAACAAGGATGTTGTTGTG-3′ (forward) and 5′-GGAACTCGAGTCATTTACAACATTGACAAGT CTGACACTCTTGCTTTGA-3′ (reverse). An *Xho*I restriction site (underlined) was added to the reverse primer for cloning purposes. 30-cycle amplification reactions were performed with a thermo-resistant Taq DNA polymerase (Expand High Fidelity PCR System, Roche) under the conditions: 2 min at 94 °C (initial denaturation), 15 s at 94°C (denaturation), 30 s at 57°C (annealing) and 30 s at 72°C (elongation). The second PCR reaction was required to amplify the whole cDNA sequence of MTT1, using a new oligonucleotide 5′-GGGGAGGATCCATGGATAAAGTTAATA GC-3′ (forward) and the product of the first PCR (reverse) as primers. Now, the *BamH*I restriction site (underlined) was added to the forward primer for cloning purposes. The 30-cycle amplification reactions were performed with the same Taq DNA polymerase as before, under the conditions: 2 min at 94°C (initial denaturation), 15 s at 94°C (denaturation), 30 s at 52°C (annealing) and 30 s at 72°C (elongation).

The MTT5 cDNA included only one TAA (encoding Gln36) that had to be mutated. Here, the first PCR amplified a MTT5 cDNA fragment using as primers: 5′-GCCGGGGATCCATGGATAAAATTTC TGGTGA-3′ (forward *BamH*I site underlined) and 5′-TCTCCTGAACCGACACAACATTGTTTATCATC AGAATTGCAGCAA-3′ (reverse). The 30-cycle amplification reactions were performed with the same Taq DNA polymerase as for MTT1, under the following conditions: 2 min at 94°C (initial denaturation), 15 s at 94°C (denaturation), 30 s at 57°C (annealing) and 30 s at 72°C (elongation). The second PCR was performed using the product of the previous PCR as forward megaprimer and the oligonucleotide 5′-AAAAGCTCGAGTCAGCAACTACCTCCAGGGC -3′ (*Xho*I restriction site underlined) as reverse primer. The procedure and reagents in the second PCR were the same as for the first reaction.

As mentioned before, the MTT3 cDNA was mutagenized by using the QuickChange Lightning Multi Site-Directed Mutagenesis Kit (Agilent Technologies), because the location of the involved codons (one TAG, encoding Glu81) and four TAA (encoding Gln102, Gln111, Gln117, Gln118 and Gln159)) made it impossible to use the megaprimer strategy. Four oligonucleotides were required to introduce the desired mutations: *ol-1:* (to mutate the T nucleotide in the 159-TAA triplet) 5′-ACTTCAAAGAAAGAGTG TCAGGTATGTCAATGTTGTAAATGA-3′;

ol-2: (to mutate the T nucleotide in the 111-, 117- and 118-TAA triplet) 5′-CACTAATTGTCAATGC TACAAACAAGCTCAACAAGGATGTTGTTG-3′;

ol-3: (to mutate the T nucleotide in the 102-TAA triplet) 5′-CTAAAGAATGTTGTACTGGCACTCAA GAAGGATG-3′; and *ol-4:* (to mutate the T nucleotide in the 81-TAG triplet) 5′-TTAGATCCAAATA GTGGATATCAGTGTGCAAGTAAAACTG-3′. The 30-cycle amplification reactions were performed following the kit instructions: 20 s at 95°C (initial denaturation), 30 s at 55°C (annealing) and 30 s at 65°C (elongation). Finally, an additional PCR reaction added the suitable restriction sites for cloning into the expression vector (*BamH*I in forward and *Xho*I in reverse, underlined), to the fully mutated cDNA product. The designed primers were: 5′-GGGAAGGATCCATGGAAAAAATTAATAAC-3′ (forward) and 5′-GGGGACTCGAGTCATTTACA ACATTGACA-3′ (reverse) and the PCR conditions were the same as before.

The MTT2 and MTT4 cDNA sequences were directly amplified using the following oligonucleotides as primers: 5′- GGGGAGGATCCATGGACACTCA-3′ (forward) and 5′-GAAACTCGAGTCAGCATTTGC ATT-3′ (reverse) for MTT2; and 5′-GGGGAGGA TCCATGGACACCCA-3′ (forward) and 5′-GGGG

ACTCGAGTCAGCATTTGC-3′ (reverse) for MTT4. These primers introduced the 5′ *BamH*I and 3′ *Xho*I restriction sites required for subsequent subcloning. The PCR conditions and reagents were the same as before.

In all cases, the final PCR products were analyzed by 1% agarose gel electrophoresis and the expected bands were excised and purified (Genelute™ Gel Extraction Kit, Sigma Aldrich) to be subcloned into the *BamH*I/*Xho*I sites of the pGEX-4T1 *E.coli* expression vector (GE Healthcare) by ligation using the DNA Ligation Kit 2.1 (Takara Bio Inc.). The recombinant vectors were transformed into *E. coli MachI* strains. All the mutated MTT cDNAs were sequenced before expression, using the Big Dye Terminator 3.1 Cycle Sequencing Kit (Applied Biosystems). The recombinant clones were then transformed into BL21 *E. coli* protease deficient cells for GST-MTT fusion protein synthesis.

Synthesis and purification of recombinant and *in vitro*-constituted metal-MTT complexes.

5-l Luria-Bertani (LB) cultures of the transformed BL21 *E. coli* strains were the source of recombinant metal-MTT complexes. Gene induction was switched on with 100 µM (final concentration) of isopropyl β-D-thiogalactopyranoside (IPTG) 30 min before the addition of the suitable metal supplement (300 µM $ZnCl_2$, 300 µM $CdCl_2$ or 500 µM $CuSO_4$, final concentrations) to allow the synthesis of the corresponding metal complex. The cultures grew for 3 h, and in the case of Cu-supplementation, cultures were aerated to obtain either a normal oxygenation (1-l of LB media in a 2-l Erlenmeyer flask at 250 rpm) or a low oxygenation (1.5-l of LB media in a 2-l Erlenmeyer flask at 150 rpm), since this condition highly determines the level of intracellular copper in the host cells, as described in [50]. It is worth noting that to prevent oxidation of the metal–MTT complexes, argon was bubbled in all the subsequent steps of the purification protocol. The 2.5-h cultures were centrifuged and the recovered cell mass was resuspended in ice-cold PBS (1.4 M NaCl, 27 mM KCl, 101 mM Na_2HPO_4, 18 mM KH_2PO_4)-0.5% v/v β-mercaptoethanol, and disrupted by sonication. The total protein extract was obtained in the supernatant of a 12,000 x*g*, 30 min centrifugation, which was then incubated with Glutathione-Sepharose 4B (GE Healthcare) beads at gentle agitation for 1 h at room temperature, for GST–MTT purification by batch affinity chromatography. After three washes in PBS, the GST-MTT proteins were digested with thrombin (10 u per mg of fusion protein, overnight at 17 °C) to separate the metal-MTT complexes from the GST fragment, which remains bound to the gel matrix. The recovered solution was concentrated using Centriprep 3 kDa cut-off Microcons (Amicon) and finally fractionated through a Superdex-75 FPLC column (GE Healthcare) equilibrated with 50 mM Tris-HCl, pH 7.0, and run at 0.8 ml min^{-1}. Aliquots of the protein-containing fractions were identified by their absorbance at 254 and 280 nm, and later analyzed in 15% SDS-PAGE gels stained with Coomassie Blue. MTT-containing samples were pooled and stored at -80 °C until further use. Due to the pGEX recombinant expression system specificities, the five synthesized MTT isoforms contained two additional residues (Gly-Ser) as their N-termini, but these amino acids have been shown not to alter the MT metal-binding features ([51]). Further details about the synthesis and purification procedures can be found in our previous publications ([51, 52]).

The so-called "*in vitro* complexes", to differentiate them from the "*in vivo*" recombinantly synthesized complexes, were prepared *via* metal replacement by adding the corresponding metal ions (Cd^{2+} or Cu^{+}) to the recombinant Zn-MTT samples. These reactions were performed at pH 7.0 following the procedures previously reported for mammalian MTs ([52, 53]). Characterization of the *in vitro* complexes was performed by UV–Vis and CD spectroscopies, as well as ESI-MS analysis, as explained below for the recombinant complexes. All assays were carried out in an Ar atmosphere, and the pH remained constant throughout all the experiments, without the addition of any extra buffers.

Spectroscopic characterization of the metal-MTT complexes

The S, Zn, Cd and Cu content of all the metal-MTT preparations was analyzed by Inductively Coupled Plasma Atomic Emission Spectroscopy (ICP-AES), using a Polyscan 61E (Thermo Jarrell Ash) spectrometer, measuring S at 182.040 nm, Zn at 213.856 nm, Cd at 228.802 nm, and Cu at 324.803 nm. Samples were routinely treated as reported in [54]. Alternatively their incubation in 1 M HCl at 65 °C for 15 min prior to analyses allowed the elimination of labile sulfide ions [55]. Protein concentrations were calculated from the ICP-AES sulfur measurement, assuming that all S atoms were contributed by the MTT peptides. CD spectra were recorded in a Jasco spectropolarimeter (Model J-715) interfaced to a computer (J700 software), where a 25 °C temperature was maintained constant by a Peltier PTC-351S equipment. Electronic absorptions measurements were performed on an HP-8453 Diode array UV-visible spectrophotometer. 1-cm capped quartz cuvettes were used to record all the spectra, which were corrected for the dilution effects and processed using the GRAMS 32 program.

ElectroSpray ionization mass spectrometry (ESI-MS) analyses of the metal-MTT complexes

Electrospray ionization time-of-flight mass spectrometry (ESI-TOF MS) was performed on a Micro TOF-Q instrument (Bruker) interfaced with a Series 1200 HPLC Agilent pump, equipped with an autosampler, all of which controlled by the Compass Software. The ESI-L Low Concentration Tuning Mix (Agilent Technologies) was used for equipment calibration. For the analysis of Zn- and Cd-MTT complexes, samples were run under the following conditions: 20 µl of protein solution injected through a PEEK (polyether heteroketone) tubing (1.5 m x 0.18 mm i.d.) at 40 µl min^{-1}; capillary counter-electrode voltage 5 kV; desolvation temperature 90-110 °C; dry gas 6 l min^{-1}; spectra collection range 800-2500 m/z. The carrier buffer was a 5:95 mixture of acetonitrile:ammonium acetate (15 mM, pH 7.0). Instead, the Cu-MTT samples were analyzed as follows: 20 µl of protein solution injected at 40 µl min^{-1}; capillary counter-electrode voltage 3.5 kV; lens counter-electrode voltage 4 kV; dry temperature 80 °C; dry gas 6 l min^{-1}. Here, the carrier was a 10:90 mixture of acetonitrile:ammonium acetate, 15 mM, pH 7.0. Acidic-MS conditions, which causes the demetalation of the peptides loaded with divalent metal ions, but keeps the Cu^+ ions bound to the protein, were used to generate the apo-MTT forms and to analyze the Cu-containing MTT samples. For it, 20 µl of the preparation were injected under the same conditions described previously, but using a 5:95 mixture of acetonitrile:formic acid, pH 2.4, as liquid carrier. For all the ESI-MS results, the error associated with the mass measurements was always inferior to 0.1%. Masses for the holo-species were calculated according the rationale previously described ([56]).

Results and Discussion

MTT1 to MTT5 peptide identity and classification

The MTT1 to MTT5 cDNAs constructed by site-directed mutagenesis according to the standard genetic code were confirmed by DNA sequencing. In total, nine TAA and two TAG triplets (coding for Gln in *Tetrahymena* and Stop in the standard genetic code) had been replaced by CAA and CAG codons: five in MTT1, five in MTT3, and one in MTT5 (protein positions indicated in Figure 1). SDS-PAGE analyses of total protein extracts from BL21 cells transformed with each one of the pGEX-MTT plasmids revealed the presence of bands corresponding to the expected GST-MTT sizes (data not shown). Homogeneous metal-MTT complex preparations were obtained from 5-l *E. coli* cultures at final concentrations varying in the 10^{-4} M range, as detailed in Table 1. Firstly, Zn-MTT and Cd-MTT aliquots were acidified to pH 2.4 to verify the molecular weight of the corresponding apo-forms, since this acid pH conventionally results in demetalation of the complexes formed by MTs and divalent metal ions. Some unusual results were already obtained at this stage. Since it was impossible to recover the corresponding Zn- or Cd-complexes for MTT2, no apo-MTT2 could be characterized. Nevertheless, the coherent results obtained for the Cu-MTT2 species (which will be analyzed in a following section) led to assuming the correct identity and integrity of the MTT2 peptide. For MTT4 and MTT5, the molecular masses of the acidified samples were in accordance with the expected values calculated from their respective amino acid sequences (Figure 1 and Table 1). Strikingly, the MTT1 and MTT3 isoforms, those first classified as Cd-thioneins according to gene induction criteria, yielded both Zn- and Cd-complexes that were extremely resistant to demetalation (Figure 2 and Table 1). Hence, the Zn-MTT1 preparation acidified to pH 2.4 yielded a mixture of almost equimolar apo-MTT1 and Zn_4-MTT1 forms, while in the acidified Cd-preparations, a major Cd_{12}-MTT1 and minor Cd_{11}-MTT1 were detected. In contrast, the Zn-MTT3 complexes exhibited the usual complete demetalation at pH 2.4, yielding an apo-form with the expected molecular weight, and only the Cd-MTT3 preparation was reluctant to yield the corresponding apo-form, yielding Cd_8-MTT3 complexes instead (Figure 2). Since the Cys content of MTT1 (48 Cys/162 aa) is considerably higher than that of MTT3 (42 Cys/162 aa) it is sensible to hypothesize that the resistance to acid demetalation exhibited by the Cd-MTT1 in relation to the Cd-MTT3 complexes may be related to the capacity of the former to fold into a more compact cluster, which would be stabilized by a higher number of Cd-thiolate bonds, the Cd content of both, Cd-MTT1 and Cd-MTT3, being roughly equivalent (*cf.* Table 2). Also the fact that, for both isoforms, the Zn species are more prone to demetalation than the Cd species is concordant with the higher strength of Cd-thiolate than Zn-thiolate bonds. These results suggest that the Cd-MTT1 and Cd-MTT3 complexes include highly stable Cd-SCys cores, which are formed by coordination of 4, or multiples of 4, Cd^{2+}, and that the bound Cd^{2+} ions are only released under harsh acidification conditions. Therefore, the incubation of the Zn-MTT1, Cd-MTT1, and Cd-MTT3 preparations with increasing strength of formic acid (final pH of 1.82) yielded the expected apo-MTT1 and apo-MTT3 polypeptides, as shown in both cases by the single ESI-MS peak corresponding to the expected molecular size (Figure 2).

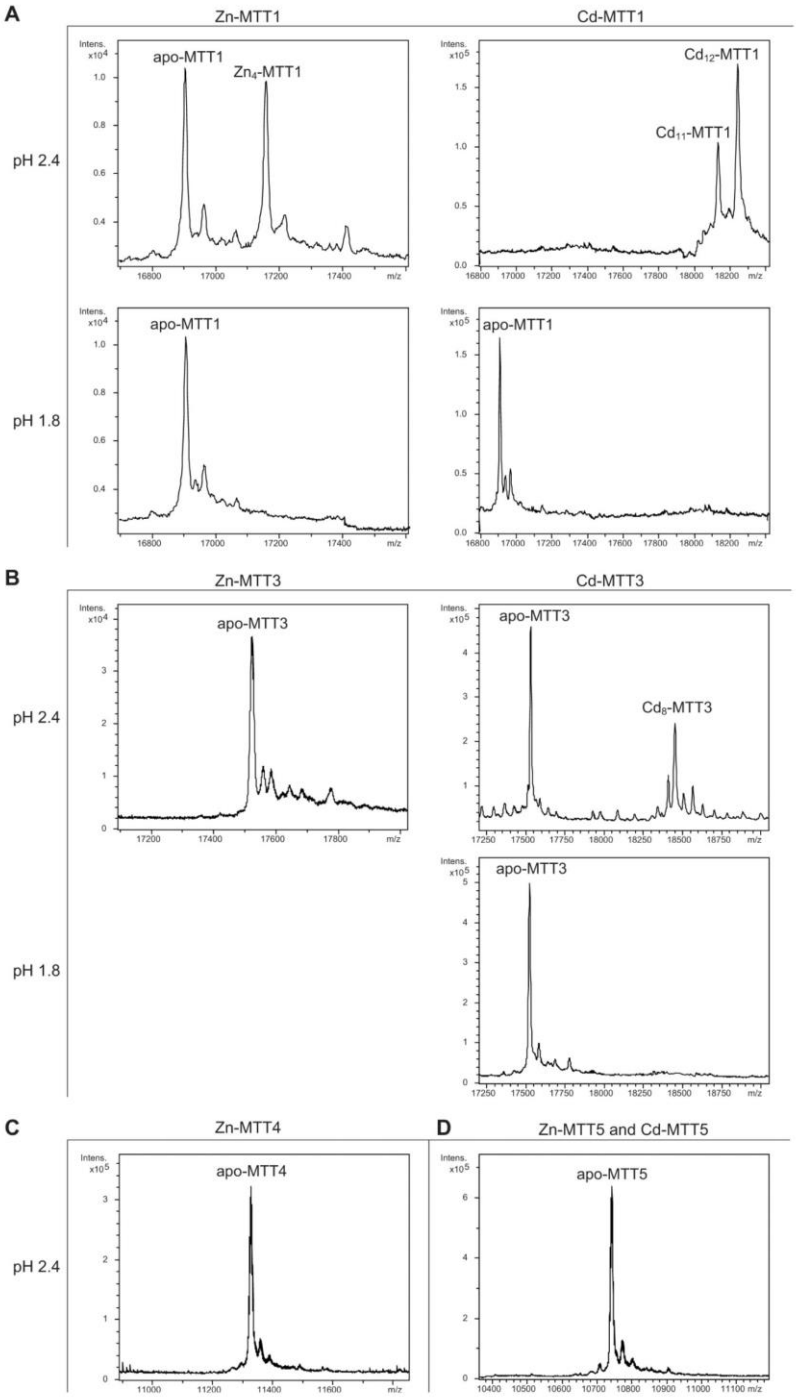

Figure 2. Deconvoluted ESI-MS spectra of the demetalated Zn- and Cd-MTT complexes, recorded at acidic pH. The spectra correspond to the demetalated preparations in Zn- and/or Cd-enriched cultures of (A) MTT1, (B) MTT3, (C) MTT4, and (D) MTT5. For those isoforms that were resistant to demetalation, the ESI-MS was run at pH 2.4 and pH 1.8.

Table 1. General features of the recombinant MTT syntheses. Total protein yield of the recombinant metal-MTT preparations. The molecular weight of the acidified (pH 2.4) Zn-, and Cd- MTT preparations compared to the expected theoretical MW of the respective apo-MTT polypeptides.

	[MT][a] (mg per L of culture)			Molecular Weight (Da)		
Isoform	Zn supplemented in culture	Cd supplemented in culture	Cu supplemented in culture	Acidified (pH 2.4) Zn- and Cd-complexes[b]	Acidified (pH 1.8)	Theoretical value for the apoforms
MTT1	1.21-1.62	2.55	0.54	16903.0 + Zn_4-MTT1 Cd_{12}->Cd_{11}-MTT1	16903.0 16903.0	16901.5
MTT2[c]	---	---	0.32-3.15	---	---	11316.0
MTT3	1.90-2.27	6.31-7.36	0.11	17530.0 Cd_8-MTT3	17530.0 17530.0	17529.9
MTT4	0.49-1.47	0.21	0.32-1.14	11328.0	---	11330.1
MTT5	1.67	1.72-2.36	0.86-2.40	10739.6	---	10741.4

a The values were calculated from the sulphur content in normal ICP-AES measurements.
b Acidification of complexes with divalent metal ions commonly renders the demetalated polypeptides, as observed for MTT3, MTT4 and MTT5. The cases of MTT1 and MTT3 are fully commented in the text.
c MTT2 failed to yield Zn- and Cd-complexes.

Table 2. Summary of the metal-to-protein-stoichiometries found in the recombinant metal-MTT preparations.

MT Isoform	Zn supplemented in culture	Cd supplemented in culture	Cu supplemented in culture (normal aeration)	Cu supplemented in culture (low aeration)
MTT1	Zn_{17}- Zn_{16}-, Zn_{18}-	**Cd_{17}-** Cd_{12}-	---	---
MTT3	**Zn_{12}-** **Zn_{11}-, Zn_{13}-** Zn_{10}-, Zn_{14}-	**$Cd_{15}S$-, $Cd_{16}S$-,Cd_{18}-** several Cd_X- and Cd_yS-	**Zn_x(Cu_8, Cu_4, Cu_{12})**	---
MTT5	**Zn_6-, Zn_5-** Zn_7-, Zn_4- Zn_8-, Zn_3-	**Cd_8-** Cd_9-	**M_{12}-** M_9-, M_8- Zn_x(Cu_8, Cu_9, Cu_{12})	**(Cu_8, Cu_4)**
MTT2	---	---	**Cu_{20}-** Cu_{16}- Zn_5Cu_{12}-	**Cu_{20}-** Cu_{23}- Cu_{21}-, Cu_{22}-
MTT4	**Zn_{10}-** Zn_{11}-, Zn_9- Zn_{12}-, Zn_8-	---	**M_{16}-, M_{13}-** Zn_x(Cu_8, Cu_4, Cu_{12})	**Cu_{20}-** Cu_{23}-, Cu_{24}- Cu_{21}-, Cu_{22}-

Major species are highlighted in bold. (---) means that neither protein nor metal complexes were recovered.

Zn-, Cd- and Cu-binding abilities of the Cd-MTT isoforms (family 7a): MTT1, MTT3 and MTT5

The metal binding abilities of the *T. thermophila* MTs previously described as Cd-thioneins (*i.e.* family 7a, including MTT1, MTT3 and MTT5) ([17]) were studied using ESI-MS and spectroscopic characterization of their corresponding recombinant Zn^{2+}, Cd^{2+} and Cu^{+}-complexes (Figure 3 and 4, respectively).

MTT1 could only be recovered from Zn^{2+}- and Cd^{2+}-supplemented cultures, this pointing to a complete inability of the protein for folding *in vivo* into stable Cu-complexes. MTT1 yielded a major Zn_{17}-MTT1, together with minor Zn_{18}-, Zn_{16}- and other much minor complexes of lower and higher stoichiometry, when synthesized in the presence of Zn^{2+} (Table 2, Figure 3). Conversely, an almost unique peak was detected as the result of the synthesis by Cd^{2+}-enriched bacteria, which corresponded to Cd_{17}-MTT1, accompanied only by a very minor Cd_{12}-complex, in total coincidence with the major Zn_{17}- stoichiometry found for the Zn-MTT1 preparation (Table 2, Figure 3). Interestingly, although both syntheses yielded major M_{17} complexes, their CD fingerprints are quite different, and reflect the nature of the samples. Zn-MTT1 shows a practically featureless CD envelope, mainly contributed by the protein, and where the absorptions expected at *ca.* 240 nm for the $Zn(SCys)_4$ chromophores are not perceptible, it is probably as a consequence of the mixture of coexisting species. Conversely, Cd-MTT1 gives rise to a very intense CD spectrum with maxima at 245(+) and 260(-) that can be attributed to the major Cd_{17}-MTT1 species. This fingerprint could be contributed by a Gaussian band centered at the characteristic wavelength of the $Cd(SCys)_4$ chromophores, 250 nm, and an exciton coupling at the same wavelength. The presence of two types of Cd-thiolate entities could be hypothesized, so that perhaps the exciton coupling signal arises from the Cd_{12} "robust cluster", while the remaining Cd-SCys units forming the Cd_{17}-MTT1 complex just generate a Gaussian band in the spectrum. Finally, it is worth noting that the results reported here are highly consistent with the stoichiometric data recently reported after apo-MTT1 metal reconstitution experiments, which showed the formation of Cd_{16}-MTT1 ([44]), and the theoretical Cd_{17} maximum capacity, estimated from the available coordinating Cys residues of the polypeptide ([18]).

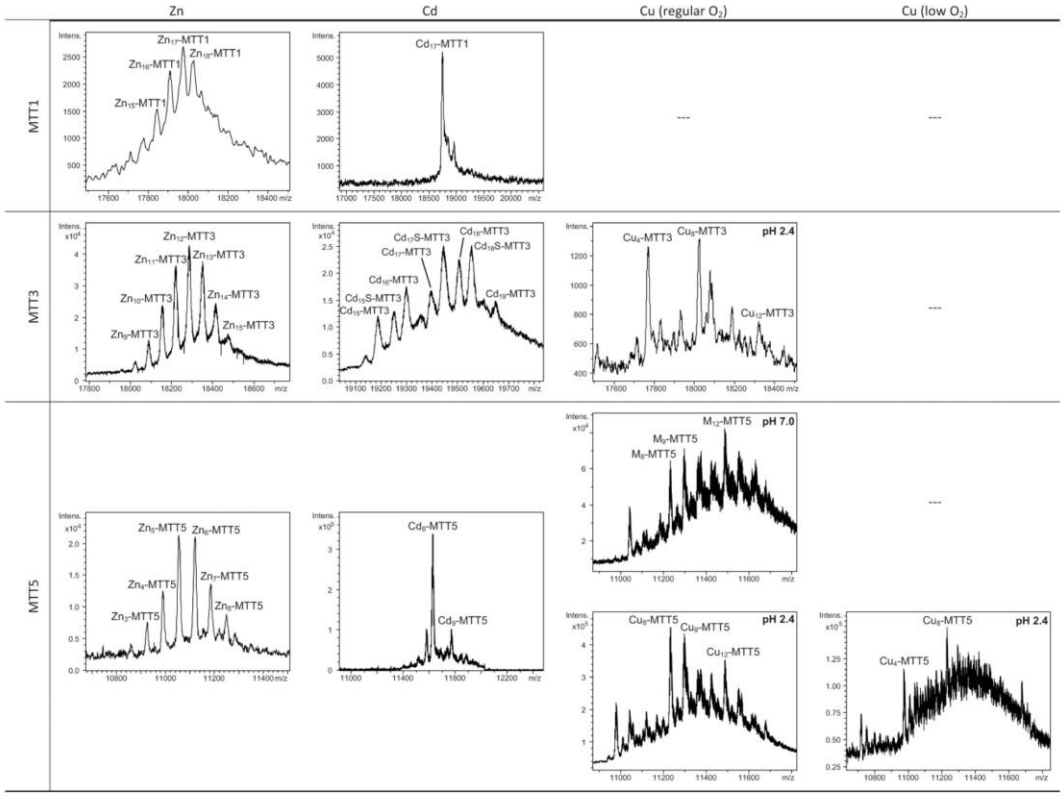

Figure 3. Deconvoluted ESI-MS spectra of the recombinant preparations of MTT1, MTT3 and MTT5. The metal-MTT complexes were synthesized in recombinant cultures supplemented with Zn, Cd, or Cu, and in the case of Cu-enriched media, the synthesis was carried out under regular and low aeration conditions. (---) denotes that no metal-MTT complexes could be purified from the corresponding cultures.

MTT3 could be recovered from Zn^{2+}, Cd^{2+} and also Cu^{2+}-supplemented cultures, but the latter only if they had been grown under normal aeration (normal cell Cu content), so that high Cu may be assumed to preclude the folding into stable complexes. Synthesis of MTT3 in Zn-supplemented *E. coli* cells yielded a mixture of species ranging from major Zn_{12}-MTT3 complexes to minor Zn_9- to Zn_{15}-MTT3 species (Table 2, Figure 3), and this sample showed a CD spectrum such as that expected for an apo-MT, *i.e.* a silent to CD above 250 nm (Figure 4), once again reflecting the mixture of species in the sample. Although this multiplicity of Zn species resembled the behavior of MTT1, MTT3, unlike the former isoform, also yielded a mixture of complexes when synthesized under Cd supplementation, which, most significantly, included sulfide-containing species as major components (Table 2, Figure 3). Hence, $Cd_{16}S$-, $Cd_{15}S$-, and Cd_{18}-MTT3 were predominant, but $Cd_{13}S$-, $Cd_{14}S$-, Cd_{15}-, Cd_{16}-, Cd_{17}- and Cd_{19}-MTT3 were also clearly identifiable. The presence of sulfide-containing species was confirmed by the corresponding ICP measurements, in which the S content proved to be significantly different depending on whether or not the sample had been subjected to acid treatment prior to analysis (data not shown). Additionally, the recombinant Cd-MTT3 sample exhibited a CD profile very similar to that of the Cd-MTT1 preparation, but the latter including the typical absorption of the $Cd\text{-}S^{2-}$ binding motifs absorbing at *ca.* 280 nm(-) (Figure 4). The synthesis in Cu^{2+}-supplemented media also yielded poor results, consisting of heterometallic complexes (ICP-AES results of almost equimolar Zn:Cu content) where only Cu_8- and Cu_4- and minor Cu_{12}- cores were stable enough to resist ESI-MS analysis conditions. Furthermore, these complexes were invariably CD silent at the metal-to-protein transition wavelength range (*cf.* Table 2, Figures 3 and 4). Therefore, MTT3 had a very atypical behavior, since it yielded mixtures of species with the three assayed metal ions.

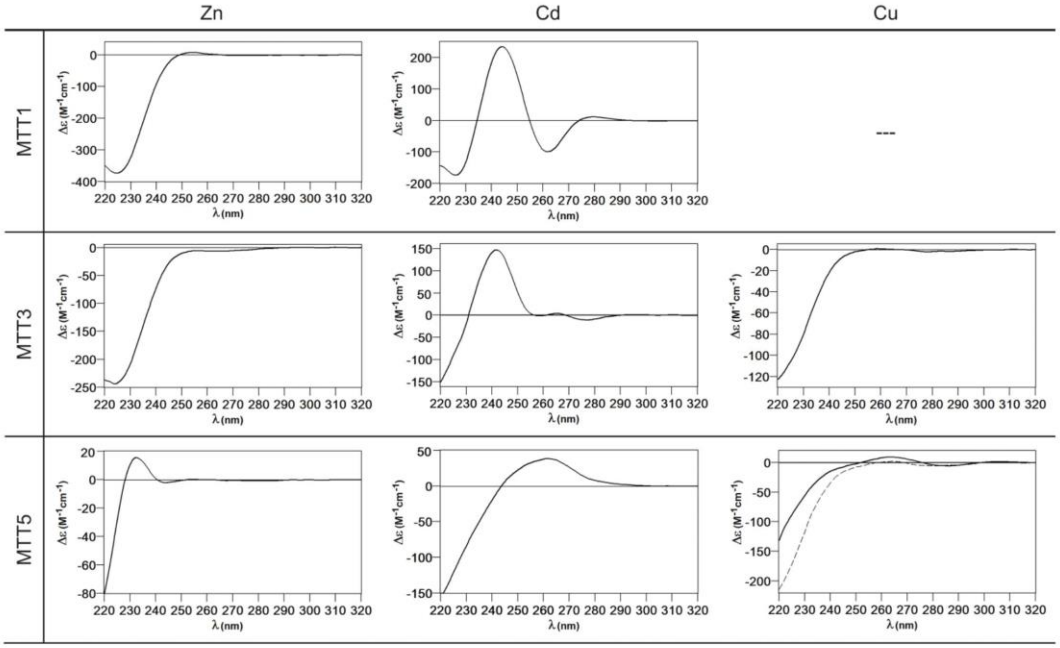

Figure 4. Circular dichroism spectra of the recombinant preparations of MTT1, MTT3 and MTT5. The metal-MTT complexes were synthesized in recombinant cultures supplemented with Zn, Cd, or Cu, and in the case of Cu-enriched media, the synthesis was carried out under regular (solid line) and low aeration (dashed line) conditions.

Finally, MTT5 results were significantly interesting, because it was the unique isoform that yielded stable complexes with the three metal ions analyzed, although the better results for Zn^{2+} and Cd^{2+} than for Cu^{+} confirmed their classification as a 7a-subfamily MT. In view of this special behavior, the *in vitro* Zn/Cd and Zn/Cu replacement reactions were studied for this isoform. The recombinant synthesis of MTT5 in Zn-enriched bacteria yielded two major Zn species (Zn_6- and Zn_5-MTT5, as revealed by ESI-MS (Table 2, Figure 3), together with minor Zn_7-, Zn_8- and Zn_4-, Zn_3-MTT5. The CD spectrum of this preparation exhibited a low intensity Gaussian band centered at 240(+) nm, in correspondence with the typical signals of the Zn-thiolate chromophores. Following a behavior similar to MTT1, MTT5 yielded an almost unique Cd-complex when synthesized in the presence of Cd^{2+}, here Cd_8-MTT5, and only very minor Cd_9-MTT5 species accompanied it (Table 2, Figure 3). However, this Cd_8-MTT5 complex exhibited a CD fingerprint less intense, and different in shape, to those of Cd-MTT1 and Cd-MTT3, with a wide Gaussian band ranging from 240 to 280 nm indicative of the different folding of this Cd_8 complex (Figure 4). For MTT5, the Zn/Cd exchange reaction was followed in detail by CD and UV-Vis spectrophotometry and ESI-MS at discrete steps of the Cd^{2+} addition to the Zn-MTT5 preparation (Figure 5). This reaction demonstrated the progressive incorporation of Cd^{2+} ions into MTT5 (Figure 5A), but this caused the generation of a considerable mixture of Cd_x-MTT5 species, (x = from 3 to 9), even for 10 Cd^{2+} ions added (Figure 5B). Hence, it is clear that the composition of the *in vivo* preparations (*i.e.* an almost unique Cd_8-MTT5 species, Figure 3) could not be reproduced by the Zn^{2+}/Cd^{2+} replacement, which was also highly evident by the comparison of the CD spectra of the respective samples (Figure 5C).

As commented before, the biosynthesis of Cu-loaded MTT5 proved to be feasible in both normal- and low-aerated Cu-supplemented cultures. Under normal Cu conditions, a mixture of M_x-MTT5 (major peaks being, in decreasing order, M_{12}- > M_9- > M_8-MTT5, M=Zn or Cu) was detected by ESI-MS at neutral pH. Since ICP-AES analyses of this sample showed a ratio of 1.6 Zn:11.2 Cu, and acid ESI-MS of the sample revealed a major content of Cu_9- and Cu_8-MTT5, followed by Cu_{12}-MTT5 cores (Table 2, Figure 3), it was reasonable to conclude that some of the recombinant complexes were indeed heterometallic Zn,Cu-MTT5 species. Conversely, cultures grown at high intracellular copper concentrations (*i.e.* low

culture aeration) led to the formation of homonuclear Cu-MTT5 species, which, however, showed an extremely high instability, and only Cu_8- and Cu_4-cores were clearly identified among a myriad of peaks in the corresponding acid ESI-MS analyses (Table 2, Figure 3). The Zn/Cu replacement studies on Zn-MTT5 demonstrated the successive incorporation of Cu^+ into the protein (Figure 5D) and revealed that a mixture of heterometallic species, similar to that yielded *in vivo* when this peptide was synthesized in regular cell copper concentrations, was reached at the interval of 6-to-8 Cu^+ eq added (Figure 5E), despite the fact that the CD fingerprint of this sample was not reproduced at this stage of the Cu^+ addition (Figure 5F). The addition of further Cu^+ ions led to the detection of apo-MTT5, for 12 eq added if the sample was analyzed at neutral ESI-MS conditions, and already at 8 eq added if the sample was subjected to acid (pH 2.4) ESI-MS. This was consistent with a high instability of these complexes, which, logically, was more apparent under the harsh acid ESI-MS conditions.

Metal-binding ability comparison between the three MTT isoforms classically classified as *Tetrahymena* Cd-thioneins (MTT1, MTT3 and MTT5) is not straightforward, because, unlike the Cu-thionein MTT isoforms, they differ either in size and/or in Cys content and patterns (*cf.* Figure 1). However, several of the Zn/Cd- *vs*. Cu-thionein classification criteria coincide in pointing to MTT1 as the isoform with a more pronounced Zn/Cd-thionein character, because, according to these ([5,10]): (i) MTT1 is unable to yield stable Cu-complexes in any of the conditions assayed for Cu-supplemented cultures; (ii) the Zn-MTT1 preparation is a mixture of multiple species, exhibiting an almost silent CD spectrum, and (iii) in contrast with the two preceding points, an almost unique Cd_{17}-MTT1 species, with very particular CD features, is the result of MTT1 folding upon Cd^{2+} ions. Unlike this clearly defined MTT1 behavior, MTT3 and MTT5 somehow present contradictory results. Both isoforms yield several complexes when synthesized under Zn^{2+} surplus, this suggesting a non-optimized polypeptide composition for Zn^{2+} coordination. If considering Cd^{2+}, results clearly indicate the patent ability of MTT5 to fold into a unique, well folded complex, while MTT3 yields a poor mixture of species, the most abundant of which being sulfide-containing complexes, a feature typical of Cu-thioneins ([5,10]). However, the synthesis of MTT3 in Cu-supplemented media was only successful under regular intracellular Cu concentrations, and it only yielded heterometallic species with a high Zn^{2+} content; while MTT5, yielded stable Cu-species also at high Cu concentrations (low aeration of the cultures), with a markedly minimum Zn^{2+} content. All these consideration led us to suggest that MTT5 may be considered as a *second-best* Zn/Cd-thionein, while MTT3 would in fact behave as a MT peptide with patent deficiencies whatever the metal ion considered.

Zn-, Cd- and Cu-binding abilities of the Cu-MTT isoforms (family 7b): MTT2 and MTT4

According to their gene expression profile, the MTT2 and MTT4 isoforms were previously classified as Cu-thioneins (*i.e.* family 7b MTs) ([17]). Following the same approach described above for family 7a MTTs, we studied here the features of their Zn^{2+}-, Cd^{2+}- and Cu^+-complexes, in order to corroborate if the copper responsiveness of their genes was coincident with the metal binding abilities of the encoded peptides and, furthermore, to evaluate if there was any differential behavior between these two *T. thermophila* MT isoforms. First, their divalent metal ion binding abilities were studied. Very significantly, and even after repeated attempts, no MTT2 complexes could be recovered from the Zn- and Cd-supplemented bacterial cells, this indicating the incapacity of MTT2 to fold into stable Zn- or Cd-complexes in an intracellular environment. It is worth commenting that we have commonly encountered this situation the other way round, *i.e.* when attempting to synthesize non-strict Cu-thioneins in copper-enriched host cells ([57,58]), but never in the case of divalent metal ion supplementation. Therefore, it is the first time that we report a Cu-thionein unable to bind Zn^{2+} or Cd^{2+} *in vivo*. Conversely, and for both MTT2 and MTT4, the two types of Cu-supplemented cultures (*i.e.*, low aeration -meaning high cell Cu content-; and regular aeration -meaning normal cell Cu content-), respectively, yielded stable heterometallic and homometallic Cu-containing complexes. Hence, at normal aeration, a major M_{20}-MTT2 complex (M=Zn or Cu) coexisted with minor M_{16}- and M_{17}-MTT2 species, as revealed by ESI-MS at neutral pH (Table 2, Figure 6). Since the major peaks detected at acid ESI-MS were Cu_{20}-, Cu_{16}- and Cu_{12}-MTT2, it is reasonable to deduce that the species present in this sample were homometallic Cu_{20}- and Cu_{16}-MTT2 complexes, together with heterometallic Zn_5Cu_{12}-MTT2, which fits with the ICP-AES-quantification of the total metal in these preparations (3.0 Zn:15.1 Cu per MTT2).

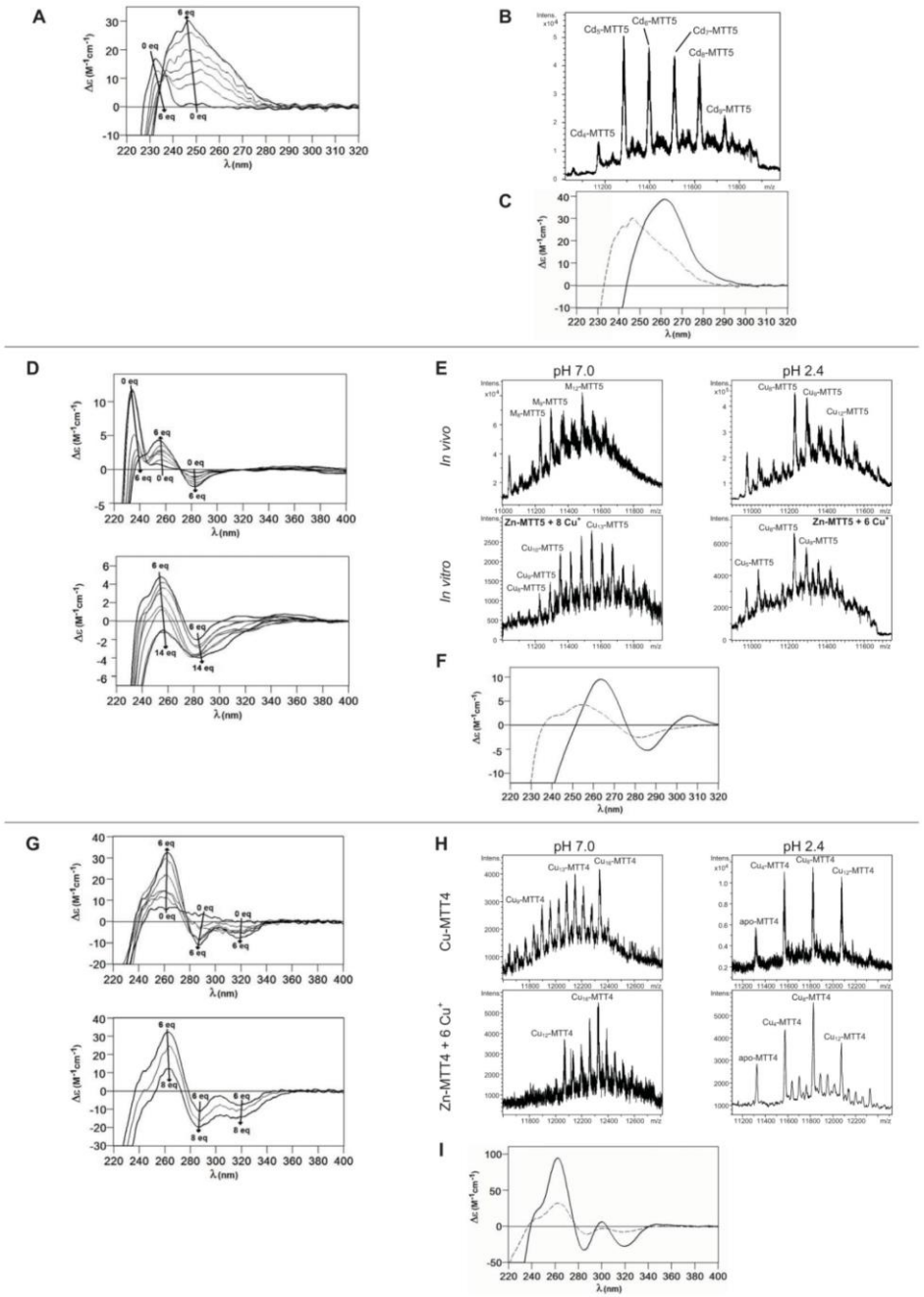

Figure 5. Characterization of *in vitro* prepared metal-MTT5 and metal-MTT4 complexes. (A) Circular dichroism -CD- spectra recorded after the addition of up to 6 Cd^{2+} eq to Zn-MTT5 at pH 7.0. (B) Deconvoluted ESI-MS spectrum recorded after the addition of 10 Cd^{2+} eq to Zn-MTT5. (C) CD spectra corresponding to the Cd-MTT5 preparation (solid line) and that recorded after the addition of 10 Cd^{2+} eq to Zn-MTT5. (D) CD spectra recorded after the addition of up to 14 Cu^{+} eq to Zn-MTT5 at pH 7.0. Comparison of (E) the deconvoluted ESI-MS and (F) the CD spectra of the recombinant Cu-MTT5 preparation (solid line) and those recorded at several stages of the titration of Zn-MTT5 with Cu^{+} (dashed line for the addition of 6 Cu^{+} eq). (G) CD spectra recorded after the addition of up to 8 Cu^{+} eq to Zn-MTT4 at pH 7.0. Comparison of (H) the deconvoluted ESI-MS and (I) the CD spectra of the recombinant Cu-MTT4 preparation (solid line) and those recorded after the addition of 6 Cu^{+} eq to Zn-MTT4 (dashed).

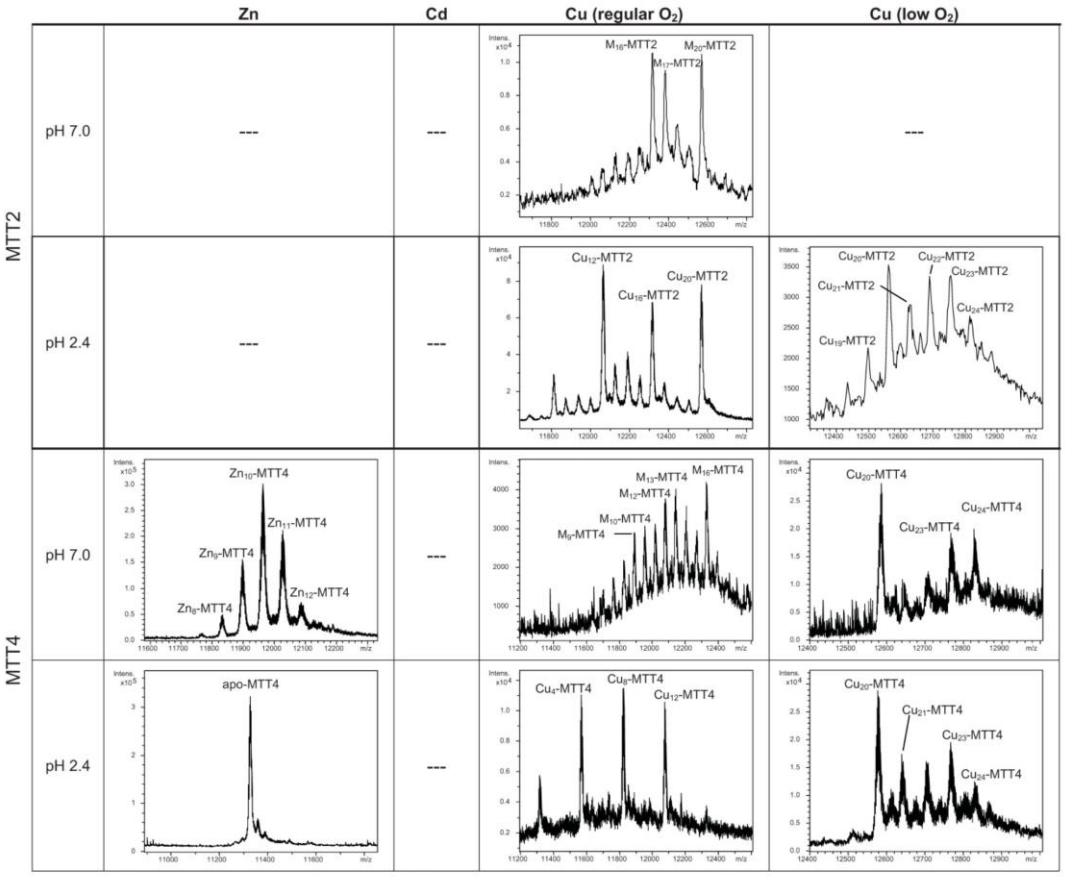

Figure 6. Deconvoluted ESI-MS spectra of the recombinant preparations of MTT2 and MTT4. The metal-MTT complexes were synthesized in recombinant cultures supplemented with Zn, Cd, or Cu, and in the case of Cu-enriched media, the synthesis was carried out under regular and low aeration conditions. ESI-MS was run at pH 7.0 and pH 2.4. (M=Zn or Cu). (---) denotes that no metal-MTT complexes could be purified from the corresponding cultures.

When MTT2 was synthesized by high Cu-enriched cells, the ICP-AES results indicated the total absence of Zn, and therefore all the complexes detected in the acid ESI-MS spectra (Figure 6) were interpreted as homometallic species, major Cu_{20}- and minor Cu_{21}- to Cu_{23}-MTT2. In summary, Cu_{20}-MTT2 was therefore assumed as the principal Cu-containing complex yielded by MTT2, which is also in good agreement with the data estimated in ([18]). The CD spectra of both Cu-MTT2 preparations (regular and normal aerated cultures) showed very similar profiles, with the typical bands at 260(+) and 285(-) nm of tetrahedrally and/or trigonally coordinated Cu^+, as well as absorbances above 300 nm (320-325(-) and 365(+)), which are attributable to digonal Cu^+. The latter are consistently more intense in the *low aeration* sample, which contains homometallic Cu^+ complexes (Figure 7).

MTT4, like MTT2, was unable to fold *in vivo* onto Cd-complexes but, at least it yielded analyzable Zn-MTT4 species, where major Zn_{10}-MTT4 appeared accompanied by several minor species, ranging from Zn_8- to Zn_{12}-MTT4. The multiplicity of peaks in the Zn-preparations (Figure 6) and, as a matter of fact, the impossibility of recovering Cd-MTT4 complexes, was highly concordant with the behavior of a typical Cu-thionein. Conversely, MTT4 folded into stable complexes when coordinating Cu^+ ions. At regular aeration, the producing cells yielded a mixture of Zn,Cu-containing complexes, as revealed by the ICP-AES analyses (9.0 Cu:4.0 Zn per MTT4) and the divergence of the ESI-MS species detected at neutral (major M_{16}- and M_{13}-MTT4, together with significantly intense M_9- to M_{17}-MTT4 peaks) and acid pH (major Cu_8-, and minor Cu_{12}- and Cu_4-MTT4 peaks) (Figure 6). These results are easily interpreted if as-

suming the presence of heterometallic Zn_xCu_4-, Zn_yCu_8-, and Zn_zCu_2-MTT4 species (where x, y, and z are a variable number of Zn^{2+} ions that added to 4, 8 or 12 Cu^+ ions end up in the 9-to-17 metal ion content), and maybe some homometallic Cu_{12}-MTT4 species. Contrarily, with a high Cu, MTT4 yields major homometallic Cu_{20}-MTT4, together with higher nucleation species (Figure 6). The CD spectra of the Cu-MTT4 preparations drew the typical Cu-MT fingerprints already observed for the Cu-MTT2 complexes, and as for MTT2, they were more intense for the homometallic Cu-MTT4 than for the heterometallic Zn,Cu-MTT4 samples (Figure 7). Owing to the availability of Zn-MTT4 preparations, it was possible to perform Zn^{2+}/Cu^+ replacement studies for this isoform, in order to obtain a deeper insight into its *in vitro* Cu^+ binding abilities (Figures 5G to 5I). It is worth noting that, starting from the uninformative Zn-MTT4 CD spectra (marked as 0 in the titration, Figure 5G), a typical Cu-MT CD profile developed, with absorptions at 260(+), 285(-), and 320(-) nm. Remarkably, when 6 Cu^+ equivalents had been added to the initial Zn-MTT4, the CD fingerprint closely resembled that of Cu-MTT4 synthesized in regularly aerated cultures (Figure 5H), also coincident with the composition of the mixture (Figure 5I).

Comparison of the metal binding abilities of MTT2 and MTT4 reveal significant information, because, noteworthy, these two peptides only differ in one amino acid position (#89: Asn in MTT2 and Lys in MTT4, *cf.* Figure 1). Both MTTs bind up to 20 Cu^+, which is consistent with their close similarity and conserved Cys pattern, but several points converge in supporting a more marked Cu-thionein character for MTT2 than for MTT4: i) it was impossible to recover Zn- and Cd-MTT2 complexes, while Zn-MTT4 species are stable; ii) when synthesized under normal Cu, MTT2 is already able to yield Cu_{20}-MTT2 complexes, while this is not the case for MTT4; iii) under these synthesis conditions, MTT2 forms heterometallic species with stable Cu_{12}-cores, while for MTT4, the most stable core is Cu_8, with Cu_4 and Cu_{12} as minor ones; iv) in surplus Cu conditions, MTT2 yields homometallic species with a higher Cu stoichiometry than MTT4. These differential Cu-binding features have to be attributed to the unique amino acid substitution, and therefore it is reasonable to conclude that the presence of Asn89 (MTT2) instead of Lys (MTT4) greatly favors the character of Cu-thionein of the polypeptide. This is in total agreement with the situation found in snail MTs, where the comparative analysis of their homologous and metal-specific CuMT and CdMT protein sequences recently revealed the respective major presence of Asn *vs.* Lys residues in several positions ([59]).

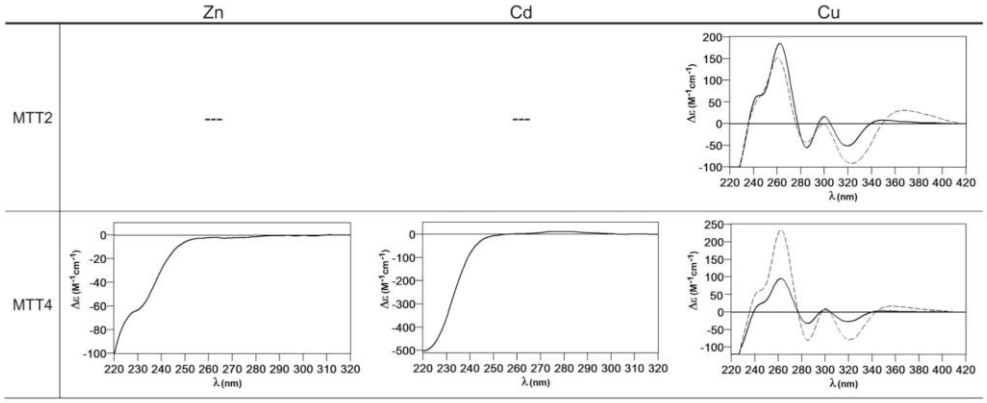

Figure 7. Circular dichroism spectra of the recombinant preparations of MTT2 and MTT4. The metal-MTT complexes were synthesized in recombinant cultures supplemented with Zn, Cd, or Cu, and in the case of Cu-enriched media, the synthesis was carried out under regular (solid line) and low aeration (dashed line) conditions. (---) denotes that no metal-MTT complexes could be purified from the corresponding cultures.

Conclusions

Overall, the results of the current study show the thorough analysis of the Zn^{2+}, Cd^{2+} and Cu^+ binding abilities of each one of the five metallothionein peptides composing the *Tetrahymena thermophila* MT system. These allow the polypeptides to be classified as Zn/Cd- or Cu-thioneins, a metal-binding property that is globally concordant with their specificity previously evaluated from gene response criteria. Hence, in this organism divergence evolution of cysteine-rich sequences and of gene expression regulation has led to the generation of two clear Zn/Cd-thioneins (MTT1 and MTT5), an undefined MT (MTT3), and two

Cu-thioneins (MTT2 and MTT4). The comprehensive comparison of the recombinant complexes yielded by the encoded peptides towards the three metal ions allows their gradual classification from Zn/Cd-thionein to Cu-thionein as follows: MTT1>MTT5>MTT3>MTT4>MTT2; and *vice versa* for the Cu- to Zn/Cd-thionein gradation. Strikingly, the MTT3 isoform is an intermediate isoform, which is not particularly suitable for coordination of any of these three metal ions, if considering the poor features of the corresponding metal complexes. Data in the literature on the type of metal ion inducing expression of the *T. thermophila MTT* genes ([17]) agree with the classification suggested in this work by the features of the metal-MTT complexes. Although MTT3 was then unambiguously considered as a Cd-thionein, a peculiar behavior was already noted for the *MTT3* gene inducibility pattern. Hence, all MTT Cd-thioneins are induced by divalent metal ions, but Cd^{2+} is the best inducer for *MTT1*, and Cd^{2+} is also better than Zn^{2+} for *MTT5*. But for the *undefined* MTT3 isoform, its gene is more responsive to Zn^{2+} at a short inducibility time, while for long treatments, Cd^{2+} is the most effective inducer, so that it is tempting to hypothesize that its lack of a definite metal preference responds to a need of plasticity, allowing it to develop diverse physiological tasks. It is captivating to hypothesize on how evolution may have modulated the amino acid sequences of these paralogous sequences in order to achieve such metal binding preferential behavior, since *T. thermophila* MTs are among the longest MT peptides ever reported. Duplication and subsequent variation of short Cys-rich sequence modules has long been proposed as the basic building mechanism for these long MTs, especially for the three Cd-thioneins, which are far more dissimilar, both in length and in Cys-patterns, than the two Cu-MTTs ([17]). The MTT Zn/Cd-isoforms are also characterized by the high occurrence of Cys doublets and triplets in their sequences (Figure 1B). Although the former are common in MTs, being, for example a signature for the vertebrate α-domains, the Cys-triplet motif is scarcely found among MTs; but here it appears undoubtedly associated to an increased ability for Cd^{2+} coordination. No complex modular structure has been defined for the MTT Cu-thioneins (MTT2 or MTT4) beyond the evidence that they encompass repetitions of a ($CysLysCysX_{2\text{-}5}CysXCys$) motif, and thus the total absence of Cys triplets and doublets appears intrinsically related with an optimal Cu-binding performance. Taking into account that MTT2 and MTT4 only differ in one amino acid position, it can be assumed that they have recently differentiated in evolution. It is relevant how this amino acid change increases the Cu-thionein character of MTT2 (Asn) in relation to MTT4 (Lys), consistently with the respective identification of these amino acids as Cu-thionein and Cd-thionein determinants in snail MTs ([59]). In conclusion, this work confirms how the *Tetrahymena* MT system constitutes an invaluable model for MT evolutionary studies, a subject that is lately revealing extraordinary convergent strategies, even if analyzed in highly distinct organisms. Hence, the need for high-capacity chelating polypeptides seems to have been tackled by tandem repetition of basic building blocks, as we recently described for the pathogenic fungus *Cryptococcus neoformans* Cu-thioneins ([45,46]), and the same amino acids appear to tip the balance in favor of Zn/Cd-thioneins (Lys) or Cu-thioneins (Asn) both in snails ([59]) and ciliates (this work). Therefore, and despite their complete disparity in protein sequence, MTs from the most diverse organisms seem to have adopted common evolutionary trends in order to achieve their functional differentiation and specialization along the tree of life.

Acknowledgements

This work was supported by the Spanish Ministerio de Economía y Competitividad (MINECO), grants BIO2012-39682-C02-01 (to SA), -02 (to MC), and grant CGL2008-00317/BOS (to JCG), which are co-financed by the European Union through the FEDER program. Authors from both Barcelona universities are members of the 2014SGR-423 Grup de Recerca de la Generalitat de Catalunya. AE was the recipient of a predoctoral grant from the MINECO (BES-2010-036553). We thank the Centres Científics i Tecnològics (CCiT) de la Universitat de Barcelona (ICP-AES, DNA sequencing) and the Servei d'Anàlisi Química (SAQ) de la Universitat Autònoma de Barcelona (CD, UV-vis, ESI-MS) for allocating instrument time.

Competing Interests

The authors have declared that no competing interest exists.

References

1. Wolfe KH, Shields DC. Molecular evidence for an ancient duplication of the entire yeast genome. Nature 1997; 387:708-713.
2. Lundin LG. Gene duplications in early metazoan evolution. Semin Cell Dev Biol 1999; 10:523-530.
3. Holland PW, Garcia-Fernandez J, Williams NA, Sidow A. Gene duplications and the origins of vertebrate development. Dev Suppl 1994; 43:125-133.
4. Capdevila M, Bofill R, Palacios O, Atrian S. State-of-the-art of metallothioneins at the beginning of the 21st century. Coord Chem Rev 2012; 256:46–62.
5. Palacios O, Atrian S, Capdevila M. Zn- and Cu-thioneins: a functional classification for metallothioneins? J Biol Inorg Chem 2011; 16:991–1009.
6. Capdevila M, Atrian S. Metallothionein protein evolution: a miniassay. J Biol Inorg Chem 2011; 16: 977–989.
7. Seren N, Glaberman S, Carretero MA, Chiari Y. Molecular evolution and functional divergence of the Metallothioneins gene family in Vertebrates. J Mol Evol 2014; 78:217-233.
8. Palmiter R. The elusive function of metallothioneins. Proc Natl Acad Sci USA 1994; 95:8428-8430.

9. Blindauer CA, Leszczyszyn OI. Metallothioneins: unparalleled diversity in structures and functions for metal ion homeostasis and more. Nat Prod Rep 2010; 27:720-741.
10. Bofill R, Capdevila M, Atrian S. Independent metal-binding features of recombinant metallothioneins convergently draw a step gradation between Zn- and Cu-thioneins. Metallomics 2009; 1:229-234.
11. Waldron JK, Robinson NJ. How do bacterial cells ensure that metalloproteins get the correct metal? Nature Rev Microbiol 2009; 6:25-35.
12. Waldron JK, Rutherford JC, Ford D, Robinson NJ. Metalloproteins and metal sensing. Nature 2009; 460:823-830.
13. Palacios O, Pagani A, Perez-Rafael S, Egg M, Höckner M, Brandstätter A, Capdevila M, Atrian S, Dallinger R. Shaping mechanisms of metal specificity in a family of metazoan metallothioneins: evolutionary differentiation of mollusc metallothioneins. BMC Biology 2011; 9:4.
14. Palacios O, Perez-Rafael S, Pagani A, Dallinger R, Atrian S, Capdevila M. Cognate and noncognate metal ion coordination in metal-specific metallothioneins: the *Helix pomatia* system as a model. J Biol Inorg Chem 2014; 19:923-935.
15. Nemer M, Wilkinson DG, Travaglini EC, Sternberg EJ, Butt TR. Sea urchin metallothionein sequence: key to an evolutionary diversity. Proc Natl Acad Sci USA 1985; 82:4992-4994.
16. [Internet] Metallothioneins: classification and list of entries.www.uniprot.org/docs/metallo.txt
17. Diaz S, Amaro F, Rico D, Campos V, Benitez L, Martin-Gonzalez A, Hamilton EP, Orias E, Gutierrez JC. *Tetrahymena* Metallothioneins Fall into Two Discrete subfamilies. PlosOne 2007; 3:e291.
18. Gutierrez JC, Amaro F, Diaz S, de Francisco P, Cubas LL, Martin-Gonzalez A. Ciliate metallothioneins: unique microbial eukaryotic heavy-metal-binder molecules. J Biol Inorg Chem 2011; 16:1025-1034.
19. Parfrey LW, Lahr DJG, Knoll AH, Katz L. Estimating the timing of early eukaryotic diversification with multigene molecular clocks. Proc Natl Acad Sci USA 2011; 108:13624-13629.
20. Boldrin F, Santovito G, Negrisolo E, Piccinni E. Cloning and Sequencing of Four New Metallothionein Genes from *Tetrahymena thermophila* and *T. pigmentosa*. Evolutionary Relationships in *Tetrahymena* MT Family. Protist 2003; 154:431-442.
21. Boldrin F, Santovito G, Gaerteig J, Wlonga D, Cassidy-Hanley D, Clark TG, Piccinni E. Metallothionein Gene from *Tetrahymena thermophila* with a Copper-Inducible- Repressible Promoter. Eukaryot Cell 2006; 5:422-425.
22. Boldrin F, Santovito G, Formigari A, Bisharyan Y, Cassidy-Hanley D, Clark TG, Piccinni E: MTT2, a copper-inducible metallothionein gene from *Tetrahymena thermophila*. Comp Biochem Physiol C Toxicol Pharmacol 2008; 147:232-240.
23. Santovito G, Formigari A, Boldrin F, Piccinni E. Molecular and functional evolution of *Tetrahymena* metallothioneins: New insights into the gene family of *Tetrahymena thermophila*. Comp Biochem Physiol C Toxicol Pharmacol 2007; 144:391-397.
24. Chang Y, Feng L-F, Xiong J, Miao W. Function comparison and evolution analysis of metallothionein gene MTT2 and MTT4 in *Tetrahymena thermophila*. Zool Res 2011; 32:476-484.
25. Piccinni E, Staudenmann W, Albergoni V, De Gabrieli R, James P. Purification and primary structure of metallothioneins induced by cadmium in the protists *Tetrahymena pigmentosa* and *Tetrahymena pyriformis*. Eur J Biochem 1994; 226:853-859.
26. Santovito G, Irato P, Palermo S, Boldrin F, Sack R, Hunziker P, Piccinni E. Identification, Cloning and Characterisation of a Novel Copper-Metallothionein in *Tetrahymena pigmentosa*. Sequencing of cDNA and Expression. Protist 2001; 152:219-229.
27. Boldrin F, Santovito G, Irato P, Piccinni E. Metal Interaction and Regulation of *Tetrahymena pigmentosa* Metallothionein Genes. Protist 2002; 153:283-291.
28. Guo L, Fu C, Miao W. Cloning characterization, and gene expression analysis of a novel cadmium metallothionein gene in *Tetrahymena pigmentosa*. Gene 2008; 423:29-35.
29. Piccinni E, Irato P, Coppellotti O, Guidolin L. Biochemical and ultrastructural data on *Tetrahymena pyriformis* treated with copper and cadmium. J Cell Sci 1987; 88:283-293.
30. Piccinni E, Bertaggia D, Santovito G, Miceli C, Kraev A. Cadmium metallothionein gene of *Tetrahymena pyriformis*. Gene 1999; 234:51-59.
31. Fu C, Miao W: Cloning and characterization of a New Multi-Stress Inducible Metallothionein Gene in *Tetrahymena pyriformis*. Protist 2006; 157:193-203.
32. Amaro F, de Lucas M, Martin-Gonzalez A, Gutierrez JC. Two new members of the *Tetrahymena* multi-stress-inducible metallothionein family: Characterization and expression analysis of *T. rostrata* Cd/Cu metallothionein genes. Gene 2008, 423:85-91.
33. Shuja RN, Shakoori AR. Identification, cloning and sequencing of a novel stress inducible metallothionein gene from locally isolated *Tetrahymena tropicalis lahorensis*. Gene 2007; 405:19-26.
34. Chaundhry R, Shakoori AR. Isolation and characterization of a novel copper-inducible metallothionein gene of a ciliate, *Tetrahymena tropicalis lahorensis*. J Cell Biochem 2010; 110:630-644.
35. Shuja RN, Taimuri SUA, Shakoori FR, Shakoori AR. Efficient expression of truncated recombinant cadmium-metallothionein gene of a ciliate, *Tetrahymena tropicalis lahorensis* in *Escherichia coli*. Mol Biol Rep 2013; 40:7061-7068.
36. Chang Y, Liu G, Guo L, Liu H, Yuan D, Xiong J, Ning Y, Fu C, Miao W. Cd-Metallothioneins in Three Additional *Tetrahymena* Species: Intragenic Repeat Patterns and Induction by Metal Ions. J Eukaryot Microbiol 2014, 61:333-342.
37. Valls M, Bofill R, Gonzalez-Duarte R, Gonzàlez-Duarte P, Capdevila M, Atrian S. A new insight into Metallothionein (MT) classification and evolution. The *in vivo* and *in vitro* metal binding features of *Homarus americanus* recombinant MT. J Biol Chem 2001; 276:32835-32843.
38. Shang Y, Song X, Bowen J, Corstanje R, Gao Y, Gaertig J, Gorovsky MA. A robust inducible-repressible promoter greatly facilitates gene knockouts, conditional expression, and overexpression of homologous and heterologous genes in *Tetrahymena thermophila*. Proc Natl Acad Sci USA 2002; 99:3734-3739.
39. Dondero F, Cavaletto M, Ghezzi AR, La Terza A, Banni M, Viarengo A. Biochemical Characterization and Quantitative Gene Expression Analysis of the Multi-Stress Inducible Metallothionein from *Tetrahymena thermophila*. Protist 2004; 155:157-168.
40. Gutiérrez JC, Amaro F, Martín-González A. From heavy metal-binders to biosensors: Ciliate metallothioneins discussed. BioEssays 2009; 31:805-816.
41. Amaro F, Turkewitz AP, Martin-Gonzalez A, Gutierrez JC. Whole-cell biosensors for detection of heavy metal ions in environmental samples based on metallothionein promoters from *Tetrahymena thermophila*. Microb Biotechnol 2011; 4:513-522.
42. Amaro F, Turkewitz AP, Martin-Gonzalez A, Gutierrez JC. Functional GFP-metallothionein from *Tetrahymena thermophila*: a potential whole-cell biosensor for monitoring heavy metal pollution and a cell model to study metallothionein overproduction effects. Biometals 2014; 27:195-205.
43. Domenech J, Bofill R, Tinti A, Torreggiani A, Atrian S, Capdevila M. Comparative insight into the Zn(II)-, Cd(II)- and Cu(I)-binding features of the protozoan *Tetrahymena pyriformis* MT1 metallothionein. Biochim Biophys Acta 2008; 1784:693-704.
44. Wang Q, Xu J, Chai B, Liang A, Wang W. Functional comparison of metallothioneins MTT1 and MTT2 from *Tetrahymena thermophila*. Arch Biochem Biophys 2011; 509:170-176.
45. Ding C, Festa RA, Chen YL, Espart A, Palacios O, Espin J, Capdevila M, Atrian S, Heitman J, Thiele D. *Cryptococcus neoformans* copper detoxification machinery is critical for copper virulence. Cell, Host & Microbe 2013; 13:265-276.
46. Palacios O, Espart A, Espin J, Ding C, Thiele D, Atrian S, Capdevila M. Full characterization of the Cu-, Zn-, and Cd-binding properties of CnMT1 and CnMT2, two metallothioneins of the pathogenic fungus *Cryptococcus neoformans* acting as virulence factors. Metallomics 2014; 6:279-291.
47. Fogel S, Welch JW, Cathala G, Karin M. Gene amplification in yeast: CUP1 copy number regulates copper resistance. Curr Genet 1983; 7:347-355.
48. Horowitz S, Gorovsky MA. An unusual genetic code in nuclear genes of *Tetrahymena*. Proc Natl Acad Sci USA 1985; 82:2452-2455.
49. Landt O, Grunert HP, Hahn U. A general method for rapid site-directed mutagenesis using the polymerase chain reaction. Gene 1990; 96:125-128.
50. Pagani A, Villarreal L, Capdevila M, Atrian S. The *Saccharomyces cerevisiae* Crs5 metallothionein metal-binding abilities and its role in the response to zinc overload. Mol Microbiol 2007; 63: 256-269.
51. Cols N, Romero-Isart N, Capdevila M, Oliva B, González-Duarte P, González-Duarte R, Atrian S. Binding of excess cadmium(II) to Cd_7-metallothionein from recombinant mouse Zn_7-metallothionein 1. UV-VIS absorption and circular dichroism studies and theoretical location approach by surface accessibility analysis. J Inorg Biochem 1997; 68:157-166.
52. Capdevila M, Cols N, Romero-Isart N, González-Duarte R, Atrian S, González-Duarte P. Recombinant synthesis of mouse Zn_7-ß and Zn_4-α metallothionein 1 domains and characterization of their cadmium(II) binding capacity. Cell Mol Life Sci 1997; 53:681–688.
53. Bofill R, Palacios O, Capdevila M, Cols N, González-Duarte R, Atrian S, González-Duarte P. A new insight into the Ag^+ and Cu^+ binding sites in the metallothionein β domain. J Inorg Biochem 1999; 73:57–64.
54. Bongers J, Walton CD, Richardson DE, Bell JU. Micromolar protein concentrations and metalloprotein stoichiometries obtained by inductively coupled plasma atomic emission spectrometric determination of sulfur. Anal Chem 1988; 60:2683–2686.
55. Capdevila M, Domenech J, Pagani A, Tio L, Villarreal L, Atrian S. Zn- and Cd-metallothionein recombinant species from the most diverse phyla may contain sulfide (S^{2-}) ligands. Angew Chem Int Ed Engl 2005; 44:4618–4622.
56. Fabris D, Zaia J, Hathout Y, Fenselau C. Retention of Thiol Protons in Two Classes of Protein Zinc Coordination Centers. J Am Chem Soc 1996; 118:12242-12243.
57. Perez-Rafael S, Mezger A, Lieb B, Dallinger R, Capdevila M, Palacios O, Atrian S. The metal binding abilities of Megathura crenulata metallothionein (McMT) in the frame of Gastropoda MTs. J Inorg Biochem 2012; 108:84-90.
58. Perez-Rafael S, Kurz A, Guirola M, Capdevila M, Palacios O, Atrian S. Is MtnE, the fifth Drosophila metallothionein, functionally distinct from the other members of this polymorphic protein family? Metallomics 2012; 4:342-349.
59. Perez-Rafael S, Monteiro F, Dallinger R, Atrian S, Palacios O, Capdevila M. Cantareus aspersus metallothionein metal binding abilities: The unspecific CaCd/CuMT isoform provides hints about the metal preference determinants in Metallothioneins. BBA-Proteins and Proteomics 2014; 1844:1694-1707.

International Journal of
Molecular Sciences

MDPI

Article

Does Variation of the Inter-Domain Linker Sequence Modulate the Metal Binding Behaviour of *Helix pomatia* Cd-Metallothionein?

Selene Gil-Moreno [1,†], Elena Jiménez-Martí [2,†], Òscar Palacios [1], Oliver Zerbe [3], Reinhard Dallinger [4], Mercè Capdevila [1] and Sílvia Atrian [2,*]

Received: 17 November 2015; Accepted: 14 December 2015; Published: 22 December 2015
Academic Editor: Nick Hadjiliadis

1 Departament de Química, Facultat de Ciències, Universitat Autònoma de Barcelona, E-08193 Cerdanyola del Vallès, Spain; selenebdn89@gmail.com (S.G.-M.); oscar.palacios@uab.cat (O.P.); merce.capdevila@uab.cat (M.C.)
2 Departament de Genètica, Facultat de Biologia, Universitat de Barcelona, Av. Diagonal 643, E-08028 Barcelona, Spain; ejimenezmarti@gmail.com
3 Institute of Organic Chemistry, University of Zurich, 8057 Zurich, Switzerland; zerbe@oci.uzh.ch
4 Institute of Zoology, University of Innsbruck, Technikerstraße 25, A-6020 Innsbruck, Austria; reinhard.dallinger@uibk.ac.at
* Correspondence: satrian@ub.edu; Tel.: +34-93-4021501; Fax: +34-93-4034420
† These authors contributed equally to this work.

Abstract: Snail metallothioneins (MTs) constitute an ideal model to study structure/function relationships in these metal-binding polypeptides. *Helix pomatia* harbours three MT isoforms: the highly specific CdMT and CuMT, and an unspecific Cd/CuMT, which represent paralogous proteins with extremely different metal binding preferences while sharing high sequence similarity. Preceding work allowed assessing that, although, the Cys residues are responsible for metal ion coordination, metal specificity or preference is achieved by diversification of the amino acids interspersed between them. The metal-specific MT polypeptides fold into unique, energetically-optimized complexes of defined metal content, when binding their cognate metal ions, while they produce a mixture of complexes, none of them representing a clear energy minimum, with non-cognate metal ions. Another critical, and so far mostly unexplored, region is the stretch linking the individual MT domains, each of which represents an independent metal cluster. In this work, we have designed and analyzed two HpCdMT constructs with substituted linker segments, and determined their coordination behavior when exposed to both cognate and non-cognate metal ions. Results unequivocally show that neither length nor composition of the inter-domain linker alter the features of the Zn(II)- and Cd(II)-complexes, but surprisingly that they influence their ability to bind Cu(I), the non-cognate metal ion.

Keywords: Cd-isoform; domain linker sequence; *Helix pomatia*; metallothionein; metal binding

1. Introduction

Metallothioneins (MTs) are a super-family of mostly small, ubiquitous, but highly heterogeneous, proteins that coordinate heavy-metal ions owing to the metal-thiolate bonds contributed by their abundant cysteine residues (recent reviews in [1,2]). They have been traditionally associated with different biological roles mainly related to physiological metal (Zn and Cu) homeostasis and/or to toxic heavy metal chelation, but also to different stress responses, such as free radical scavenging. It has been hypothesized that this multitude of possible functions may be the basis of the high heterogeneity of the MT proteins reported up to now, so that MTs may have evolved

differently in certain groups of organisms according to precise physiological requirements. Hence, the extraordinary diversity of MT isoforms -MTs are polymorphic in almost all organisms analyzed up to now—along all kinds of taxa seem to be related to their plasticity to perform a great multiplicity of functions [3]. At first, several classifications of this heterogeneous group of proteins had been first proposed on the basis of sequence similarity and taxonomic criteria [4,5], but most significantly, our group later proposed a functional classification of MTs founded on the analysis of their preference for divalent metal ion coordination, grouping them into the so-called Zn-thioneins (accounting for both Zn(II) or Cd(II)-binding MTs), and the so called Cu-thioneins (accounting for monovalent ion binding MTs). Each type of MT is characterized by yielding unique, well-folded, homometallic complexes when it coordinates its cognate metal ion [6]. Although originally this classification only proposed these two MT categories [7], it was later extended to a step-wise gradation between extreme, or genuine, Zn- (or divalent metal-ions)-thioneins and Cu-thioneins [8].

Gastropoda pulmonates is one of the Mollusca classes with a higher number of species, and they constitute an ideal model system to study the structure/function relationship and the evolutionary differentiation of polymorphic MTs. The different MT isoforms combine two valuable properties that allow to precisely recognize the features that confer the Zn- or Cu-thionein character to an MT polypeptide: the paralogous proteins are highly specialized for binding distinct metal ions while retaining high sequence similarities. Hence, the best characterized snail MT systems, those of the terrestrial snails *Helix pomatia* and *Cantareus aspersus* include three paralogous MT peptides with different metal binding preferences: the CdMT and CuMT isoforms which, respectively, bind cadmium and copper with high specificity, and an unspecific Cd/CuMT isoform that was isolated as a mixed Cd and Cu native complex. The CdMT and CuMT proteins were first extensively characterized in the species *Helix pomatia* [9], whereas the unspecific Cd/CuMT was initially isolated from cadmium-intoxicated garden snails (*Cantareus aspersus*) [10]. Nevertheless, its presence was later also corroborated in *H. pomatia* [11]. Since the synthesis of the *H. pomatia* Cd-specific isoform (HpCdMT) was shown to be inducible by cadmium food supplementation, and since it yielded homonuclear Cd_6-complexes, a metal detoxification role in the snail digestive tract was assigned to this peptide [12,13]. Contrarily, the Cu-specific isoform (HpCuMT), natively isolated as homonuclear Cu_{12}-complexes, is constitutively synthesized in the rhogocytes, which suggested a possible involvement in hemocyanin synthesis through storage and delivery of the required copper [14]. Further data from recombinantly-synthesized metal-complexes allowed to demonstrate that variations of the amino acid sequence interspersed between their fully conserved cysteines had led to the metal binding specificity these two *H. pomatia* MTs [11]. More recently, studies of the metal-binding behavior towards either cognate or non-cognate metal ions revealed that MT biosynthesis in the presence of the former renders unique, energetically optimized complexes, which is what outlines their metal specificity or preference. In contrast, the binding of non-cognate metal ions results in a mixture of complexes, with varied stoichiometries and folds [15]. Thus, the thermodynamic stability of the metal-MT complexes appears not exclusively related to their metal-thiolate bonds, as could have been theorized from strict chemical considerations, but is rather determined by the nature of the non-coordinating residues of each MT sequence [15].

In addition to Cys patterns and the nature of the intercalated residues, a third element that may modulate the binding behavior of an MT polypeptides are the linker stretches between the domains (metal-clusters). Their length and composition may influence the stability and independency of the metal-MT structural domains. This is a rather unexplored aspect of MT structures, mainly because the number of 3D structures available is still limited and, therefore, does not provide a sound statistical basis to study this aspect. In fact, among the 16 MT structures available in PDB [2], only one—the rat liver Zn_2, Cd_5–MT2 complex—reveals the relative orientation of the two domains. This structure displays the paradigmatic dumbbell shape that vertebrate MTs yield when they coordinate divalent metal ions: the N-terminal segment (β domain), with 9 cysteines in Cys–X–Cys arrays, which binds three M(II) ions, and the C-terminal segment (α domain), with 11 cysteines, which

binds four M(II) ions [16]. In all the other proteins, the putative independent domains have been solved independently by NMR, and were assumed to be connected more or less flexibly by the linker residues. However, for some MTs despite the absence of resolved 3D structures, some clear data have been reported, about the influence of both the linker composition and the N-term and C-term MT flanking regions for their metal binding capabilities, such as in the case of arsenic chelation by *Fucus vesiculosus* MT [17], cadmium scavenging by the type 2 *Quercus suber* QsMT [18] or, most recently, copper coordination by the two fungal *Cryptococcus neoformans* CnMT1 and CnMT2 isoforms [19].

In this report, we aimed at investigating the influence of the amino acid sequence in the linker connecting the two nine-Cys moieties of HpCdMT for the stoichiometry and folding of the corresponding Zn(II), Cd(II), or Cu(I) complexes. Although no crystal or solution structure of the Cd-HpCdMT complex is yet available (work is in progress), the results from its spectroscopic characterization fully support the existence of two domains constituting separate Cd_3Cys_9 clusters [20], as observed for the marine crustaceans [21,22] and the *C. elegans* MTs [23]. To this end, two mutant HpCdMT proteins with prolonged linkers (eight instead of the two native residues) were designed and expressed in *E. coli*. Thereafter, the metal binding behavior of these two mutants (called HpCdMcMT and HpCdPlMT from now on) was assessed for recognizing both their cognate metal ions (*i.e.*, Zn(II) and Cd(II)), but also the non-cognate monovalent Cu(I) ions, and all the data were compared with those from the wild-type HpCdMT isoform.

2. Results and Discussion

2.1. The HpCdMcMT and HpCdPlMT Recombinant Peptides

The two HpCdMT mutants designed contained longer linkers than the -KT- dipeptide of the wild type protein: one of them—that of HpCdMcMT—reproduces the one of another gastropod MT, *M. crenulata*, and exhibits a clear polar character (-VKTEAKTT-) [24]. The other linker—that of HpCdPlMT—derives from a plant MT (the wheat Ec-1 protein), and is of clear apolar composition (-SARSGAAA-) [25]. DNA sequencing of the HpCdMcMT- and HpCdPlMT-coding pGEX-4T-1 constructs ruled out any nucleotide mutation, and confirmed that the cDNAs were cloned in correct frame. After expression in *E. coli* and purification, acidification of the recombinant Zn-HpCdMcMT and Zn-HpCdPlMT samples yielded the corresponding apo-forms, with respective molecular masses of 7254.7 and 7066.6 Da, in accordance with the respective theoretical values of 7255.7 and 7067.9 Da (Figures 1 and 2). This confirmed the correctness of both synthesized proteins.

```
HpCdMT    GSGKGKGEKCTSACRSEPCQCGSKCQCGEGCTCAAC---KT---CNCTSDGCKCGKECTGPDSCKCGSSCSCK
HpCdMcMT  GSGKGKGEKCTSACRSEPCQCGSKCQCGEGCTCAACVKTEAKTTCNCTSDGCKCGKECTGPDSCKCGSSCSCK
HpCdPlMT  GSGKGKGEKCTSACRSEPCQCGSKCQCGEGCTCAACSARSGAAACNCTSDGCKCGKECTGPDSCKCGSSCSCK
```

Figure 1. Sequence alignment of the recombinant proteins studied in this work: the constructs HpCdMcMT and HpCdPlMT are aligned with the HpCdMT wild-type form. The Cys residues are written in red, and the linker residues are shaded in grey. The initial Gly, which is a remainder from the thrombin cleavage site, is printed in italics.

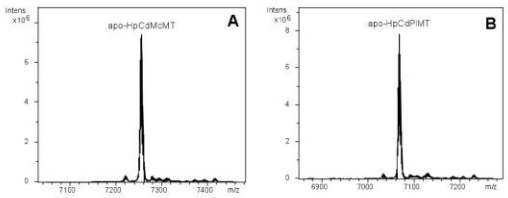

Figure 2. Deconvoluted ESI-MS spectra of the recombinant preparations of (**A**) HpCdMcMT; and (**B**) HpCdPlMT purified from bacterial cultures grown under Zn-supplementation, analyzed at acid pH (2.4).

2.2. Zn and Cd Binding Abilities of HpCdMcMT and HpCdPlMT

Both HpCdMcMT and HpCdPlMT polypeptides synthesized in Zn-supplemented *Escherichia coli* cultures folded into unique Zn_6-complexes, (*cf.* the ESI-MS spectra shown in Figure 3A, where only very minor, negligible accompanying peaks are detected, attributable to frequently observed NH_4^+ adducts, and Table 1). The syntheses in Cd-supplemented cultures equally yielded almost unique peaks corresponding to the Cd_6-complexes of both peptides, as identified in the respective ESI-MS analyses at neutral pH (Figure 3A and Table 1). These results fully coincide with the Zn- and Cd-species afforded by the wild-type HpCdMT synthesized under equivalent conditions, that affords unique $M(II)_6$ complexes, as we demonstrated in [11]. Analysis of the CD spectra of the Zn- and Cd-preparations of HpCdMcMT and HpCdPlMT totally confirmed that these two mutants exhibit equivalent folds when coordinating Zn(II) ions, and also when coordinating Cd(II) ions, which are also practically indistinguishable from those of the respective wild-type HpCdMT complexes (Figure 3B). For example, the Zn-MT complexes show the typical Gaussian band centred at *ca.* 240 nm, while the Cd-MT species display the exciton coupling envelop at *ca.* 250 nm characteristic of the Zn- and Cd-thiolate chromophores.

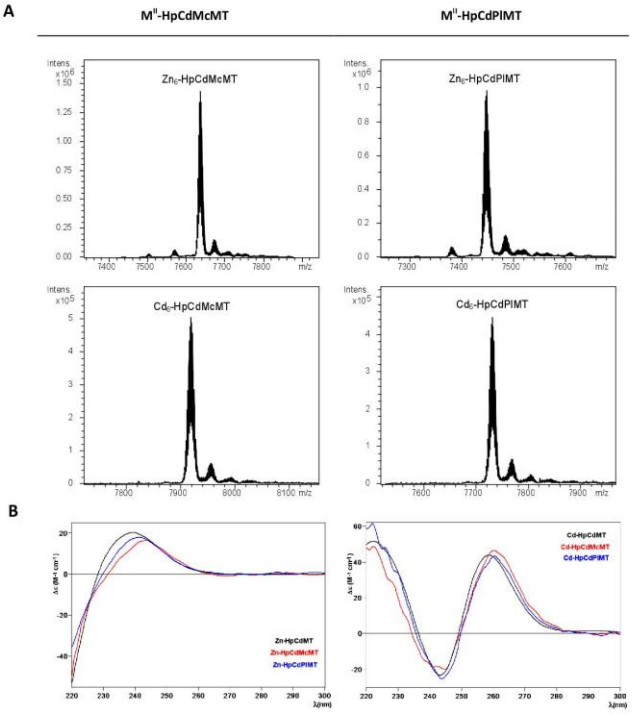

Figure 3. Analysis of the Zn- and Cd-HpCdMcMT and -HpCdPlMT complexes. (**A**) Deconvoluted ESI-MS spectra of the recombinant preparations of HpCdMcMT and HpCdPlMT purified from Zn- and Cd-supplemented cultures, analyzed at neutral pH (7.0); (**B**) CD spectra of the corresponding recombinant preparations. For comparative purposes, the CD spectra of the recombinant preparations yielded by the wild-type HpCdMT protein [11] have been included.

Table 1. Analytical characterization of the recombinant Zn(II)- and Cd(II)-complexes of the HpCdMT mutants studied in this work. For comparative purposes, data for the recombinantly-synthesized wild-type HpCdMT are included [11].

MT	ICP-AES [a]	Neutral ESI-MS [b]	Experimental MM [c]	Calculated MM [d]
HpCdMT [11]	5.8	Zn_6-MT	7005	7005.6
HpCdMcMT	5.9	Zn_6-MT	7635	7635.6
HpCdPlMT	6.0	Zn_6-MT	7448	7448.3
HpCdMT [11]	6.2	Cd_6-MT	7287	7287.8
HpCdMcMT	6.1	Cd_6-MT	7917	7917.7
HpCdPlMT	6.6	Cd_6-MT	7730	7730.4

[a] Zn(II)-to-peptide ratio calculated from S and Zn content (ICP-AES data); [b] The deduced Zn(II)-species were calculated from the mass difference between the holo- and apo-peptides; [c] experimental molecular masses corresponding to the detected M(II)-complexes. The corresponding ESI-MS spectra are shown in Figure 3; [d] theoretical molecular masses corresponding to the M(II)-complexes.

Furthermore, the Zn^{2+}/Cd^{2+} displacement process in Zn_6-HpCdMcMT and Zn_6-HpCdPlMT was a straight reaction that exclusively yielded Cd_6-complexes after the addition of 6 Cd^{2+} eq (Figure 4A,B, respectively), in agreement with the behavior in wild-type Zn_6-HpCdMT [15]. Most significantly, not only the final step of this reaction was the same, and also equivalent to the respective recombinant Cd-complexes, but CD spectra recorded at progressive stages of the reaction revealed identical profiles (*cf.* Figure 4). These basically consist in the evolution of the initial Gaussian band at *ca.* 240 nm characteristic of the Zn-complexes to the exciton-coupling signal centered at *ca.* 250 nm, typical of Cd-complexes. This suggests that the Zn(II)/Cd(II) substitution proceeds in an almost parallel way in all three cases, *i.e.*, for the wild-type HpCdMT and for the two mutant forms.

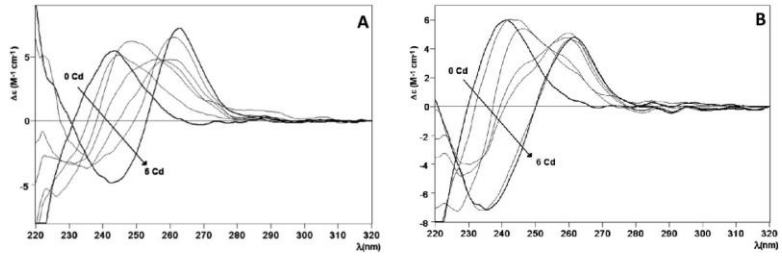

Figure 4. Zn(II)/Cd(II) replacement reaction of the Zn-HpCdMcMT and Zn-HpCdPlMT complexes. (**A**) CD spectra of a 10 μM solution of the Zn-HpCdMcMT sample titrated with $CdCl_2$ at neutral pH up to six Cd(II) equivalent; (**B**) CD spectra of a 10 μM solution of the Zn-HpCdPlMT sample titrated with $CdCl_2$ at neutral pH, up to six Cd(II) equivalent.

Therefore, it can be concluded that the different composition of the amino acid sequence linking the two putative domains of the HpCdMT proteins does affect neither the stoichiometry nor the folding of the complexes formed when coordinating divalent metal ions. To conclude, the linker length and compositions do not seem to alter the binding behavior towards a cognate metal ion.

2.3. Cu Binding Abilities of HpCdMcMT and HpCdPlMT

Before going into the details of the Cu(I) binding analysis of the two mutant constructs HpCdMcMT and HpCdPlMT, it is worth remembering that the data of the previous Cu(I) binding study performed with the wild-type HpCdMT form already exhibited a high degree of complexity, typical of the recombinant samples obtained when synthesizing a MT protein (here HpCdMT) in the presence of its non-cognate metal ion (here Cu(I)) [15]. As previously described [26], we perform two types of Cu-supplemented productions: at standard and at low aeration conditions.

This responds to the known influence of culture oxygenation on the amount of internal copper in bacteria, which determines the composition of the final Cu-species. But unfortunately, several efforts to purify HpCdMcMT and HpCdPlMT from *E. coli* cultures grown at low oxygen conditions were not successful. Contrarily, the synthesis of both polypeptides performed at regular oxygen conditions yielded preparations that allowed their analysis by ESI-MS and CD, and facilitated the comparison of all their features with those of the complexes obtained from HpCdMT.

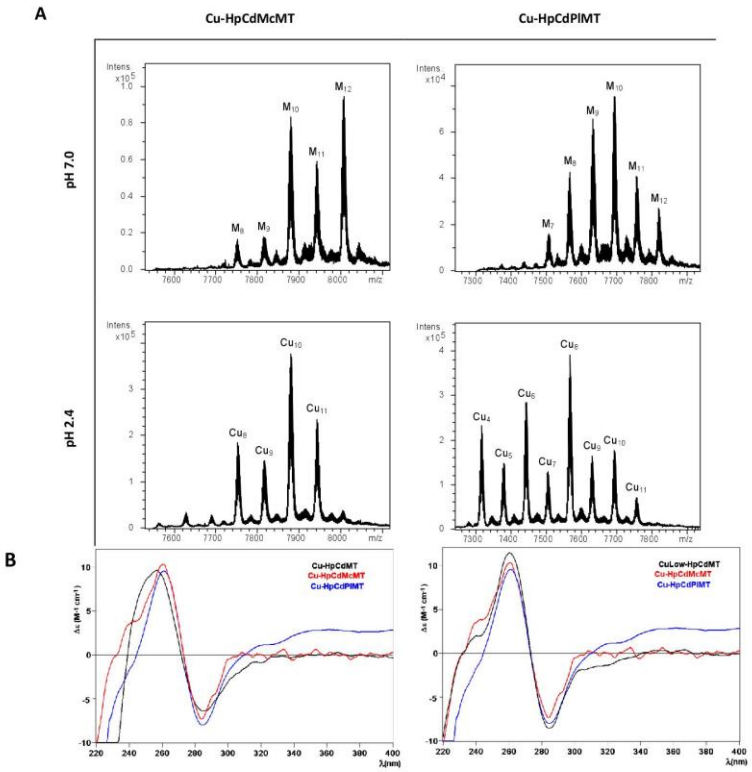

Figure 5. Analysis of the Cu-HpCdMcMT and Cu-HpCdPlMT complexes. (**A**) Deconvoluted ESI-MS spectra of the recombinant preparations of HpCdMcMT and HpCdPlMT purified from Cu-supplemented cultures, analyzed at neutral pH (7.0); (**B**) CD spectra of the same recombinant preparations. For comparative purposes, the CD spectra of the corresponding recombinant preparations yielded by the wild-type HpCdMT protein [15] have been included.

The first noticeable observation was that the composition of the Cu-HpCdMcMT and Cu-HpCdPlMT purified samples was significantly different, and in turn different from that of the wild-type Cu-HpCdMT preparations [15]. For example, the ESI-MS spectra of the Cu-HpCdMcMT sample recorded at neutral pH exhibited two clear major peaks corresponding to M_{12}- and M_{10}-HpCdMcMT complexes, an intermediate M_{11}-HpCdMT and very minor M_9- and M_8-HpCdMcMT species (Figure 5A, Table 2), where M can be either Zn(II) or Cu(I) because the similarity of their atomic masses. When this same preparation was analyzed at pH 2.4—which allows the release of all bound Zn(II) but not of Cu(I) [27,28]—one major peak corresponding to homonuclear Cu_{10}-HpCdMT together with minor peaks of Cu_{11}-, Cu_8- and Cu_9-complexes were observed (Figure 5A, Table 2). Taking into consideration that the ICP-AES analyses of the purified Cu-HpCdMcMT sample yielded an average metal content of 1.32 Zn and 12.25 Cu per MT,

the most straightforward explanation for these results is to assume the presence of a mixture of major homonuclear complexes (Cu_{11}-, Cu_{10}-, Cu_9- and Cu_8-HpCdMcMT) together with some minor amounts of heteronuclear CuZn-HpCdMcMT species, mainly accounting for the M_{12}-HpCdMcMT species. On the other hand, a slightly poorer Cu-binding capacity can be attributed to HpCdPlMT for the following reasons: First, the ICP-AES analysis indicated a Zn:Cu mean content in the purified preparation of 2.17 Zn:7.87 Cu, corresponding to higher Zn:Cu ratio than in the HpCdMcMT sample. Second, the Cu-HpCdPlMT sample presents a more complex mixture, in terms of the number of ESI-MS detected species, both at neutral and acid pH. Thus, the ESI-MS spectrum at pH 7.0 allows the detection of a major M_{10}-HpCdPlMT peak, followed by M_9-, M_{11}-, M_8-, M_{12}-, and M_7-HpCdPlMT species, in decreasing order of intensity. This sample exhibited a mixture of major Cu_8-, and then minor Cu_6-, Cu_4-, and all the rest of peaks between Cu_4- and Cu_{11}-HpCdPlMT when analyzed at acidic ESI-MS, which would point to a continuum of heterometallic ZnCu-HpCdPlMT species (Figure 5A, Table 2).

Table 2. Analytical characterization of the recombinant complexes obtained from Cu supplemented cultures of the HpCdMT mutants studied in this work. All data for the two mutant proteins correspond to normal aerated cultures, since no complexes could be recovered from low aeration conditions. For comparative purposes, data for the wild-type HpCdMT, recombinantly-synthesized in Cu-supplemented cultures grown at both aeration conditions, are included [15].

MT	ICP-AES [a]	Neutral ESI-MS [b]	MM_{Exp} [c]	MM_{Theor} [d]	Acidic ESI-MS [b]	MM_{Exp} [c]	MM_{Theor} [d]
HpCdMT Normal aeration [15]	2.6 Zn 1.9 Cu	**M_5-MT**	6932	6938.1			
		M_4-MT	6867	6875.5	**apo-MT**	6623	6625.5
		M_6-MT	6996	7000.6	Cu_4-MT	6873	6875.5
		M_7-MT	7062	7063.2	Cu_5-MT	6930	6938.1
		M_8-MT	7124	7125.7			
HpCdMT Low aeration [15]	0.8 Zn 8.3 Cu	**M_{10}-MT**	7251	7250.8	**Cu_8-MT**	7120	7,125.7
		M_{11}-MT	7313	7313.4	Cu_{10}-MT	7248	7,250.8
		M_{12}-MT	7379	7375.9	Cu_{11}-MT	7312	7313.4
		M_8-MT	7122	7125.9	Cu_9-MT	7184	7188.3
		M_9-MT	7182	7188.3	Cu_5-MT	6929	6938.1
HpCdMcMT	1.3 Zn 12.3 Cu	**M_{12}-MT**	8006	8005.8			
		M_{10}-MT	7878	7880.7	**Cu_{10}-MT**	7879	7880.7
		M_{11}-MT	7942	7943.3	Cu_{11}-MT	7942	7943.3
		M_9-MT	7816	7818.2	Cu_8-MT	7753	7755.6
		M_8-MT	7753	7755.6	Cu_9-MT	7816	7818.2
HpCdPlMT	2.2 Zn 7.9 Cu				**Cu_8-MT**	7566	7568.3
		M_{10}-MT	7692	7693.4	Cu_6-MT	7442	7443.2
		M_9-MT	7631	7630.9	Cu_4-MT	7316	7318.1
		M_8-MT	7566	7568.3	Cu_{10}-MT	7692	7693.4
		M_{11}-MT	7755	7755.9	Cu_9-MT	7629	7630.9
		M_{12}-MT	7818	7818.5	Cu_5-MT	7377	7380.7
		M_7-MT	7505	7505.8	Cu_7-MT	7503	7505.8
					Cu_{11}-MT	7755	7755.9

[a] Zn(II) and Cu(I)-to-peptide ratio calculated from S, Zn, and Cu content (ICP-AES data); [b] the deduced species (M = Zn or Cu) were calculated from the mass difference between the holo- and the respective apo-peptides. The major species are indicated in bold, and the rest are in decreasing order of ESI-MS peak intensity; [c] experimental molecular masses corresponding to the detected complexes. The corresponding ESI-MS spectra are shown in Figure 5; [d] theoretical molecular masses corresponding to the metal-complexes.

Finally, comparison of these results with those from the wild-type HpCdMT protein also differed considerably (included in Table 2 for comparative purposes). Synthesis of Cu-HpCdMT yielded very poor results when performed in normally aerated cultures [15], only allowing recognizing major M_5-HpCdMT and minor M_4- to M_8-complexes that contained Cu_4- or Cu_5-cores. In fact, the results for the two mutant constructs analyzed in this work resembled far more those of Cu-HpCdMT produced in low aerated cultures, this means in the presence of higher intracellular copper levels,

because in that case also major M_{10}-HpCdMT, together with minor M_8- to M_{12}-complexes were identified by neutral ESI-MS, which were composed of major Cu_8-cores [15]. However, despite the diversity of results about the species composition yielded from the three HpCdMT proteins when coordinating Cu(I), they all gave rise to comparable CD signals, both in shape and intensity, which display the typical envelope of the Cu-MT complexes with absorption maxima at *ca.* 260 nm and minima at *ca.* 280 nm. The CD fingerprint of the Cu-HpCdMcMT and Cu-HpCdPlMT samples was more similar to that of the Cu-HpCdMT synthesized at low aeration [15] (Figure 5B), in concordance with the above-commented species composition.

Therefore, it can be unambiguously concluded that the inter-domain linker features (length and composition) greatly influences the Cu(I) binding behavior of the HpCdMT protein, so that the capacity to bind Cu(I) for the mutant HpCdMcMT and HpCdPlMT constructs, with eight amino acid-long linkers between the ninth and tenth Cys in their sequence, appears considerably enhanced in comparison with HpCdMT whose linker contains only two residues between the homologous Cys residues (*cf.* Figure 1). However, the differences in Cu-binding capabilities between HpCdMcMT and HpCdPlMT reveals that not only the length, but also the composition of the linker is important. Hence, the linker of the HpCdMcMT construct, containing two lysine, one glutamic acid and three threonine residues, seems to favor the formation of higher nuclearity homonuclear Cu(I) complexes, over the highly apolar HpCdPlMT linker, that is composed of only one arginine and two serine residues and that also contains five apolar amino acids (four alanine and a glycine).

3. Experimental Section

3.1. Construction and Cloning of the cDNAs Encoding the HpCdMT Linker Mutants

Two HpCdMT mutants were designed to replace the only two residues (-KT-) that act as a linker between the two nine-Cys domains in the HpCdMT sequence with the corresponding linkers from the (giant keyhole limpet) *M. crenulata* MT [24] (-VKTEAKTT-; HpCdMcMT protein) or from wheat (*T. aestivum*) Ec-1 MT [25] (-SARSGAAA-; HpCdPlMT protein) (Figure 1). The cDNAs encoding for these sequences were designed on the basis of the flanking regions in wild-type HpCdMT cDNA, and to encode the new linkers in the corresponding limpet or wheat cDNAs. Additionally, the restriction sites for *BamH*I and *Xho*I were added to the 5′ and 3′ ends respectively for cloning purposes (Supplementary Materials, Figure S1). The HpCdMcMT and HpCdPlMT coding sequences designed this way were purchased as synthetic DNAs from ID & Conda Labs (Spain). After PCR amplification (35 cycles: 95 °C 30 s, 50 °C 30 s, and 72 °C 30 s, using Expand High Fidelity (Roche) thermostable DNA polymerase) of the synthetic cDNAs using the flanking primers: 5′-TTTATTGGATCCGGTAAGGG-3′ (HpCdMcMT forward); 5′-TTTCTCGAGTTACTTACAGG-3′ (HpCdMcMT reverse); 5′-TTTATTGGATCCGGCAAAGGG-3′ (HpCdPlMT forward); and 5′-TTTCTCGAGTTATTTGCAAG-3′ (HpCdPlMT reverse). They were subsequently digested with *BamH*I and *Xho*I restriction enzymes, and the resulting products were ligated in-frame (DNA ligation kit, Takara Bio, Kusatsu, Shiga, Japan) in the pGEX-4T-1 (Amersham-GE Healthcare Europe, Cerdanyola del Valles, Spain) *E. coli* expression vector, which yields GST-fusion proteins. DNA sequencing allow confirming all the DNA constructs (ABIPRISM 310, Applied Biosystems, Foster City, CA, USA), using BigDye Terminator. The *E. coli* MachI strain was used for cloning and sequencing. The expression plasmids were then transformed into the protease-deficient strain BL21 for protein synthesis. The construction of the pGEX plasmid encoding for the wild type HpCdMT isoform has been previously described [11].

3.2. Synthesis and Purification of the Recombinant Zn-, Cd-, and Cu-Complexes of the HpCdMT Linker Mutants

All the purifications of the metal-MT complexes were carried out as reported in [29] for the wild-type HpCdMT isoform, which ensured full comparative results. Hence, the GST-HpCdMT

fusions were produced in 5-L cultures (Luria Bertani medium) of transformed *E. coli* BL21 bacteria. Induction of gene expression was achieved with 100 μM (final concentration) of isopropyl β-D-thiogalactopyranoside (IPTG). After 30 min of induction, 300 μM $ZnCl_2$ or 500 μM $CuSO_4$ (final concentration) were supplemented to the cultures, which grew for a further 2.5 h, for the synthesis of the respective metal complexes. The Cu-cultures were grown both under normal (1-L medium in a 2-L Erlenmeyer flask, at 250 rpm) and low oxygen conditions (1.5-L medium in a 2-L Erlenmeyer flask at 150 rpm). It is well known that the culture aeration determines the amount of intracellular copper in the host cells available for the newly synthesized MTs [26].

Harvesting and centrifugation of the grown cells renders a cell mass that, resuspended in ice-cold PBS (1.4 M NaCl, 27 mM KCl, 101 mM Na_2HPO_4, 18 mM KH_2PO_4) with 0.5% *v*/*v* β-mercaptoethanol, is disrupted by sonication (20 s pulses for 5 min). All solutions used were oxygen-purged by saturating them with pure-grade argon to prevent metal-MT oxidation. The suspension was centrifuged at 12,000× *g* for 30 min, and the incubation of the resulting supernatant (gentle agitation for 60 min at room temperature) with Glutathione-Sepharone 4B (GE Healthcare) allowed batch affinity purification of the GST-HpCdMT species. The MT portion was recovered after thrombin cleavage (10 μ per mg of fusion protein at 17 °C over-night). The solution containing the cleaved metal-MT complexes was concentrated by Centriprep Microcon 3 (Amicon, cut-off of 3 kDa, Merck-Millipore, Darmstadt, Germany) centrifugation. The final metal complexes were purified through FPLC size-exclusion chromatography in a Superdex75 column (GE Healthcare) equilibrated with 50 mM Tris-HCl, pH 7.0 and run at 0.8 mL· min^{-1}. Absorbances at 254 and 280 nm signaled the fractions to be collected and analyzed for protein content.

3.3. Cd(II) Replacement Reactions with the Zn(II)-HpCdMT Mutants

The so-called "*in vitro* complexes" were obtained by metal displacement reactions using the recombinant Zn-HpCdMT preparations, by adding several molar equivalents of Cd^{2+} ions from a standard solution. As described elsewhere [29], the titrations were performed at pH 7.0, and all assays were performed under an Ar atmosphere. The pH remained constant throughout all experiments without the addition of any extra buffers.

3.4. Spectroscopic Analyses (ICP-AES and CD) of the Metal Complexes Formed by the HpCdMT Linker Mutants

The sulfur and metal content of all the metal-MT samples was determined by Inductively Coupled Plasma Atomic Emission Spectroscopy (ICP-AES) in a Polyscan 61E (Thermo Jarrel Ash, Franklin, MA, USA) spectrometer, measuring S at 182.040 nm, Zn at 213.856 nm, and Cu at 324.803 nm. Conventional treatment [30] and incubation in 1 M HNO_3 at 65 °C for 10 min before measurements to avoid possible traces of labile sulfide anions [31] were used to obtain the protein concentration, by considering that all S atoms were provided by the MT peptides.

CD measurements were performed at 25 °C in a Jasco spectropolarimeter (Model J-715, JASCO, Groß-Umstadt, Germany) interfaced to a computer (J700 software, JASCO, Groß-Umstadt, Germany) by using Peltier PTC-351S equipment (TE Technology, Traverse City, MI, USA). An HP-8453 Diode array UV-VIS spectrophotometer (GIM, Ramsey, MN, USA) was used for the electronic absorption measurements. 1-cm capped quartz cuvettes were employed for spectra recording, and the dilution effects were corrected and processed using the GRAMS 32 software (Thermo Fisher Scientific, Waltham, MA, USA).

3.5. Electrospray Ionization Time-of-Flight Mass Spectrometry (ESI-TOF MS) of the Metal Complexes Obtained from the HpCdMT Linker Mutants

A Micro TOF-Q instrument (Bruker Daltonics, Bremen, Germany) interfaced with a Series 1200 HPLC Agilent pump and equipped with an autosampler, all of which controlled by the Compass Software, allowed MW determinations by Electrospray ionization time-of-flight mass spectrometry

(ESI-TOF MS). ESI-L Low Concentration Tuning Mix (Agilent Technologies, Santa Clara, CA, USA) was used for calibration. The conditions for the Zn-MT complex analyses were the following: 20 µL of sample solution injected through a PEEK (polyether heteroketone) tubing (1.5 m–0.18 mm i.d.) at 40 µL· min^{-1}; capillary counter-electrode voltage 5 kV; desolvation temperature 90–110 °C; dry gas 6 L· min^{-1}; spectra collection range 800–2500 m/z. A 5:95 mixture of acetonitrile:ammonium acetate (15 mM, pH 7.0) was the carrier buffer.

The conditions for the Cu-MT complex analyses were: 20 µL of sample solution injected at 40 µL· min^{-1}; capillary counter-electrode voltage 3.5 kV; lens counter-electrode voltage 4 kV; dry temperature 80 °C; dry gas 6 L· min^{-1}; and a 10:90 acetonitrile:ammonium acetate 15 mM, pH 7.0 mixture as carrier. The apo-proteins and the Cu-complexes at acid pH were analyzed following the same conditions previously described, but using a liquid carrier consisting of a 5:95 acetonitrile:formic acid mixture at pH 2.4. This causes the release of Zn(II), but keeps Cu(I) bound to the peptides. Experimental mass values were calculated as described in [32], and the error associated with the measurements resulted to be always smaller than 0.1%.

4. Conclusions

In summary, in this study we investigated the influence of the polypeptide region linking the two nine-Cys moieties of the CdHpMT isoform, hypothesized to give rise to two independent domains when coordinating divalent metal ions, into the stoichiometry and folding of the corresponding complexes. This was performed by constructing two mutant CdHpMT proteins with longer linkers than the wild-type (eight instead of the two residues), one of them derived from another snail MT sequence: *M. crenulata*, with a clear polar character (HpCdMcMT); and the other derived from a plant MT (the wheat Ec-1 protein), of clear apolar composition (HpCdPlMT). Thereafter, the metal binding behavior of the two mutants was assessed not only for the CdHpMT cognate metal ions (*i.e.*, the divalent Zn(II) and Cd(II)), but also for the non-cognate monovalent Cu(I) ions. The results clearly show that both HpCdMcMT and HpCdPlMT form unique Zn_6- and Cd_6-complexes, of the same stoichiometry than HpCdMT, and with indistinguishable CD fingerprints. On the contrary, when synthesized in normally-aerated Cu-enriched cultures, the two mutants behave like the wild-type form only in the sense that they yielded a mixture of heterometallic species—expected from their character as non-Cu-thioneins—but otherwise they differed a lot, in comparison to each other as well as in comparison to the wild-type protein. Hence, HpCdMcMT (with a polar linker) yields major M_{12}-species (M = Zn or Cu), with Cu_{10} and Cu_{11} cores, and HpCdPlMT (with an apolar linker) yields major M_{10}-species (M = Zn or Cu), with a major Cu_8 core (M = Zn or Cu). Under the same culture conditions, HpCdMT was only capable of folding into major M_5-species (M = Zn or Cu), with a Cu_4 core, and only when synthesized at high intracellular Cu concentrations (low culture aeration), similarly to HpCdPlMT major M_{10}-species (M = Zn or Cu) with Cu_8 cores were observed. No Cu(I)-MT complexes were obtained for the mutants at low oxygenation conditions, a fact that is in agreement with the observation that Cu(I)-complexes formed by Cu-thioneins unfold at high Cu concentrations, as has been described for *Drosophila* MtnE [33] or even *M. crenulata* MT [24].

To summarize, variation of the linker (length and amino acid features) does not alter the divalent metal ion (Zn(II) or Cd(II)) binding behavior of HpCdMT, probably because of the independence of the two separate domains. In contrast, variation of the linker (length and sequence) has an influence on the Cu(I) binding behavior of this MT, so that the mutants with the elongated linker better bind Cu(I) ions compared to the wild-type form. Moreover, the more polar the linker, the higher the Cu-thionein character of the protein, as shown by the higher nuclearity and the higher Cu *vs.* Zn content of the heterometallic species resulting from biosynthesis in Cu-enriched cultures. Interestingly, the *C. aspersus* Cu-specific MT (CaCuMT), which has a four-amino acid linker, exhibits a better Cu-binding behavior than the orthologous HpCuMT isoform, which possesses a two-residue linker [34]. This fact is worth considering even if Cu(I) is the non-cognate metal ion for this isoform,

because it can provide valuable information about the determinants of the Cu(I) binding capabilities of a great number of MTs with intermediate Zn- *vs.* Cu-thionein character [8].

Supplementary Materials: Supplementary materials can be found at http://www.mdpi.com/1422-0067/17/1/6/s1.

Acknowledgments: This work was supported by the DACH (International Cooperation) Project ref. I-1482-N28 of the Austrian Science Fund (FWF) to RD and the Swiss National Science Foundation (SNF) to OZ. Authors from both Barcelona universities are members of the 2014SGR-423 Grup de Recerca de la Generalitat de Catalunya, and they are recipients of MINECO-FEDER grants (BIO2012-39682-C02-01 to SA), and (BIO2012-39682-C02-02 to MC). We thank the Centres Científics i Tecnològics (CCiT) de la Universitat de Barcelona (ICP-AES, DNA sequencing) and the Servei d'Anàlisi Química (SAQ) de la Universitat Autònoma de Barcelona (CD, UV-vis, ESI-MS) for allocating instrument time.

Author Contributions: Oliver Zerbe, Reinhard Dallinger, Mercè Capdevila and Sílvia Atrian designed experiments and discussed the results. Elena Jiménez-Martí performed the cloning and recombinant synthesis of the analyzed proteins and Selene Gil-Moreno and Òscar Palacios performed their ESI-MS and CD characterization. Òscar Palacios, Mercè Capdevila and Sílvia Atrian prepared the manuscript.

Conflicts of Interest: The authors declare no conflict of interest.

References

1. Capdevila, M.; Bofill, R.; Palacios, O.; Atrian, S. State-of-the-art of metallothioneins at the beginning of the 21st century. *Coord. Chem. Rev.* **2012**, *256*, 46–62. [CrossRef]
2. Blindauer, C. Metallothioneins. In *RSC Metallobiology: Binding, Transport and Storage of Metal Ions in Biological Cells*; Maret, W., Wedd, A., Eds.; The Royal Society of Chemistry: Cambridge, UK, 2014; Volume 2, pp. 594–653.
3. Capdevila, M.; Atrian, S. Metallothionein protein evolution: A miniassay. *J. Biol. Inorg. Chem.* **2011**, *16*, 977–989. [CrossRef] [PubMed]
4. Kägi, J.H.R.; Kojima, Y. Chemistry and biochemistry of metallothionein. In *Metallothionein II*; Kägi, J.H.R., Kojima, Y., Eds.; Birkhäuser Verlag: Basel, Switzerland, 1987; pp. 25–61.
5. Binz, P.A.; Kägi, J.H.R. Metallothionein: Molecular evolution and classification. In *Metallothionein IV*; Klassen, C.D., Ed.; Birkhäuser Verlag: Basel, Switzerland, 1999; pp. 7–13.
6. Palacios, O.; Atrian, S.; Capdevila, M. Zn- and Cu-thioneins: A functional classification for metallothioneins? *J. Biol. Inorg. Chem.* **2011**, *16*, 991–1009. [CrossRef] [PubMed]
7. Valls, M.; Bofill, R.; González-Duarte, R.; González-Duarte, P.; Capdevila, M.; Atrian, S. A new insight into metallothionein classification and evolution. The *in vivo* and *in vitro* metal binding features of *Homarus americanus* recombinant MT. *J. Biol. Chem.* **2001**, *276*, 32835–32843. [CrossRef] [PubMed]
8. Bofill, R.; Capdevila, M.; Atrian, S. Independent metal-binding features of recombinant metallothioneins convergently draw a step gradation between Zn- and Cu-thioneins. *Metallomics* **2009**, *1*, 229–234. [CrossRef] [PubMed]
9. Dallinger, R.; Berger, B.; Hunziker, P.E.; Kägi, J.H.R. Metallothionein in snail Cd and Cu metabolism. *Nature* **1997**, *388*, 237–238. [CrossRef] [PubMed]
10. Hispard, F.; Schuler, D.; de Vaufleury, A.; Scheifler, R.; Badot, P.M.; Dallinger, R. Metal distribution and metallothionein induction after cadmium exposure in the terrestrial snail *Helix aspersa* (Gastropoda, Pulmonata). *Environ. Toxicol. Chem.* **2008**, *27*, 1533–1542. [CrossRef] [PubMed]
11. Palacios, O.; Pagani, A.; Pérez-Rafael, S.; Egg, M.; Höckner, M.; Brandstätter, A.; Capdevila, M.; Atrian, S.; Dallinger, R. Shaping mechanisms of metal specificity in a family of metazoan metallothioneins: Evolutionary differentiation of mollusc metallothioneins. *BMC Biol.* **2011**, *9*, 4. [CrossRef] [PubMed]
12. Chabicovsky, M.; Klepal, W.; Dallinger, R. Mechanisms of cadmium toxicity in terrestrial pulmonates: Programmed cell death and metallothionein overload. *Environ. Toxicol. Chem.* **2004**, *23*, 648–655. [CrossRef] [PubMed]
13. Chabicovsky, M.; Niederstaetter, H.; Thaler, R.; Hödl, E.; Parson, W.; Rossmanith, W.; Dallinger, R. Localisation and quantification of Cd- and Cu-specific metallothionein isoform mRNA in cells and organs of the terrestrial gastropod *Helix pomatia*. *Toxicol. Appl. Pharmacol.* **2003**, *190*, 25–36. [CrossRef]

14. Dallinger, R.; Chabicovsky, M.; Hödl, E.; Prem, C.; Hünziker, P.; Manzl, C. Copper in *Helix pomatia* (Gastropoda) is regulated by one single cell type: Differently responsive metal pools in rhogocytes. *Am. J. Physiol.* **2005**, *189*, R1185–R1195. [CrossRef] [PubMed]
15. Palacios, O.; Pérez-Rafael, S.; Pagani, A.; Dallinger, R.; Atrian, S.; Capdevila, M. Cognate and noncognate metal ion coordination in metal-specific metallothioneins: The *Helix pomatia* system as a model. *J. Biol. Inorg. Chem.* **2014**, *19*, 923–935. [CrossRef] [PubMed]
16. Braun, W.; Vasak, M.; Robbins, A.H.; Stout, C.D.; Wagner, G.; Kagi, J.H.; Wuthrich, K. Comparison of the NMR solution structure and the x-ray crystal structure of rat metallothionein-2. *Proc. Natl. Acad. Sci. USA* **1992**, *89*, 10124–10128. [CrossRef] [PubMed]
17. Ngu, T.T.; Lee, J.A.; Rushton, M.K.; Stillman, M.J. Arsenic metalation of seaweed *Fucus vesiculosus* metallothionein: The importance of the interdomain linker in metallothionein. *Biochemistry* **2009**, *48*, 8806–8816. [CrossRef] [PubMed]
18. Domenech, J.; Orihuela, R.; Mir, G.; Molinas, M.; Atrian, S.; Capdevila, M. The Cd^{2+}-binding abilities of recombinant *Quercus suber* metallothionein, QsMT: Bridging the gap between phytochelatins and metallothioneins. *J. Biol. Inorg. Chem.* **2007**, *12*, 867–882. [CrossRef] [PubMed]
19. Espart, A.; Gil-Moreno, S.; Palacios, P.; Capdevila, M.; Atrian, S. Understanding the internal architecture of long metallothioneins: 7-Cys building blocks in fungal (*C. neoformans*) MTs. *Mol. Microbiol.* **2015**. [CrossRef]
20. Dallinger, R.; Wang, Y.; Berger, B.; Mackay, E.A.; Kägi, J.H.R. Spectroscopic characterization of metallothionein from the terrestrial snail, *Helix pomatia*. *Eur. J. Biochem.* **2001**, *268*, 4126–4133. [CrossRef] [PubMed]
21. Zhu, Z.; de Rose, E.F.; Mullen, G.P.; Petering, D.H.; Shaw, C.F., III. Sequential proton resonance assignments and metal cluster topology of lobster metallothionein-1. *Biochemistry* **1994**, *33*, 8858–8865. [CrossRef] [PubMed]
22. Narula, S.S.; Brouwer, M.; Hua, Y.; Armitage, I.M. Three-dimensional structure of *Callinectes sapidus* metallothionein-1 determined by homonuclear and heteronuclear magnetic resonance spectroscopy. *Biochemistry* **1995**, *34*, 620–631. [CrossRef] [PubMed]
23. Bofill, R.; Orihuela, R.; Romagosa, M.; Domenech, J.; Atrian, S.; Capdevila, M. *C. elegans* metallothionein isoform specificity: Metal binding abilities and histidine role in CeMT1 and CeMT2. *FEBS J.* **2009**, *276*, 7040–7056. [CrossRef] [PubMed]
24. Perez-Rafael, S.; Mezger, A.; Lieb, B.; Dallinger, R.; Capdevila, M.; Palacios, O.; Atrian, S. The metal binding abilities of *Megathura crenulata* metallothionein (McMT) in the frame of gastropoda MTs. *J. Inorg. Biochem.* **2012**, *108*, 84–90. [CrossRef] [PubMed]
25. Peroza, E.A.; Schmucki, R.; Güntert, P.; Freisinger, E.; Zerbe, O. The β(E)-domain of wheat E(c)-1 metallothionein: A metal-binding domain with a distinctive structure. *J. Mol. Biol.* **2009**, *387*, 207–218. [CrossRef] [PubMed]
26. Pagani, A.; Villarreal, L.; Capdevila, M.; Atrian, S. The *Saccharomyces cerevisiae* Crs5 metallothionein metal-binding abilities and its role in the response to zinc overload. *Mol. Microbiol.* **2007**, *63*, 256–269. [CrossRef] [PubMed]
27. Orihuela, R.; Domenech, J.; Bofill, R.; You, C.; Mackay, E.A.; Kägi, J.H.R.; Capdevila, M.; Atrian, S. The metal-binding features of the recombinant mussel *Mytilus edulis* MT-10-IV metallothionein. *J. Biol. Inorg. Chem.* **2008**, *13*, 801–812. [CrossRef] [PubMed]
28. Palacios, O.; Espart, A.; Espín, J.; Ding, C.; Thiele, D.J.; Atrian, S.; Capdevila, M. Full characterization of the Cu-, Zn- and Cd-binding properties of CnMT1 and CnMT2, two metallothioneins of the pathogenic fungus *Cryptococcus neoformans* acting as virulence factors. *Metallomics* **2014**, *6*, 279–291. [CrossRef] [PubMed]
29. Capdevila, M.; Cols, N.; Romero-Isart, N.; Gonzalez-Duarte, R.; Atrian, S.; Gonzalez-Duarte, P. Recombinant synthesis of mouse Zn3-β and Zn4-α metallothionein 1 domains and characterization of their cadmium(II) binding capacity. *Cell. Mol. Life Sci.* **1997**, *53*, 681–688. [CrossRef] [PubMed]
30. Bongers, J.; Walton, C.D.; Richardson, D.E.; Bell, J.U. Micromolar protein concentrations and metalloprotein stoichiometries obtained by inductively coupled plasma. Atomic emission spectrometric determination of sulfur. *Anal. Chem.* **1988**, *60*, 2683–2686. [CrossRef] [PubMed]
31. Capdevila, M.; Domenech, J.; Pagani, A.; Tio, L.; Villarreal, L.; Atrian, S. Zn- and Cd-metallothionein recombinant species from the most diverse phyla may contain sulfide (S^{2-}) ligands. *Angew. Chem. Int. Ed. Engl.* **2005**, *44*, 4618–4622. [CrossRef] [PubMed]

32. Fabris, D.; Zaia, J.; Hathout, Y.; Fenselau, C. Retention of thiol protons in two classes of protein zinc ion coordination centers. *J. Am. Chem. Soc.* **1996**, *118*, 12242–12243. [CrossRef]
33. Perez-Rafael, S.; Kurz, A.; Guirola, M.; Capdevila, M.; Palacios, O.; Atrian, S. Is MtnE, the fifth *Drosophila metallothionein*, functionally distinct from the other members of this polymorphic protein family? *Metallomics* **2012**, *4*, 342–349. [CrossRef] [PubMed]
34. Perez-Rafael, S.; Monteiro, F.; Dallinger, R.; Atrian, S.; Palacios, O.; Capdevila, M. *Cantareus aspersus* metallothionein metal binding abilities: The unspecific CaCd/CuMT isoform provides hints about the metal preference determinants in metallothioneins. *Biochim. Biophys. Acta* **2014**, *1884*, 1694–1707. [CrossRef] [PubMed]

International Journal of
Molecular Sciences

MDPI

Article

Analysis of Metal-Binding Features of the Wild Type and Two Domain-Truncated Mutant Variants of *Littorina littorea* Metallothionein Reveals Its Cd-Specific Character

Òscar Palacios [1], Elena Jiménez-Martí [2], Michael Niederwanger [3], Selene Gil-Moreno [1], Oliver Zerbe [4], Sílvia Atrian [2,†], Reinhard Dallinger [3] and Mercè Capdevila [1,*]

1 Departament de Química, Facultat de Ciències, Universitat Autònoma de Barcelona, E-08193 Cerdanyola del Vallès, Spain; oscar.palacios@uab.cat (Ò.P.); selenebdn89@gmail.com (S.G.-M.)
2 Departament de Genètica, Facultat de Biologia, Universitat de Barcelona, Av. Diagonal 643, E-08028 Barcelona, Spain; ejimenezmarti@gmail.com (E.J.-M.)
3 Institute of Zoology and Center of Molecular Biosciences Innsbruck (CMBI), University of Innsbruck, Technikerstraße 25, A-6020 Innsbruck, Austria; michael.niederwanger@uibk.ac.at (M.N.); reinhard.dallinger@uibk.ac.at (R.D.)
4 Department of Chemistry, University of Zurich, 8057 Zurich, Switzerland; oliver.zerbe@chem.uzh.ch
* Correspondence: merce.capdevila@uab.cat; Tel.: +34-935-81-33-23
† Deceased.

Received: 31 May 2017; Accepted: 1 July 2017; Published: 6 July 2017

Abstract: After the resolution of the 3D structure of the Cd_9-aggregate of the *Littorina littorea* metallothionein (MT), we report here a detailed analysis of the metal binding capabilities of the wild type MT, LlwtMT, and of two truncated mutants lacking either the N-terminal domain, Lltr2MT, or both the N-terminal domain, plus four extra flanking residues (SSVF), Lltr1MT. The recombinant synthesis and in vitro studies of these three proteins revealed that LlwtMT forms unique M_9-LlwtMT complexes with Zn(II) and Cd(II), while yielding a complex mixture of heteronuclear Zn,Cu-LlwtMT species with Cu(I). As expected, the truncated mutants gave rise to unique M_6-LltrMT complexes and Zn,Cu-LltrMT mixtures of lower stoichiometry with respect to LlwtMT, with the SSVF fragment having an influence on their metal binding performance. Our results also revealed a major specificity, and therefore a better metal-coordinating performance of the three proteins for Cd(II) than for Zn(II), although the analysis of the Zn(II)/Cd(II) displacement reaction clearly demonstrates a lack of any type of cooperativity in Cd(II) binding. Contrarily, the analysis of their Cu(I) binding abilities revealed that every LlMT domain is prone to build Cu_4-aggregates, the whole MT working by modules analogously to, as previously described, certain fungal MTs, like those of *C. neoformans* and *T. mesenterica*. It is concluded that the *Littorina littorea* MT is a Cd-specific protein that (beyond its extended binding capacity through an additional Cd-binding domain) confers to *Littorina littorea* a particular adaptive advantage in its changeable marine habitat.

Keywords: *Littorina littorea*; metallothionein; metal binding; tridominial MT

1. Introduction

Metallothioneins (MTs) constitute a monophyletic superfamily [1] of highly heterogeneous proteins of, generally [2], a small size. They are present in almost all living organisms, and are able to coordinate a number of heavy-metal ions through the formation of metal-thiolate bonds via their highly abundant cysteine residues [3,4]. Their biological functions have been ascribed to the physiological regulation of Zn and Cu homeostasis and/or the detoxification of Cd and other toxic metals, although they also respond to

different stress situations. In any case, the biological roles of MTs seem to be cell- and species-dependent, based on their reported heterogeneity. The latter has apparently evolved in a lineage-specific manner, according to the particular physiological requirements of the respective species [5]. Only rarely, however, was it so far shown how MT isoforms in a given species have adapted structural and metal-binding features in order to optimize metal-specific functions. One of the best-documented examples of this may be the metal-selective MT isoforms that evolved in certain terrestrial gastropods like the Roman snail (*Helix pomatia*) and some of its relatives [6,7]. On the other side, the plasticity required to perform a great multiplicity of functions could explain the extraordinary polymorphism reported for MTs, considering that in nearly all organisms analyzed so far, several coexisting MT isoforms have been found. After two decades devoted to the study of the metal binding abilities of a considerable number of MTs from diverse organisms [8], our group proposed a functional classification of MTs on the basis of their metal-binding preferences. This proposal, while acknowledging the classification of MTs according to sequence similarities within the taxonomic subfamilies [1,9], initially recognized two major groups [10]: Zn-thioneins (including both Zn(II) or Cd(II)-preferring MTs) and Cu-thioneins (i.e., Cu(I)-preferring MTs). Later, a step-wise gradation between genuine, Zn-(or divalent metal-ions)-thioneins and genuine Cu-thioneins was established [11]. In both of the extreme situations unique, well-folded, homometallic complexes were observed when bound to its cognate metal ion [8].

An ideal model system to study the evolutionary differentiation of polymorphic MTs, and the structure/function relationship in these metalloproteins, is the MT subfamily from the Mollusk class of Gastropoda (snails and slugs). Gastropods have existed as a distinct monophyletic clade for more than 500 million years [12]. Presently, they comprise a huge number of species (about 80,000) that have since successfully adapted to marine, freshwater, and terrestrial environments. As a reflection of this, gastropod MTs provide a fascinating example of how these proteins have evolved and diversified in such an ancient and diverging animal phylum. One of the most interesting aspects of gastropod MT evolution arises from the fact that species of the terrestrial helicid family possess metal-selective MT isoforms. The study of these peptides provided us with valuable data to recognize some distinct features that confer to them their specific Zn/Cd or Cu-thionein character. The paralogous MT proteins of these snails are, in fact, highly specialized for binding distinct metal ions while retaining high primary sequence similarities. Hence, the terrestrial snails *Helix pomatia* [6,7,13–16] and *Cantareus aspersus* [17–19], the best characterized snail MT systems so far, include three paralogous MT peptides with differentiated metal binding preferences: the Cd-specific (CdMT) and the Cu-specific (CuMT) isoforms, and an unspecific Cd/CuMT isoform that can be isolated as a mixed Cd,Cu-containing native complex, which have all been extensively studied by our group.

The marine common periwinkle *Littorina littorea* is also a member of Gastropoda that, in contrast to the terrestrial gastropods, has a unique MT. Interestingly it possesses a much longer sequence with 27 cysteine residues (Cys) instead of the 18 Cys commonly found in the other snails. *Littorina littorea* lives in a habitat (rocky sea shores) with rapidly changing environmental conditions due to tidal and microclimatic fluctuations, exposing snails to both marine and terrestrial conditions and alternating mineral and trace element availabilities, with an increasing risk of metal ion disbalances. Our research group has recently succeeded in determining the Nuclear Magnetic Resonance (NMR) structure of the Cd(II)-complexed form of *Littorina littorea* metallothionein, Cd_9-LlMT. It appears that the protein possesses three individual domains, each of them forming an independent metal-chelating module that folds into a single, well-defined Cd_3 cluster [20]. In comparison to MTs from other snail species that are only comprised by two domains, this novel three-domain MT is likely to confer to *Littorina littorea* an evolutionary advantage by structural adaptation to the higher risk of metal exposure in the marine tidal zone, through a simple domain duplication event. Overall, the MT of *Littorina littorea* seems to have adapted to stressful environmental conditions in a twofold manner: first, by increasing the metal binding specificity of the protein towards Cd(II) (present study); and second, by addition of an extra metal binding domain so as to increase the metal/protein stoichiometry from six to nine Cd(II) ions [20].

Hence, in the present study we explored in depth the Zn(II)-, Cd(II)- and Cu(I)-binding capabilities of the wild type *Littorina littorea* metallothionein, from now on referred to as LlwtMT, and of two designed mutants (Lltr1MT, Lltr2MT), comprising only two of the putative metal binding domains, with or without four N-terminal flanking residues.

2. Results and Discussion

2.1. Characterization of the Metallothionein (MT) System of Littorina littorea

The first primary structure knowledge of an MT from *Littorina littorea* goes back to studies of English and Storey [21], who recognized the important role of this MT in response to environmental stressors such as freezing and anoxia, to which the snail may intermittently be exposed in its tidal habitat. A screening of transcriptome from the midgut gland of Cd-exposed *Littorina littorea* for possible additional MT isoforms of this species by our team was negative, while the originally proposed sequence could be retrieved and confirmed via Polymerase Chain Reaction (PCR). Hence, it is actually assumed that the formerly identified MT of *Littorina littorea* [21] may be the only isoform from this species. Its sequence was therefore used in the present study. Interestingly, however, we found some variability of this MT in terms of an allelic variant that differs from the wild type MT in a few amino acid positions (Figure 1). While these slight primary structure differences may not significantly impact the overall metal binding behavior between wild type and allelic variants, their sequence composition with 9 Cys residues (i.e., 9 metal binding sulfur atoms) for each putative cluster suggest the presence of three individual domains, each of them carrying one metal cluster with a stoichiometric ratio of 9 Cys residues versus 3 divalent or 6 monovalent metal ions (Figure 1). The three-domain structure of this MT was in fact recently confirmed by our group using solution NMR [20]. In contrast, the metal binding features of the *Littorina littorea* MT remained still uncharacterized, and are now presented in this study.

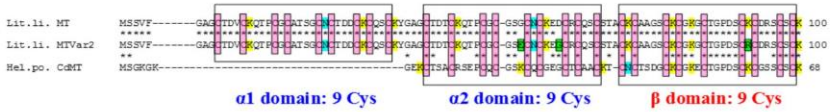

Figure 1. Alignment of *Littorina littorea* Metallothionein (MT) (Lit.li. MT, GenBank Acc. No. AAK56498), with its allelic variant (Lit.li. Var2, GenBank Acc. No. KY963497), and with the paradigmatic Cd-specific MT isoform of the terrestrial snail, *Helix pomatia* (Hel.po. CdMT, GenBank Acc. No. AAK84863.1). Throughout, conserved cysteine (Cys) positions in the peptide chains are highlighted by a **pink** box. In the sequence of the allelic Lit.li. MTVar2, the amino acid positions exchanged with respect to the wildtype Lit.li. MT sequences are shown in **green**. Also highlighted in **yellow** are the Lysine (K) residues whose preponderance over Aspargine (N) (highlighted in **blue**) in the sequences is supposed to confer to the respective peptides a high Cd(II) binding preference [19]. The transparent boxes indicate the supposed three-domain structure of the three MT proteins, which has been experimentally verified by solving the structure of *Littorina littorea* MT [20]. According to this, the *Helix pomatia* CdMT consists of two modular domains (one α2 and one β domain), whereas the two MT variants of *Littorina littorea* comprise three modular domains (two α domains, i.e., α1 and α2, and one β domain). In each of the above-shown proteins, every domain includes 9 Cys residues that provide 9 sulfur atoms for the binding of 3 divalent metal ions (such as Cd(II)). Identical positions between adjacent sequences are indicated by stars. The number of residues in the respective peptide chains is specified near their C-terminal end.

2.2. The LlwtMT, Lltr1MT and Lltr2MT Recombinant Polypeptides

In order to understand the possible impact of the number and length of domains on the metal binding properties of the *Littorina littorea* MT, the wild type MT was compared with

two domain-truncated mutants lacking one of the two α-domains. As shown in our previous publication [20], the increase in Cd loading capacity of the *Littorina littorea* MT has been achieved by duplication of the N-terminal α-domain (resulting in an MT with two N-terminal α-domains and one C-terminal β-domain). Our hypothesis was that the evolutionary duplication of the α-domain (and resulting addition of one more domain) should confer to the MT an increased loading capacity without grossly impairing its metal specificity features and metal binding behavior. Therefore, the two MT mutants were designed in order to contain only two metal binding domains (one single α and one single β domain), like the most common snail MTs (Figure 2). One of them (Lltr1MT) lacks the N-terminal metal binding domain from amino acid positions 2 to 37. In the Lltr2MT mutant residues 6 to 37 were removed, so that the truncated protein presents the two C-terminal metal binding domains and a small stretch of four additional amino acids (-SSVF-) at its N-terminus. DNA sequencing of the cDNA of the three proteins confirmed their sequence. Expression in *E. coli* cultured in Zn-enriched media and purification rendered the corresponding recombinant Zn-LlwtMT, Zn-Lltr1MT, and Zn-Lltr2MT samples. These, once acidified, yielded the corresponding apo-forms, with respective molecular masses of 10,183, 6425, and 6846 Da, in accordance with the respective theoretical values of 10,183.59, 6426.35, and 6846.82 Da (Figures 2 and 3, Table 1), respectively.

Figure 2. Sequences of the recombinant proteins studied in this work: the constructs Lltr1MT (GeneBank Accession No. MF326202) and Lltr2MT (GeneBank Accession No. MF326203) are aligned with the LlwtMT (UniProt #Q962G0) wild-type form. Cysteine residues are written in **red**, Methionine residues in **blue**, and the SSVF N-terminal flanking amino acids are highlighted in **green**.

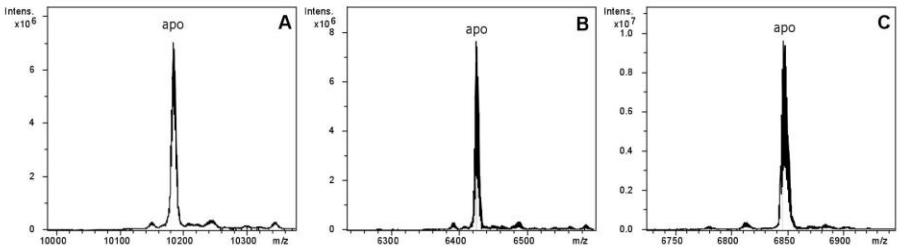

Figure 3. Deconvoluted Electrospray Ionization Mass Spectrometry (ESI-MS) spectra of the recombinant preparations of (**A**) LlwtMT; (**B**) Lltr1MT; and (**C**) Lltr2MT, purified from bacterial cultures grown under Zn-supplementation and analyzed at acid pH (2.4).

Table 1. Analytical characterization of the recombinant Zn- and Cd-complexes of LlwtMT, Lltr1MT, and Lltr2MT.

MT	ICP-AES [a]	Neutral ESI-MS [b]	Experimental MM [c]	Theoretical MM [d]
LlwtMT	9.5	Zn_9-MT	10,753	10,754.1
Lltr1MT	5.9	Zn_6-MT	6807	6806.7
Lltr2MT	6.1	Zn_6-MT	7226	7227.2
LlwtMT	8.7	Cd_9-MT	11,177	11,177.3
Lltr1MT	6.3	Cd_6-MT	7089	7088.8
Lltr2MT	6.5	Cd_6-MT	7509	7509.3

[a] M(II)-to-peptide ratio calculated from S and Zn or Cd content (Inductively Coupled Plasma Atomic Emission Spectroscopy, ICP-AES, data); [b] the metal contents of the M(II)-LlMT species were calculated from the mass difference between the holo- and the respective apo-peptides; [c] experimental molecular masses corresponding to the detected M(II)-LlMT complexes. The corresponding ESI-MS spectra are shown in Figure 3; [d] theoretical molecular masses corresponding to the M(II)-LlMT complexes.

2.3. Zn(II) and Cd(II) Binding Capabilities of LlwtMT, Lltr1MT, and Lltr2MT

The recombinant synthesis of LlwtMT in M^{II}-supplemented (M^{II} = Zn(II) or Cd(II)) *Escherichia coli* cultures yielded almost unique peaks corresponding to M^{II}_9-complexes, while those of the truncated mutants, Lltr1MT and Lltr2MT, gave rise to M^{II}_6-complexes for both peptides, as identified in the respective ESI-MS analyses at neutral pH (Figure 4A and Table 1). The only minor accompanying peaks were attributed to frequently observed NH_4^+ adducts. These results are in good concordance with those obtained previously for LlwtMT synthesized under equivalent conditions [20], and nicely match with those expected after removing one of the structural domains, and therefore reduce the initial 27 to 18 Cys coordinating amino acids. Analysis of the Circular dichroism (CD) spectra of the Zn- and Cd-preparations of LlwtMT and of those of the Lltr1MT and Lltr2MT truncated mutants (Figure 4B) confirmed that, irrespective of their metal loading (9 M^{II} metal cations but 6 M^{II} in the truncated forms), (1) the three Zn-loaded proteins showed equivalent folds, and (2) the three Cd-loaded proteins also showed equivalent folds. However (3), the Zn(II) and the Cd(II) complexes of these three proteins did not show the same level of structuration; in fact, peptides loaded with Cd(II) were more well-structured in solution, as can be deduced from the *exciton coupling* signal centered at ca. 255 nm, which is a characteristic wavelength of the Cd-thiolate chromophores (Figure 4B, right hand). In contrast, the corresponding Zn-loaded complexes gave rise to the typical $Zn(SCys)_4$ absorption, with a Gaussian band centered at ca. 240 nm (Figure 4B, left hand), representative of a lower degree of compactness and a less defined 3D structure in solution. Furthermore, the Zn(II)/Cd(II) displacement reaction in Zn_9-LlwtMT, Zn_6-Lltr1MT, and Zn_6-Lltr2MT proceeded gradually from the Zn_x-LlMT complexes to the respective Cd_x-LlMT species (x = 9 or 6), giving rise to all the Zn_aCd_b-LlMT (a + b = x) intermediate species in the transitional steps (Figure 5). The CD spectra recorded at progressive stages of the reaction revealed identical profiles (cf. Figure 5A) for the three polypeptides. The observed changes basically consisted in the transition of the initial Gaussian band at ca. 240 nm, characteristic of the Zn-complexes, into the exciton coupling signal centered at ca. 250 nm, typical of Cd-complexes. This suggests that the Zn(II)/Cd(II) substitution proceeds in an almost parallel way for the wild-type LlwtMT and the two mutant forms. The CD spectra of the Zn/Cd replacement steps also suggest non-cooperative replacement (Figure 5A), which is supported by the ESI-MS data (Figure 5B).

After the respective additions of 9 and 6 Cd(II) equivalents to the recombinant Zn-LlMT preparations, the respective peptides exclusively yielded the expected Cd_9-LlwtMT, Cd_6-Lltr1MT, and Cd_6-Lltr2MT complexes (Figure 5C), in agreement with the results obtained in the in vivo recombinant preparations and the reported NMR results [20]. These in vitro-generated complexes show CD fingerprints almost equivalent to those of the in vivo-synthesized species (Figure 5B).

Therefore, it can be concluded that the removal of one of the structural domains of the LlwtMT protein does obviously affect the overall metal content of the final aggregates but likely not the structure of the individual domains.

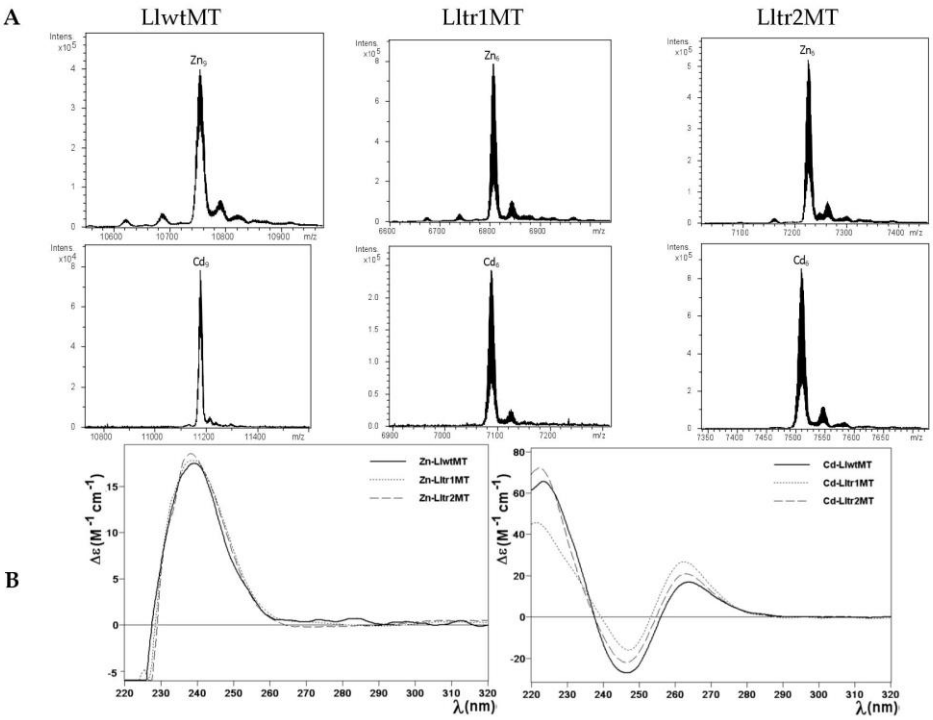

Figure 4. Analysis of the Zn- and Cd-LlwtMT, -Lltr1MT, and -Lltr2MT complexes. (**A**) Deconvoluted ESI-MS spectra of the recombinant preparations of LlwtMT, Lltr1MT, and Lltr2MT, purified from Zn- and Cd-supplemented cultures, analyzed at neutral pH (7.0); (**B**) CD spectra of the corresponding Zn- and Cd-LlMT recombinant preparations.

2.4. Cu(I) Binding Capabilities of LlwtMT, Lltr1MT, and Lltr2MT

Due to the known influence of oxygenation on the amount of internal copper in the cultured bacteria [22], and following our established methodology [8], we performed two types of Cu-supplemented productions: one under standard and one under low aeration conditions. The synthesis of the three polypeptides at regular oxygenation conditions yielded preparations that allowed their analysis by ESI-MS and CD, and facilitated the comparison of all their features. Unfortunately, several efforts to purify LlwtMT, Lltr1MT, and Lltr2MT from *E. coli* cultures grown under low oxygen conditions failed. This fact, together with the results described below (that clearly illustrate the degree of heterogeneity of the Cu-LlMT recombinant samples (Figure 6A)) and the results obtained in the M^{II} binding studies (see above), already suggest a low specificity of these three proteins for Cu(I). At this point we would like to remind the reader of data obtained in some of our previous Cu(I) binding studies, performed with other snail MTs [15], where other Cu-MT preparations also exhibited a high degree of complexity when synthesized in the presence of a non-cognate metal ion.

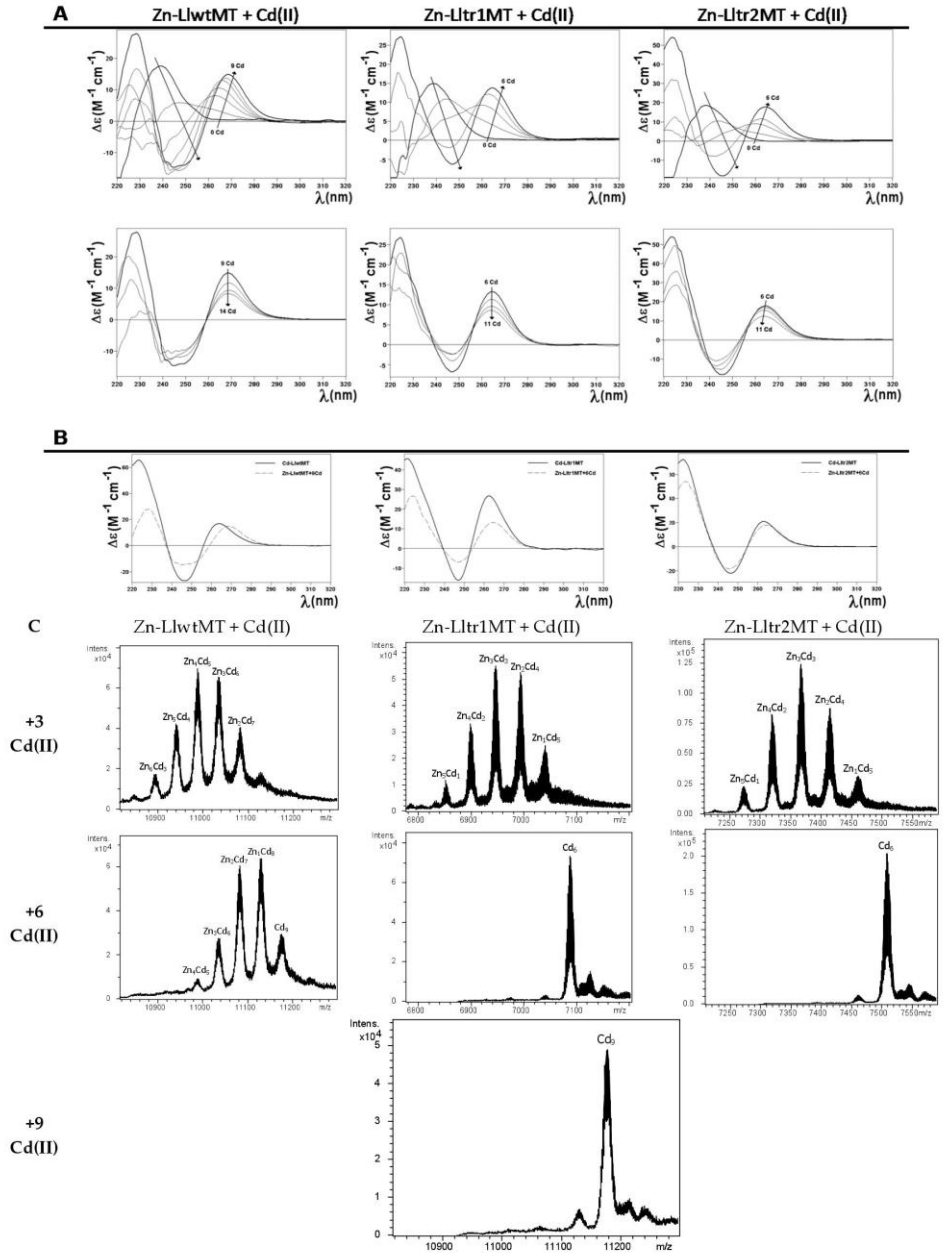

Figure 5. Zn(II)/Cd(II) replacement reaction on the Zn_9-LlwtMT, Zn_6-Lltr1MT, and Zn_6-Lltr2MT complexes. (**A**) CD spectra of a 10 μM solution of the Zn-LlMT samples, titrated with $CdCl_2$ at neutral pH up to 14 (LlwtMT) or 11 (Lltr1MT and Lltr2MT) Cd(II) equivalents; (**B**) Comparison of the CD spectra of the three recombinant productions of Cd-LlMT with those obtained at the end of the in vitro metal displacement reactions; (**C**) Deconvoluted ESI-MS spectra recorded after the addition of 3, 6, and 9 equivalents of $CdCl_2$ to the recombinant Zn-LlMT preparations.

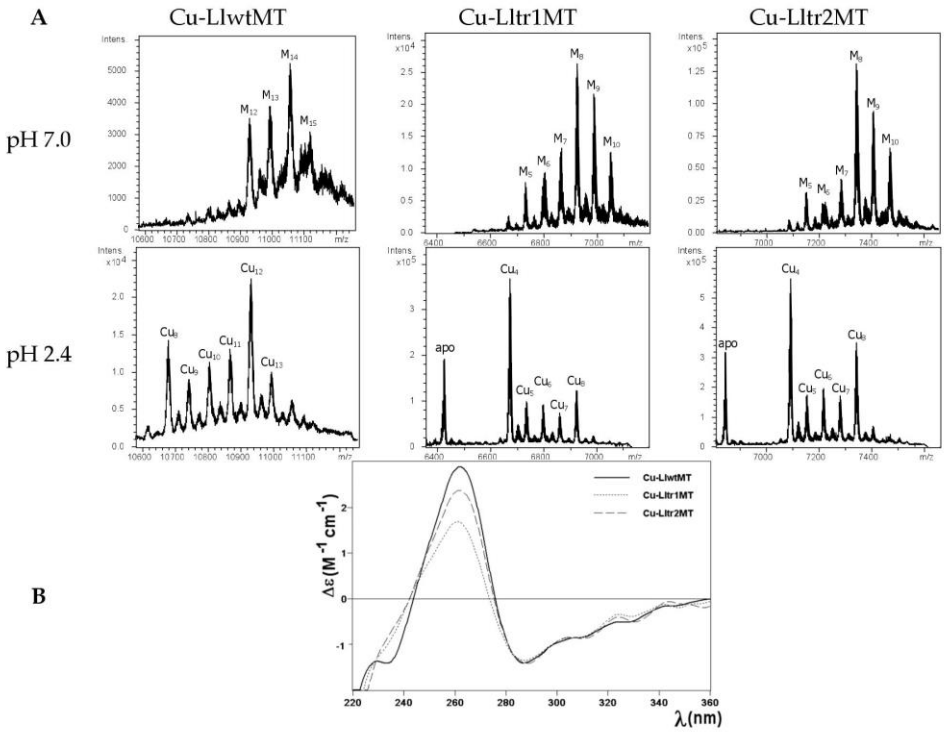

Figure 6. Analysis of the Cu-LlwtMT, Cu-Lltr1MT, and Cu-Lltr2MT complexes. (**A**) Deconvoluted ESI-MS spectra of the recombinant preparations of LlwtMT, Lltr1MT, and Lltr2MT, purified from Cu-supplemented cultures, analyzed at neutral pH (7.0) and acid pH (2.4); (**B**) CD spectra of the three recombinant Cu-LlMT preparations.

The first noticeable observation was that the composition of the Cu-LlwtMT and Cu-LltrMT purified samples was significantly different (obviously, this was expected, owing to their different number of coordinating residues), apart from the manifold of different species and the heteronuclear nature (i.e., Cu,Zn-species) of the complexes found in the three Cu-LlMT samples. For example, the ESI-MS spectra of the Cu-LlwtMT sample recorded at neutral pH exhibited one major peak, corresponding to the M_{14}-LlwtMT complexes; two less abundant M_{13}- and M_{12}-LlwtMT, and one very minor M_{15}-LlwtMT species (Figure 6A, Table 2). Due to the similarity of their atomic masses M can be either Zn(II) or Cu(I). The same preparation was analyzed at acidic pH, as this allows the release of all bound Zn(II) but not of Cu(I) [23,24]. At pH 2.4 the major peak corresponded to homonuclear Cu_{12}-LlwtMT, and a smaller peak for Cu_8-LlwtMT as well as minor peaks for Cu_9-, Cu_{10}-, Cu_{11}-, Cu_{13}- and Cu_{14}-LlwtMT (Figure 6A, Table 2). Analogously, the Cu-Lltr1MT and Cu-Lltr2MT preparations resulted in major M_8- with also abundant M_9-complexes, while the M_{10}-, M_7-, and M_6-species appeared as minor MS peaks. At acidic pH these samples rendered major Cu_4-complexes, less abundant Cu_8-species, and minor Cu_5-, Cu_6- and Cu_7-species, together with a relatively intense peak (corresponding to the truncated apo-proteins, a peak that was not observed for wild type Cu-LlwtMT). In any case, the ESI-MS data at acidic pH clearly indicated that the Cu_4-, Cu_8-, and Cu_{12}-aggregates were the most favored ones in these LlMTs, thus suggesting an optimal occupancy of 4 Cu(I) ions per structural domain. The ICP-AES results obtained for the purified Cu-LlwtMT, -Lltr1MT, and -Lltr2MT samples (4.0 Zn:13.3 Cu; 3.5 Zn:5.8 Cu; and 3.2 Zn:6.5 Cu, respectively, for LlwtMT, Lltr1MT, and Lltr2MT, see Table 2) revealed that the deletion of one out of the three structural

domains of LlwtMT has drastically reduced the copper content to one half, but practically maintained that of Zn. The most straightforward explanation for the overall results may be that according to our previous observations [19], the small number of asparagine (N) residues (two in the LlwtMT, see Figures 1 and 2) was reduced by half in the two truncated LlMTs (one asparagine residue left in each, Lltr1MT, and Lltr2MT), hence decreasing the already low Cu(I) binding character of the LlwtMT even further in the two truncated Lltr1MT and Lltr2MT. Another explanation would be that Cu-LlwtMT contains Cu_{12}- and Cu_8-aggregates, which also enclose some Zn(II) ions to finally render the observed M_{12}-, M_{13}-, and M_{14}-LlwtMT species. In contrast, the truncated mutants present Cu_4-aggregates that, however, still contain Zn(II) to yield the observed M_8- and M_9-complexes. The fact that these preparations also showed a significantly intense peak corresponding to their apo-peptides, at pH 2.4, suggests that some of the complexes are only loaded with Zn(II). Finally, the relative higher intensity of Cu_8-Lltr2MT, in comparison to that of Cu_8-Lltr1, seems to indicate that the SSVF fragment perhaps has a role in the stabilization of the aforementioned Cu_4-aggregates.

Table 2. Analytical characterization of the recombinant Cu-complexes of LlwtMT, Lltr1MT, and Lltr2MT, obtained from cultures grown with normal aeration (no complexes could be recovered from low aeration conditions).

MT	ICP-AES [a]	Neutral ESI-MS [b]	Exp MM [c]	Theor MM [d]	Acidic ESI-MS [b]	Exp MM [c]	Theor MM [d]
LlwtMT	4.0 Zn 13.3 Cu	M_{14}-MT M_{13}-MT M_{12}-MT M_{15}-MT	11,058 10,995 10,934 11,122	11,059.3 10,996.7 10,934.2 11,121.8	Cu_{12}-MT Cu_8-MT Cu_{11}-MT Cu_{10}-MT Cu_{13}-MT Cu_9-MT Cu_{14}-MT	10,934 10,682 10,869 10,808 10,995 10,747 11,061	10,934.2 10,684.0 10,871.6 10,809.1 10,996.7 10,746.5 11,059.3
Lltr1MT	3.5 Zn 5.8 Cu	M_8-MT M_9-MT M_{10}-MT M_7-MT M_6-MT	6925 6988 7050 6862 6796	6926.8 6989.3 7051.9 6864.2 6801.7	Cu_4-MT apo-MT Cu_8-MT Cu_5-MT Cu_6-MT Cu_7-MT	6675 6425 6925 6738 6801 6865	6676.6 6426.4 6926.8 6739.1 6801.7 6864.2
Lltr2MT	3.2 Zn 6.5 Cu	M_8-MT M_9-MT M_{10}-MT M_7-MT M_6-MT	7344 7407 7471 7285 7224	7347.2 7409.8 7472.3 7284.7 7222.1	Cu_4-MT apo-MT Cu_8-MT Cu_5-MT Cu_6-MT Cu_7-MT	7095 6845 7344 7161 7220 7286	7097.0 6846.8 7347.2 7159.6 7222.1 7284.7

[a] The Zn(II) and Cu(I)-to-peptide ratio calculated from S and Cu content (ICP-AES data); [b] the deduced M-LlMT (M = Zn or Cu) species were calculated from the mass difference between the holo- and the respective apo-peptides. The major species are indicated in bold, and the rest are in decreasing order of ESI-MS peak intensity; [c] experimental molecular masses corresponding to the detected M-LlMT complexes. The corresponding ESI-MS spectra are shown in Figure 5; [d] theoretical molecular masses corresponding to the M-LlMT complexes.

Interestingly, despite the diversity of species formed by the three LlMT proteins when coordinating Cu(I), they all gave rise to comparable CD spectra, both in shape and intensity (Figure 6B). Their envelopes display the typical fingerprints of the Cu-MT complexes with absorption maxima at ca. 260 nm and minima at ca. 280 nm.

To further explore the Cu(I)-binding capabilities of these three peptides, their Zn-loaded forms were treated with increasing amounts of a Cu(I) solution. The distinct stages reached during the titrations were analyzed by CD and ESI-MS, and compared with the results obtained from the recombinant Cu-LlMT preparations (Figures 7 and 8). As expected, the Zn(II)->Cu(I) displacement reaction in Zn_9-LlwtMT, Zn_6-Lltr1MT, and Zn_6-Lltr2MT gave rise, at pH 7, to a complex mixture of heterometallic M_x-LlMT species (Figure 8). The 240 nm Gaussian band in the CD spectra, characteristic of the Zn-loaded form, decreased in intensity in all three peptides and shifted towards the red with the incoming Cu(I). After the addition of 8 equivalents of Cu(I), the typical CD envelop characteristic of Cu-loaded MTs (with absorptions at ca. 260, 290, and 320 nm (cf. Figure 7A)) was observed. At this stage both, the CD fingerprints (Figure 7B) and the metal composition (Figure 8), as deduced from the

MS data, were quite close (but not exactly equal) to those observed in the recombinant synthesis of the three proteins (Figure 6). Further addition of Cu(I) beyond 8 Cu(I) equivalents resulted in all three samples in a decrease of the CD signal (Figure 7B). The Zn(II)->Cu(I) substitutions in vitro proceeded in an almost parallel way for the wild-type LlwtMT and the two truncated LltrMT forms, showing CD fingerprints almost equivalent to those of the in vivo synthesized species (Figure 7B).

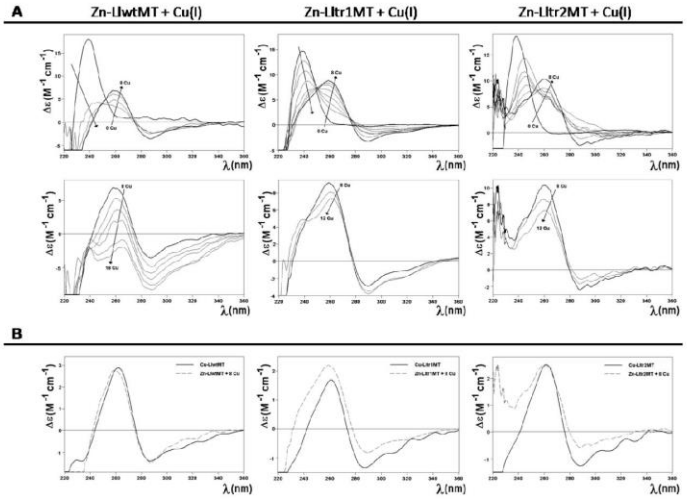

Figure 7. Zn(II)->Cu(I) replacement reaction on the Zn_9-LlwtMT, Zn_6-Lltr1MT, and Zn_6-Lltr2MT complexes. (**A**) CD spectra of a 10 μM solution of the Zn-LlMT samples, titrated with a Cu(I) solution at neutral pH; (**B**) Comparison of the CD spectra (normalized) of the three recombinant productions of Cu-LlMT with those obtained from the in vitro metal displacement reactions.

The ESI-MS data at acidic pH, however, revealed a distinctly different behavior for each peptide. First of all, it is worthwhile to highlight that the spectrometric measurements at acidic pH revealed that the three peptides formed copper aggregates on the basis of Cu_4-clusters, in closer resemblance to the behavior observed for the two MTs (CnMT1 and CnMT2) of the pathogenic fungus *Cryptococcus neoformans*. It was recently suggested that these MTs are built from a modular structure of Cu_5 clusters [24], in response to a highly selective pressure to chelate copper. Hence in our present study, the addition of a few Cu(I) equivalents at the beginning of the three experiments already gave rise to the appearance of Cu_4-LlMT clusters, which remained very abundant, while Cu_8-LlMT clusters gained in importance when further Cu(I) was added. After the addition of the fourth Cu(I) equivalent, at which a significant amount of the apo protein was still present, M-LlwtMT species already contained a significant fraction of the Cu_8 cluster. This was not the case for both truncated mutants, for which the apo-protein and Cu_4 presented the major species. Interestingly for the six Cu(I) equivalents added, Cu_8 was already the major species for LlwtMT. Oppositely, Lltr1Mt maintained a small proportion of the apo-protein and showed an increased amount of Cu_8, while Lltr2 had no apo-protein and a higher amount of Cu_8, in regards to that of Cu_4. With 8 Cu(I) equivalents added, Cu_8 was the major species for LlwtMT and Lltr2MT but not for Lltr1MT, for which a significant fraction was present as the Cu_4 aggregate. Addition of excess Cu(I) did not induce further changes in the metal content of the truncated mutants, which indicates that Lltr2MT, but not Lltr1MT, can easily reach a state in which both domains are loaded with 4 Cu(I). We suspect that the additional presence of the SSVF amino acid motif at the N-terminus of Lltr2MT is important for that feature. On the other hand, and as expected, LlwtMT can bind more Cu(I) equivalents so that its third domain becomes loaded with further 4 Cu(I) ions, resulting in a Cu_{12} cluster as the fully saturated species.

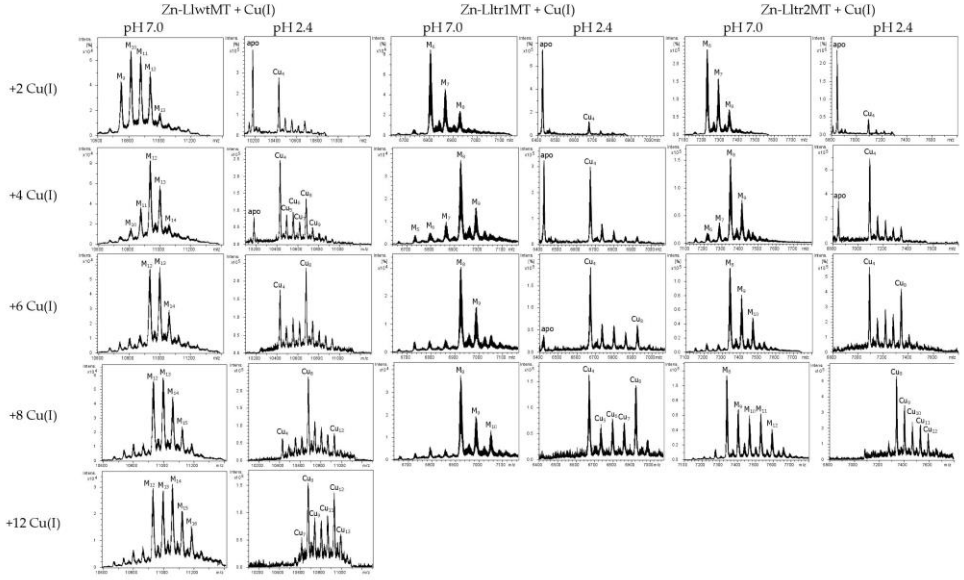

Figure 8. Zn(II)->Cu(I) replacement reaction on the Zn_9-LIwtMT, Zn_6-LItr1MT, and Zn_6-LItr2MT complexes. Deconvoluted ESI-MS recorded, at pH 7.0 and 2.4, after the addition of 2, 4, 6, 8, and 12 equivalents of Cu(I) to the recombinant Zn-LIMT preparations.

3. Materials and Methods

3.1. Confirmation of the MT System of Littorina littorea

Individuals of *Littorina littorea* (20–30 mm high) collected in Scrabster (Scotland) were obtained through a commercial dealer in Bilbao (Arrainko SL, Mercabilbao, Bilbao, Spain). After an acclimation period of two weeks, twenty snails were dissected at the Research Centre for Experimental Marine Biology and Biotechnology (University of the Basque Country) in Plentzia (Bizkaia, Basque Country, Spain). Midgut gland aliquots (~10 µg) were separated and stored in RNA-later for subsequent RNA isolation at the Institute of Zoology of the University of Innsbruck (Innsbruck, Austria). RNA isolation of homogenized (Precellys, Bertin Instruments, Montigny-le-Bretonneux, France) hepatopancreatic tissue was performed using the RNeasy®Plant Mini Kit (Qiagen, Hilden, Germany), applying on-column DNase 1 digestion (Qiagen). RNA was quantified using RiboGreen®RNA Quantification Kit from Molecular Probes (Invitrogen, Karlsruhe, Germany). The RNA sample of one individual was sent to Duke University (Durham, NC, USA) for Illumina HiSeq Sequencing, in order to screen the transcriptome for the presence of additional MT isoforms (which, however were not present). The allelic variant 2 was discovered in a screen of twenty individuals of *Littorina littorea*.

cDNA was synthesized from 450 ng of total RNA with the Superscript® IV Reverse Transcriptase synthesis kit (Invitrogen, Life Technologies, Waltham, MA, USA) on a 20 µL scale. The primary structure of the *Littorina littorea* MT (GenBank Acc.Nr. AAK56498) and the allelic variant 2 (GenBank Acc.Nr. KY963497) were confirmed by PCR. To this aim, the Titanium® Taq PCR Kit (Clontech, Mountain View, CA, USA) was used with the following primers: 5′UTR primer, 5′-CTGACGAGTGAACTGTTTTT-3′; 3′UTR primer, and 5′-GATGGGGAATGAGAAAATG-3′.

3.2. Construction and Cloning of the cDNAs Encoding the LlwtMT, Lltr1MT, and Lltr2MT Proteins

Two LltrMT truncation mutants (LltrMT1 and LltrMT2) were designed to lack the first metal binding domain completely. In Lltr1, the N-terminal domain (including all amino acid positions from 2 to 37) were deleted, while in Lltr2 the N-terminal domain was truncated too, but the N-terminal amino acid positions from 1 to 5 were maintained (Figure 2).

For the construction of the pGEX plasmids containing the wild type sequence of *Littorina littorea* or the mutants, the cDNAs encoding for these sequences were designed on the basis of the flanking regions in wild-type LlwtMT cDNA, and to encode the truncated sequences in the corresponding Lltr1MT and Lltr2MT cDNAs, taking out nucleotides 4 to 111 and 16 to 111, respectively. Additionally, the restriction sites for *BamHI* and *XhoI* were added to the 5′ and 3′ ends, respectively, for cloning purposes (Supplementary Materials, Figure S1). The LlwtMT, Lltr1MT, and Lltr2MT coding sequences designed this way were purchased as synthetic DNAs IDT & Conda Labs (Madrid, Spain). After PCR amplification (35 cycles: 95 °C 30 s, 50 °C 30 s, and 72 °C 30 s, using Expand High Fidelity (Roche Diagnostics S.L:, San Cugat del Vallès, Spain) thermostable DNA polymerase) of the synthetic cDNAs using the flanking primers 5′-TTTATTGGATCCATGA GCTC-3′ (LlwtMT forward); 5′-TTTCTCGAGTCATTTGCATG-3′ (LlwtMT reverse); 5′-TTTATTGGATC CGGTAAGGG-3′ (Lltr1MT forward); 5′-TTTCTCGAGTTACTTACAGG-3′ (Lltr1MT reverse); 5′-TTTATTGGATCCGGCAAAGGG-3′ (Lltr2MT forward); and 5′-TTTCTCGAGTTATTTGCAAG-3′ (Lltr2MT reverse), they were subsequently digested with *BamHI* and *XhoI* restriction enzymes, and the resulting products were ligated in-frame (DNA ligation kit, Takara Bio, Kusatsu, Shiga, Japan) in the pGEX-4T-1 (Amersham-GE Healthcare Europe, Cerdanyola del Valles, Spain) *E. coli* expression vector, which yields GST-fusion proteins. DNA sequencing allowed confirming of all the DNA constructs (ABIPRISM 310, Applied Biosystems, Foster City, CA, USA) using the BigDye Terminator. The *E. coli* MachI strain was used for cloning and sequencing. The expression plasmids were then transformed into the protease-deficient *E. coli* strain BL21 (*fhuA2 [lon] ompT gal [dcm] ΔhsdS*) for protein synthesis.

3.3. Synthesis and Purification of the Recombinant Zn-, Cd-, and Cu-Complexes of LlwtMT and the Lltr1MT and Lltr2MT Mutants

Purification of all the metal-MT complexes of the LlwtMT, Lltr1MT, and Lltr2MT proteins was carried out, as reported previously [25], to ensure fully comparable results. Hence, the GST-LlMT fusions were produced in 5-L cultures (Luria Bertani medium) of transformed *E. coli* BL21 bacteria. Induction of gene expression was achieved with 100 μM (final concentration) of isopropyl β-D-thiogalactopyranoside (IPTG). After 30 min of induction, 300 μM $ZnCl_2$, 300 μM $CdCl_2$, or 500 μM $CuSO_4$ (final concentrations) were supplemented to the cultures, which grew for a further 2.5 h, for the synthesis of the respective metal complexes. Owing to the well-known fact that culture aeration determines the amount of available intracellular copper [22], the Cu-cultures were grown both under normal (1-L medium in a 2-L Erlenmeyer flask, at 250 rpm) and low-oxygen conditions (1.5-L medium in a 2-L Erlenmeyer flask at 150 rpm).

Harvesting and centrifugation of the grown cells produced a cell mass that, resuspended in ice-cold PBS (1.4 M NaCl, 27 mM KCl, 101 mM Na_2HPO_4, 18 mM KH_2PO_4) with 0.5% v/v β-mercaptoethanol, was disrupted by sonication (20 s pulses for 5 min). All solutions used were oxygen-purged by saturating them with pure-grade argon to prevent metal-MT oxidation. The suspension was centrifuged at 12,000× *g* for 30 min, and the incubation of the resulting supernatant (gentle agitation for 60 min at room temperature) with Glutathione-Sepharone 4B (GE Healthcare) allowed batch affinity purification of the GST-LlMT species. The MT portion was recovered after thrombin cleavage (10 μ per mg of fusion protein at 17 °C over-night). The solution containing the cleaved metal-MT complexes was concentrated by Centriprep Microcon 3 (Amicon, cut-off of 3 kDa, Merck-Millipore, Darmstadt, Germany) centrifugation. The final metal complexes were purified through FPLC size-exclusion chromatography in a Superdex75 column (GE Healthcare), equilibrated with 50 mM Tris-HCl (pH 7.0), and run at 0.8 $mL \cdot min^{-1}$. Absorbances at 254 and 280 nm signaled the fractions to be collected and analyzed for protein content.

3.4. Zn(II)/Cd(II) and Zn(II)/Cu(I) Replacement Reactions in the Zn(II)-LlMT Proteins

Metal displacement reactions on the recombinant Zn-LlMT preparations allowed formation of the alleged Cd- or Cu-LlMT "in vitro complexes". As described elsewhere [25,26], the respective additions of several molar equivalents of Cd^{2+} or Cu^{+} ions from standard solutions were performed at constant pH 7.0 without the addition of any extra buffers, and under argon atmosphere.

3.5. Spectroscopic Analyses (ICP-AES, UV-Vis and CD) of the Metal Complexes Formed by the Llmt Proteins

Inductively Coupled Plasma Atomic Emission Spectroscopy (ICP-AES) in a Polyscan 61E (Thermo Jarrel Ash, Franklin, MA, USA) spectrometer allowed determination of the sulfur and metal content of all the metal-MT samples, by measuring S at 182.040 nm, Zn at 213.856 nm, and Cu at 324.803 nm. The protein concentration was determined both by conventional treatment [27] and by incubation in 1 M HNO_3 at 65 °C for 10 min, before measurements to avoid possible traces of labile sulfide anions [28], by assuming that all S atoms were provided by the MT proteins. Circular dichroism measurements were performed at 25 °C in a Jasco spectropolarimeter (Model J-715, JASCO, Groß-Umstadt, Germany) interfaced to a computer (J700 software, JASCO, Groß-Umstadt, Germany) by using Peltier PTC-351S equipment (TE Technology, Traverse City, MI, USA). An HP-8453 Diode array UV-vis spectrophotometer (GIM, Ramsey, MN, USA) was used for the electronic absorption measurements. In all cases, 1-cm capped quartz cuvettes were employed for spectra recording, and the dilution effects were corrected and processed using the GRAMS 32 software (Thermo Fisher Scientific, Waltham, MA, USA).

3.6. Electrospray Ionization Time-of-Flight Mass Spectrometry (ESI-TOF MS) of the Metal Complexes Obtained from the LlMT Proteins

Mass determinations by Electrospray ionization time-of-flight mass spectrometry (ESI-TOF MS) were carried out in a Micro TOF-Q instrument (Bruker Daltonics, Bremen, Germany) interfaced with a Series 1200 HPLC Agilent pump and equipped with an autosampler, all of which were controlled by the Compass Software. The ESI-L Low Concentration Tuning Mix (Agilent Technologies, Santa Clara, CA, USA) was used for calibration.

A 5:95 mixture of acetonitrile:ammonium acetate (15 mM) was the carrier buffer for measurements at pH 7.0, while the measurements at acidic pH (2.4) were carried out using a 5:95 acetonitrile:formic acid solution, which causes the release of Zn(II) but keeps Cu(I) bound to the peptides. Experimental mass values were calculated as described previously [29], and the error associated with the measurements was always smaller than 0.1%.

4. Conclusions

In summary, we have explored and analyzed the metal binding capabilities of wild type *Littorina littorea* MT (LlwtMT) and two truncated mutants that either lack the N-term domain (Lltr2MT), or both the N-term domain plus a short fragment (residues SSVF) at the N-terminus of its sequence (Lltr1MT).

The LlwtMT protein, with 27 Cys distributed equally in 3 structural domains [20], rendered unique M_9-LlwtMT species—both in vivo and in vitro—when bound to divalent metal ions (M = Zn(II) or Cd(II)), while affording a complex mixture of heteronuclear Zn,Cu-LlwtMT species if Cu(I) was introduced. This already excludes that LlwtMT behaves like a Cu-thionein. Both truncated mutants matched the expectation that metal binding is simply scaled when removing a single domain from the full-length protein, e.g., obtaining unique M_6-LltrMT complexes with divalent metal ions and a complex mixture of heteronuclear Zn,Cu-LltrMT species of lower stoichiometry, compared to the wild type protein (M_8 instead on M_{14}, M = Zn + Cu).

The characterization of recombinant preparations of these three proteins revealed increased specificity for Cd(II) over Zn(II), as clearly revealed by the CD fingerprints of their in vivo and in vitro preparations, that displayed Gaussian bands for the Zn-loaded complexes (Zn_9-LlwtMT and Zn_6-LltrMT) but clear *exciton couplings* for the Cd-loaded complexes (Cd_9-LlwtMT and Cd_6-LltrMT) at the corresponding wavelengths (ca. 240 nm for Zn(II) complexes, and ca. 250 for Cd(II) complexes). Despite the observed better folding of the proteins with Cd(II) compared to those with Zn(II), the metal displacement reaction of Zn(II) by Cd(II) did not reveal any type of cooperativity upon Cd(II) binding. The spectrometric data clearly revealed that the incoming Cd(II) ions gradually displaced the bound Zn(II) ions, initially yielding all the possible Zn_X,Cd_y-LlMT (x + y = 9 for LlwtMT, and x + y = 6 for LltrMT) species, until only Cd(II) was present in the final homonuclear Cd-LlMT complexes. Contrarily, the analysis of the Cu(I) binding capabilities of these proteins has revealed that the three domains are prone to form Cu_4-aggregates in separate modules, as previously described for other MTs (like those of *Cryptococcus neoformans* [24] and *Tremella mesenterica* [2], which have been reported to have been built by tandem amplification of a basic unit).

Overall, the MT of *Littorina littorea* must be considered as a particularly efficient Cd-specific MT. It confers to the snail an evolutionary advantage in a twofold manner, because: (1) it is prone to preferentially bind Cd^{2+}; and (2) as shown by us previously [20], its Cd binding capacity has been increased during evolution through the addition of a third metal binding domain.

Supplementary Materials: Supplementary materials can be found at www.mdpi.com/1422-0067/18/7/1452/s1.

Acknowledgments: This work was supported by the DACH (International Cooperation) Project ref. I-1482-N28 of the Austrian Science Fund (FWF) to Reinhard Dallinger and the Swiss National Science Foundation (SNF) to Oliver Zerbe. Authors from both Barcelona universities are members of the 2014SGR-423 Grup de Recerca de la Generalitat de Catalunya, and they are recipients of MINECO-FEDER grants (BIO2015-67358-C2-1-P) to Sílvia Atrian) and (BIO2015-67358-C2-2-P to Mercè Capdevila). We thank the Centres Científics i Tecnològics (CCiT) de

la Universitat de Barcelona (ICP-AES, DNA sequencing) and the Servei d'Anàlisi Química (SAQ) de la Universitat Autònoma de Barcelona (CD, UV-Vis, ESI-MS) for allocating instrument time.

Author Contributions: Oliver Zerbe, Reinhard Dallinger, Mercè Capdevila, and Sílvia Atrian conceived and designed experiments. Michael Niederwanger and Reinhard Dallinger confirmed the MT system and designed mutant MTs. Mercè Capdevila, Oscar Palacios, and Sílvia Atrian analyzed the data and discussed the experimental results. Elena Jiménez-Martí performed the cloning and recombinant synthesis of the analyzed proteins and Selene Gil-Moreno and Òscar Palacios performed their ESI-MS and CD characterization. Òscar Palacios, Mercè Capdevila, and Reinhard Dallinger were primarily responsible for writing the manuscript. All authors—except Silvia Atrian, who passed away on 5 December 2016, and is sorely missed—edited and approved the final version of the manuscript.

Conflicts of Interest: The authors declare no conflict of interest.

References

1. Binz, P.A.; Kägi, J.H.R. Metallothionein: Molecular evolution and classification. In *Metallothionein IV*; Klassen, C.D., Ed.; Birkhäuser Verlag: Basel, Switzerland, 1999; pp. 7–13.
2. Iturbe-Espinoza, P.; Gil-Moreno, S.; Lin, W.; Calatayud, S.; Palacios, O.; Capdevila, M.; Atrian, S. The fungus *Tremella mesenterica* encodes the longest metallothionein currently known: Gene, protein and metal binding characterization. *PLoS ONE* **2016**, *4*, e0148651. [CrossRef] [PubMed]
3. Capdevila, M.; Bofill, R.; Palacios, O.; Atrian, S. State-of-the-art of metallothioneins at the beginning of the 21st century. *Coord. Chem. Rev.* **2012**, *256*, 46–62. [CrossRef]
4. Blindauer, C. Metallothioneins. In *RSC Metallobiology: Binding, Transport and Storage of Metal Ions in Biological Cells*; Maret, W., Wedd, A., Eds.; The Royal Society of Chemistry: Cambridge, UK, 2014; Volume 2, pp. 594–653.
5. Capdevila, M.; Atrian, S. Metallothionein protein evolution: A miniassay. *J. Biol. Inorg. Chem.* **2011**, *16*, 977–989. [CrossRef] [PubMed]
6. Dallinger, R.; Berger, B.; Hunziker, P.E.; Kägi, J.H.R. Metallothionein in snail Cd and Cu metabolism. *Nature* **1997**, *388*, 237–238. [CrossRef] [PubMed]
7. Palacios, O.; Pagani, A.; Pérez-Rafael, S.; Egg, M.; Höckner, M.; Brandstätter, A.; Capdevila, M.; Atrian, S.; Dallinger, R. Shaping mechanisms of metal specificity in a family of metazoan metallothioneins: Evolutionary differentiation of mollusc metallothioneins. *BMC Biol.* **2011**, *9*, 4. [CrossRef] [PubMed]
8. Palacios, O.; Atrian, S.; Capdevila, M. Zn- and Cu-thioneins: A functional classification for metallothioneins? *J. Biol. Inorg. Chem.* **2011**, *16*, 991–1009. [CrossRef] [PubMed]
9. Kägi, J.H.R.; Kojima, Y. Chemistry and biochemistry of metallothionein. In *Metallothionein II*; Kägi, J.H.R., Kojima, Y., Eds.; Birkhäuser Verlag: Basel, Switzerland, 1987; pp. 25–61.
10. Valls, M.; Bofill, R.; González-Duarte, R.; González-Duarte, P.; Capdevila, M.; Atrian, S. A new insight into metallothionein classification and evolution. The in vivo and in vitro metal binding features of Homarus americanus recombinant MT. *J. Biol. Chem.* **2001**, *276*, 32835–32843. [CrossRef] [PubMed]
11. Bofill, R.; Capdevila, M.; Atrian, S. Independent metal-binding features of recombinant metallothioneins convergently draw a step gradation between Zn- and Cu-thioneins. *Metallomics* **2009**, *1*, 229–234. [CrossRef] [PubMed]
12. Lieb, B.; Altenheim, B.; Markl, J. The sequence of a gastropod hemocyanin (HtH1 from Haliotis tuberculata). *J. Biol. Chem.* **2000**, *275*, 5675–5681. [CrossRef] [PubMed]
13. Chabicovsky, M.; Niederstaetter, H.; Thaler, R.; Hödl, E.; Parson, W.; Rossmanith, W.; Dallinger, R. Localisation and quantification of Cd- and Cu-specific metallothionein isoform mRNA in cells and organs of the terrestrial gastropod *Helix pomatia*. *Toxicol. Appl. Pharmacol.* **2003**, *190*, 25–36. [CrossRef]
14. Dallinger, R.; Chabicovsky, M.; Hödl, E.; Prem, C.; Hünziker, P.; Manzl, C. Copper in *Helix pomatia* (Gastropoda) is regulated by one single cell type: Differently responsive metal pools in rhogocytes. *Am. J. Physiol.* **2005**, *189*, R1185–R1195. [CrossRef] [PubMed]
15. Palacios, O.; Pérez-Rafael, S.; Pagani, A.; Dallinger, R.; Atrian, S.; Capdevila, M. Cognate and noncognate metal ion coordination in metal-specific metallothioneins: The *Helix pomatia* system as a model. *J. Biol. Inorg. Chem.* **2014**, *19*, 923–935. [CrossRef] [PubMed]

16. Gil-Moreno, S.; Jiménez-Martí, E.; Palacios, O.; Zerbe, O.; Dallinger, R.; Capdevila, M.; Atrian, S. Does variation of the inter-domain linker sequence modulate the metal binding behaviour of *Helix pomatia* Cd-metallothionein? *Int. J. Mol. Sci.* **2016**, *17*, 1–13. [CrossRef] [PubMed]
17. Hispard, F.; Schuler, D.; de Vaufleury, A.; Scheifler, R.; Badot, P.M.; Dallinger, R. Metal distribution and metallothionein induction after cadmium exposure in the terrestrial snail *Helix aspersa* (Gastropoda, Pulmonata). *Environ. Toxicol. Chem.* **2008**, *27*, 1533–1542. [CrossRef] [PubMed]
18. Höckner, M.; Stefanon, K.; de Vaufleury, A.; Monteiro, F.; Pérez-Rafael, S.; Palacios, Ò.; Capdevila, M.; Atrian, S.; Dallinger, R. Physiological relevance and contribution to metal balance of specific and non-specific metallothionein isoforms in the garden snail, *Cantareus aspersus*. *Biometals* **2011**, *24*, 1079–1092. [CrossRef] [PubMed]
19. Pérez-Rafael, S.; Monteiro, F.; Dallinger, R.; Atrian, S.; Palacios, Ò.; Capdevila, M. *Cantareus aspersus* metallothionein metal binding abilities: The unspecific CaCd/CuMT isoform provides hints about the metal preference determinants in metallothioneins. *Biochim. Biophys. Acta* **2014**, *1844*, 1694–1707. [CrossRef] [PubMed]
20. Baumann, C.; Beil, A.; Jurt, S.; Niederwanger, M.; Palacios, O.; Capdevila, M.; Atrian, S.; Dallinger, R.; Zerbe, O. Structural adaptation of a protein to increased metal stress: NMR structure of a marine snail metallothionein with an additional domain. *Angew. Chem. Int. Ed.* **2017**, *56*, 4617–4622. [CrossRef] [PubMed]
21. English, T.E.; Storey, K.B. Freezing and anoxia stresses induce expression of metallothionein in the foot muscle and hepatopancreas of the marine gastropod *Littorina littorea*. *J. Exp. Biol.* **2003**, *206*, 2517–2524. [CrossRef] [PubMed]
22. Pagani, A.; Villarreal, L.; Capdevila, M.; Atrian, S. The Saccharomyces cerevisiae Crs5 metallothionein metal-binding abilities and its role in the response to zinc overload. *Mol. Microbiol.* **2007**, *63*, 256–269. [CrossRef] [PubMed]
23. Orihuela, R.; Domenech, J.; Bofill, R.; You, C.; Mackay, E.A.; Kägi, J.H.R.; Capdevila, M.; Atrian, S. The metal-binding features of the recombinant mussel *Mytilus edulis* MT-10-IV metallothionein. *J. Biol. Inorg. Chem.* **2008**, *13*, 801–812. [CrossRef] [PubMed]
24. Palacios, O.; Espart, A.; Espín, J.; Ding, C.; Thiele, D.J.; Atrian, S.; Capdevila, M. Full characterization of the Cu-, Zn- and Cd-binding properties of CnMT1 and CnMT2, two metallothioneins of the pathogenic fungus *Cryptococcus neoformans* acting as virulence factors. *Metallomics* **2014**, *6*, 279–291. [CrossRef] [PubMed]
25. Capdevila, M.; Cols, N.; Romero-Isart, N.; Gonzalez-Duarte, R.; Atrian, S.; Gonzalez-Duarte, P. Recombinant synthesis of mouse Zn3-(and Zn4-(metallothionein 1 domains and characterization of their cadmium(II) binding capacity. *Cell. Mol. Life Sci.* **1997**, *53*, 681–688. [CrossRef] [PubMed]
26. Bofill, R.; Palacios, O.; Capdevila, M.; Cols, N.; Gonzalez-Duarte, R.; Atrian, S.; Gonzalez-Duarte, P. A new insight into the Ag+ and Cu+ binding sites in metallothionein β domain. *J. Inorg. Biochem.* **1999**, *73*, 57–64. [CrossRef]
27. Bongers, J.; Walton, C.D.; Richardson, D.E.; Bell, J.U. Micromolar protein concentrations and metalloprotein stoichiometries obtained by inductively coupled plasma. Atomic emission spectrometric determination of sulfur. *Anal. Chem.* **1988**, *60*, 2683–2686. [CrossRef] [PubMed]
28. Capdevila, M.; Domenech, J.; Pagani, A.; Tio, L.; Villarreal, L.; Atrian, S. Zn- and Cd-metallothionein recombinant species from the most diverse phyla may contain sulfide (S2-) ligands. *Angew. Chem. Int. Ed. Engl.* **2005**, *44*, 4618–4622. [CrossRef] [PubMed]
29. Fabris, D.; Zaia, J.; Hathout, Y.; Fenselau, C. Retention of thiol protons in two classes of protein zinc ion coordination centers. *J. Am. Chem. Soc.* **1996**, *118*, 12242–12243. [CrossRef]